Ministero dell'Università e della Ricerca

Università degli studi di Palermo

DIN
Dipartimento di Ingegneria Nucleare
Università di Palermo

Dipartimento di Ingegneria Nucleare

INNOVATIVE CHEMICAL PROCESSES FOR THE TREATMENT OF WATERS POLLUTED BY RECALCITRANT ORGANIC SUBSTANCES

PhD thesis of **Serena Randazzo**

Supervisors
Dott. Ing. Galia Alessandro

Dott. Ing. Scialdone Onofrio

Head of the PhD board
Prof. Francesco Castiglia

Ciclo XXII: 2008-2010

INDEX

INTRODUCTION

In the last years many research groups have focused their attention on the innovative chemical processes adopted for the treatment of water effluents polluted by recalcitrant organic substances, i.e. substances resistant to biological treatment. The main oxidative processes that could be used are: the incineration, the wet oxidation (realized at high pressures and temperatures by air or oxygen and at milder conditions by stronger oxidants like hydrogen peroxide), the anodic oxidation and the electro-Fenton process. Some of these technologies are fully known and are widely applied in the industries while others are in experimental route. In particular, the latter two processes have been taken in consideration in this work.

The electrochemical oxidation is one of the more studied technology because it presents high versatility and low costs, it is realized at mild condition of pressure and temperature and generally not involve the use of toxic substances.

The objectives of my PhD's thesis were:

1. to study the influence of the operative parameters on the electrochemical incineration of some organic pollutants chosen as model molecules, at different anodes, in order to better understand and optimize the process;
2. to study different electrochemical approaches such as direct processes, oxidation by means of electro-generated chlorine and electro-Fenton to compare their performances.

In particular, in the first year of my PhD, it was carried out an experimental investigation aimed to study the influence of numerous parameters, such as the current density, the flow rate, the initial concentration of the substrate, the nature of the supporting electrolyte, the anodic material, the pH and the temperature on the performances of the process of electrochemical incineration of oxalic acid to individuate the optimal operative conditions. Oxalic acid is often the main and ultimate intermediate for the chemical and electrochemical oxidation of many organic compounds that have more than two carbons atoms in their cycle or chain. It

was chosen as model molecule because it is generally resistant to electrochemical oxidation more than that of the starting compounds.

Experiments were performed at BDD (boron-doped diamond), which presents a high oxygen overpotential and is up to now one of the more promising materials for the direct electrochemical incineration and IrO_2-Ta_2O_5, which is known to present a quite low oxygen overpotential and to give rise to low efficient removal of organics and in particular of oxalic acid.

This study concerned the electrochemical direct processes, i. e. when the anodic oxidation takes place directly at the anode or is mediated by hydroxyl radicals. Hence, in the second year of my PhD, several studies on the oxidation of the oxalic acid in homogeneous phase by means of electro-generated oxidants such as active chlorine, were accomplished. In particular, in a first moment, a set of electrolyses was carried out only with sodium chloride in order to understand the mechanism of development of active chlorine at different operative conditions. In a second moment, a study on the influence of the main operative parameters on the electrochemical incineration of oxalic acid in the presence of sodium chloride was carried out, focusing on how the presence of this salt could change the results obtained before.

Moreover, in the last part of the second year and in the first part of the third, the study of the electrochemical direct anodic oxidation was extended to other carboxylic acids, such as formic and maleic acids, in order to evaluate the effect of the nature of the substrate on the performances of the process.

Theoretical considerations on the oxidation mechanism of these organics at the two different anodes employed were also included in this work. In particular, various expressions were elaborated for the processes under the mass transport control, oxidation reaction control and mixed kinetic regimes. Furthermore, different considerations about the experiments conducted with an amperostatic and with a potentiostatic alimentation, and in the presence of one or more organics in the electrolytic solution, were discussed. In each case, a good agreement between theoretical predictions and experimental data were observed.

The second part of the third year was dedicated to the study of the degradation of chlorinated aliphatic hydrocarbons, namely 1,2-dichloroethane and 1,1,2,2-tetrachloroethane, by anodic oxidation and by electro-Fenton processes. In particular, this last aspect was studied at the Faculty of Chemistry of Barcelona, during a stage of three months. Chlorinated aliphatic hydrocarbons are often toxic and they are frequently found in many surface and ground waters, as a result of their widespread use in industry and in various household products and their poor biodegradability. Since recent researches have demonstrated that some advanced oxidation processes, both simple and coupled, offer an attractive alternative to traditional routes for treating wastewaters containing toxic and refractory organic pollutants, these compounds were chosen as model molecules to reach our purposes.
Electro-Fenton, classified as one of the electrochemical advanced oxidation process, is a coupled process in which hydrogen peroxide, produced by the two-electron reduction of oxygen at an appropriate cathode, reacts with iron (II) ions added in the electrolytic solution to generate a very power oxidizing specie that oxidize the organic substrate. In particular, hydrogen peroxide can be produced by reduction of oxygen at certain electrodes such as reticulated vitreous carbon, graphite and gas diffusion electrode, but also at the anode, especially in the case of anodes with high oxidation power, by water discharge. Thus, through this coupled process, the pollutants can be destroyed by the simultaneous action of the Fenton's reaction and of the anodic oxidation at the anode. A set of electro-Fenton experiments under different operative conditions was carried out in order to investigate the effect of some operative parameters. Indeed, electrolyses were performed at various applied current density values, initial chlorinated compound concentrations and at BDD and Pt anodes. In particular, a time course of the intermediates detected during these experiments, such as some short-chain carboxylic acids and chlorinated ions, were also reported.

CHAPTER 1

ADVANCED OXIDATION PROCESSES (AOPs)

1.1 INTRODUCTION

In the last decades, industrial processes have generated a large variety of molecules that polluted air and waters due to negative impacts for ecosystems and humans (toxicity, carcinogenic and mutagenic properties) (Busca et al., 2008).

Furthermore, the protection and conservation of natural resources is one of the main priorities of modern society. Thus water, that is perhaps our most valuable resource, should be recycled. In particular, in appropriate circumstances, the organic pollutants contained in wastewaters can be economically recovered, but usually the best method to treat these streams involves the destruction of these substances (Cañizares et al., 2009; Poyatos et al., 2010).

In this sense, several research activities devoted to environment protection have been recorded as the consequence of the special attention paid to the environment by national and international authorities (Andreozzi et al., 1999).

In many cases organic substances are refractant[1] to biological degradation processes but they can be removed by chemical technologies.

Different chemical oxidation processes can be used. For high concentrations of organic substances, i.e., COD major than 20 g/ml, incineration or wet air oxidation processes are the most convenient ones, even if high pressure and high temperature have to be settled.

For low concentrations of organics, advanced oxidation processes (AOPs) are recommended.

These processes can be broadly defined as aqueous phase oxidation methods based on the intermediacy of highly reactive species such as hydroxyl radicals in the mechanisms leading to the destruction of the target pollutant (Comninellis et al., 2008).

[1] recalcitrance is the ability of a substance to remain in a particular environment in an unchanged form (Gulyas, 1997)

$$AOPs \rightarrow {}^{\bullet}OH \xrightarrow{pollutant} CO_2 + H_2O + \text{inorganic ions}$$

A chemical wastewater treatment using AOPs can produce the complete mineralization of pollutants to CO_2, water, and inorganic compounds, or at least their transformation into more innocuous products (Poyatos et al., 2010). In particular, the decomposition of non-biodegradable organic pollutants can lead to biodegradable intermediates, thus it can be recommended in some case to set AOPs as pre-treatments, followed by biological processes.

Key AOPs include photocatalysis based on near ultraviolet (UV) or solar visible irradiation, electrochemical processes, ultrasound (US) and chemical oxidation with use of oxidants, in particular ozone and Fenton's reagent, all these methods producing ·OH radicals. These radicals are very reactive, attack most organic molecules and are not highly selective (Skoumal et al., 2006).

Furthermore, less conventional but evolving processes exist including ionising radiation, microwaves, pulsed plasma and the utilisation of ferrate reagent.

Furthermore, it has been shown that coupled AOPs can lead to higher removal efficiencies. Thus often more AOPs are used at the same time as UV/O_3, UV/H_2O_2, photo-Fenton, O_3/H_2O_2 and others.

Some authors, such as Poyatos et al., have classified AOPs, both singles and combined, differentiating them as homogeneous or heterogeneous. Homogeneous processes have been further subdivided into processes that use energy and processes that do not use energy as shown in Fig. 1.1 (Poyatos et al., 2010).

Interestingly, AOPs are considered as very important tools, particularly for two reasons, namely the diversity of technologies involved and the areas of potential application.

In fact, although water and wastewater treatment is by far the most common area for their utilization, AOPs have also found applications as groundwater treatment, soil remediation, municipal wastewater sludge conditioning, ultrapure water production, volatile organic compound treatment and odour control.

Substantially, nowadays, AOPs can provide effective technological solutions for water treatment, which are vital for supporting and enhancing the competitiveness of

different industrial sectors, including the water technology sector, in the global market (Comninellis et al., 2008).

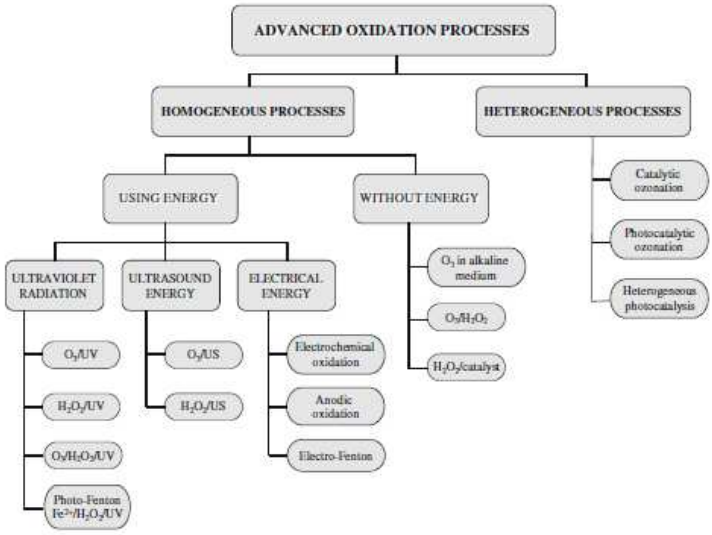

Fig. 1 Advanced oxidation processes (AOPs) classification. Abbreviations used: O_3 ozonation; H_2O_2 hydrogen peroxide; *UV* ultraviolet radiation; *US* ultrasound energy; Fe^{2+} ferrous ion

In the following paragraphs, a wide range of advanced oxidation systems that are used or currently being studied for their possible use in wastewater treatment will be briefly described.

1.2 OXIDATIVE DEGRADATION WITH CHEMICAL OXIDANTS

Different chemical oxidants have been reported to be active in the oxidation of recalcitrant substances in water solution. The most used are however, ozone and hydrogen peroxide.

1.2.1 OXIDATIVE DEGRADATION WITH OZONE

Ozonation consists in molecular ozone acting directly on the nucleophilic sites and unsaturated bonds of the organic compounds. Ozone is one of the strongest

oxidants technically applied, according to its high reduction potentials in principle both at acid and basic pHs (Busca et al., 2008):

$O_3 + 2H^+ + 2e^- \rightarrow O_2 + H_2O$ $E^\circ = 2.07$ V/SHE

$O_3 + H_2O + 2e^- \rightarrow O_2 + 2OH^-$ $E^\circ = 1.24$ V/SHE

The utilisation of ozone for the oxidative elimination of wastewater components has been known for a long time. This strong oxidant was used even earlier for the sterilization of air and the treatment of drinking water. Its effectiveness is highly dependent on the pH and is based essentially on two mechanisms (Ullmann's):

1) So- called direct oxidation occurs under acidic conditions. This is a fairly slow process, but the conversion can be accelerated greatly if the energy necessary for radical formation is provided in the form of UV light from a Hg low-pressure radiation source;

$$O_3 \xrightarrow{h\nu} O^\bullet + O_2$$
$$O^\bullet + H_2O \longrightarrow H_2O_2$$
$$H_2O_2 \xrightarrow{h\nu} 2\,HO^\bullet$$

2) Alkaline oxidation also takes place via the intermediate formation of hydroxyl radicals

$$O_3 + HO^- \rightarrow HO_2^- + O_2$$
$$HO_2^- + O_3 \rightarrow {}^\bullet O_2^- + O_2 + HO^\bullet$$
$$H_2O + O_3 + {}^\bullet O_2^- \rightarrow HO^- + 2\,O_2 + HO^\bullet$$

In the last reaction mechanism, OH^- ion has the role of initiator and the active species is the conjugate base of hydrogen peroxide, HO_2^-, which is formed from ozone and whose concentration is strictly dependent upon pH. The increase of pH to the aqueous O_3 solution will thus result into higher rates of $^\bullet$OH radicals production and the attainment of higher steady-state concentrations of $^\bullet$OH radicals in the radical chain decomposition process.

The action of ozone is selective, and the kinetics of reaction depends on the nature of the organic compounds (Busca et al., 2008).

As an example of application of ozonation in the treatment of wastewaters, it can be considered the degradation of phenol, a core theme of the contemporary research mainly for two reasons, namely the high toxicity even at low concentrations of this compound and its presence in natural waters that can lead further to the formation of substituted compounds during disinfection and oxidation processes. Indeed, some authors have observed that the kinetic of the reaction between ozone and phenol is fast. In particular, Gimeno et al. (2005) have shown that ozone (C_{O3} 10^{-4} mol/l) allows the almost complete conversion of 200mg/l phenol in 2 h at 20 °C without any buffer. However, the removal of COD is only 35% and that of TOC is less than 20% since hydroquinone, benzoquinone, catechol and mainly oxalic acid at higher conversion are generated as main intermediates (Busca et al., 2008.).

Nevertheless, some authors observed that the presence of catalysts, transition metal ions such as Mn^{2+}, Fe^{2+}, Ni^{2+}, Co^{2+}, Zn^{2+}, Cu^{2+}, and Ag^{+}, may enhance the conversion of ozone and of COD and TOC (Busca et al., 2008).

1.2.2 OXIDATIVE DEGRADATION WITH HYDROGEN PEROXIDE (Busca et al., 2008; Ullmann's)

The direct oxidation of organic compounds by hydrogen peroxide under acidic conditions is a well-known but relatively seldom-employed process.

The special advantage of this process is that the technological effort required is small, an especially positive factor in the case of dilute wastewater (i.e., < 10 g COD/l).

Oxidation with H_2O_2 proceeds at atmospheric pressure and room temperature within 60 –90 min.

Hydrogen peroxide is not toxic, has low cost, is easy and safe to handle and has an environmentally friendly nature since it decomposes into oxygen and water.

The standard reduction potentials of hydrogen peroxide

$H_2O_2 + 2H^+ + 2e^- \rightarrow 2\ H_2O$ $\quad E^\circ = 1.77$ V/SHE

$HO_2^- + H_2O + 2e^- \rightarrow 3\ OH^-$ $\quad E^\circ = 0.87$ V/ SHE

imply that it is a strong oxidant in both acidic and basic solutions.

Large-scale use of this virtually universal oxidizing agent is restricted by the high price of H_2O_2 itself, together with the fact that although self-decomposition proceeds with the formation of oxygen according the next reaction, the resulting oxygen contributing almost nothing to the oxidation process (Eq. 1.1).

$$H_2O_2 \rightarrow H_2O + ½\ O_2 \quad (1.1)$$

The reactivity of hydrogen peroxide is generally low and largely incomplete due to kinetics, in particular in acidic media, while being much enhanced by homogeneous and/or heterogeneous catalysts.

1.2.2.1 PROCESS INVOLVING IRON CATALYSTS: FENTON PROCESS

The conventional Fenton reaction uses hydrogen peroxide in conjunction with an iron(II) salt to produce high fluxes of hydroxyl radicals which can oxidise organic compounds in solution. Use of Fenton's reagent is one of the most effective ways for $^{\bullet}OH$ radical generation. In addition, due to the simplicity of equipment and mild operation conditions (atmospheric pressure and room temperature), this method has been postulated as the most economic oxidation alternative.

The mechanism of $^{\bullet}OH$ generation, which has been well established in the literature, is quite complex. Briefly, H_2O_2 decomposes catalytically by means of Fe^{2+} at acid pH giving rise to hydroxyl radicals (Eq. 1.2):

$$Fe^{2+} + H_2O_2 \rightarrow Fe^{3+} + OH^- + {}^{\bullet}OH \quad (1.2)$$

$$Fe^{3+} + H_2O_2 \rightarrow Fe^{2+} + {}^{\bullet}OOH + H^+ \quad (1.3)$$

Furthermore, Fe^{3+} can react, at acid pH, with H_2O_2 in the so-called Fenton's reaction, regenerating the catalyst and producing the $^{\bullet}HO_2$ radical, thus sustaining the process (Eq. 1.3). The technique becomes operative if the contaminated solution is at the optimum pH of 2.8-3.0, where it can be propagated by the catalytic behavior of the Fe^{3+}/Fe^{2+} couple. Interestingly, only a small catalytic amount of Fe^{2+} is required whereas this ion is regenerated (see Eq. 1.3) (Brillas et al., 2009). In particular, reaction (1.3) is associated with a two-step transformation in which the adduct $[FeIII(HO_2)]^{2+}$ formed in the equilibrium (1.3a) is subsequently converted into Fe^{2+}

and hydroperoxyl radical (HO_2•) following the first-order reaction (1.3b) (Brillas et al., 2009):

$$Fe^{3+} + H_2O_2 \rightarrow [FeIII(HO_2)]^{2+} + H^+ \quad (1.3a)$$

$$[FeIII(HO_2)]^{2+} \rightarrow Fe^{2+} + HO_2\bullet \quad (1.3b)$$

Generated HO_2• exhibits such a low oxidization power compared with •OH that it is quite unreactive toward organic matter. As can be observed, Fenton-like reaction (1.3) is much slower than Fenton's reaction (1.2). Fortunately, Fe^{2+} can be regenerated more rapidly by the reduction of Fe^{3+} with HO_2• from reaction (1.3c), with an organic radical R• from reaction (1.3d) and with superoxide ion (O_2•$^-$) from reaction (1.3e) (Brillas et al., 2009).

$$Fe^{3+} + HO_2\bullet \rightarrow Fe^{2+} + O_2 + H^+ \quad (1.3c)$$

$$Fe^{3+} + R\bullet \rightarrow Fe^{2+} + R^+ \quad (1.3d)$$

$$Fe^{3+} + O_2\bullet^- \rightarrow Fe^{2+} + O_2 \quad (1.3e)$$

Interestingly, this process can lead to the complete mineralization of the organics and is considered an attractive oxidative system for wastewater treatment due to the fact that iron is a very abundant and non toxic element even if usually significant quantities of ferric salts need to be disposed off. Furthermore, technical requirements for optimization or monitoring of the Fenton's reaction efficiency are complex and costly (i.e., GC–MS), which inhibits its common usage. Moreover, it is necessary to control pH carefully to prevent precipitation of iron hydroxide which occurs at basic pH. Even with optimization of the reaction efficiency this treatment technique implies significant operative costs, which can be an important limitation in the choice of treatment.

Recently, the use of ferrous waste metals as a source of iron ions to be used as catalysts has been proposed. Indeed, in acidic conditions, the surface of iron corrodes giving rise to ferrous ions and hydrogen gas. The former, in the presence of hydrogen peroxide, reacts rapidly to produce hydroxyl radicals in the normal Fenton reaction and leads to the formation of ferric ions. The zero-valent iron metal surface can then reduce the ferric ions down to ferrous (so increasing the reaction rate) or

indeed may interact with hydroxyl radicals resulting in oxidation to hydroxide ions, so limiting the reaction rate.

Furthermore, the application of conventional homogeneous Fenton reaction is complicated by the problems typical of homogeneous catalysis, such as catalyst separation, regeneration, etc. Thus, Fenton like heterogeneous catalysts, i.e., solids containing transition metal cations (mostly iron ions) have been developed and tested.

1.2.2.2 PROCESSES INVOLVING NON-IRON CATALYSTS

Non-iron catalysts may also work to enhance water peroxide oxidation reaction rate, namely copper containing microporous or mesoporous materials such as Cu-Al pillared clays and Cu-zeolite.

Additionally, it can be interestingly to cite the case of phenolic waste treatment with peroxidase enzymes, about which the most commonly used is horseradish peroxidase, in order to remove phenols from aqueous solutions in the presence of hydrogen peroxide. In this treatment, phenolic compounds are polymerized through a radical oxidation–reduction mechanism. High molecular weight polymers are insoluble and non-toxic and can be easily separated by filtration. It has been indicated that by using enzymes, treatment costs would be less than those in the conventional processes. In this case, treatment costs are significant not only due to the price of the purified enzyme but, also, because peroxidase is susceptible to permanent inactivation by various undesirable side reactions of the treatment process.

1.2.3 OXIDATIVE DEGRADATION WITH OTHER CHEMICAL OXIDANTS (Busca et al., 2008)

The oxidation of organic pollutants can be obtained also using other efficient oxidants as chlorine, chlorine dioxide and potassium permanganate. In fact, some authors, Throop et al. reported usage of these oxidants for the destruction of phenol.

These methods are certainly not environmentally friendly, due in particular to the formation of chlorinated organic compounds and the dispersion of Mn compounds. Furthermore, they are expensive due to the cost of the reagents, as well as the need for quite precise control of pH.

In recent years increasing interest has been devoted to ferrate (VI) ion as environmentally friendly oxidant. The ferrate ion, whose reduced form is ferric ions, is in fact a strong oxidant:

$FeO_4^{2-} + 8H^+ + 3e^- \rightarrow Fe^{3+} + 4\ H_2O$ $\quad E^\circ = 2.20$ V/SHE

but its redox potential strongly decreases by increasing pH.

1.3 PHOTOCATALYTIC OXIDATION

Photocatalytic processes make use of a semiconductor metal oxide as catalyst and of oxygen as oxidizing agent. Many catalysts have been so far tested for their application to the destruction of environmental toxic pollutants, although only TiO_2 in the anatase form seems to have the most interesting attributes such as high stability, in terms of resistance to photo-corrosion, good performance, namely high oxidative power and non-toxicity, and low cost. Additionally, it has a moderate Lewis-type acid–base character, allowing the adsorption of pollutants but also the desorption of intermediates and products (Busca et al., 2008; Andreozzi et al., 1999).

The strong oxidizing ability of TiO_2 photocatalysts has been ascribed to highly oxidative holes of the valence band and various oxygen-containing radical species (e.g., $^{\bullet}OH$, $O_2^{\bullet -}$, $HO_2^{\bullet}$). Among these species, holes and $^{\bullet}OH$ radicals play the most important roles in the photodegradation of organic pollutants.

As shown in Fig. 1.2, the primary event occurring on the UV-illuminated TiO_2 is the generation of photo-induced electron/hole (e^-/h^+) pairs.

$$TiO_2 \xrightarrow{h\nu} e^- + h^+$$

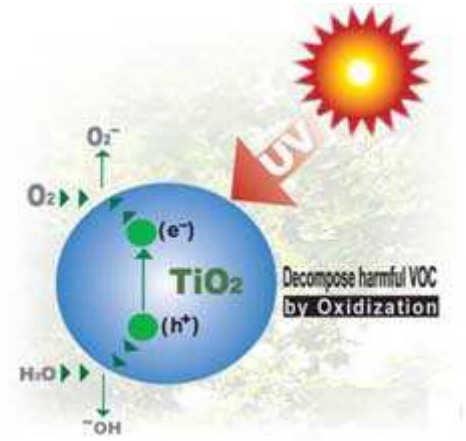

Fig. 1.2 Schematic representation of the generation of photo-induced electron/hole (e^-/h^+) pairs, referred as an example, to the decomposition of harmful VOC (Volatile Organic Compounds) by oxidization.

These charge carriers can rapidly migrate to the surface where they are captured by a suitable electron donor and acceptor, initiating an oxidation and reduction reaction, and/or they are recombined, dissipating the input light energy onto heat (Busca et al., 2008).

The considerable reducing power of formed electrons allows them to reduce some metals and dissolved oxygen with the formation of the superoxide radical ion $^{\bullet}O_2^-$, as also shown in Fig. 1.2, whereas remaining holes are capable of oxidizing adsorbed H_2O or HO^- to reactive $^{\bullet}HO$ radicals:

$$TiO_2(h^+) + H_2O_{ad} \rightarrow TiO_2 + HO_{ad}^{\bullet} + H^+$$

$$TiO_2(h^+) + HO_{ad}^- \rightarrow TiO_2 + HO_{ad}^{\bullet}$$

These reactions are of great importance in oxidative degradation processes due to the high concentration of H_2O and HO^- adsorbed on the particle surface.

Some adsorbed substrate can be directly oxidized by electron transfer:

$$TiO_2(h^+) + RX_{ad} \rightarrow TiO_2 + RX_{ad}^{\bullet +}$$

Unfortunately a significant part of electron-hole pairs recombine thus reducing the quantum yield. Thus, improving photocatalytic efficiency requires primarily a decreased e^-/h^+ recombination rate, which is generally achieved by the increase of the rate of photogenerated electrons transfer to the oxidant at the interface and/or the capture of holes via oxidation process (Andreozzi et al., 1999).

However, homogeneous AOPs using UV radiation are generally employed for the degradation of compounds that absorb UV radiation within the corresponding range of the spectrum. In fact, a consideration of the associated energy factors shows that titanium dioxide absorbs light only at wavelengths below 390 nm because of its relatively large band gap of 3.2 eV. Thus, the compounds that absorb UV light at lower wavelengths are excellent candidates for photo-degradation. Unfortunately, in the treating wastewaters, the compounds to be destructed can be of very different nature, thus the large band gap can be an important drawback of TiO_2 for photocatalysis (Busca et al., 2008; Poyatos et al., 2010).

For these reasons, various efforts for enhancing photocatalytic efficiency have to be studied and among these, the surface modification of TiO_2 seems the most interesting. In fact, in order to reduce the too large band gap of TiO_2, its surface can be modified by depositing noble metal clusters on its surface, as platinum, carbon, copper, fluorine and nitrogen. In this way, TiO_2-anatase can be photocatalytically active under visible light and thus more useful for the degradation of a wide set of pollutants.

As all the heterogeneous processes, one of the most drawback of the photocatalytic oxidation can be referred to optimize the mass transfer between the different phases. Thus, reactors operating photocatalytically use semiconductor such as TiO_2 in different ways, i.e. in suspension as a fluidised bed or internally supported as a fixed bed. Generally the presence of a heterogeneous catalysts lead to the advantage of a easy separation and regeneration of themselves, even if in this case, the formation of a slurry of TiO_2 could lead to onerous and long recovering processes.

1.4 ELECTROCHEMICAL OXIDATION PROCESSES

Nowadays, electrochemical processes are also receiving increasing attention for wastewater treatment. Indeed, recent researches have demonstrated that electrochemical methods offer an attractive alternative to traditional routes for treating wastewaters containing toxic or/and refractory organic pollutants (Chen, 2004; Martinez-Huitle and Ferro, 2006).

This method is characterized by two processes, the anodic oxidation that usually occurs with complete mineralization of organics and the cathodic reduction which is used to convert organic pollutants in not toxic substances. Among these, the most common is by far the anodic oxidation in which organic pollutants are usually destroyed with $^{\bullet}OH$ formed at the surface of the anode, by the oxidation of water (Guinea et al., 2009). Thus, electrochemical oxidation process is an AOP.

Recently, this electrolytic technology has been widely studied with both real and synthetic industrial wastes. The main results are that this route allows the almost complete mineralization of the organics contained in the wastes with, in some cases, very high current efficiencies (Cañizares et al., 2009).

The oxidation mechanisms involved in this technology have also been characterized and include direct electro-oxidation, hydroxyl radical-mediated oxidation, and oxidation mediated by oxidants generated during the treatment from the salts contained in the waste.

In the first case, direct electron transfer from the anode to the molecule occurs but fast deactivation of the anode is often observed, due to deposition of a carbonaceous film. This condition is usually achieved in the potential region before oxygen evolution (water stability).

On the other hand, at high anodic potentials, the water oxidation is involved giving rise to the electro-generation of hydroxyl radicals on the anodes. These species are known as "active oxygen", that can be physically adsorbed (adsorbed hydroxyl radicals, $^{\bullet}OH$) or chemisorbed (oxygen in the oxide lattice, MO_{x+1}). In this case, total mineralization of organic pollutants may occur with no anode deactivation. Interestingly, the physically adsorbed "active oxygen" may cause the complete mineralization of organic compounds, while the chemisorbed "active oxygen" may participate in the formation of selective oxidation products. Thus, in general, $^{\bullet}OH$ is more effective for pollutant oxidation than O in MO_{x+1} (Busca et al., 2008; Kapalka et al., 2008).

Besides the advantages typical of every AOP, the anodic oxidation does not need additions of a large amount of chemicals to wastewater, with no tendency of producing secondary pollution.

However, the effectiveness of the electrochemical treatment depends on many factors including the nature of the electrodic material. In fact, several anode materials had been investigated, including graphite, Pt, PbO_2, IrO_2, TiO_2, SnO_2, and diamond film. Among these, conductive-diamond anode, in particular boron-doped diamond (BDD), is by far preferred, despite of its expensive costs, because of its high over-potentials for O_2 evolution, high stability even in strong acid media and wide potential window of water discharge.

Interestingly, this anode is among those interact very weakly with $^{\bullet}OH$ (Eq. 1.4), thus resulting in high organic removals.

$$BDD(H_2O) \rightarrow BDD(^{\bullet}OH) + H^+ + e^- \quad (1.4)$$

Interestingly, the high oxidation power of BDD also allows the production of other weaker oxidants such as reactive oxygen species like H_2O_2 and ozone, as well as peroxo-derivatives coming from the oxidation of the anion of the background electrolyte. These characteristics have led to CDEO (Conductive-Diamond Electrochemical Oxidation (CDEO)) being classified as an AOP (Cañizares et al., 2009).

1.5 PROCESSES INVOLVING ULTRASOUND (Poyatos et al., 2010; Mahamuni and Adewuyi, 2010; Oturan et al., 2008)

In recent years, ultrasound has been extensively used as an advanced oxidation process for wastewater treatment. This is owing to the production of $^{\bullet}OH$ radicals in aqueous solutions and subsequent oxidation of pollutants in the presence of ultrasound.

$$H_2O \xrightarrow{)))} H^{\bullet} + OH^{\bullet}$$

$$H^{\bullet} + O_2 \xrightarrow{)))} HOO^{\bullet}$$

$$\text{Pollutants} + OH^{\bullet} \xrightarrow{)))} \text{Degradation products}$$

$$\text{Pollutants} + HOO^{\bullet} \xrightarrow{)))} \text{Degradation products}$$

The well-known effect of ultrasound is the cavitation, which is the formation, growth and collapse of microbubbles that concentrate the acoustic energy into

micro-reactors leading to extreme conditions within a short time (<1 ns). In fact, very high temperatures are reached during cavitation, even in the range of 5200 K and 1900 K in the cavity and interfacial region, respectively.

In this scenario, the formation of ˙OH radicals takes place inside the cavity, whereas these conditions are so extreme that they are capable of breaking up the water molecules and producing radicals. Thus, pyrolysis of organics takes place inside the cavity and near the interface of the cavity and surrounding liquid at the time of collapse of the cavity in the presence of ultrasound.

Moreover, during sonication, the formation of hydrogen peroxide was observed that also helps in the degradation of pollutants in wastewater, according the following reaction:

$$\text{Pollutants} + H_2O_2 \xrightarrow{)))} \text{Degradation products}$$

Process involving ultrasound has been studied for the wastewater treatment of various pollutants such as aromatic compounds, chlorinated aliphatic compounds, explosives, herbicides and pesticides, organic dyes, organic and inorganic gaseous pollutants, organic sulfur compounds, oxygenates and alcohols, pharmaceuticals, personal care products, pathogens and bacteria in water. Thus, it has virtually been proved beyond doubt that ultrasound can be used for the treatment of any kind of wastewater.

Generally, this type of advanced oxidation process reduces costs since no radiation is needed, and it can be combined with other oxidation processes.

Nevertheless, due to the inefficient conversion of energy in producing ultrasonic cavitation and possible difficulties in its scale up, no industrial installations for waste water treatment have been reported in the literature, since the technology necessary is still in its initial phases, and thus not as well developed as other options.

Finally, efforts have been made to use ultrasound in the presence of ozone, hydrogen peroxide (see par. 1.6.7), Fenton's reagent, photocatalysts and enzymes.

1.6 COMBINED PROCESSES

The combination of different techniques has been found frequently very useful to improve the performances in organics degradation processes. Many different solutions are reported in the literature.

Among these, the coupling of UV irradiation with chemical oxidation with ozone or/and hydrogen peroxide has to be considered convenient and seems to have already industrial application in water treatment. Interestingly, according to Gimeno et al. (2005), the coupling of ozonation with photochemical and/or photocatalytic oxidation are the most attractive technologies.

Furthermore, some authors have noted that the Fenton-type oxidation is made more efficient by coupling with sonication and hydrodynamic cavitation. Additionally, the coupling of adsorption on alumina with electrical discharges as well as of adsorption on polymeric materials with sonication have been reported as very efficient methods to remove phenol (Busca et al., 2008).

Nevertheless, the most famous coupled processes are the electro-Fenton (EF) and photoelectro-Fenton (PEF), H_2O_2/UV and O_3/UV. In this frame, it is also important to consider the possibility of the degradation of organic pollutants by the contemporary effectiveness of electrochemical anodic and cathodic processes. AOPs involving electrochemical process are also known as EAOPs, i.e. electrochemical advanced oxidation processes (Brillas et al., 2009).

Finally, apart from the combination of AOPs, it is important to enunciate the possibility of put in sequence some degradation processes in order to improve the treating of wastewaters. In particular, whereas oxidation processes could transform refractory pollutants in more innocuous products and thus biodegradable, it was considered that AOPs could be an optimal pretreatments for a successive biological degradation step, to limit toxicity of the solution with respect to the microbial cultures.

1.6.1 ELECTROCHEMICAL REDUCTION AND OXIDATION (Scialdone et al., 2010)

An electrochemical cell is a particular heterogeneous reactor that, owing to the charge conservation law, requires the coupling of at least two spatially separated redox processes: an anodic oxidation and a cathodic reduction. The most frequent condition is that only one of these processes is of applicative interest and the other one is simply used to close the circuit.

In particular, in the case of treatment of wastewaters:

- in adopted reduction process, oxygen evolution by water oxidation occurs at anodic surface that is useless for the abatement of the organic pollutant;
- in the oxidation route, the cathodic process, that is not of applicative interest, is the hydrogen evolution.

Nevertheless in some cases, both anodic oxidation and cathodic reduction processes are useful for the abatement of pollutants, as in the case of chlorurated aliphatics. Indeed, these substance can be mineralized to carbon dioxide and water at anodic compartment and de-halogenated to correspondent alkenes at the cathodic one.

Interestingly, if we denote with E the cell voltage, we can express the rate of consumption R of the pollutant and the molar energy consumption η (kJ/mol) respectively by the Eq. (1.5) and (1.6) both implicitly based on the Faraday law.

$$R = \frac{ICE}{nF} \tag{1.5}$$

$$\eta = \frac{nFE}{CE} \tag{1.6}$$

In particular, when the reactant is consumed in paired anodic and cathodic processes, aforementioned equations becomes:

$$\eta = \frac{FE}{CE_1/n_1 + CE_2/n_2} = \frac{n_1 FE}{CE_1}\frac{1}{1+\frac{n_1 CE_2}{n_2 CE_1}} \tag{1.7}$$

$$R = I\frac{CE_1}{n_1 F} + I\frac{CE_2}{n_2 F} = I\frac{CE_1}{n_1 F}\left(1+\frac{n_1 CE_2}{n_2 CE_1}\right) \tag{1.8}$$

where CE_1 and CE_2 are the faradic yields of the two redox reactions and n_1 and n_2 the number of electrons exchanged for each them.

From these equations one can easily understand that when paired electrochemical processes can be adopted for the abatement of a pollutant, without significantly increase of the cell voltage E, it is possible to obtain a faster elimination of the compound at the same current intensity coupled with a better utilization of the electric power driving the reactor.

In this frame, some authors have coupled the anodic oxidation of various organic compounds with the cathodic formation of oxidants, as in the electro-Fenton process (Fockedey et al., 2002; Guinea et al., 2009; Montanaro et al., 2008; Skoumal et al., 2009) (see par. 1.6.2).

1.6.2 ELECTRO-FENTON PROCESS

EAOPs based on Fenton's reaction chemistry are emerging technologies for water remediation. Over the past decade, they have experienced a significant development showing great effectiveness for the decontamination of wastewater polluted with toxic and persistent pesticides, organic synthetic dyes, pharmaceuticals and personal care products, and a great deal of industrial pollutants (Brillas et al., 2009).

During the electrochemical treatment of wastewaters, hydrogen peroxide can be produced continuosly by the two-electron reduction of oxygen (Eq. 1.9) at appropriate cathodic potential on certain electrodes such as reticulated vitreous carbon, graphite and gas diffusion electrode (Busca et al., 2008) (as shown in Fig. 1.3):

$$O_2 + 2H^+ + 2e^- \rightarrow H_2O_2 \qquad (1.9)$$

Furthermore, water discharge at the anode occurs, leading, especially in the case of anodes with high oxidation power, to the generation of hydrogen peroxide besides oxygen and hydroxyl radicals. In the electro-Fenton process, the oxidation ability of electrogenerated H_2O_2 is strongly enhanced by adding to the solution a small

quantity of catalytic Fe^{2+} to produce $^{\bullet}OH$ thus following Fenton's reaction (Skoumal et al., 2009).

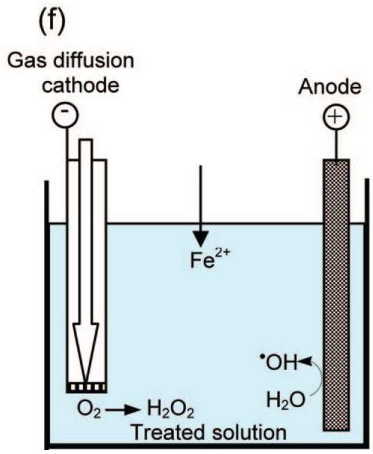

Fig. 1.3 *A schematic representation of a bench-scale undivided cell with a gas diffusion cathode used in EF process* (*Brillas et al.*, 2009)

The major advantages of this indirect electro-oxidation method compared with the chemical Fenton process are (Brillas et al., 2009):

- (i) the on-site production of H_2O_2 that avoids the risks related to its transport, storage, and handling,
- (ii) the possibility of controlling degradation kinetics to allow mechanistic studies,
- (iii) the higher degradation rate of organic pollutants because of the continuous regeneration of Fe^{2+} at the cathode, which also minimizes sludge production;
- (iv) the feasibility of overall mineralization at a relatively low cost if the operation parameters are optimized.

In EF and most related technologies, soluble Fe^{3+} can be cathodically reduced to Fe^{2+} by reaction (1.9b), which is known as electrochemical catalysis, with $E°$ = 0.77 V/SHE:

$$Fe^{3+} + e^{-} \rightarrow Fe^{2+} \qquad (1.9b)$$

The fast regeneration of Fe^{2+} by reaction (1.9b) accelerates the production of $^{\bullet}OH$ from Fenton's reaction (1.2). This enhances the decontamination of organic solutions achieved with these EAOPs, which possess much greater degradation ability than similar anodic oxidation and Fenton processes used separately.

1.6.2.1 INFLUENCE OF OPERATION PARAMETERS (Brillas et al., 2009)

The degradation rate of organic wastewater in the EF process depends on operation parameters such as O_2 feeding, stirring rate or liquid flow rate, temperature, solution pH, electrolyte composition, applied potential or current, and iron catalyst and initial pollutant concentration. Most of these parameters are optimized in the cell used for achieving the best current efficiency and lowest energy cost. High flow rates of pure O_2 or air are normally used either to feed the gas diffusion electrode (GDE) cathode or maintain the solution saturated with O_2 to obtain the maximum H_2O_2 production rate. Similarly, the solution stirring rate in tank reactors or liquid flow rate in flow cells is chosen at sufficiently high values to obtain fast homogenization of treated solutions and enhance the mass transfer of reactants toward the electrodes to yield the maximum rates of electrode reactions. Ambient temperatures are normally employed. A rise in temperature to 35-40 °C increases the mineralization rate, but greater temperatures are detrimental because of the strong acceleration of chemical H_2O_2 decomposition. Several authors have reported that the maximum efficiency of the process in undivided cells with carbon-felt and GDE cathodes is achieved at pH 3.0, which is close to pH 2.8 where the maximum production of $^{\bullet}OH$ is expected from Fenton's reaction (1.2). The concentration of Fe^{2+} required as catalyst, which is a function of the cathode employed, have not to be much higher. Indeed, for example, values of 0.5-1.0 mM are employed for carbon-PTFE/GDE cathodes, since for higher catalyst concentrations the following reaction should be favoured:

$$Fe^{2+} + {}^{\bullet}OH \rightarrow Fe^{3+} + OH^{-}$$

An increase in initial pollutant concentration always causes its slower kinetic decay and lower percentages of pollutant removals. The electrolyte composition is limited

to sulfate and chloride ions, since media involving perchlorate ions with lower complexing power are toxic and not environmentally viable. The oxidation power related to the applied current in undivided two-electrode cells depends on the pollutant concentration, cell configuration, and anodes utilized, which can electrogenerate competitive strong oxidants such as BDD(•OH) (see section 1.4) . In general, lower currents and greater organic contents lead to higher current efficiency with smaller energy consumption but requiring longer times for attaining acceptable mineralization degrees.

1.6.3 PHOTOELECTRO-FENTON PROCESSES

In this scenario, an interesting possibility could be to profit from the potential oxidant power of electrogenerated H_2O_2 via photo-Fenton. Indeed, it was demonstrated that the mineralization process can be accelerated using the photoelectro-Fenton method, where the solution treated under electro-Fenton conditions is exposed to an UVA light of wavelength max = 360 nm (Gimeno et al., 2005; Skoumal et al., 2009).

The photocatalytic action of this irradiation is complex and its main effects can be related to:

- the photolysis of $Fe(OH)^{2+}$, which is the predominant Fe(III) species at pH 3.0, regenerating greater amount of Fe^{2+} and producing more quantity of •OH via photo-Fenton reaction, according Eq. 1.10:

  $$Fe(OH)^{2+} + h\nu \rightarrow Fe^{2+} + {}^{\bullet}OH \qquad (1.10)$$

- the photolysis of complexes of Fe(III) with generated carboxylic acids (Skoumal et al., 2009).

Nevertheless, some authors (Flox et al., 2007; Guinea et al., 2009; Skoumal et al., 2009) have used sunlight irradiation as alternative treatment, since it represents an inexpensive and potent source of UV light, giving rise to the so-called solar photoelectro- Fenton method.

Hence, both these combined processes are an extension of Fenton process which takes advantages from UV-VIS light irradiation (Andreozzi et al., 2009).

Finally, to our knowledge, it is important to consider another kind of electro-oxidation process, known as mediated electro-oxidation, concerning the oxidation on an anode of metal ions, usually called mediators, from a stable, low valence state to a reactive, high valence state. Then, the oxidized mediators, typically Ag^{2+}, Co^{3+}, Fe^{3+}, Ce^{4+} and Ni^{2+}, attack organic pollutants directly, and may also produce hydroxyl free radicals that promote destruction of the organic pollutants. Subsequently, these species are regenerated on the cathode, forming a closed cycle. This process was proposed for treating mixed and hazardous wastes (Busca et al., 2008).

On the other hand, mediated electro-oxidation as well as electro-Fenton usually need to operate in acidic media to avoid precipitation of metal hydroxides and, in addition, there exists the secondary pollution from the heavy metals added. These disadvantages limit the application of these processes (Busca et al., 2008).

1.6.4 OZONATION AND ULTRAVIOLET RADIATION (O_3/UV) (Andreozzi et al., 1999; Poyatos et al., 2010)

Oxidation processes using ozone and ultraviolet radiation is an advanced water treatment method for the effective oxidation and destruction of toxic and refractory organics in water.

Basically, aqueous systems saturated with ozone are irradiated with UV light of 254 nm; the photolysis of the ozone leading to the formation of hydroxyl radicals as shown in the following reaction (Eq. 1.11):

$$H_2O + O_3 \rightarrow 2\ ^{\bullet}OH + O_2 \qquad (1.11)$$

The extinction coefficient of O_3 at 254 nm is $3600 M^{-1}\ cm^{-1}$, much higher than that of H_2O_2. By the way, O_3/UV oxidation process is more complex than the other ones, since $^{\bullet}OH$ radicals are produced through different reaction pathways. There is a general agreement about involved reactions:

$$O_3 \xrightarrow[k_{O_3}]{h\nu} O^1(D) + O_2$$

$$O^1(D) + H_2O \rightarrow H_2O_2$$

$$H_2O_2 \xrightarrow{h\nu} HO^{\bullet} + {}^{\bullet}OH$$

By using an O_3/UV process, as an example, Chen et al. (2007) obtained a very effective mineralization of the total organic carbon (TOC) (94%) of a solution containing dinitrotoluene (DNT) and trinitrotoluene (TNT), with a UV radiation of 96 W and an ozone dosage of 3.8 g/h. The use of UV radiation improved performance by 76.4% on the respect of results obtained when only ozone was used for the degradation of the compounds.

1.6.5 OZONATION WITH HYDROGEN PEROXIDE (O_3/ H_2O_2) (Poyatos et al., 2010)

Hydrogen peroxide in an aqueous solution is partially dissociated to hydroperoxide anion (HO_2^-), which reacts with ozone giving rise to a series of chain reactions including hydroxyl radicals (Eq. 1.12-1.13):

$$H_2O_2 + 2O_3 \rightarrow 2\,{}^{\bullet}OH + 3O_2 \quad (1.12)$$

$$HO_2^- + O_3 \rightarrow {}^{\bullet}HO_2 + {}^{\bullet}O_3 \quad (1.13)$$

This method, which can be easily automated, can be used for the degradation of practically all compounds.

1.6.6 HYDROGEN PEROXIDE AND ULTRAVIOLET RADIATION (H_2O_2/UV) (Andreozzi et al., 1999; Poyatos et al., 2010)

This advanced oxidation process entails the formation of hydroxyl radicals generated by the photolysis of H_2O_2 and the corresponding propagation reactions. The photolysis of hydrogen peroxide occurs when UV radiation (with wavelengths smaller than 280 nm) is applied, causing the homolytic cleavage of H_2O_2, as shown in the following reaction:

$$H_2O_2 \xrightarrow{h\nu} 2OH^{\bullet}$$

Moreover, the propagation reactions are the following, since H_2O_2 itself is attacked by OH radicals (Eq. 1.14):

$$H_2O_2 + {}^{\bullet}OH \rightarrow {}^{\bullet}HO_2 + H_2O \quad (1.14)$$

$$2\ {}^{\bullet}HO_2 \rightarrow H_2O_2 + O_2 \quad (1.15)$$

Nevertheless, the major drawback of this process is due to the small molar extinction coefficient of H_2O_2 which is only 18.6 $M^{-1}cm^{-1}$ at 254 nm, thus only a relative small fraction of incident light is therefore exploited.

Furthermore, the rate of photolysis of aqueous H_2O_2 has been found to be pH dependent and to increase when more alkaline conditions are used. This may be primarily due to the higher molar absorption coefficient of the peroxide anion HO_2^- which at 254 nm is 240 $M^{-1}cm^{-1}$, since hydrogen peroxide dissociate in aqueous solution (Eq. 1.16).

$$H_2O_2 \rightarrow HO_2^- + H^+ \quad (1.16)$$

However, an H_2O_2/UV system can totally mineralize any organic compound, reducing it to CO_2 and water. Indeed this method have been employed for the mineralization of many toxic organics.

For instance, De Laat et al. (1994) demonstrated the effectiveness of this method even for dilute aqueous solution of chloroethanes. In particular, using a H_2O_2 concentration of $5 \cdot 10^{-4}$ mol/L, pH of 7.5, a temperature of 20°C, and a photonic flux at 254 nm of $4{,}4 \cdot 10^{-}$ (Einstein s^{-1}) to treating water with a 1,1,2-trichloroethane concentration of 0.5 µmol/L, they observed a conversion of the pollutant of about 87%.

1.6.7 OZONE, HYDROGEN PEROXIDE AND ULTRAVIOLET RADIATION (O_2/H_2O_2/UV) (Poyatos et al., 2010)

When hydrogen peroxide is used in an O_3/UV process, it accelerates the decomposition of ozone and increases the generation of OH radicals. This process is the result of the combination of two binary systems, O_3/UV and O_3/H_2O_2, in such a way that the resulting action is the following:

$$2\,O_3 + H_2O_2 \xrightarrow{h\nu} 2\,OH^{\bullet} + 3O_2$$

Obviously, O_3/H_2O_2/UV processes are the most expensive because of the use of two types of reagents as compared to processes that use only one.

As an example, some authors used these methods for the decolorization of a dye in the textile industry. These authors found that the H_2O_2/UV process took longer to remove the color than ozonation. In contrast, the H_2O_2/UV method eliminated the TOC from the effluent more efficiently (99%) than ozonation (33%) for 160 min of retention time. Consequently, a combination of both methods was proposed in order to reduce both of these parameters, thus, with 15 min of pre-ozonation followed by a H_2O_2/UV treatment, the dye and TOC removal efficiency were 90%.

1.6.8 OZONE AND HYDROGEN PEROXIDE WITH ULTRASOUND (Poyatos et al., 2010)

The reactions that occur in the presence of ozone and ultrasounds (represented as "))))") are shown below:

$$H_2O \xrightarrow{)))} H^{\bullet} + OH^{\bullet}$$
$$O_3 \xrightarrow{)))} O_2(g) + O(^3P)$$
$$O(^3P)(g) + H_2O \rightarrow 2OH^{\bullet}$$
$$O_3 + OH^{\bullet} \rightarrow O_2 + HO_2^{\bullet}$$
$$O_2 + H^{\bullet} \rightarrow HO_2^{\bullet}$$
$$O_3 + HO_2^{\bullet} \rightarrow 2\,O_2 + OH^{\bullet}$$
$$OH^{\bullet} + OH^{\bullet} \rightarrow H_2O_2$$
$$HO_2^{\bullet} + OH^{\bullet} \rightarrow H_2O + O_2$$

Moreover, by combining ultrasounds and H_2O_2, it was possible to achieve the formation of free radicals in gaseous phase of the cavitation bubbles formed during the US sonication, thus increasing the destruction yeld of organic pollutants. The reactions produced are the following:

$$H_2O_2 \xrightarrow{)))} OH^{\bullet} + OH^{\bullet}$$
$$H_2O_2 + O_2 \xrightarrow{)))} HO_2^{\bullet} + HO_2^{\bullet}$$
$$H_2O_2 + OH^{\bullet} \rightarrow HO_2^{\bullet} + H_2O$$

In fact, although hydrogen peroxide can be produced by application of ultrasounds alone to a diluted aqueous solution, the amount may be too small to be significant. For this reason, it was considered best to add it in order to speed up the oxidation process of the substance to be degraded. On occasions, these processes are enhanced when UV radiation is also included because more free radicals are formed.

CHAPTER 2

ELECTROCHEMICAL INCINERATION

2.1 INTRODUCTION

Electrochemical technologies have gained importance in the world during the past two decades and offer promising approaches for the treatment of industrial effluents contaminated by organic and inorganic pollutants.

In particular, by an electrochemical treatment of wastes, either a partial (reduction of toxicity) or a complete decomposition of the pollutants can be achieved. In the second case, the organic substances are totally oxidize to carbon dioxide and this electrolytic approach is known as “electrochemical incineration”, because of the obvious similarity with the thermal incineration process (Zhi et al., 2003).

Furthermore, removal and destruction of pollutant species can be carried out directly or indirectly by electrochemical oxidation processes in an electrochemical cell without continuous feed of redox chemicals. Nevertheless, the inherent advantage of the electrochemical technology is its environmental compatibility, due to the fact that the main reagent, the electron, is a ‘clean reagent’. In addition, the high selectivity of many electrochemical processes helps to prevent the production of unwanted by-products, which in many cases have to be treated as waste.

More specifically, attractive advantages of electrochemical processes are generally (Jüttner et al., 2000):

1. Versatility — they are used for direct or indirect oxidation and reduction, phase separation, concentration or dilution, biocide functionality, applicability to a variety of media and pollutants in gases, liquids, and solids;
2. Energy efficiency — electrochemical processes generally have lower temperature and pressure requirements, as the other AOPs, and electrodes and cells can be designed to minimize power losses caused by inhomogeneous current distribution, voltage drop and side reactions;

3. Amenability to automation — the system inherent variables of electrochemical processes, e.g. electrode potential and cell current, are particularly suitable for facilitating process automation;
4. Cost effectiveness — cell constructions and peripheral equipment are generally simple and, if properly designed, also inexpensive.

Therefore, this technology can be considered environmentally compatible, versatile, safe and easy to handle.

Despite these advantages, electrochemical processes are of a heterogeneous nature, which means that the reactions are taking place at the interface of an electronic conductor (the electrode) and an ion conducting medium (the electrolyte). This implies that the performance of electrochemical processes may suffer from limitations of mass transfer and the size of specific electrode area.

Another crucial point is the chemical stability of the cell components in contact with an aggressive medium and in particular the long term stability and activity of the electrode material. Therefore, an efficient, stable and environmentally compatible anode material is required for future technology.

Moreover, electrochemical methods are recommended for low concentration (COD < 5 g/L) of organics because in this way they can work more economically and ecologically (Gulyas, 1997; Kapalka et al., 2008).

2.2 MECHANISM PATHWAYS

Electrochemical incineration processes can be grouped in two categories (Jüttner et al., 2000; Zhi et al., 2003):

- direct oxidation at the anode;
- indirect oxidation involving the electrochemical generation of powerful oxidants, such as Cl_2, hypochlorite, peroxide, ozone, Fenton's reagent, peroxodisulphate and metal ions with high oxidation potential.

Furthermore, most of the electrochemical incineration processes on the anode are reported to be mediated by hydroxyl radicals and other active intermediates that are produced on the anode surface by the discharge of water.

Generally, authors refer to this pathway as a direct oxidation process mediated by $^{\bullet}OH$ radicals, physically or chemically adsorbed on the anode surface, distinguishing it from the direct electron-transfer reaction (Zhi et al., 2003).

2.2.1 DIRECT OXIDATION MECHANISM

Electrochemical oxidation of pollutants can occur directly at the anode through the generation of physically adsorbed "active oxygen", i.e. adsorbed hydroxyl radicals $^{\bullet}OH$ or chemisorbed "active oxygen", i.e. oxygen in the oxide lattice MO_{x+1}.

The overall electrochemical oxidation mechanism involves the transferring of oxygen from water to the organic pollutant using electrical energy. As an example, here is reported the anodic oxidation of phenol (Eq. 2.1):

$$C_6H_5OH + 11H_2O \rightarrow 6CO_2 + 28H^+ + 28\ e^- \quad (2.1)$$

In this reaction, water is the source of oxygen atoms for the complete oxidation of phenol to CO_2 at the anode of the electrolytic cell. The liberated protons in this reaction are usually discharged at the cathode to hydrogen molecules (Eq. 2.2).

$$28H^+ + 28e^- \rightarrow 14H_2 \quad (2.2)$$

According to the literature (Jüttner et al., 2000; Kapalka et al., 2008), water is firstly discharged (at potentials above 1.23 V/SHE under standard conditions) at the anode active sites M producing adsorbed hydroxyl radicals (Eq. 2.3).

$$H_2O + M \rightarrow M(^{\bullet}OH)_{ads} + H^+ + e^- \quad (2.3)$$

These electro-generated hydroxyl radicals, that represent the "activated state" of water in O-transfer reactions, are then involved in the mineralization of organic pollutants R (present in an aqueous solution) (Eq. 2.4):

$$R_{(aq)} + xM(^{\bullet}OH)_{ads} \rightarrow xM + \text{Mineralization products} + yH^+ + ye^- \quad (2.4)$$

where x and y are the stoichiometric coefficients.

This reaction (Eq. 2.4) is in competition with the side reaction of the anodic discharge of these radicals to dioxygen (Eq. 2.5), diminishing the current efficiency.

$$M(^{\bullet}OH)_{ads} \rightarrow M + \tfrac{1}{2}\ O_2 + H^+ + e^- \quad (2.5)$$

Thus, for the direct oxidation, beside the properties above mentioned (see par. 2.1), the most important request for a suitable anode is the high oxygen over-potential or catalytic activity for the requisite anodic O-transfer mechanism.
Several authors have employed the direct anodic oxidation process in their study on the electrochemical incineration of organic pollutants. In particular, phenol and derivates, likewise the carboxylic acids, their main intermediates, are the mostly investigated examples of the electrochemical studies (Cañizares et al., 2002, 2003, 2004a, 2004b; Chatzisymeon et al., 2010; Gandini et al., 2000; Martinez-Huitle et al., 2004a, 2005a; Panizza et al., 2001). Generally, a complete oxidation of these substances was achieved even if at optimum operative conditions.
Other applications have been researched for direct anodic oxidation involving sugars, alcohols, distillery effluents, dyes, aromatics and many other compounds (Jüttner et al., 2000).

2.2.2 INDIRECT OXIDATION MECHANISM

The electro-oxidation of pollutants can be performed through indirect oxidation, with the involvment of oxidants that can be added or electrochemically generated at the electrodes. The most known are the peroxide, Fenton's reagent, peroxidisulphate, besides chlorine, hypochlorite and ozone. These oxidants react with the organic substrates, eventually leading to their complete conversion to carbon dioxide or other innocuous components.
In particular, most of these compounds can be produced directly in the electrochemical assay trough oxidation or reduction processes. In this case, some specie present in the electrolytic solution are reduced or oxidized with the formation of oxidants which then oxidize the organic pollutants in the bulk of the solution (Fig. 2.1).
The most used electrochemical oxidant are by far chlorine and/or hypochlorite, (depending on the pH of the media), due to their quite effective action. In most cases they could be anodically generated in the presence of chlorides ions in the electrolytic solution (Martinez-Huitle et al., 2006). In this example of indirect process, the possible formation of chlorinated organic intermediates or final

products could represents a possible limitation for the real application of this technique.

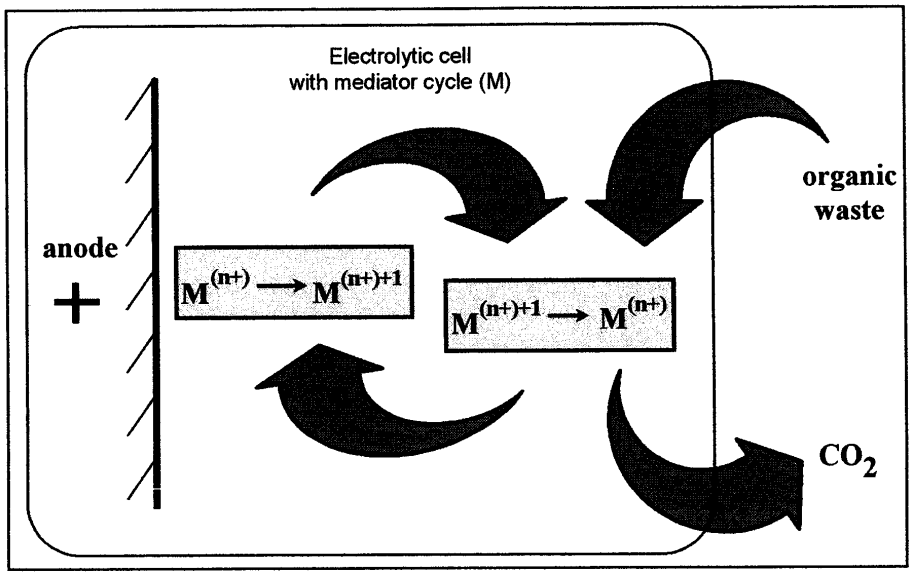

Fig. 2.1 *Principle of the mediated electrochemical oxidation process*

In particular, a whole paragraph will be dedicated more specifically to the influence of the presence of NaCl in the electrolytic solution on the electrochemical incineration process (see par. 2.4.7).

As far as other chemicals agents are concerned, other two oxidants can be enounced among those more diffused, able to degraded several pollutants, i.e. electrochemically generated hydrogen peroxide and electrically generated ozone.

2.3 INFLUENCE OF THE ANODIC MATERIAL

The effectiveness of the electrochemical incineration depends on many factors, but the nature of the electrodic material is by far the most important parameter because it strongly influences both the selectivity and the efficiency of the process.

In order to discover an anode material with high stability and high activity towards organic oxidation, several electrodes have been tested, but some of them

demonstrated a rapid loss of activity due to surface fouling (as for the glassy carbon), others gave only selective oxidation (as for the IrO_2), others showed a limited service life (as for the SnO_2). (Panizza and Cerisola, 2005). Moreover, although PbO_2 is a good anodic material for the detection of organic pollutants, its application in the water treatment may be limited by the risk of lead contamination, due to its dissolution under specific anodic polarization and solution composition (Murugananthan et al., 2007).

In particular, these conventional electrodes are already used for anodic oxidation even if they led to quite poor mineralization rates.

On the contrary, one of the most promising anodic material is the synthetic boron-doped diamond, characterized by a high anodic stability and a wide potential window for water discharge. It has undoubtedly proved to be an excellent material for the complete combustion of organics in wastewater treatment and water disinfection (Cañizares et al., 2004b; Kapalka et al., 2008; Panizza and Cerisola, 2005). This table shows that the oxidation potential of the anode (which corresponds to the onset potential of oxygen evolution) is directly related to the over-potential for oxygen evolution and to the adsorption enthalpy of hydroxyl radicals on the anode surface i.e. for a given anode material the higher the O_2 overvoltage the higher its oxidation power. A low oxidation power anode is characterized by a strong electrode-hydroxyl radical interaction resulting in a high electrochemical activity for the oxygen evolution reaction (low overvoltage anode) and to a low chemical reactivity for organic oxidation (low current efficiency for organics oxidation). These anodes are called “active” electrodes and a typical example are the iridium based anodes (see Table 2.1).

In contrast to this low oxidation power anode, the high oxidation power anode is characterized by a weak electrode hydroxyl radical interaction resulting in a low electrochemical activity for the oxygen evolution reaction (high overvoltage anode) and to a high chemical reactivity for organics oxidation (high current efficiency for organic oxidation). These anodes are called “nonactive” electrodes and a typical example is the boron doped diamond (BDD) anode (see Table 2.1).

Table 2.1 *Oxidation power of the anode material used in the electrochemical mineralization process in acid media (Kapalka et al., 2008)*

Electrode	Oxidation potential / V	Overpotential of O_2 evolution / V	Adsorption enthalpy of M-OH	Oxidation power of the anode
RuO_2-TiO_2 (DSA-Cl_2)	1.4-1.7	0.18	Chemisorption of OH radical	
IrO_2-Ta_2O_5 (DSA-O_2)	1.5-1.8	0.25		
Ti/Pt	1.7-1.9	0.3		
Ti/PbO_2	1.8-2.0	0.5		
Ti/SnO_2-Sb_2O_5	1.9-2.2	0.7		
p-Si/BDD	2.2-2.6	1.3	Physisorption of OH radical	

Interestingly, many studies are conducted on the influence of the nature of the anode, in particular comparing the performances of BDD and DSA anodes. Let us consider, in particular, the case of carboxylic acids, and of BDD and iridum anodes which are of particular interest for the objectives of this thesis.

The group of research of Prof. De Battisti (Ferro et al., 2010; Martinez-Huitle et al., 2004a) have carried out some cyclovoltammetries on the electroxidation of oxalic acid on Ti/IrO_2-Ta_2O_5. They observed that the addition of the organic substrate had no significant effect on the shape of the curves, with the exception of a quite modest increase in currents in the oxygen evolution potential range (E > 1.15V) at high concentrations. This behavior could be due to a weak interaction between the organic substrate and the oxide metal, leading to a preferential interaction between active sites and hydroxyl radicals rather than oxalic acid adsorption as well.

On the contrary, the experiments performed at BDD demonstrated that oxalic acid is electroactive on this anode and its oxidation takes place about 0.1 V before oxygen evolution reaction. Hence, oxalic acid oxidation can take place even without involvement of the adsorbed hydroxyl radicals.

Furthermore, these authors performed some electrolyses confirming the different performances of the anodes considered: a complete elimination of the organic reagent has been achieved at BDD electrodes, while only a minor attack takes place at the IrO_2 anode.

Analogue results were achieved by Martinez-Huitle et al. (2004b) who conducted similar studies for the electrochemical oxidation of chloranilic acid (CAA). At the Ti/IrO_2 electrode, they observed a slower CAA electro-oxidation, as indicated by residual COD values that are very close to the initial one. Indeed, in the second case, a complete elimination of CAA from the electrolyzed solution requires only about 4 $Ahdm^{-3}$ at 6.3 and 12.5 $mAcm^{-2}$, thus clearly showing the effectiveness of the BDD electrode for the anodic mineralization of organic pollutants. Similar results were obtained for a very large number of organics, thus confirming the crucial role of the anode material on the elimination of organic compounds, BDD being the electrode at which the best incineration efficiency has usually been attained.

In order to better understand the different performances of the two electrodes considered in our discussion, let us focus on their properties and on the interpretative models elaborated by some groups of research on the respective principles of electrochemical oxidation process of organics.

2.3.1 IRIDIUM BASED ANODES

As before specified, a typical low oxidation power anode is the IrO_2 based electrode.

It has been demonstrated, using differential electrochemical mass spectrometry (DEMS) (Kapalka et al., 2008), that the interaction between IrO_2 and hydroxyl radical at this electrode is so strong that a higher oxidation state oxide IrO_3 can be formed. This higher oxide can act as mediator for both organics oxidation and oxygen evolution.

Furthermore, IrO_2 based anodes, and in particular the binary system IrO_2 –Ta_2O_5, are reported to exhibit good anodic stability and electrocatalytic activity towards the oxygen evolution and are, actually, one of the most adopted catalyst for oxygen evolution in industrial electroplating processes (Morimtsu et al., 2000).

On the other hand, these anodes are reported to give rise only to selective oxidation of organics (Comninellis, 1994; Simond et al., 1997), thus strongly limiting the possible utilization of these materials for electrochemical incineration processes.

A generalized scheme of the electrochemical incineration of organics on oxide anode (MO_x) is shown in Fig. 2.2 (Comninellis, 1994; Simond et al., 1997).

In the first step (Eq. 2.6), water is discharged at the anode producing adsorbed hydroxyl radicals:

$$MO_x + H_2O \rightarrow MO_x(^{\bullet}OH) + H^+ + e^- \quad (2.6)$$

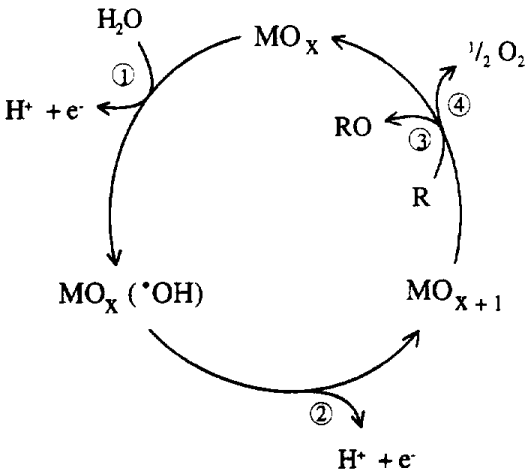

Fig. 2.2 *Schematic representation of the electrochemical oxidation of organics on oxide anodes (MO_x)forming the higher oxide (MO_{x+1}). ①water discharge; ② higher oxide formation; ③organics oxidation; ④oxygen evolution (Simond et al., 1997).*

In the second step (Eq. 2.7) the adsorbed hydroxyl radicals may interact with the oxygen already present in the oxide anode with possible transition of oxygen from

the adsorbed hydroxyl radical to the lattice of the anode, leading to the formation of the active species (MO_{x+1}), called higher oxide.

$$MO_x(^{\bullet}OH) \rightarrow MO_{x+1} + H^+ + e^- \quad (2.7)$$

This species is considered responsible for both organics oxidation (Eq. 2.8) and oxygen evolution (Eq. 2.9). Thus, there is a competition between these two reactions that give rise to the regeneration of the metal oxide MO_x

$$MO_{x+1} + R \rightarrow MO_x + RO \quad (2.8)$$

$$MO_{x+1} \rightarrow MO_x + \tfrac{1}{2} O_2 \quad (2.9)$$

Moreover, Comninellis (1994) speculated that the "active oxygen" present in the specie $MO_x(^{\bullet}OH)$ is physically adsorbed and it should cause predominantly the complete incineration of organics (Eq. 2.10), in the presence of oxidizable organics, while the "active oxygen" present in MO_{x+1} is chemically adsorbed and participates in the formation of selective oxidation products (Eq. 2.8).

$$R + MO_x(^{\bullet}OH)_z \rightarrow CO_2 + zH^+ + ze^- + MO_x \quad (2.10)$$

2.3.2 BORON DOPED DIAMOND (BDD) ANODES

Owing to its extraordinary chemical stability, diamond undoubtedly is a promising candidate as electrode material. However, unlike other carbonaceous materials which have found practical use (graphite, glassy carbon, pyrolytic graphite, carbon fiber, etc.) for a long time, the electrochemical studies of diamond were started relatively late, approximately twenty three years ago (Pleskov, 2002).

Initially, such studies were essentially impeded by two factors: first, diamond remained an exotic, hardly accessible material, whose preparation required very high temperature and pressure, and second, diamond is an insulator, it does not conduct electric current and is therefore inapplicable as an electrode material as it is.

The situation changed basically upon invention of an improved technology for fabricating thin diamond films from a gas phase under subatmospheric pressure.

Effective methods for growing polycrystalline diamond films on diamond and non-diamond substrates were developed. These films undoubtedly will be not very much expensive if produced on a large scale.

Additionally, to impart conduction to diamond films, they are doped during their growth with an acceptor impurity (boron); thus a *p*-type semiconductor material is obtained.

These first studies of diamond electrodes opened a new area in the electrochemistry of semiconductors: the electrochemistry of diamond.

Hence, highly boron-doped diamond exhibits several technologically important properties that distinguish it from conventional electrodes, such as (Panizza and Cerisola, 2005):

- An extremely wide potential window in aqueous and non-aqueous electrolytes: in the case of high-quality diamond, hydrogen evolution commences at about −1.25V versus SHE and oxygen evolution at +2.3V versus SHE, then the potential window may exceed 3V. The width of the window decreases with the quality of the film and with the incorporation of non-diamond sp^2 carbon impurities its response resembles that obtained from glassy carbon and highly oriented pyrolytic graphite;
- Corrosion stability in very aggressive media: the morphology of diamond electrodes is stable during long-term cycling from hydrogen to oxygen evolution even in acidic fluoride media;
- An inert surface with low adsorption properties and a strong tendency to resist to deactivation: the voltammetric response towards ferri/ferrocyanide is remarkably stable for up to 2 weeks of continuous potential cycling;
- Very low double-layer capacitance and background current: the diamond-electrolyte interface is ideally polarizable and the current between −1000 and +1000mV versus SCE is < 50 A/cm^2. The double-layer capacitance is up to one order of magnitude lower than that of glassy carbon.

Depending on the applied potential, the oxidation of organics at BDD electrodes can follow two mechanisms: direct electron transfer in the potential region before oxygen evolution (water stability), and indirect oxidation via electro-generated hydroxyl radicals, in the potential region of oxygen evolution (water decomposition) (Panizza and Cerisola, 2005).

It has been shown that only reactions involving simple electron transfer processes are active on diamond electrodes in the potential region of water stability. For reactions with more complex mechanism, oxidation can take place on diamond electrodes only in the potential region of supporting electrolyte or/and water discharge (Gandini et al., 2000; Iniesta et al., 2001).

Canizares et al. (2003) reported some ciclovoltammetric studies conducted on different carboxylic acids where an anodic current peak is observed at about 2.3V versus SCE, close to the water decomposition region. They showed that this peak often overlapped with oxygen evolution and that the current density increased with carboxylic acid concentration, thus suggesting the possible existence of a direct electrochemical reaction involving oxidation of the carboxylic acids.

In fact, some authors have observed that the onset potential of oxygen evolution reaction on BDD surface is about 2.3 V, potential at which is thermodynamically possible to form hydroxyl radicals (Kaplaka et al., 2009). The presence of electrogenerated hydroxyl radicals on BDD surface was detected by means of spin-trapping (Kapalka et al., 2008).

Moreover, it has been reported that the BDD-hydroxyl radical interaction is so weak (no free p or d orbitals on BDD) that the $^{\bullet}OH$ can even be considered as quasi free (Kapalka et al., 2008). In fact, the boron-doped diamond based anode (BDD) is a typical high oxidation power anode and it is classified as a “non-active” electrode.

The reason of this weak interaction can be ascribed to the surface of BDD, consisting of sp^3 carbon, responsible of its excellent chemical stability. Hence, this type of stable surface might not favor adsorption or accumulation of polar molecules, due to a lack of adsorption sites (Zhi et al., 2003).

2.3.2.1 KINETIC MODELS

Kapalka et al. (2008) have proposed the following reactions scheme for the mechanism of electrochemical mineralization of organics on BDD anodes.

Water is firstly discharged at the BDD anode producing free or weakly adsorbed hydroxyl radicals (Eq. 2.11). These species are the intermediated for both the main

reaction of organics oxidation (Eq. 2.12) and the side reaction of oxygen evolution (Eq. 2.13).

$$H_2O + BDD \rightarrow BDD(^{\bullet}OH)_{ads} + H^+ + e^- \quad (2.11)$$

$$R + xBDD(^{\bullet}OH) \rightarrow xBDD + \text{Mineralization products} + yH^+ + ye^- \quad (2.12)$$

$$BDD(^{\bullet}OH) \rightarrow BDD + \tfrac{1}{2} O_2 + H^+ + e^- \quad (2.13)$$

When the rate of the mass transfer of the pollutant is dramatically lower than that of its anodic oxidation, the concentration of the pollutant at the anodic surface/reaction layer C^0 is close to zero and the oxidation process is under mass transfer control. This case arises, for an oxidation process that proceeds up to the total oxidation of the organic pollutant, when the limiting current density $i_{lim} = nFk_m[RH]^b << i_{app} ICE^{OC}$ (where n is the number of electrons exchanged for the anodic oxidation of *RH* to carbon dioxide, F the Faraday constant (96487 C mol^{-1}), $[RH]^b$ and k_m the bulk concentration and the mass transfer coefficient of the organic *RH*, respectively, i_{app} the applied current density and ICE^{OC} the instantaneous current efficiency for the oxidation of *RH* under oxidation reaction control under adopted operative conditions).

Conversely, when $i_{lim} >> i_{app} ICE^{OC}$, mass transfer is significantly faster with respect to oxidation rate, C^0 is very close to the concentration in the bulk C^b and the process is under reaction oxidation control. When more pollutants are present in the bulk during the electrolysis, one can focus on the chemical oxygen demand *COD* of the solution. In particular, the limiting current density, for a process that proceed up to the total oxidation of organics, is given by $i_{lim} = 4Fk_mCOD$ and a mass transfer control will arise if $i_{lim} << i_{app} ICE^{OC}$ (where ICE^{OC} is the average current efficiency for a process under oxidation reaction control and *COD* the chemical oxygen demand computed on a molar base).

The theoretical works of Comninellis and co-authors

Comninellis and co-authors observed that the oxidation of many organics proceeds at BDD, under usually adopted operative conditions, towards the complete incineration with very high current efficiency if no mass transfer limitations arise

(Iniesta et al., 2001; Panizza et al., 2001; Rodrigo et al., 2001). On the bases of these results, the authors developed a very simple kinetic model for a batch recirculation system with galvanostatic alimentation based on the assumption that when the oxidation of organics is performed at BDD at high anodic potentials, close to oxygen evolution, the electrochemical incineration of the organic compound is a fast reaction and it is controlled by mass transport towards the anode. Particularly, authors assumed that:

- The reservoir volume (*V*) is much greater than that of the electrochemical reactor
- The electrochemical reactor and the reservoir are perfectly mixed.
- The oxidation in the bulk by electrogenerated oxidants is not considered.

The limiting current density for the electrochemical mineralization of an organic compound under given hydrodynamic conditions can be written as (Eq. 2.14):

$$i_{lim} = 4Fk_mCOD \qquad (2.14)$$

where i_{lim} is the limiting current density for organics mineralization (A m^{-2}), 4 is the number of electrons involved for one mole of O_2, k_m is the mass transport coefficient (m s^{-1}), F is the Faraday constant (C mol^{-1}) and COD is the chemical oxygen demand ($molO_2$ m^{-3}).

- for $i_{appl} < i_{lim}$ the concentration of organic is sufficiently high and the electrolysis is under current limited control, the current efficiency is 100% and the rate of COD removal decreases linearly;
- for $i_{appl} > i_{lim}$ the electrolysis is controlled by the mass transport control and the instantaneous current efficiency (ICE) decreases since secondary reactions, such as oxygen evolution, commence. In this regime the trend of COD versus charge passed is exponential because of mass transport limitation.

The equations that describe the trend of COD and ICE (instantaneous current efficiency) in the two regimes are:

- for $i_{appl} < i_{lim}$ $\quad ICE = 1 \qquad (2.15)$

$$COD(t) = COD° \left(1 - \frac{Akm\alpha}{Vr} t\right) \qquad (2.16)$$

- for $i_{appl} > i_{lim}$ $$ICE = \exp\left(-\frac{Akm}{Vr}t + \frac{1-\alpha}{\alpha}\right) \quad (2.17)$$

$$COD(t) = \alpha COD^{\circ} \exp\left(-\frac{Akm\alpha}{Vr}t + \frac{1-\alpha}{\alpha}\right) \quad (2.18)$$

where:

- COD° is the initial chimical oxygen demand (mol O_2/m^3);
- V_r is the reaction volume (m^3);
- k_m is the mass transport coefficient (m/s);
- A is the electrode area (m^2);
- $\alpha = i_{appl} / i^{\circ}_{lim.}$

As shown in Fig. 2.3, this model can predict very satisfactory the trend of COD and of ICE for all the applied operative conditions.

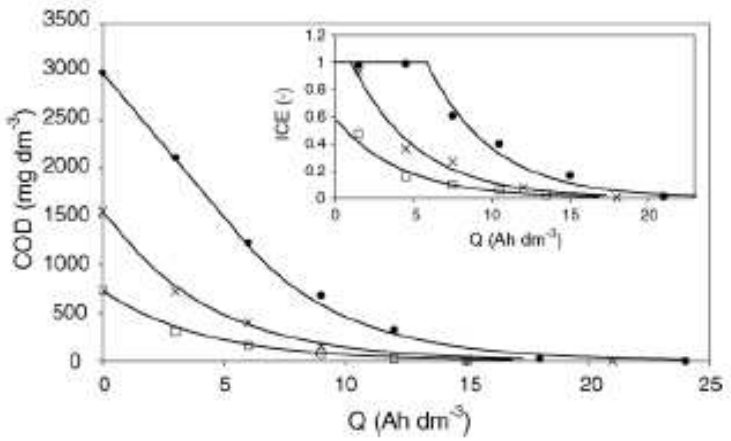

Fig. 2.3 *Influence of 4-chlorophenol (4-CP) concentration on the trends of COD and ICE (inset) during electrolysis on BDD anode. (□) 3.9 mM 4-CP ; (×) 7.8 mM 4-CP;and (●) 15.6 mM 4-CP. Electrolyte 1 M sulphuric acid, T = 25°C; i = 30 mA/cm². (—)Represents model prediction (Rodrigo et al., 2001).*

The same group of research have proposed a simple model for the oxidation of water on BDD surface (Michaud et al., 2003), performing some experiments with aqueous

solutions 1 M of sulphuric and perchloric acids. They observed the formation of peroxidisulfuric acid in the first case and of oxygen in the second case, besides ozone and hydrogen peroxide in both the cases.
The model proposed is shown in Fig. 2.4.

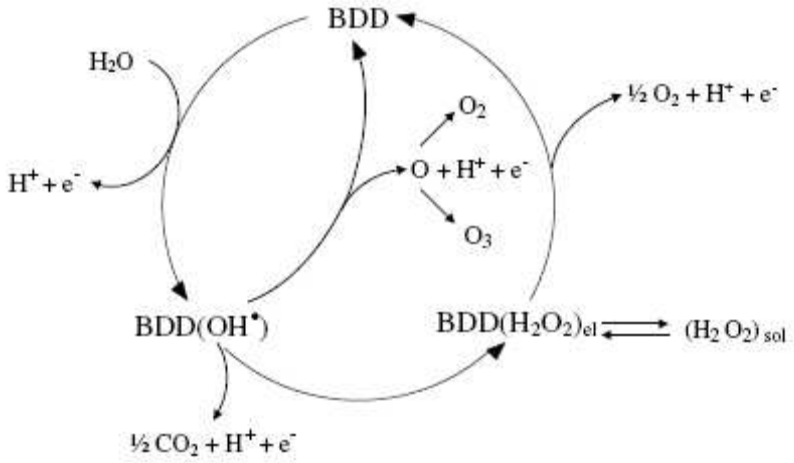

Fig. 2.4 *Scheme of the proposed mechanism for water oxidation on BDD electrode in acidic solution containing a non electroactive supporting electrolyte ($HClO_4$) (Michaud et al., 2003).*

According to this model, the first step is water discharge on BDD with the formation of hydroxyl radicals. Then, the electrogenerated hydroxyl radicals can be involved in four parallel reactions:

(i) Oxidation of supporting electrolyte: in the case of H_2SO_4 supporting electrolyte, electrogenerated hydroxyl radicals react with sulphuric acid giving peroxodisulphfuric acid:

$$2\ H_2SO_4 + 2(^{\bullet}OH)_{ads} \rightarrow H_2SO_8 + 2\ H_2O \qquad (2.19)$$

(ii) H_2O_2 formation: mainly in the solution containing $HClO_4$:

$$2\ ^{\bullet}OH \rightarrow H_2O_2 \qquad (2.20)$$

Then, it can diffuse through the bulk solution or it can be transformed into oxygen;

(iii) O_3 production:

$$^{\bullet}OH \rightarrow {}^{\bullet}O + H^+ + e^- \quad (2.21)$$

$$^{\bullet}O + O_2 \rightarrow O_3 \quad (2.22)$$

considering that atomic oxygen can be also evolved in oxygen:

$$2\,{}^{\bullet}O \rightarrow O_2 \quad (2.23)$$

(iv) BDD corrosion: another possible reaction pathway for the electrogenerated hydroxyl radicals is the combustion of BDD to CO_2 during the anodic polarization at high current density:

$$C_{BDD} + 2\,{}^{\bullet}OH \rightarrow CO_2 + 2H^+ + 2e^- \quad (2.24)$$

The theoretical works of Cañizares and co-authors

To describe the electrochemical oxidation of organics aqueous wastes, the group of research of Prof. Cañizares (2002, 2003) proposed a cell model which relies upon the existence of two zones in the electrochemical reactor (Fig. 2.5):

- a first zone close to the anode surface with a thickness equivalent to the Nernst diffusion layer (reaction zone), where electrochemical and fast mediated oxidation processes take place;
- the remaining reactor volume (bulk zone), where slow mediated oxidation reactions can occur.

In both zones, the concentration of every compound is considered to be constant with position and only time-dependent. Mass transport processes between both zones were quantified by assuming that the local rate of exchange is proportional to the concentration difference in the two zones.

This description allows one to simplify significantly the mathematical complexity of the reaction system and can yield, together with an appropriate kinetic model, good agreements between experimental and simulation results.

Experimentally, inorganic oxidants were not found in the system although their presence was confirmed by the increase in the organic oxidation rate observed in sulfuric acid media. This fact indicates that these compounds must react rapidly with carboxylic acids to form carbon dioxide or oxygen (side reaction), with both

reactions developing mainly in the reaction zone, because the concentration of oxidants is higher in this region. In this zone, the nature of the oxidation process cannot be identified because there is no possibility of discerning whether the oxidation of a carboxylic acid is performed directly on the electrode surface or by an inorganic oxidant.

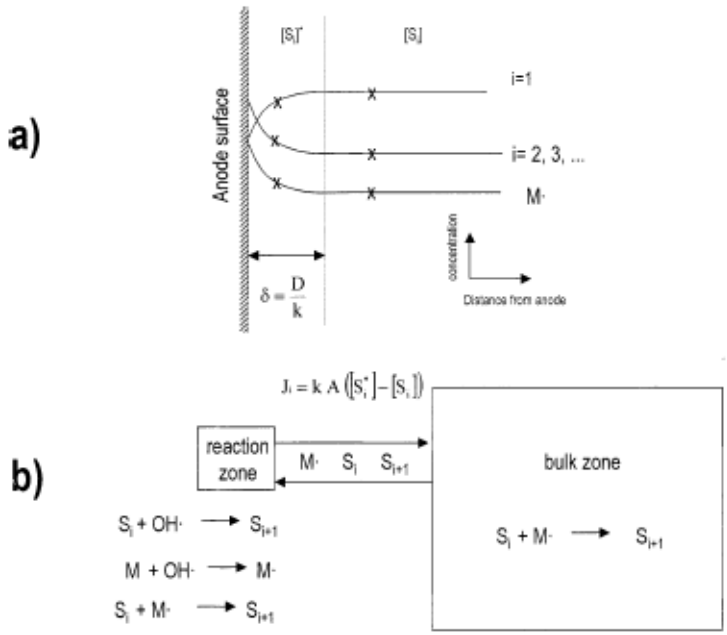

Fig. 2.5 *Sketch of the model for process characterization: [Si], concentration of compound Si; M/M•, redox couple of an inorganic reagent;×, average concentration of each organic compound in the two zones (Cañizares et al., 2003).*

For this reason, kinetic expression (Eq. 2.25) is proposed to model the oxidation process, where k_{ox} (the maximum oxidation rate) is multiplied by ICE to take into account the oxidants that attack organic matter under total diffusion control and by the adjustable parameter σ to determine the effectiveness of the oxidation.

$$r = k_{ox}(ICE)\sigma \qquad (2.25)$$

Parameter k_{ox} is assumed to include the oxidation carried out directly by the electrode surface and those performed by indirect electroreagents. Its value can be

estimated from the current intensity *I* (Cs^{-1}) and the Faraday constant *F* (96 485 C mol^{-1}) using Eq. (2.26).

$$k_{ox} = I/F \quad (2.26)$$

The ICE can be calculated from the following equations:

$$ICE = 1 \quad \text{se } I < I_{lim} \quad (2.27)$$

$$ICE = [S_1]/ [S_1]_{lim} \quad \text{se } I > I_{lim} \quad (2.28)$$

Hence, it is assumed equal to unity under charge transfer control, while it is proportional to 1 the concentration of organics under mass transport control. Parameter σ depends on the waste composition and on the operation conditions.

Oxidation reactions in the bulk zone can only occur for large excesses of electrogenerated inorganic oxidants in comparison to the carboxylic acid concentration. The rate of this reaction must be low because such oxidizing species are present in very low concentrations. A first-order kinetic model was assumed (Eq. 2.29) in order to quantify their effect.

$$r = K_b[S_1] \quad (2.29)$$

In this kinetic model, it is clear that the reaction rate in the bulk zone $\sigma < 1$, $K_b = 0$, than reaction rate is equal to zero. Thus, it does mean that all inorganic oxidants react in the reaction zone and therefore cannot reach the bulk zone.

By using the mass transport and kinetics expressions proposed, they obtained and resolved a system of differential equations leading them to a mathematical model, that have permitted to obtain a good agreement between the model and the experimental data, as shown in the next figure.

The theoretical works of Polcaro and co-authors

Polcaro and co-authors reported a more complex model with the aim of evaluating the trends of the concentrations of the starting pollutant and intermediate products in the stagnant layer and in the bulk (Polcaro et al., 2003). Thus, it has been shown that the incineration of some organics at BDD proceeds trough the formation of some intermediates. As an example, the oxidation of phenol can be represented by the following schematic reaction path:

Phenol → Cyclic intermediates → Aliphatic acids → CO_2

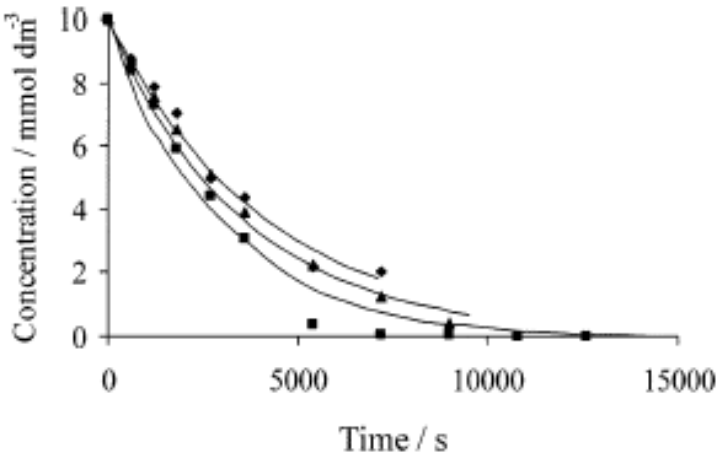

Fig. 2.6 *Results obtained [simulation (line) versus experimental (points) data] for three experimental runs: ◆, formic acid; ▲,oxalic acid; ■, maleic acid. Experimental conditions: n^0, 10 mmoldm^{-3}; T, 20 °C; j, 30 mA cm^{-2}; supporting medium, H_2SO_4/Na_2SO_4 (Cañizares et al., 2003).*

Furthermore, this model applies also to the case of an oxidation process that gives rise to a current efficiency lower than 100% in the absence of mass transfer limitations. The model was based on the following assumptions:

- Oxidation of pollutants and intermediate compounds takes place by homogeneous chemical reaction with hydroxyl radicals (with first order kinetic with respect to both organics and hydroxyl radicals concentrations) in the diffusion layer in competition with the chemical deactivation of hydroxyl radicals which is described by a first order kinetic reaction not depending on the working potential;
- A diffusion-reaction model is used to model the diffusion layer while the bulk of the solution is represented by a stirred-tank reactor.

By a numerical solution of pertaining equations (mass balance equations in the bulk and in the stagnant layer for the starting pollutant and intermediates and in the diffusion layer for hydroxyl radicals), authors were able to predict the trend with

time of the different compounds present in the bulk of the solution during the electrolyses, as well as the evolution of the space profile of the species.
As an example, authors used their model to predict with a good accuracy, for the oxidation of phenol, the trend with time of the concentrations of phenol and main intermediates (aromatic and aliphatic acids) by changing significantly the current density and the flow dynamic regime and using only one adjustable parameter (the average kinetic constant between hydroxyl radicals and aromatic compounds) (Polcaro et al., 2003). A good agreement between theoretical predictions and experimental data was reported by the authors also in the cases of cyanuric acid and atrazine by using in this case, as an adjustable parameter, the kinetic constant between hydroxyl radicals and the adopted pollutant (Polcaro et al., 2003). As above mentioned, the model involved also the calculation of the concentration profiles in the diffusion layer of hydroxyl radicals, pollutants and intermediates with the time. Quite interestingly, according to this model, hydroxyl radicals diffuse in the stagnant layer for few tens of nanometers in agreement with literature.

2.4 INFLUENCE OF SOME OPERATIVE PARAMETERS ON THE ELECTROCHEMICAL INCINERATION PROCESS

Numerous authors have studied the effect of numerous operative parameters, such as the nature of the supporting electrolyte, pH, current density and flow rate, temperature, nature of the organic substrate and presence of sodium chloride in the electrolytic solution, on the performances of the electrochemical incineration processes. In the following we will focus on the studies performed at BDD and/or Iridium anodes. Studies on the abatement of carboxylic acids will be, in particular, reviewed with a more detail.

2.4.1 SUPPORTING ELECTROLYTE

Various authors have studied the effect of the supporting electrolyte on the electrochemical oxidation of organics.
Cañizares et al. (2003) have performed a set of experiments in order to study the effect of supporting electrolyte on the anodic oxidation at diamond anodes of three

carboxylic acids, namely formic, oxalic and maleic acids. The average composition of the wastewater used in the experiments was 10 mmol dm^{-3} of carboxylic acid, 5000 mg of Na_2SO_4 dm^{-3} and H_2SO_4 (pH of 2). In order to determine the influence of supporting media, an experiment using Na_3PO_4/H_3PO_4 media was also carried out.
Authors observed a higher degradation rate in media containing sulfate ions probably due to the generation of peroxodisulfate (Eq. 2.30), a powerful oxidizing agent that can oxidize organic substrates.

$$2\ H_2SO_4 \rightarrow H_2S_2O_8 + 2e^- + 2H^+ \qquad (2.30)$$

Interestingly, this effect was marked for formic acid and very small for oxalic acid.
Same authors have reported the effect of supporting electrolyte also for the anodic oxidation of three chlorophenols, namely 4-chlorophenol, 2,4-dichlorophenol and 2,4,6-trichlorophenol (Cañizares et al., 2004a). Even in this case, they observed that the oxidation rate was higher in media containing sulphates than in media containing phosphates.
Analogue conclusions are achieved by Murugananthan et al. (2007) who compared the effect of sulfate and nitrate ions in the electrolytic solution on the electrochemical degradation of 17ß-estradiol (E2) at BDD thin film electrode. They detected a poorer degradation efficiency, and a request of three-fold higher electrolysis time to attain about 75% degradation, in the case of medium containing NO_3^- than in the medium containing SO_4^{2-} ion.
Quite different results were obtained by Michaud et al. (2003) when they performed some polarization curves at Si/BDD in 1 M $HClO_4$ and 1 M H_2SO_4 at a scan rate of 100 mV s^- They observed very similar current-potential curves in perchloric acid and sulphuric acid media, although the reactions that take place are different: in l M $HClO_4$ the main reaction is oxygen evolution, while in H_2SO_4 the main reaction is the formation of $H_2S_2O_8$.

2.4.2 pH

The effect of pH on the electrochemical incineration of organics has been investigated by many authors. Results are often contradictory, thus probably

showing that the effect of this parameter strongly depends on the nature of the investigated organics and of the electrodes.

In particular, several authors have studied the influence of pH at BDD anode obtaining very different results.

Murugananthan et al. (2007) analyzing the degradation of 17β-estradiol, at different values of pH, precisely 2, 4, 6, 8 and 10, observed that the rate of degradation was highly depended on initial pH of the electrolyte and enhanced in alkaline conditions. In particular, a very rapid 100% degradation was accomplished within a very short period of 7.5 min at pH 10.

A very different result was achieved by Flox et al. (2005) who found a higher mineralization rate for 4,6-dinitro-*o*-cresol in acid medium by anodic oxidation at BDD. They related this result to a faster reaction of intermediates formed under these conditions with $^{\bullet}OH$ produced on the anode surface.

Interestingly, concerning carboxylic acids, Martinez-Huitle et al. (2005b) observed that low pH favours the incineration of OA at platinum anode with respect to high ones.

A more complicated scenario was shown by Polcaro et al. (2005), which in their study on the electrochemical oxidation of triazines, observed a very complex dependence of this process on pH. In particular, higher abatements were evaluated when the pH increased from 1 to 7, than worse results were obtained increasing the pH until 12. They found a possible explanation of this result in a variation of reactivity with pH of either the organic compound or $^{\bullet}OH$ radicals. In particular, the oxidative potential of the latter decreases as pH increases while the reactivity of the organic compound increases with pH, thus the global trend of reaction rate may result as a combination of these two contrasting effects.

Interestingly, Cañizares et al. (2004b) observed different results depending on the nature of the substrate. In particular they showed that incineration of chlorophenols depends on the pH, alkaline pH favoring the accumulation of carboxylic acid intermediates and in particular of oxalic acid. In fact, they observed that the initial oxidation rate was higher in alkaline media, while, as the galvanostatic electrolysis goes on, the oxidation rate in acidic media surpasses those in the alkaline media.

Furthermore, in the presence of 10 mM of formic, oxalic and maleic acids in water (5000 mg Na_2SO_4 dm^{-3}; T = 25°C; i = 30 $mAcm^{-2}$), they observed a lower mineralization rate at pH 12, mainly for the maleic acid case. Thus, the larger amounts of aliphatic acids generated at alkaline pH were a result of the slower oxidation rate for these compounds.

Nevertheless, when they used polyhydroxybenzenes as substrates (Cañizares et al., 2004b), they observed that the global oxidation rate of the electrochemical treatment does not depend on the pH, at least in the experimental conditions studied. In fact, a complete mineralization of organic waste was obtained both at pH 2 and 12.

2.4.3 FLOW RATE AND CURRENT DENSITY

From a theoretical point of view, when the process is under mass transport control regime, the flow dynamic conditions, imposed by the flow rate, are expected to affect the mass transfer coefficient and as a consequence the abatement of the organics. Furthermore, under mass transfer control, the oxidation rate is not controlled by applied current density, thus higher current densities does not affect the abatement of the organic for a given time but results in lower current efficiencies. Conversely, when the process is under reaction oxidation control, the flow dynamic conditions are not expected to affect the abatement of the organics while a higher current density should determine lower times of treatment (Scialdone et al., 2010).

Many authors have performed some experiments in electrochemical flow cell, thus in order to study the influence of flow rate on the electrochemical oxidation of organics.

In particular, Martinez-Huitle et al. (2005a) have found that the anodic oxidation of oxalic acid at BDD at a fixed current density of 10 mA/cm^2 is enhanced upon increasing the flow rate.

Furthermore, different research groups have investigated the effect of current density at fixed hydrodynamics conditions.

Gandini et al. (2000), studying the influence of applied current density on the electrochemical oxidation of acetic acid, have found that a decrease in the current density (from 90 to 30 mA/cm^2) influences the process resulting in higher faradic efficiency only when an high degree of conversion was achieved. In particular they observed that, depending on the degree of oxidation, two regions can be distinguished:

1. at low degree of conversion ($Q < 20$ $Ahdm^{-3}$), thus under charge transfer control, the oxidation rate of acetic acid is not influenced by the current density within the domain investigated;
2. at high degree of conversion ($Q > 25$ Ah dm^{-3}), thus under mass transport control, the oxidation rate of acetic acid decrease with increasing current density.

This behaviour is due to the fact that at high degree of conversion the oxidation rate is diffusion controlled and consequently the current efficiency decreases with the applied current density.

Interestingly, opposite results, but very similar considerations were reported by Cañizares et al. (2004b) when they conducted some electrolyses using polyhydroxybenzenes as substrates. In particular, they observed that the oxidation rate of these substances increases with the current density, altough this increase is not proportional in the whole range of COD. In fact, they explained taht at high COD values the process is kinetically controlled, thus the increase in the oxidation rate is proportional to the increase in current density, while and mass transport controls at low values of COD.

Similary, Brillas et al. (2005) detected an increase in removed TOC with increasing of the current, when some electrolyses with paracetamol as substrate were performed at BDD. They related this result to a concomitant generation of more $^{\bullet}OH$ on the anode surface.

For what concerning the electrochemical oxidation of oxalic acid at BDD, very different results were obtained. Indeed, while Martinez-Huitle et al. (2004a) have found that a dramatic improvement of the incineration efficiency occurs by decreasing the current density from 60 to 10 mA/cm^2, Cañizares et al. (2003)

observed that an increase of current density from 30 to 60 mA/cm^2 leads to a very slight improvement of the performances.

Evidently, these strong observed differences are likely to arise from the fact that different operative conditions were used in these investigations.

Interestingly, for what concern the case of electrochemical oxidation of oxalic acid at IrO_2-Ta_2O_5, Martinez-Huitle et al. (2004a) have found that higher current densities give rise to lower abatement of oxalic acid, as in the case of BDD.

2.4.4 INFLUENCE OF INITIAL SUBSTRATE CONCENTRATION

The concentration of organics can, in principle, affect the kinetics of both its mass transfer from the bulk of the solution to the electrodic surface and of the oxidation reactions which take place at the anode or in its proximity. The effect of the organic concentration, at BDD anode, under mass transfer control regimes was studied by various authors. In particular, under these operative conditions, Palma-Goyas R.E. and co-authors (2010) observed that the higher was the concentration of crystal violet, the higher was the initial decomposition rate, while Choi J.Y. et al. (2010), in their study about the electrochemical degradation of 1,4-dioxane, observed that COD decreased firstly linearly, implying that these reactions are in the current control regime, and then exponentially, implying mass transport control regime.

On the other hand, it is difficult to found in literature data on the effect of the organic concentration on the performances of the process when a fast mass transfer kinetic is involved. More precisely, this latter condition was usually investigated at BDD anodes under conditions when the current efficiency of the process is close to 100 % so that no an appreciable effect of the organic pollutant concentration can be expected.

2.4.5 TEMPERATURE

Different authors have reported some studies on the effect of the temperature on the electrochemical oxidation process of organic pollutants at different electrodic materials.

Canizares et al. have studied the influence of temperature on the electrochemical oxidation of different organic substrates, as carboxylic acids, chlorophenols, phenol, and polyhydroxybenzenes, at BDD anode (Cañizares et al., 2002, 2003, 2004a, 2004b). They generally observed that direct electrochemical oxidation processes remain almost unaffected by temperature, thus ascribing the effect of this parameter to the presence of inorganic electrogenerated reagents, mainly hypochlorite and peroxodisulphates. In fact, the oxidation carried out by these redox reagents is a chemical reaction and, consequently, its rate normally increases with temperature.

In particular they reported that peroxidisulfate is chemically decomposed at high temperature and is transformed into oxygen (Eq. 2.31) and in hydrogen peroxide (Eq. 2.32-2.33), thus the effect of this compound at high temperatures is less significant since these species are less powerful oxidant than peroxidisulfate.

$$H_2S_2O_8 + H_2O \rightarrow 2\ H_2SO_4 + 2H^+ + ½\ O_2 \quad (2.31)$$

$$H_2S_2O_8 + H_2O \rightarrow H_2SO_5 + H_2SO_4 + 2H^+ \quad (2.32)$$

$$H_2SO_5 + H_2O \rightarrow H_2O_2 + H_2SO_4 \quad (2.33)$$

In the case of carboxylic acids (Cañizares et al., 2003), they have found a negative effect of the temperature, obtaining lower abatements of he organics when they set the temperature at 60°C instead of 20°C and this effect was more marked for formic acid and very small for oxalic acid. They explained these results considering the effects of the temperature on the sodium sulphate, present as supporting electrolyte in the electrolytic solution.

Different results were obtained in the case of electrochemical oxidation of aqueous phenol and of chlorophenols when they observed that higher temperatures leaded to an increase in the mineralization process rate.

Thus, they enounced (Cañizares et al., 2004b) that the presence of peroxidisulfuric acid in the electrolytic solution can lead to a different effect of the temperature on the electrochemical oxidation process of organics of different nature, depending

from which of these two processes is favored by increasing the temperature: the oxidation rate of the organics with peroxodisulfate (positive effect) and peroxodisulfate decomposition (negative effect).

Similar results were obtained by Panizza et al. (2001) that have studied the effect of temperature on the electrochemical oxidation of 2-naphthol at BDD anodes. They observed different results at the beginning and after passing about 4.5 $Ahdm^{-3}$: in the first case, no significant differences were found between the different temperature investigated (30, 40 and 60°C), while in the second case higher removal was detected probably for the production of peroxidisulphuric acid, which can oxidize more quickly the organic oxidation at high temperature, whereas in these conditions, the rate of this reaction increases.

Different results were obtained when were used Ti/IrO_2-Ta_2O_5 electrodes as anodes. Chatizisymeon et al. have conducted a set of experiments at different values of temperatures (30, 60 and 80°C) in order to study the effect of this parameter on the phenol oxidation rate (Chatzisymeon et al., 2010). They observed that oxidation of phenol was more efficient at high temperatures, since for example, at 80°C and after 48 $Ahdm^{-3}$ of charge passed, phenol degradation reached 72% while at 30°C it was only 42%.

Similar results were obtained by Martinez-Huitle et al. (2004a) that have found a drastic increase of the anodic oxidation of oxalic acid at, when temperature was increased (25 – 40 – 60 – 80°C). They explained this result relating the effect of temperature to the different activation energies characterizing the different rate-determining step for oxalic acid mineralization and for oxygen evolution reaction, since the former reaction exhibits the higher activation energy, with respect to the latter.

Hence, the effect of the temperature on the performances of the process strongly depends on the nature of the anodic material. In particular, for example in the case of carboxylic acids abatements, an increase of the temperature gives rise to a decrease of some carboxylic acids abatement at BDD (Cañizares et al., 2003) and to a drastic increase at IrO_2 based anodes (Martinez-Huitle et al., 2004a).

2.4.6 NATURE OF THE ORGANIC SUBSTRATE

Several authors have studied the influence of the nature of substrate on the electrochemical oxidation process.

Cañizares et al. (2004b) reported the electrochemical oxidation of three polyhydroxybenzenes, namely phenol, hydroquinone and 1,2,4-trihydroxybenzene, at BDD anode. They observed a complete mineralization of the organic matter in all cases, thus the rate of mineralization does not depend on the particular organic compound. A very similar study was performed by the same group of research comparing the galvanostatic electrolysis of three chlorophenols, namely 4-chlorophenol, 2,4-dichlorophenol and 2,4,6-trichlorophenol, under the same operation conditions (C_0 = 1.1 mM; T = 25°C; i = 30 $mAcm^{-2}$; pH = 2; BDD anode) in supporting media containing sulphates or phosphates in water. In this case, they observed a smaller difference for the dichlorophenol and trichlorophenol that can be easily justified in terms of the formation of hypochlorite by means of the oxidation of the chloride ions released from the chlorophenols. In particular, the concentration of hypochlorite increases with the chlorine content in the organic pollutant and so it also increases the rate of the oxidation processes (Cañizares et al., 2004a).

Quite different results were obtained when carboxylic acids were used in order to investigate the influence of the nature of the substrate on the electrochemical oxidation process at BDD anode. In particular, some authors observed a quite complete oxidation indifferently for all the acids investigated, while others observed a more precise order of mineralization rate.

Gandini et al. (2000) reported quite similar removals of formic, oxalic and acetic acids, resulting on a complete oxidation to carbon dioxide on diamond electrodes with current efficiencies, after a circulated charge of 12.0, 23.5 and 43.7 $Ahdm^{-3}$.

Very similar results were obtained by Cañizares et al (2003) who detected the evolution of the total organic and inorganic carbon concentration in the electrochemical oxidation of formic, oxalic and maleic acids for a specific set of experimental conditions (C_0 = 10 mM; T = 20°C; i = 30 $mAcm^{-2}$; pH = 2; supporting medium Na_2SO_4; BDD anode). They observed that the electrochemical process could successfully treat the three carboxylic acids under investigation, transforming

these compounds into carbon dioxide, after a circulated charge of about 18 $Ahdm^{-3}$. The formation of intermediates could not be observed, suggesting that the oxidation of the carboxylic acids can be considered as an electrochemical combustion reaction. Nevertheless, the study of undoubted importance of Brillas and coauthors (Guinea et al., 2009) had lead to different results. They have studied the degradation of carboxylic acids, carrying out three comparative experiments involving direct anodic oxidation, anodic oxidation with addition of $Fe3^{+}$ in solution and anodic oxidation with addition of $Fe3^{+}$ in solution coupled with solar irradiation. They have shown that the degradation rate of carboxylic acids depends on both the AOP employed and the nature of the Acid. In particular, the tested acids resulted more quickly oxidized in direct anodic oxidation in the sequence: oxalic < acetic < maleic < formic << pyruvic. Thus, the oxalic acid seemed to be the more resistant, even in electro-Fenton processes.

In order to better understand the effect of the nature of the organic substrate on the electrochemical oxidation processes, Weiss et al. (2007) conduced a very interesting study. They demonstrated the presence of of oxalic and formic acids as the main intermediates during the electrochemical oxidation of maleic acid at BDD. Thus, they studied the influence of the presence of these compounds adding them at the initial electrolytic solution, containing maleic acid as substrate. Investigating simultaneously formic and maleic acids, they observed that the latter was rapidly oxidized while the first was slowly oxidized, since the rate of formic acid oxidation increased as the concentration of maleic acid decreased. They ascribed this result to the different rate constants for the reaction between hydroxyl radicals and formic and maleic acids, of 1.3×10^{8} $Lmol^{-1}s^{-1}$ and 6×10^{9} $Lmol^{-1}s^{-1}$, respectively.

On the contrary, when maleic and oxalic acids are put together in the initial electrolytic solution, they observed that the concentration of both acids decreased at rates of same order. Since the rate constant for the reaction between hydroxyl radicals and oxalic acid is 1.4×10^{6} $Lmol^{-1}s^{-1}$, this result could not ascribed to this reaction, but to the possibility of a direct transfer of electrons of the oxalic acid.

2.4.7 INFLUENCE OF SODIUM CHLORIDE CONCENTRATION

The effect of chloride ions on the performances of the process has been the object of numerous researches (Martinez-Huitle and Ferro, 2006) for two main reasons. First, the addition of chloride ions can cause an increase in the removal efficiency due to the involvement of active chlorine in the oxidation process. Second, chloride ions are often present in liquid effluents and in natural waters, which makes the involvement of active-chlorine in these media inevitable. On the other hand, the addition of chloride ions can give rise in some cases to the formation of halogenated intermediates more toxic than the starting compounds (Bergmann and Rollin, 2007).

In order to explain the positive effect of the addition of sodium chloride towards the electrochemical oxidation of many organics, it has been pointed out, since the first works on the topic, that the chloride ions oxidation can lead to the formation of chlorine, hypochlorous acid and/or hypochlorite, depending on the pH (Eqs. 2.34-2.36), that can oxidize the organics near to the anode or/and in the bulk of the solution (Eq. 2.37 in alkaline medium).

$$2\ Cl^- \rightarrow Cl_2 + 2e^- \quad (2.34)$$

$$Cl_2 + H_2O \rightarrow HOCl + H^+ + Cl^- \quad (2.35)$$

$$HOCl \leftrightarrow H^+ + OCl^- \quad (2.36)$$

$$Organics + OCl^- \rightarrow intermediates \rightarrow CO_2 + Cl^- + H_2O \quad (2.37)$$

These reactions should take place in competition with oxygen evolution (Eqs. 2.38-2.39), chlorate chemical and electrochemical formation (Eqs. 2.40-2.41) and cathodic reduction of oxidants in the presence of undivided cells (Eq. 2.42) (Coninellis and Nerini, 1995; Szpyrkowicz et al, 1994).

$$4\ OH^- \rightarrow 2\ H_2O + O_2 + 4\ e^- \quad (2.38)$$

$$2\ H_2O \rightarrow 4\ H^+ + O_2 + 4\ e^- \quad (2.39)$$

$$OCl^- + 2\ HClO \rightarrow ClO_3^- + 2\ HCl \quad (2.40)$$

$$6\ OCl^- + H_2O \rightarrow 2\ ClO_3^- + 4Cl^- + 6\ H^+ + 1.5\ O_2 + 6\ e^- \quad (2.41)$$

$$OCl^- + H_2O + 2\ e^- \rightarrow Cl^- + 2\ OH^- \quad (2.42)$$

To account for some experimental results and in particular for the different distribution of byproducts observed in the electrochemical treatment in the presence of Cl^- and in the chemical oxidation with NaClO, some authors have suggested that an important role can be played also by surface electrochemical reactions (Bonfatti et al., 2000; Szpyrkowicz et al, 1994). In particular, some authors (Bonfatti et al., 2000; Israelides et al., 1997; Martinez-Huitle et al., 2005b) have proposed that adsorbed chloro- and oxychloro-radicals could be involved in the oxidation mechanism (see as an example Eqs. (2.43-2.44) for the oxychlroradicals).

$$MO_x(OH) + Cl^- \rightarrow MO_x(HOCl) + e^- \quad (2.43)$$

$$\text{Organics} + MO_x(HOCl) \rightarrow \text{intermediates} \rightarrow MO_x + CO_2 + Cl^- + H_2O + H^+ \quad (2.44)$$

Furthermore, the possibility that some role could be played by the anodic shift of the oxygen evolution, caused by Cl^- ions in the solution, has also been taken in consideration. Interestingly, up to now, it cannot be excluded that all these routes are simultaneously involved in the anodic oxidation of organics in the presence of chlorides. Furthermore, the oxidation performed by means of active-chlorine could coexist with the direct oxidation of the organics at the electrode surface, the indirect oxidation mediated by electrogenerated hydroxyl or oxychloro radicals or with both these paths thus giving rise to a complex system which does not easily allow to predict the role of operative parameters on the performances of the process.

The complexity of the system gives rise to a difficult optimization of the process and to a discrepancy between literature data for what concern the effect of the various operative parameters on the performances of the process. As an example, Polcaro et al. (2002) report that higher current density results in an higher abatement of 2,6-dichlorophenol at Ti/RuO_2 in phosphate buffer at pH = 7, Panizza and Cerisola (2003) do not observe a significant effect of the current density for the incineration of 2-naphtol at Ti-Ru-Sn, while Comninellis and Nerini (1995) show that in the case of the oxidation of phenol at Ti/IrO_2, higher current density leads to lower current efficiencies. In this study, no effect of chloride concentration was observed, while higher NaCl concentrations gave rise to higher removal efficiencies in the treatment of landfill leachate (Chiang et al., 1995). Importantly, many authors have shown that the effect of NaCl drastically depends on the anodic material. Coninellis and Nerini

(1995) have studied the influence of this parameter on the electrochemical oxidation of phenol at Ti/IrO_2 and Ti/SnO_2. They observed that the presence of chloride ions resulted in an increase of the current efficiency for the former anode, in contrast to the latter for which the presence of NaCl did not influence this value. Moreover, Chiang et al. (1995), in their study about the indirect oxidation effect in electrochemical oxidation treatment of landfill leachate at Sn-Pd-Ru oxide coated titanium (SPR) and at PbO_2/Ti anodes, observed that the treatment efficiency of the SPR anode was higher than that of the other with the addition of chloride.

CHAPTER 3

EXPERIMENTALS

In order to pursue the objectives of my thesis, the following kinds of study were performed:

1) Electroanalytical experiments and polarization curves.

- chronoamperometric measurements and polarization curves conducted on the carboxylic acids used as organic substrates in the electrochemical oxidation process.
- current/potential curves for the couple Fe^{2+}/Fe^{3+} in order to determine the limit current value at the different experimental assays.

2) Electrolyses experiments, conducted in two types of cell, in order to study the electrochemical and the Electro-Fenton oxidation processes of some organic substrates;
- electrochemical oxidation of carboxylic acids.
- electrochemical oxidation of chlorinated aliphatic hydrocarbons.
- electro-Fenton oxidation of chlorinated aliphatic hydrocarbons (study effectuated at the faculty of chemistry of Barcelona).

3) Analytical methods for the detection of the organic substances used as substrates and of the possible byproducts.

3.1 CHEMICALS

The electrolytic solution was constituted of distillate water as solvent and Na_2SO_4 (Janssen Chimica) 0.035 M as supporting electrolyte. The solution pH was settled adding H_2SO_4 (Sigma Aldrich) or NaOH (Applichem) in order to obtain acid and basic solution, respectively.

In some experiments, NaCl (Sigma-Aldrich) was added to the system in order to study the effect of the presence of chloride ions in the electrolytic solution. Moreover, in the solutions prepared for the study of the electro-Fenton process, ferrous sulphate eptahydrate from Fluka was used as source of Fe^{2+} ions.

Several compounds were used as organic substrates:

- carboxylic acids, in particular bi-hydrate oxalic acid 99% (Aldrich), formic acid 98% (J.T. Baker) and maleic acid >99% (Fluka).
- chlorinated aliphatic hydrocarbons, in particular 1,2-dichloroethane 99,8% (Aldrich) and 1,1,2,2-tetrachloroethane 98% (Fluka).

All these chemicals were analytical grade.

Different electrodic materials were used during the electrolyses in dependence of the process and organic substrate studied. In particular:

- BDD and Iridium anodes were used as anodic material, supplied by Condias and De Nora S.p.A. (Milano, Italy), respectively and nichel as cathode, for the oxidation of carboxylic acids;
- BDD and Pt 99.99% purity anodes were used as anodic material, supplied by Adamant Technologies (La Chaux-de-Fonds, Switzerland) and SEMPSA, respectively and Carbon-PTFE oxygen diffusion from E-TEK 8Somerset,Nj, USA) as cathode were used for the Electro-Fenton oxidation.

All the experiments with carboxylic acids as substrate were conducted under nitrogen atmosphere (Air Liquid-Rivoira), while those conducted with aliphatic chlorides were conducted in a sealed assay.

3.2 EXPERIMENTAL SETTINGS

3.2.1 ELECTROANALYTICAL EXPERIMENTS

Some electroanalytical experiments, in particular polarization curves and chronoamperometric measurements, were performed during my PhD thesis as preliminary studies in order to best understand the mechanism of oxidation of the organic substances used as substrates in the electrochemical processes, even at

different operative conditions. In particular, some of these experiments were conducted at temperature higher than 25°C, at both basic and acid pH, at different electrodes and at different potentials, with the aim to evaluate the effect of these parameters on the mechanism of oxidation and reduction of the organic substrates.

Chronoamperometric measurements

These electroanalytical experiments consist on the monitoring of the current versus the time, at fixed potential. In this way, adding some concentrations of the organic substrates step-by-step, at wished time, it is possible to detect the changing of the current, relating to the organic concentration. Chronoamperometric measurements were performed by an Autolab PGSTAT12.

Polarization curves

Polarization curves are carried out monitoring the current at different potential values which vary according to an imposed rate, typically of a few mV/s. In this way, it is possible to detect the potential at whitch the oxidation of the organic compound takes place at the used electrode. Amel 2053 potentiostat, Amel 567 current integrator and HP 34401A multimeter were used for quasi-steady polarization curves.

Polarization curves for the determination of the limit current

When the polarization curves are detected for the couple Fe^{2+}/Fe^{3+}, a very stable redox couple, it is possible to determine the limiting current value according the following considerations.

During the electrochemical process, the following reactions take place at the two electrodes, i.e. the reduction of the Fe^{3+} (Eq. 3.1) and the oxidation of Fe^{2+} (Eq. 3.2), at the cathode and at the anode, respectively:

$$Fe(CN)_6^{3-} + e^- \rightarrow Fe(CN)_6^{4-} \quad (3.1)$$

$$Fe(CN)_6^{4-} \rightarrow Fe(CN)_6^{3-} + e^- \quad (3.2)$$

Known the ions concentration in the bulk of the solution (C) and the limiting current values i_{lim}, obtained for the different concentrations of the redox couple, it is possible to determine the mass transfer coefficients k_m (Eq. 3.3) and consequently the thickness of the stagnant layer (δ).

$$k_m = \frac{1}{z \cdot F \cdot A} \times \frac{dI_L}{dC} \tag{3.3}$$

Polarization curves were conducted changing the potential from 0 to 1,3 V/SCE, by a linear ramp with a rate of 3 mV/s, at both system I and II (see par. 3.2.2) in order to know the mass transfer coefficient for every assay employed.

The electrolytic solutions were constituted of aqueous solutions of equitable molarity of $K_4Fe(CN)_6$ thrihydrate 99%, Carlo Erba reagents, and $K_3Fe(CN)_6$ 99%, Merk, with the concentrations of 10, 20 and 30 mM, using NaOH (99%, AppliChem) as supporting electrolyte. The diffusion coefficient D values for this couple in aqueous solution was assumed of 6.631 10^{-10} m^2/s. The values of δ detected in the different electrolytic systems (see the next paragraph) and at different operative conditions are shown in Table 3.1, while the values of D chosen from literature data for the several organics investigates in this work are reported in Table 3.2.

Tab. 3.1 *Values of the thicknesses of the stagnant layer δ for the different electrolytic systems and operative conditions adopted*

Electrolytic systems and Operative conditions	$\delta * 10^{-3}$ (cm)
System II at a flow rate of 1.2 l/min at 25°C	1.2
System II at a flow rate of 0.2 l/min at 25°C	2.8
System I at 25°C	4

Tab. 3.2 *Values of the diffusion coefficient D for the investigated organic*

Substrate	D * 10^{-5} (cm^2/s)
Oxalic Acid	1.1[a]
Formic and Maleic Acids	1[b]

[a] *Kulas J. et al., 1998*
[b] *Value assumed*

3.2.2 ELECTRODIC OXIDATION SETTINGS

Electrolyses were performed in two different systems:

System **I**

This experimental setting was constituted of a bench-scale batch undivided or divided glass cell (Fig. 3.1) equipped with a SCE reference electrode, an anode (Ti/IrO_2-Ta_2O_5 or BDD) with a wet surface area in most cases of 5.5 cm^2, and a nichel or silver cathode.

When the divided assay was employed, the anodic and cathodic compartments were divided by a cation-exchange membrane Nafion 324. Anodic solution was stirred by magnetic stir bar at a rate o 600 rpm.The volume of each compartment was generally of 50 ml for the cathodic and 70 ml for the anodic one.

The temperature of the electrolytic solution was settled at 10°C for the chlorinated aliphatic hydrocarbons (to prevent a massive evaporation) and at 25 and 50°C for carboxylic acids, thermostating the cell by the circulation of a refrigerant liquid (50% water and 50% ethylene glycol) kept at constant temperature by an ULTRATEMO 2000 julabo F30, with regulation from –50 to +200°C.

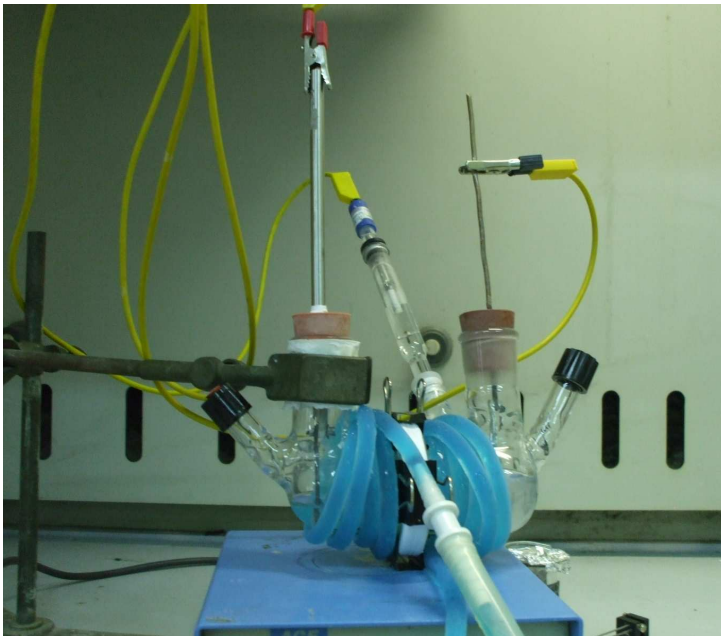

Fig. 3.1 *Scheme of a bench-scale batch glass divided for Anodic Oxidation*

System **II**

This experimental system was constituted of a continuous batch recirculation reaction system equipped with:

- a filter press undivided micro flow cell ElectroCell AB with parallel and thin sheets (Fig. 3.2);

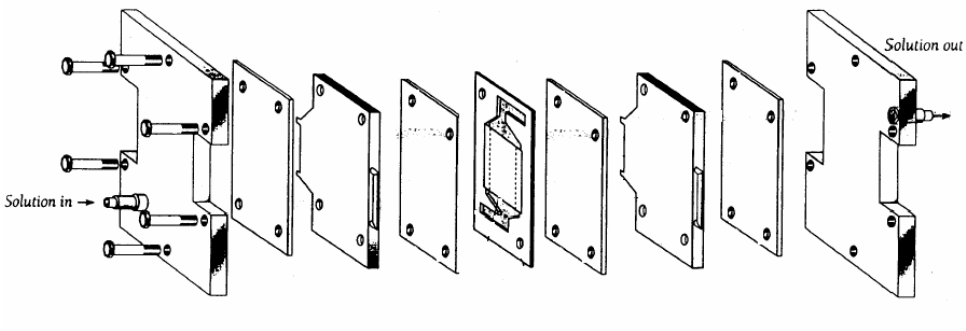

Fig. 3.2 *Scheme of a Micro flow cell ElectroCell AB*

- a centrifugal pump IWAKI mod. MD 70 RZM, with a maximum power pumping of 40 l/min and a prevalence of 14.3 m;
- a flowmeter model Picomag DMI 6530 equipped with a valve located at the exit of the electrochemical cell, in order to regulate the flow rate solution;
- a jacketed glass solution reservoir equipped with three enters: one for the circulation of the solution, one for the diffuser of a continuous stream of nitrogen dispersed in the liquid phase and a service enter to let take samples and measuring the temperature of the solution.

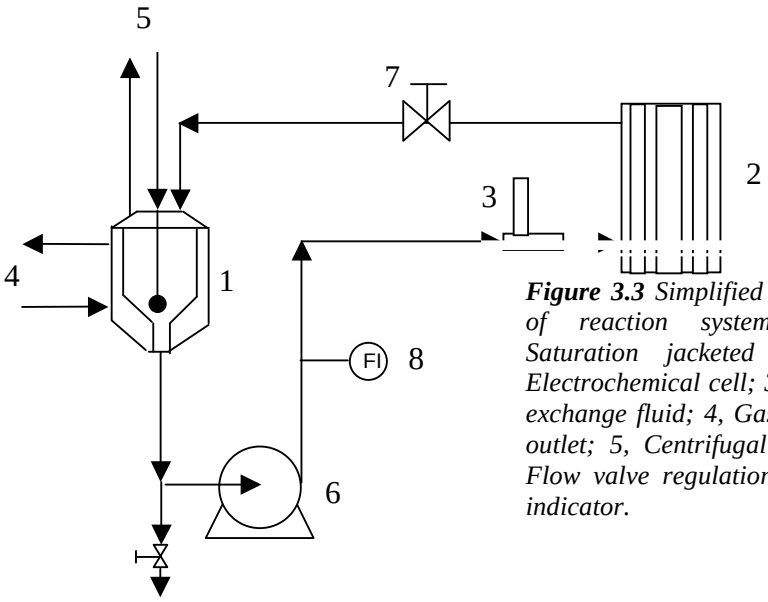

Figure 3.3 *Simplified flow-sheet of reaction system II: 1, Saturation jacketed tank; 2, Electrochemical cell; 3, Thermal exchange fluid; 4, Gas inlet and outlet; 5, Centrifugal pump; 6, Flow valve regulation; 7, Flow indicator.*

The tank is thermostated by the circulation of a refrigerant liquid (50% water and 50% ethylene glycol) kept constant temperature by an ULTRATEMO 2000 julabo F30, with regulation from –50 to +200°C.

The volume of the electrolytic solution continuously fed was 250 ml.

The system was washed by a continuous circulation of distilled water after each experiments.

The overall arrangement of the batch pilot reactor is shown in Fig. 3.3.

The cell was equipped with a BDD-Nb or a Ti/IrO_2-Ta_2O_5 thin sheet anode (surface area 9.14 cm^2) and a nickel cathode (distance between cathode and anode lower than 5 mm). Electrolyses were conducted with an Amel 2055.

3.2.3 ELECTRO-FENTON SETTING

Electrolyses were conducted in a system (system III**)**, constituted of an undivided cylindrical glass cell (Fig. 3.4) equipped with a BDD anode, a wet surface area of 3 cm^2, and a carbon-PTFE O_2-diffusion cathode (air-diffusion electrode, ADE) (Fig. 3.5).

The temperature was regulated at 10°C by circulating external thermostatated water through the double-jacket of the cell. The volume of the electrolytic solution was of about 130 ml and was stirred by magnetic stir bar.

This set of experiments was conducted with 1,2-dichloroethane and 1,1,2,2-tetracholoroethane as organic substrates and for this reason the cell was kept closed with a glass covering in order to avoid the vaporization of the volatile chlorinated compound.

The carbon-PTFE cathode was fed with an oxygen flow rate of 0.35 l/min, from an oxygen generator KNF LAB LABPORT, to continuously electrogenerate hydrogen peroxide by oxygen electrochemical reduction (see Eq. 1.9). In particular, the carbon-PTFE electrodic material was placed at the bottom of a cylindrical holder of polypropylene with an inner nickel screen of 125 mesh as current collector in contact with a nichrome wire as electrical connection.

Electrolyses were conducted with an Amel 2053.

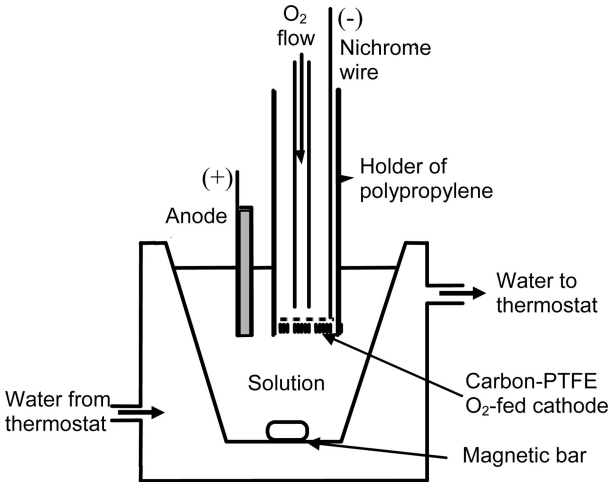

Fig. 3.4 *Scheme of a bench-scale undivided and thermostated cylindrical glass cell, where the carbon-PTFE ADE cathode was directly fed with pure O_2*

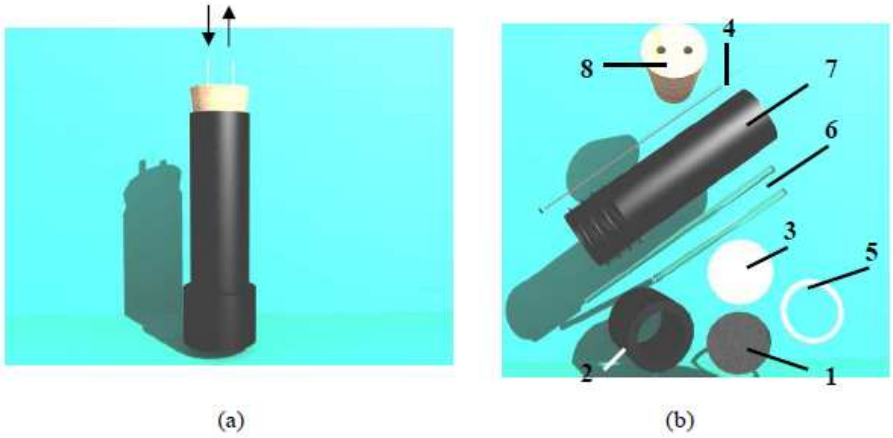

Fig. 3.5 *(a) Oxygen-diffusion cathode. (b) Components of the cathode: (1) carbon-PTFE cloth, (2) polypropylene screw plug, (3) Ni mesh, (4) Ni-Cr wire, (5) silicone gasket, (6) glass tube, (7) polypropylene support and (8) support tap.*

3.3 ANALYSIS EQUIPMENTS

Samples of the electrolytic solutions were periodically taken and analyzed during the electrolyses to evaluate the performances of the process in terms of conversion of the substrates during the different stages of the experiments and the presence of possible byproducts.

This section is devoted to give detailed information on the measurement of global parameters such as COD, pH, TOC and active chlorine, as well as individual parameters including qualitative and quantitative analysis of initial compounds and their reaction intermediates. Moreover, we also pay attention to the apparatus and equipments utilized in this work.

Quantification of the carboxylic acids, present as organic substrates or reaction intermediates, by HPLC

Carboxylic acids concentration was evaluated by liquid chromatographic analyses using HP 1100 HPLC equipped with UV-Vis detector (adopted λ=210 nm), and performed with a Alltech Platinum EPS C18 column, for the electrolyses with oxalic acid as substrate, and a Prevail Organic Acid 5u, for those conducted with formic and maleic acids.

The samples of quasi 0.2 g were taken from the electrolytic solution and were diluted until 10 ml with the buffer solution, containing KH_2PO_4 (Aldrich 99+%, A.C.S. reagents) and H_3PO_4 at pH = 2.5, prepared with water of Sigma-Aldrich G-chromasolv for gradient elution).

In the case of the oxalic acid detection, when a Alltech Platinum EPS C18 column was used, the mobile phase was constituted of a tampon solution for the 90% (aqueous solution of KH_2PO_4/H_3PO_4 at a pH of 2.5) and of methanol (99,9%, Fluka chromasolv for hplc) for the remain 10%. Instead, in the case of the formic and maleic oxalic acid detection, when a Prevail Organic Acid 5u was used, the mobile phase was constituted by the tampon solution for 100%.

When electro-Fenton oxidation process was studied, using chlorinated aliphatic hydrocarbons as organic substrates, some samples have been taken during the experiments and have been analyzed by HPLC in order to detect the possible

presence of electro-generated carboxylic acids. In particular the analyses were performed with an AMINEX Column and a mobile phase constituted of H_2SO_4 4 mM, fluxed of 0.6 mL/min.

Quantification of the chlorinated aliphatic hydrocarbons by GC

The concentrations of 1,2-dichloroethane and 1,1,2,2-tetrachloroethane were monitored during some electrolyses by Gas Cromatography using a Trace GC Ultra (Thermo Scientific) System equipped with FID, a TriPlus Autosampler GC Headspace and an Agilent J&W GC Column DB-624. Temperature at the oven was settled according the following method: an initial temperature of 60°C, a ramp until the final temperature of 220 °C at a rate of 8 degrees/min and a final hold time of 5 minutes. The identification of halogenated compounds was generally performed by GC analyses trough comparison with pure standards.

Quantification of ions released by IC

The presence of chloride, chlorate and perchlorate ions produced during the electro-Fenton oxidation of chlorinated aliphatic hydrocarbons was determined by ionic chromatography (IC). This is a liquid chromatography technique, where the stationary phase inside the column contains a synthetic ion-exchange resin with charged groups as active sites. There are two types of resins depending on the nature of the ion to be retained:

- cationic ion exchange resins contain negatively charged groups such as sulphonic or carboxylic acids (strong and weak acid, respectively);
- anionic ion exchange resins usually contain positively charged quaternary or primary amines (strong and weak base, respectively).

Consequently, there are two types of IC systems designed to separate either cations or anions. Thus, in order to detect the presence of anions, the anodic one was employed. In particular, anions concentration was evaluated using Shimadzu IC equipped with a conductivity detector (CDD-10AVP), and performed with a SHODEX Packed column SHIM-PACK IC-A15. The mobile phase was constituted

of an aqueous solution of tris(hydroxymethyl-)aminomethane 99%, from Lancaster and phtalic acid 99%, from Lancaster.

pH

The pH measurements were carried out with a Crison 2000 pH-meter, calibrated with two buffers of pH 4 and 7 purchased from Panreac for the electro-Fenton experiments and with a HI 8314 membrane pH-meter, calibrated with three buffers of pH 4, 7 and 10 purchased from Hanna for the anodic oxidation experiments.

Active chlorine

When the electrolyses were conducted in the presence of sodium chloride in the electrolytic solution in order to study the influence of the chloride ions on the electrochemical oxidation of the oxalic acid, active chlorine concentration was detected by the photometric method (Ocean Optic DH-2000) with a MerK Chlorine test containing dipropil-p-fenilendiamina (DPD).

COD (Chemical Oxygen Demand)

The trend of some of the oxidative processes was also monitored by measuring the COD. This parameter represents the measurement of the oxygen equivalent to the organic matter contained in a sample that is susceptible to be oxidized by a strong chemical oxidant. The COD value is given in concentration of oxygen (mg O_2 /l)

COD has been determined by the potassium dichromate method according to the following reaction:

$$C_xH_yO_z + m\ Cr_2O_7^{2-} + 8m\ H^+ \longrightarrow x\ CO_2 + (y+8m)/2\ H_2O + 2m\ Cr^{3+} \qquad (3.4)$$

where $m = (2x/3) + y/6 - z/3$

The oxidation takes place by adding 2 or 3 ml of solution (depending on the range of the concentration of COD) to a Merck vial containing both silver compound as catalyst to oxidize resistant organics and mercuric sulphate to reduce interference from the oxidation of chloride ions by dichromate in sulphuric acid. After reaction of the mixture for 2 h at 148 °C in a thermoreactor (Merck, Spectroquant Thermoreactors TR320) and cooling at room temperature, the COD value was

obtained from the spectrophotometric absorbance of Cr^{3+} formed, by an Ocean Optic Spectrophotometer (DH-2000).

TOC (Total Oxygen Demand)

Total Organic Carbon (TOC) analysis of a solution is based on the complete conversion of all carbon atoms present in the sample up to CO_2 and constitutes another global parameter that serves to evaluate the degree of mineralization of a pollutant during its destruction. This technique allows evaluating the degree of mineralization of the starting pollutant during the electrochemical processes. This parameter was monitored on a Shimadzu VCSN TOC analyzer. The TOC value is given in milligrams of carbon per liter (mg l^{-1}), performing the average of three consecutive measurements with a precision of about 2%. The calibration of the equipment was made using potassium hydrogen phtalate standards in the range between 20 and 400 mg l^{-1}.

Spectrophotometric determination of electrogenerated H_2O_2 by its complex with Ti(IV)

Once titrated the H_2O_2 standards, the spectrophotometric calibration curve for the peroxo-titanate complex was determined by measuring the absorbance for each standard using an Unicam UV4 Prisma double-beam spectrophotometer thermostated at 25 ºC. This method is based on the reaction between Ti(IV) and H_2O_2 in sulphuric acid medium yielding a yellow-orange peroxo-complex with λ_{max} = 408 nm, according to the reaction:

$$Ti^{4+} + H_2O_2 + 2\ SO_4^{2-} \longrightarrow (TiO_2(SO_4)_2)^{2+} + 2\ H^+ \qquad (3.5)$$

A reagent solution with Ti(IV) concentration close to 20 mM was prepared by heating a solution of solid $TiO(SO_4)$ in concentrated H_2SO_4 until it turned colorless and transparent. This solution was then cooled at room temperature before use. Interferences of yellowish Fe(III) hydroxo-complexes were easily masked by addition of some drops of H_3PO_4 to the samples prior to their spectrophotometric analysis. The concentration of H_2O_2 accumulated in the medium was calculated from

the absorbance measurements of the yellow-orange peroxo-Ti(IV) complex in the samples withdrawn at different electrolysis times.

Spectrophotometric determination of Fe^{2+}/Fe^{tot} contents by reaction with 1,10-phenantrolin

Ions Fe^{2+} form a red colour complex with 1,10-phenantrolin with λ_{max} = 510 nm. The analyses were effectuated by measuring the absorbance for each sample using an Unicam UV4 Prisma double-beam spectrophotometer thermostated at 25 ºC. The spectrophotometric calibration curves have been made using ammonium sulfate of iron (II) which is more stable than the respective sulfate.

In order to detect the concentration of iron (II) ions by spectrophotometric analyses, samples were prepared putting 1 mL of phenantrolin + 1 mL of a buffer solution constituted of sodium acetate/ acetic acid + xx mL of H_2O if is necessary to dilute + (4- xx mL) of the sample taken from the electrochemical cell during the experiments or prepared for the calibration curve.

In order to estimate the concentration of total iron (i.e. iron (II) and iron (III)), is necessary to add some ascorbic acid, which by its high reducing power, reduce Fe^{3+} ions to Fe^{2+} and make the ionic form of iron (II) stable. After 30 minutes is possible to analyse these samples.

3.4 GLOBAL ELECTROCHEMICAL PARAMETERS

In order to estimate the features of the experiments, some global electrochemical parameters were calculated such as CE and ICE.

The *current efficiency (CE)* can be defined as the part of the current directly used for the oxidation reaction. The current efficiency (CE) and the instantaneous current efficiency (ICE) were then calculated using the Eq.ns 3.6 and 3.7, respectively.

$$CE = xC^0V\frac{nF}{Q} \tag{3.6}$$

$$ICE = (C_Q - C_{Q+\Delta Q})V\frac{nF}{\Delta Q} \tag{3.7}$$

where *x* is the conversion of the pollutant, C^0 and C_Q are the concentrations of the pollutant at the beginning of the electrolysis and after Q passed charge, respectively, $C_{Q+\Delta Q}$ is the generic value of the pollutant concentration after the circulation of an incremental amount ΔQ of the passed charge. *F* is the faraday constant (96487 C mol^{-1}), *V* is the volume of the electrolyte and *n* is the number of electrons necessary for the conversion of the pollutant to carbon dioxide.

In particular, the number of electrons involved was estimated by considering the following reactions:

- for oxalic acid.....$C_2H_2O_4 \rightarrow 2\ CO_2 + 2\ e^- + 2H^+$
- for formic acid.....$CH_2O_2 \rightarrow CO_2 + 2\ e^- + 2H^+$
- for maleic acid.....$C_4H_4O_4 \rightarrow 4\ CO_2 + 12\ e^- + 12H^+$
- for 1,2-dichloroethane

.....$C_2H_4Cl_2 + 4\ H_2O \rightarrow 2\ CO_2 + 12\ H^+ + 2\ Cl^- + 10\ e^-$

- for 1,1,2,2-tetrachloroethane

.....$C_2H_2Cl_4 + 4\ H_2O \rightarrow 2\ CO_2 + 10\ H^+ + 4\ Cl^- + 6\ e^-$

CHAPTER 4

THEORETICAL CONSIDERATIONS AND MATHEMATICAL MODELS

4.1 INTRODUCTION

Quite often the high number of operative parameters which may be adjusted makes an empirical investigation exceedingly onerous in order to individuate the conditions which allow the optimization of the electrochemical process. In this perspective, theoretical models can offer useful strategies for both the individuation of the parameters that affect the competition between the targeted reactive path and side unwanted reactions and the design of new materials/apparatus that can favour the selective occurrence of the desired route. The experimental validation of mathematical models can, furthermore, furnish precious indications for scale-up stages and confirm the assumptions on which the model is based allowing a proper description of the process. For what concern the electrochemical abatement of organic pollutants in wastewater, unwanted reactions should be severely minimized in order to avoid the formation of secondary pollutants and/or an increase of energetic costs. Hence, the modelling of these processes has attracted in the last years the attention of numerous researchers (Cañizares et al., 2002, 2004c, 2004d; Comninellis, 1994; Israelides et al., 1997; Panizza et al., 2001; Polcaro et al., 2003; Rodrigo et al., 2001; Scialdone, 2009; Simond et al., 1997; Wiley, in press).

Particular attention was devoted to processes performed at BDD, due to the extreme efficacy of this electrode toward the oxidation of numerous pollutants. The modeling of both direct and indirect oxidation processes was attempted by various authors as recently reviewed (Wiley, in press). In particular, the kinetic models proposed by Comninellis, Canizares and Polcaro and their co-authors are reported in section 2.3.2.1. As an example, the simple theoretical kinetic model proposed by Comninellis for the oxidation of organics in batch systems with galvanostatic alimentation does not present adjustable parameters and it allows to fit with accuracy experimental data when the current efficiency in the absence of mass transfer limitations is close to 100%. On the other hand, this model does not describe

mixed kinetic regimes or the evolution of the concentrations of different specie present in the system.

Hence, in this chapter, the oxidation of organics at BDD and metal oxide electrodes is proposed, taking in account both the direct anodic oxidation and the oxidation of the organic by hydroxyl radicals, that are usual named as “direct processes”. Since hydroxyl radicals are expected to be chemi-adsorbed at the DSA and physi-adsorbed at the BDD anode (see par. 2.3), quite different expressions were derived. Moreover, a section will be dedicated at the theoretical modeling of electrolyses conducted with a potentiostatic alimentation, taking in account the role of the potential. Finally, theoretical considerations about the indirect oxidation by means of active chlorine generated by the oxidation of NaCl are also presented in this chapter.

Theoretical predictions based on a simple theoretical model were compared with experimental data with the aim to achieve, without a significant computational effort, a proper description of the effect of numerous operative parameters such as the current density, the flow dynamic regime and the pollutants concentration on the performances of the process for electrolyses performed in the presence of one or more organics .

4.2 THEORETICAL MODELLING

Theoretical considerations will be presented differentiating the kinetic regimes that can subsist during electrochemical experiments.

4.2.1 MASS TRANSPORT CONTROL

When the rate of the mass transfer of the pollutant is dramatically lower than that of its oxidation, the concentration of the pollutant at the anodic surface/reaction layer $[RH]^0$ is close to zero and the oxidation process is under mass transfer control. This case arises, for an oxidation process that proceeds up to the total oxidation of the organic pollutant, when the limiting current density $i_{lim} = nFk_m[RH]^b << i_{app} ICE^{OC}$ (where n is the number of electrons exchanged for the anodic oxidation of RH to carbon dioxide, F the Faraday constant (96487 C mol^{-1}), $[RH]^b$ and k_m the bulk

concentration and the mass transfer coefficient of the organic *RH*, respectively, i_{app} the applied current density and ICE^{OC} the instantaneous current efficiency for the oxidation of *RH* under oxidation reaction control under adopted operative conditions) e.g. when $[RH]^b << C^* \leq C^* \; ICE^{OC}$ (where $C^* = i_{app}/(nFk_m)$). Under mass transfer control, the current efficiency ICE^{MT} is given by the ratio between the limiting current i_{lim} and the applied current density i_{app} independently by the oxidation mechanism as previously proposed (Scialdone, 2009).

For $[RH]^b << C^* \; ICE^{OC}$

$$ICE = ICE^{MT} \approx [RH]^b/C^* = nFk_m[RH]^b/ i_{app} \quad (4.1)$$

where $C^* = i_{app} /nFk_m$.

The *ICE* should depend on the fluidodynamic of the system (trough its effect on k_m), on the applied current density and on $[RH]^b$ (with a linear dependence on this parameter). It is important to observe that, under these conditions, the performances of the process are readily predictable. Thus the mass transfer coefficient is readily given by the ratio $k_m = D/\delta$ where the diffusion coefficient D can be often found in literature or can be estimated by electroanalytical experiments or using the Wilke-Chang expression while the thickness of the diffusion layer δ is easily estimated by typical limiting-current essays using, as an example, the couple hexacyanoferrate (II)/hexacyanoferrate (III). Hence, it is also possible to predict the organics concentration as a function of the charge or of the time. Indeed, the instantaneous current efficiency is given, by definition, by:

$$ICE = - nFV \, d[RH]^b/dQ \quad (4.2)$$

and eliminating the term *ICE* by Eq.ns 4.1 and 4.2, one easily obtains the relationships reported in Eq.ns 4.3-4.4 (where *V* is the volume, *A* the anodic surface, *t* and *Q* the time and the charge passed, respectively).

$$ln[RH]^{b,Q} /[RH]^{b,Q=0} = - Q/(nFVC^*) \quad (4.3a)$$

$$\text{and then } [RH]^{b,Q} = [RH]^{b,Q = 0} \exp[-Q/(nFVC^*)] \quad (4.3)$$

$$[RH]^{b,t} = [RH]^{b,t = 0} \exp[-(Ak_m/V)t] \quad (4.4)$$

It is important to stress also the fact that under these circumstances, the adsorption of organics at the anode surface is prevented by their fast reaction with hydroxyl radicals, thus hindering passivation phenomena. When more pollutants are present in the bulk during the electrolysis, one can focus on the chemical oxygen demand *COD* of the solution. In particular, the limiting current density, for a process that proceed up to the total oxidation of organics, is given by $i_{lim} = 4Fk_mCOD$ and a mass transfer control will arise if $i_{lim} << i_{app}\ ICE^{OC}$ (where ICE^{OC} is the average current efficiency for a process under oxidation reaction control and *COD* the chemical oxygen demand computed on a molar base). The COD is expected to be given by the following relationship, previously proposed by Comninellis and co-authors (Panizza et al., 2001; Rodrigo et al., 2001):

$$[COD]^{b,t} = [COD]^{b,t=0} \exp[-(Ak_m/V)t] \quad (4.5)$$

Please, consider however that under these conditions the formation of significant concentration of intermediates is expected to be prevented by the excess of hydroxyl radicals available at the anodic surface.

4.2.2 OXIDATION REACTION CONTROL

For a process under the kinetic control of the oxidation reaction, the instantaneous current efficiency ICE^{OC} is determined by the competition between the oxidation of the organic and the evolution of the oxygen. Please, consider that the oxidation can take place by both an anodic reaction or by reaction with electrogenerated hydroxyl radicals.
Under these conditions, the current efficiency can be simply estimated by Eq. 4.6.

For $[RH]^b >> C^* ICE^{OC}$

$$ICE^{OC} = \frac{i_{RH}}{i_{app}} = \frac{i_{RH}}{i_{RH} + i_{O2}} = \frac{1}{1 + \frac{i_{O2}}{i_{RH}}} = \frac{1}{1 + \frac{[RH]^*}{[RH]^b}} \quad (4.6)$$

and thus:

$$\frac{1}{ICE} = 1 + \frac{[RH]^*}{[RH]^b} \quad (4.6b)$$

where i_{RH} and i_{O2} are the current densities involved in the oxidation of the organic and in the oxygen evolution process, respectively. [*RH*]* is defined as the value of [*RH*]^b which gives a current density for the *RH* oxidation i_{RH} equal to the current density involved for the oxygen evolution reaction i_{O2}, e.g. the value of [*RH*]^b that gives *ICE* = 50% (Scialdone, 2009). A similar expression was first proposed for the oxidation of organics at metal oxide electrodes (Scialdone, 2009).

Please consider, however, that the physical meaning of [*RH*]* depends on the oxidation route and, as a consequence, on the nature of both the organic pollutant and the electrodic material. Thus, if the oxidation of the organic takes place by direct anodic oxidation, [*RH*]* is given by $[RH]^*_{dir} = 2r(E)/nk(E)$ where *k(E)* is the heterogeneous rate constant for the oxidation of *RH* and *r(E)* is the rate of the solvent oxidation. Otherwise, if the oxidation takes place by means of hydroxyl radicals, $[RH]^*_{HO}$ is given by:

$$[RH]^*_{OH} = 2k_{or}/nk_{O2} \quad (4.7a)$$

for physically adsorbed hydroxyl radicals;

$$[RH]^*_{OH} = 2k_E/nk_O \quad (4.7b)$$

for chemically adsorbed hydroxyl radicals,

where k_{O2} (s^{-1}) and k_{or} ($M^{-1}s^{-1}$) are the rate constants of the reactions reported in Eq.ns 4.8 and 4.9 respectively, k_E and k_O are the kinetic constants of the reactions of evolution of oxygen and organics oxidation by means of "adsorbed oxygen", respectively, and *n* is the number of adsorbed hydroxyl radicals necessary to convert the substrate to carbon dioxide.

$$BDD(^{\bullet}OH) \rightarrow BDD + 0.5\ O_2 + H^+ + e^- \quad (4.8)$$

$$BDD(^{\bullet}OH) + RH \rightarrow BDD + H_2O + R^{\bullet} \quad (4.9)$$

In particular, for an oxidation process mediated by chemical adsorbed hydroxyl radicals, [RH]* describes the competition between two chemical reactions (the oxidation of organics by means of adsorbed oxygen and its evolution towards the formation of oxygen), does not depend on the working potential (Scialdone, 2009) and hence is expected to assume a constant value by changing the operative parameters at a fixed value of the temperature. Interestingly, also $[RH]_{dir}$* is expected not to depend on the potential and to assume a constant value for a fixed value of the temperature if the transfer coefficient α assumes similar values for the oxidation of water and *RH*:

$$[RH]_{dir}^* = 2r(E)/nk(E) = (2/n)\,(k'/k°_{RH})\exp[(1-\alpha)\,F(E°_{RH} - E°_{W})/(RT) \qquad (4.10)$$

where *k*' is given by the product of the standard rate constant for the oxidation of the solvent and the solvent concentration and $E°_{W}$ is the standard potential for the oxidation of the water.

Hence, in the case of a direct anodic oxidation process, expression reported in Eq. 4.6 can be readily used to predict the effect of some operative parameters such as current density and organic concentration on the performances of the process. A more complex scenario is expected for an indirect process mediated by physical adsorbed hydroxyl radicals. In this case, in fact, [*RH*]* is expected to depend on the working potential (e.g. on the applied current density) so that a less effective prediction of the effect of operative parameters on *ICE* is achievable. Anyway, this aspect is of less practical relevance if the kinetic constant of mediated reaction is so high that in any case [*RH*]* is close to zero and *ICE* under oxidation control is close to 1.

In particular, in the following a constant value of [RH]* will be considered, for the sake of simplicity. More in general, it is interesting to observe that according to Eq.ns 4.1 and 4.6, the instantaneous current efficiency of the process is expected to depend on the concentration of the organic pollutant in the bulk $[RH]^b$ for both mass transfer and oxidation reaction control. On the other hand, in the case of a mass transfer control, *ICE* should depend linearly on $[RH]^b$ while in the case of an oxidation reaction control a linear relationship is expected between 1/*ICE* and

$1/[RH]^b$. Furthermore, if the kinetic constant of the reaction between the organic pollutant and hydroxyl radical is very high as generally expected for diamond anodes, the dependence of the *ICE* by $[RH]^b$ can be practically observed only for very low values of both $[RH]^b$ and the applied current density (e.g. by working, as an example, with electrodes characterized by a very large surface area).

Please, note also that, under oxidation reaction control, the process is expected to be dramatically affected by the nature of the organic pollutant and of the anodic material through their effect on $[RH]^*$ but not by the flow dynamic regime while, in the case of a mass transfer control, the *ICE* depends strongly on the flow dynamic regime (trough its effect on k_m), slightly on the nature of the organic pollutant (trough the value of the diffusion coefficient) but not significantly on the nature of the anode. It follows that the utilization of boron doped diamond anodes is expected to affect positively the abatement of organic pollutants in water if the process is under oxidation reaction control but not if a mass transfer control arises.

If more organics are present in the system from the beginning or as a result of the formation of intermediates, Eq. 4.6 can be readily modified as follows (as an example in the case of the presence of two organics named, respectively, *RH(I)* and *RH(II)*).

$$ICE^{OC}(I) = \frac{i_{RH(I)}}{i_{app}} = \frac{i_{RH(I)}}{i_{RH(I)} + i_{RH(II)} + i_{O2}} = \frac{1}{1 + \frac{[RH(I)]^*}{[RH(I)]^b}\left(1 + \frac{[RH(II)]^b}{[RH(II)]^*}\right)} \quad (4.11)$$

$$ICE^{OC}(II) = \frac{1}{1 + \frac{[RH(II)]^*}{[RH(II)]^b}\left(1 + \frac{[RH(I)]^b}{[RH(I)]^*}\right)} \quad (4.12)$$

In Table 4.1 the fitting parameters found for all the organics investigated, namely oxalic, formic and maleic acids, at BDD and at DSA anodes, are reported. In particular, [RH]* was estimated to lead to the best fit of the experimental results using Eq. 4.6 for what concern the ICE or 4.1 and 4.6 for the concentration profiles of the organics as a function of the charge passed, when the electrolysis was

conducted under oxidation reaction control regime (see Fig. 4.1 as an example at BDD anode). The values of [*RH*]* relative to the oxidation reaction at DSA anode were detected at different temperatures and at different pH values, but only for the oxalic acid. The different [*RH*]* observed for the investigated organics correspond to different oxidation rates at BDD and at DSA anodes.

Tab. 4.1 *Fitting parameters and kinetic constants for the reaction between hydroxyl radicals and investigated organic for the BDD anode.*[a]

Substrate	[*RH*]* (mM)	*n*[*RH*]* (mM)	p_1	p_2	
at DSA anode:					Operative conditions
Oxalic Acid	18	36			T = 25°C – pH 2
Oxalic Acid	250	500			T = 25°C – pH 12
Oxalic Acid	3-4	6-8			T = 50°C – pH 2
at BDD anode:					k_{OH} [b] (l mol^{-1} s^{-1})
Oxalic Acid	13	26			9.2 10^6
Formic Acid	2	4			0.5 - 1.6 10^8
Maleic Acid	0.05	6	0.04	0.08	4.6 10^8

[a] *System solvent supporting electrolyte (SSE): Water, Na_2SO_4/H_2SO_4. T = 25° and 10 °C for experiments performed in the presence of Carboxylic Acids and Aliphatic Chlorides, respectively.*
[b] *Rate constant for the reaction between hydroxyl radicals and investigated organics (Pimblott et al., 2005; Ross and ross, 1977).*

In particular, for what concern the oxidation at BDD anode, the rate constant for the reaction between hydroxyl radicals and investigated carboxylic acids k_{OH} are also reported in Table 4.1.

Please, note that, since maleic acid at BDD is expected to proceed with the formation of three different products which are probably related to three competitive oxidation routes, namely carbon dioxide, formic acid and oxalic acid (see section

8.4.2.1), the competition between these routes was described by three competition parameters named $p_1 = r_{OA}/r_{MA}$, $p_2 = r_{FA}/r_{MA}$ and $p_3 = 1 - p_1 - p_2 = r_{CO2}/r_{MA}$ (where r_{MA} is the total oxidation rate of maleic acid and r_{OA}, r_{FA} and r_{CO2} the oxidation rate of maleic acid to oxalic, formic and carbon dioxide, respectively).

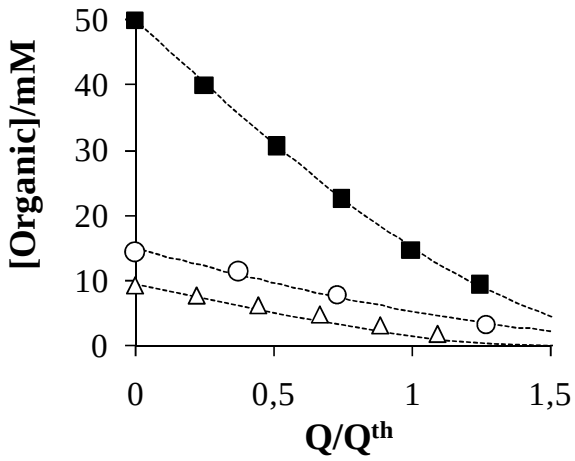

Fig.4.1 *Anodic oxidation of formic (Δ), oxalic (■) and 1,2-dichloroethane (○) performed at BDD under oxidation reaction kinetic control. Electrolyses of formic and oxalic acid were performed in system II with i_{app} = 1 and 17 mA/cm^2, respectively, flow rate = 1.2 l/min, T = 25 °C. Electrolyses of 1,2-dichloroethane were performed in system I with i_{app} = 15 mA/cm^2 at 10 °C. Other experimental conditions: Amperostatic alimentation, system solvent supporting electrolyte (SSE): Water, Na_2SO_4, H_2SO_4 (pH 2). Theoretical curves (---) obtained by Eq.ns 4.1 and 4.6 with the values of [RH]* listed in Table 1. Q^{th} theoretical charge necessary for the complete oxidation of the organic with a process with a current efficiency of 100 %.*

Two of these parameters were obtained as fitting parameters together with [*RH*]* (see Table 4.1) by comparing the theoretical predictions with the experimental trends of the concentration of maleic, formic and oxalic acid with the charge passed, while the last parameter was simply obtained by mathematical combination of the other two.

4.2.3 MIXED KINETIC REGIME

Let now us discuss the general case of a process whose rate determining step changes during the electrolysis from an oxidation reaction control in the first stages to mass transfer control in the last part with a mixed regime between them. In order to found a general expression for *ICE* which can be easily used to predict the performances of the process under different kinetic regimes, it is necessary to determine [*RH*]°. Thus, let us consider that under pseudo-steady state conditions, prevailing during an electrolysis, carried out with amperostatic alimentation the following expression should apply:

$$k_m ([RH]^b - [RH]^0) = i_{app}\, ICE/nF \tag{4.13}$$

Hence, by combination of Eq.ns 4.10 and 4.13 and elimination of the term [*RH*]°, one can obtain, as previously reported in literature (Scialdone, 2009), the expression for the *ICE* during an amperostatic electrolysis:

$$ICE = \frac{1}{1 + \frac{2[RH]^*}{[RH]' + ([RH]'^2 + 4[RH]^*[RH]^b)^{0.5}}} \tag{4.14a}$$

where $[RH]' = [RH]^b - [RH]^* - C^*$.

A first consequence of the above considerations is that the current efficiency of the process is expected to depend dramatically on $[RH]^b$, on i and k_m through their effects on the substrate concentration at the electrode and on [*RH*]*. The last is a measure of the competition between the oxidation of the organics and oxygen evolution processes and it is expected to depend dramatically for a given electrode on the nature of the organic. Interestingly, also in this case the value of *ICE* is readily predictable for different operative conditions if one estimates k_m and [*RH*]* as above mentioned. As a consequence, also the profiles of the organics concentration during the electrolysis as a function of charge or time passed can be numerically computed by combining Eq.ns 4.14 and 4.2. In particular, for what

concern the dependence with the charge passed, the following equation can be applied

$$d[RH]^b = - dQ\ ICE/nFV \quad (4.14b)$$

In the presence of two organics, the following equations can be applied:

$$k_{m(I)} ([RH(I)]^b - [RH(I)]^0) = i_{app}\ ICE(I)/nF \quad (4.15)$$

$$k_{m(II)} ([RH(II)]^b - [RH(II)]^0) = i_{app}\ ICE(II)/nF \quad (4.16)$$

$$ICE^{OC}(I) = \frac{1}{1+\frac{[RH(I)]^*}{[RH(I)]^0}(1+\frac{[RH(II)]^0}{[RH(II)]^*})} \quad (4.17)$$

$$ICE^{OC}(II) = \frac{1}{1+\frac{[RH(II)]^*}{[RH(II)]^0}(1+\frac{[RH(I)]^0}{[RH(I)]^*})} \quad (4.18)$$

If $k_{m(i)}$ and $[RH(i)]^*$ are estimated by proper experiments, one have a system of 4 equations and 4 variables that can be easily computationally solved. Of course, a simple extension of this approach is necessary in the presence of more organic pollutants in the system.

4.3 THEORETICAL MODELING FOR LECTROLYSES PERFORMED WITH A POTENTIOSTATIC ALIMENTATION

Let now us consider the aspects of the mathematical model when experiments were performed with a potentiostatic alimentation. In this case, the instantaneous current *ICE* is given by:

$$ICE = \frac{i_{RH}}{i_{RH} + i_{wat}} = \frac{k(E)[RH]^0}{k(E)[RH]^0 + k'(E)} \quad (4.19)$$

where *k(E)* is the heterogeneous rate constant for the oxidation of the generic RH and *k'(E)* is given by the product of the heterogeneous rate constant for the oxidation

of the solvent and the solvent concentration. The heterogeneous rate constant, k(E), of electron transfer to RH, is given by

$$k(E) = k^{\circ}_{RH} \exp\left[\frac{(1-\alpha)F}{RT}\left(E - E^{0}_{RH}\right)\right] \quad (4.20)$$

where F is the Faraday constant (96487 C mol^{-1}), α is the transfer coefficient and E°_{RH} and k°_{RH} are the standard potential and standard rate constant for the oxidation of RH, respectively .

Under pseudo-steady state conditions prevailing during the electrolysis:

$$k(E)\,[RH]^0 = k_m\,([RH]^b - [RH]^0) \quad (4.21)$$

where $[RH]^b$ and k_m are the bulk concentration and the mass transfer coefficient of RH, respectively. Upon eliminating $[RH]^0$ by Eqs. 4.19 and 4.21, one obtains:

$$ICE = \frac{1}{1 + k'(E)\dfrac{k(E) + k_m}{k(E)k_m[RH]^b}} = \frac{1}{1 + \dfrac{x}{[RH]^b}} \quad (4.22)$$

where $x = k'(E)\ (k(E)+k_m)/(k(E)k_m)$ assumes a constant value during a single potentiostatic experiment. Hence, Eq. 4.22 can be properly used to describe the trend of ICE in electrolyses with potentiostatic alimentation. In particular, according to Eq. 4.22, *ICE* is expected to decrease during a potentiostatic experiment for the effect of the reduction of the organic compound concentration with a linear relationship between 1/*ICE* and 1/$[RH]^b$.

$$\frac{1}{ICE} = 1 + \frac{x}{[RH]^b} \quad (4.23)$$

It can be observed that x increases with the potential as an effect of the limitations given by the mass transport rate assuming the values of $x_1 = k'(E)/k(E)$ and of $x_2 = k'(E)/k_m$ for low and high values of E, respectively (e.g. under charge transfer and mass transfer kinetic control, respectively). In particular, if the transfer coefficient α

assumes similar values for the oxidation of water and oxalic acid, x_1 is given by the following expression and does not depend on the working potential:

$$x_1 = (k'/k°_{OA}) \exp[(1- \alpha) F(E°_{OA} - E°_{W})/(RT)] \quad (4.24)$$

where k' is given by the product of the standard rate constant for the oxidation of the solvent and the solvent concentration and $E°_W$ is the standard potential for the oxidation of the water.

A different scenario is present if a mediated oxidation is involved, i.e. when hydroxyl radicals are produced by the oxidation of water at the anode, evolving towards oxygen evolution with a rate r_1 or towards organic compound oxidation with a rate $r_2 = k_{14}$ [$^{\bullet}$OH] $[RH]^0$ where [$^{\bullet}$OH] is the average concentration of hydroxyl radicals in a very small reaction volume confined nearby the electrode surface with a negligible thickness with respect to that of the stagnant layer δ.

In this scenario, the instantaneous current efficiency is given by:

$$ICE = r_2/(r_1 + r_2) \quad (4.25)$$

where

$$r_1 + r_2 = A\, k'(E)/2V \text{ under potentiostatic alimentation} \quad (4.26)$$

and under pseudo-steady state conditions prevailing during the electrolysis:

$$r_2 = k_{14} [^{\bullet}OH] [RH]^0 = k_m ([RH]^b - [RH]^0)A/V \quad (4.27)$$

Hence, the *ICE* can be calculated by solving the system composed by equations 4.25, 4.26 and 4.27. When a process under mass transfer control is performed with potentiostatic alimentation, the expression of the *ICE* depends on the mechanism involved. Indeed, if an indirect mechanism occurs, independently by the oxygen evolution mechanism, the instantaneous current efficiency is expected to depend linearly on $[OA]^b$ (see Eq. 4.28 derived by equations 4.25, 4.26 and 4.27, while a more complex relationship between *ICE* and $[RH]^b$ is expected in the case of a direct mechanism (see Eq.ns 4.29 and 4.30) which derive by Eq. 4.23 in the case of mass transfer control

$$ICE = \frac{k_m [OA]^b}{k^{'}(E)} \tag{4.28}$$

$$ICE = \frac{1}{1 + \frac{k'(E)}{k_m [OA]^b}} \tag{4.29}$$

$$\frac{1}{ICE} = 1 + \frac{k'(E)}{k_m} \frac{1}{[OA]^b} \tag{4.30}$$

Let us now discuss the expected dependence of $[OA]^b$ with the charge and the time passed for a direct process, which seems, according to previous observations, likely to be involved. For what concern the dependence with the charge passed, the following equation can be applied

$$d[RH]^b = - dQ\ ICE/(nFV) \tag{4.31}$$

and as consequence for a direct process according to Eq. 4.23,

$$d[RH]^b = - ([RH]^b/([RH]^b + x))\ dQ/(nFV) \tag{4.32}$$

Hence, by integration

$$([RH]^{b,Q=0} - [RH]^{b,Q}) + x \ln([RH]^{b,Q=0}/[RH]^{b,Q}) = Q/(nFV) \tag{4.33}$$

For what concern the dependence of $[RH]^b$, the variation of $[RH]^b$ with time for a direct process should be, simply, given by

$$d[RH]^b = - dQ\ ICE/nFV = - (I/nFV)\ ICE\ dt = - \Gamma\ [RH]^b\ A/V\ dt \tag{4.34}$$

where $\Gamma = [k(E)(D/\delta)/(k(E)+(D/\delta))]$ can be approximated to $k(E)$ and D/δ respectively under charge transfer and mass transfer control. Hence, in a potentiostatic electrolysis, by integration, one obtains:

$$\ln [OA]^{b,t}/[OA]^{b,t=o} = - \Gamma A/V\ t \tag{4.35}$$

and consequently,

$$[OA]^{b,t} = [OA]^{b,t=o} \exp(- \Gamma A/V\ t) \tag{4.36}$$

Interestingly, a slight different correlation between $[RH]^b$ and time is expected for an indirect process with the exception of the electrolyses which occur under a mass transfer control; as an example for oxidation reaction controlled processes, for an oxygen evolution based on the oxidation of the hydroxyl radical, the following expressions should apply:

$$[RH]^{b,t}-[RH]^{b,t=o} + A/V\ (k_{11}/k_{14})\ Ln\ [RH]^{b,t}/[RH]^{b,t=o} = -\ A/V\ k'(E)\ t \qquad (4.37)$$

CHAPTER 5

ELECTROCHEMICAL INCINERATION OF OXALIC ACID AT BORON DOPED DIAMOND ANODES: ROLE OF OPERATIVE PARAMETERS

5.1 INTRODUCTION

The first part of the thesis was dedicated to the study of the role of operative parameters on the electrochemical incineration of oxalic acid at BDD. The choice of this anode material was dictated by its good properties, as reported in the paragraph 2.3.2.

Oxalic acid (OA) is often the main and ultimate intermediate for the chemical and electrochemical oxidation of many organic compounds that have more than two carbons atoms in their cycle or chain and in many cases, its oxidation results to be more difficult than that of the starting compound (Gandini et al., 2000; Martinez-Huitle et al., 2004a). Hence, this acid was chosen as a very interesting model compound for its resistance to chemical and electrochemical oxidation.

In particular, electrolyses were performed at very different operative conditions with the aim of studying in a systematic way the influence of numerous parameters, such as the working potential (in potentiostatic electrolyses), the current density (in amperostatic ones), the flow rate, the OA concentration, the nature of the supporting electrolyte and the pH on the performances of the process and to individuate the optimal operative conditions.

The first experiments were carried out by maintaining the solution in acid conditions (pH = 2), while, in the last part of the study, a focused investigation on the effect of pH was carried out.

Finally, an experimental validation of mathematical model discussed in the previous chapter, in order to confirm the assumption on which the model is based, is reported in this chapter.

5.2 EXPERIMENTS AT LOW pH.

5.2.1 QUASI-STEADY POLARIZATION CURVES AND CHRONOMAPEROMETRIC MEASUREMENTS

Prior to electrochemical incineration experiments, quasi-steady polarization curves and chronoamperometric measurements were recorded in background solutions containing Na_2SO_4 and H_2SO_4, in the absence and in the presence of different concentrations of oxalic acid.

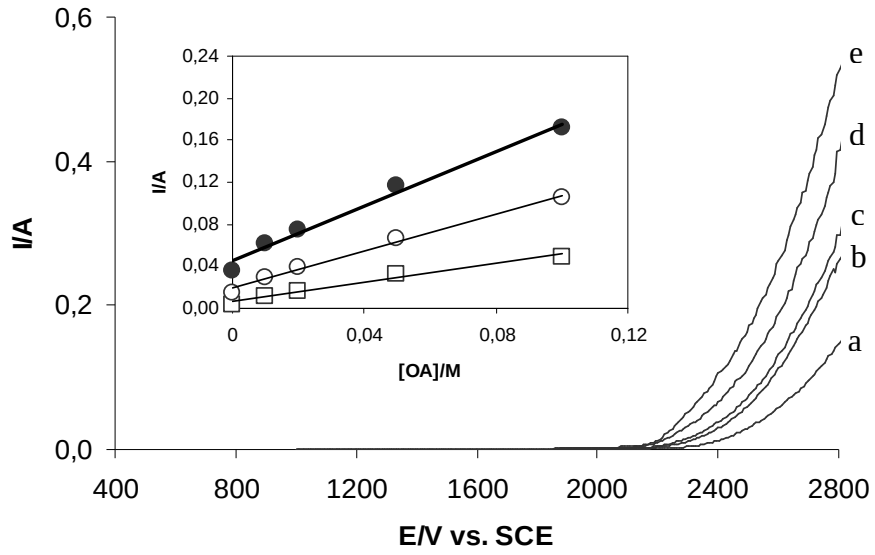

Fig. 5.1. *Current-potential curves for the BDD electrode in the presence of different amounts of oxalic acid: (a) 0; (b) 10 mM; (c) 20 mM; (d) 50 mM; (e) 100 mM. Inset: current vs. [OA] at different potentials: 2.3 ( ), 2.4 (o) and 2.5 V (•) and relative regression lines. System solvent supporting electrolyte (SSE): Water, Na_2SO_4, H_2SO_4 (pH = 2).*

As shown in Fig. 5.1, the polarization curve shifted to less positive potentials in the presence of OA and higher current densities are observed upon increasing the acid concentration. Quite interestingly, the current density increases with a linear dependence on the acid concentration.

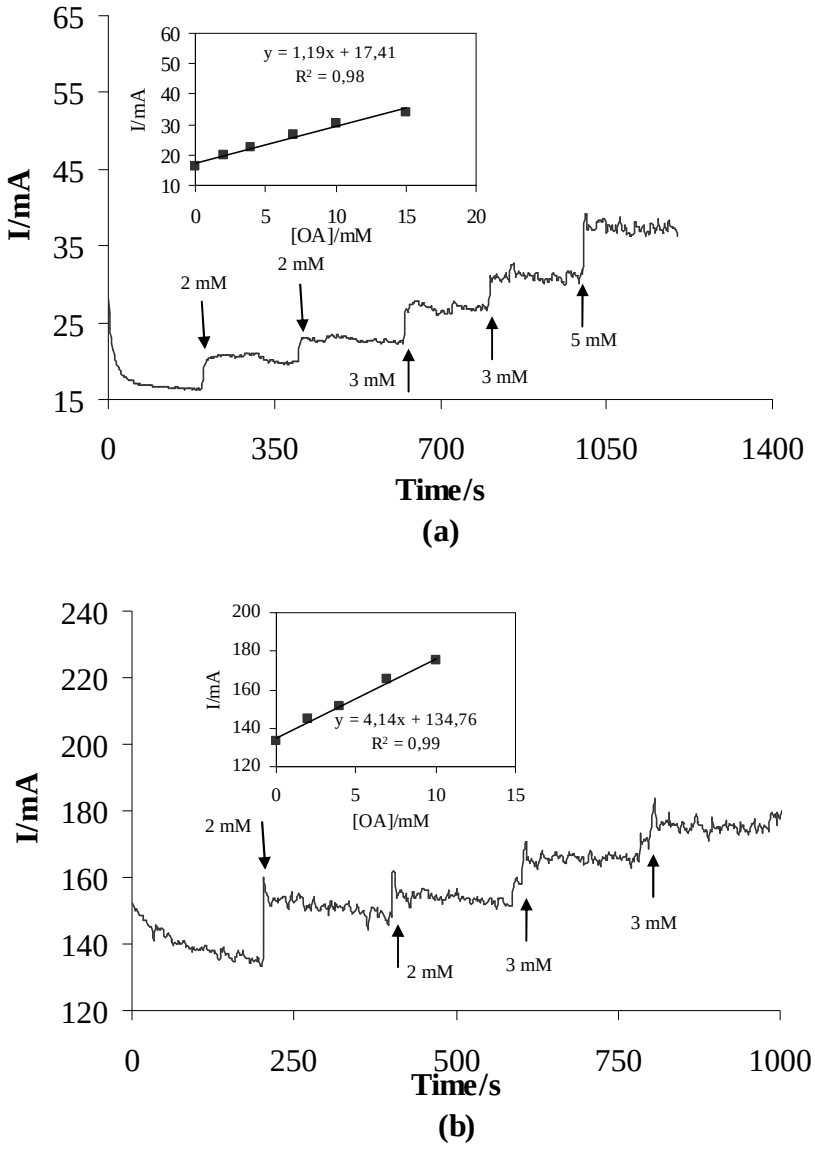

Fig. 5.2 *Chronoamperometric response of BDD anode to step-by-step injection of OA at different potentials: 2.4 V (a) and 2.7 V (b) vs. SCE. Insert shows the correspondent current increases as a function of OA concentration. System solvent supporting electrolyte (SSE): Water, Na_2SO_4, H_2SO_4 (pH = 2).*

According to Zhi et al. (2003), if the oxidation of OA occurs exclusively by the hydroxyl radical mediation, the current should be expected to be substantially independent by the acid concentration. On the other hand, it has been recently pointed out that a linear increase of the current density can be theoretically related also to the presence of an oxidation process mediated by hydroxyl radicals or to a direct anodic oxidation.

To achieve more information on the oxidation mechanism, a series of chronoamperometric measurements of current by the step-by-step injection of oxalic acid into the solution at different potentials (2.4 and 2.7 V vs. SCE) was carried out. As shown in Fig. 5.2, an increase of the steady-state current was observed, with an increasing concentration of OA, at both polarized potentials examined. Furthermore, in the adopted range of concentrations, current increased linearly with OA concentration (see inserts in Fig. 5.2).

5.2.2 INFLUENCE OF THE ANODIC POTENTIAL ON THE POTENTIOSTATIC OXIDATION EXPERIMENTS

A first set of electrolyses was performed under potentiostatic alimentation in the undivided bench-scale batch cell (see par. 3.2.2) at different applied potentials *E* with an initial $[OA]^b$ of 0.2 M. As reported in Table 5.1, in all the electrolyses the final current efficiency (*CE*) for the removal of oxalic acid was lower than 100 % as a result of the competitive oxidation of the solvent. Higher values of *E* resulted in a marked decrease of *CE* (Table 5.1). In particular, when the experiments were performed at the more positive potential adopted (2.30 V vs. SCE), a conversion of about 99%, corresponding to a final concentration of about 2 mM, was obtained after 938 minutes and a charge passed 1.3 times higher than that theoretically required for the total conversion of the acid with *CE* = 100% (Q^{th}).

Hence, the *CE* was approximately 73%. When moderate increases of *E* were adopted, to obtain the same values of conversion shorter times and higher amounts of charge (see Table 5.1 and Fig. 5.3a and 5.3b) had to pass and as consequence lower *CE* were achieved. For the electrolysis performed at more positive potentials, the conversion of 99% was obtained for Q = 4.1 Q^{th} with a final faradic efficiency of

about 22%. Hence, the utilization of low values of the working potential should be preferred to obtain high CE.

Table 5.1 *Influence of the Anodic Potential on the Incineration of Oxalic Acid*[a]

E(V) vs. ref	*CE* (%)	Conversion (%)	Time Passed (min)	Charge passed [b] (Q/Q^{th})	Initial and final Current density (mA/cm^2)	10^2 x[c] (M)	10^3 Γ[d] ($cm\ s^{-1}$)
2.30	73	99	938	1.03	34 – 5	1.07	1.00
2.35	62	99	800	1.06	98 – 7	2.03	1.08
2.40	57	98	588	1.07	136 - 10	2.08	2.02
2.50	37	99	428[e]	2.06	263 – 29	6.05	3.02
0,125	36	98	255[e]	2.06	394 – 55	7.09	5.01
0,1319	26	99	272[e]	3.06	477 - 74	12.04	5.08
0,1354	22	99	228[e]	4.01	906 - 123	16.06	5.09

[a] *potentiostatic electrolyses. Reference electrode SCE. System solvent supporting electrolyte (SSE): Water, Na_2SO_4/H_2SO_4. Initial oxalic acid concentration: 200 mM. T = 25°C.*
[b] *Q = charge passed, Q^{th} = charge necessary for a total conversion of the oxalic acid with a CE = 100%.*
[c] *x was estimated to lead to the best fit of the experimental results using Eq. 4.23 (Fig. 5.3e) or 4.33.*
[d] *Γ was estimated to lead to the best fit of the experimental results using Eq. 4.35 (Fig. 5.3f).*
[e] *Normalised time = time*(A/2.7)*(50/V) where A and V are the anode surface area and the electrolytic solution volume, respectively. A = 2.7 cm^2 and V = 50 cm^3 for the electrolyses performed at 2.30, 2.40 and 2.45 V; V = 25 cm^3 for other electrolyses; A = 1.3 cm^2 when E = 2.5 V, 1.0 when E = 2.6 and 2.7 V and 0.9 cm^2 when E = 2.75 V.*

As shown in Fig. 5.3c, a dramatic decrease of the instantaneous current efficiency (*ICE*) with the charge passed occurred during each electrolysis as a result of the diminution of [OA][b] (Fig. 5.3d).

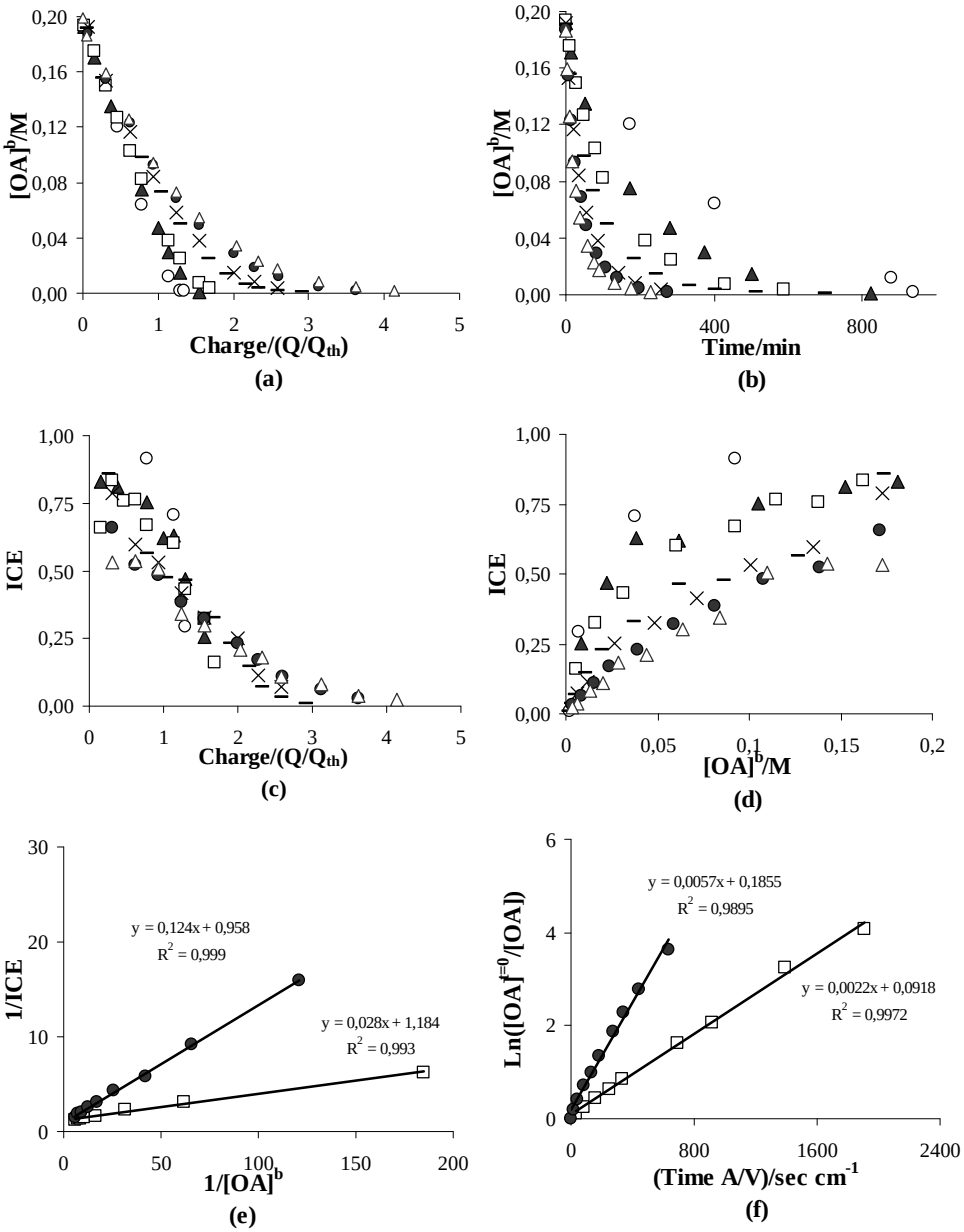

Fig. 5.3 *$[OA]^b$ vs. charge (a) and normalised time (b) passed, ICE vs. charge (c) and $[OA]^b$ (d), 1/ICE vs. $1/[OA]^b$ (e) and $\ln[OA]^{b,t=0}/\ln[OA]^{b,t}$ vs. time (f). Working potential: 2.30 V (o), 2.35 V (▲), 2.40 V (□), 2.50 V (-), 2.60 V (x), 2.70 V (•) and 2.75V (Δ). Fitting curves (—) obtained by Eq.ns 4.23 and 4.35 for Figures 5.3e and 5.3f, respectively. Experimental conditions as reported in Table 5.1.*

In particular, it is evident that quite low values of applied potential are necessary if one wants to achieve very low oxalic acid concentration in the system with at least moderate faradic efficiency. On the other hand, experiments performed at the less positive potentials present the drawback of very low current density values, especially at the end of the electrolyses, that imply very long electrolysis time (see Table 5.1 and Fig. 5.3b) to achieve high conversions.

It was observed (see Table 5.1) that during potentiostatic electrolyses a continuous decrease of current density always occurred as a result of the consumption of the acid, in agreement with the possible involvement of a direct oxidation of OA. As mentioned above, for a direct process (Eq. 4.23) under potentiostatic alimentation, $1/ICE$ should present a linear trend with $1/[OA]^b$ for any value of E. Indeed, when $1/ICE$ was plotted as a function of $1/[OA]^b$, the experimental points were well fitted by regression lines with an intercept close to 1, for all the investigated electrolyses including those operated at high values of the working potential (see, as an example, Fig. 5.3e for experiments performed at 2.40 and 2.70 V). Interestingly, as previously mentioned, for a direct process mediated by hydroxyl radicals under mass transfer control (e.g. for very positive values of the applied potential), the *ICE* should present a linear variation with the oxalic acid concentration as shown by Eq. 4.1, that was not observed in any electrolysis (see Fig. 5.3d).

For what concern the dependence with the charge passed, according to Eq.ns 4.31-4.33, plotting $\ln([OA]^{b,Q=0}/[OA]^{b,Q})$ versus $-[OA]^{b,Q=0} + [OA]^{b,Q} + Q/(nFV)$ is possible to observe a linearly dependence. In particular x was estimated from the best fit of the results using Eq.ns 4.23 or 4.33 and its value increases with the potential as expected on the basis of previous considerations (Table 5.1).

For what concern the dependence of $[OA]^b$ with the time, as observed in Fig. 5.3b, the rate of the oxalic acid oxidation decreases with the time passed and increases with E. Indeed the experimental points arranged as the $\ln [OA]^{b,t=0}/[OA]^{b,t}$ actually follow a linear trend with time, as predicted by Eq. 4.35 (as shown in Fig. 5.4f, as an example, for experiments performed at 2.40 and 2.70 V), thus leading to the estimation of Γ (see Table 5.1). The Γ value, in particular, increases with the potential even if smaller variations are observed for the more positive potentials. It is

useful to observe that, according with a rough estimation of the thickness of the stagnant layer trough a typical limiting-current essay using the redox couple hexacyanoferrate(II)/ hexacyanoferrate(III), the mass transfer coefficient $k_m = D/\delta$, should assume, under adopted conditions, a value of approximately close to the values obtained for Γ at the more positive potentials adopted (Table 5.1).

5.2.3 GALVANOSTATIC OXIDATION EXPERIMENTS

A wide set of galvanostatic experiments was performed both in the undivided bench scale batch cell (Table 5.2) and in a continuous batch recirculation reaction system (Table 5.3) at different current densities with the couple H_2SO_4–Na_2SO_4 as supporting medium.

Table 5.2. *Influence of the Current Density on the Incineration of Oxalic Acid*[a]

I/A (mA/cm^2)	*CE* (%)	Conversion (%)	Time Passed (min)	Charge passed (C)	Initial and final anodic potential vs. SCE (V)	C* (M) [b]
37	49	99%	500	3950	2.35 – 2.6	0.034
100	35	99%	263	5500	n.a.[c]	0.090
143	29	99%	215	6500	2.45- 3.0	0.13

[a] *Amperostatic electrolyses. Reference electrode SCE. System solvent supporting electrolyte (SSE): Water, Na_2SO_4, H_2SO_4 (pH = 2). Initial oxalic acid concentration: 200 mM. T = 25°C. V = 50 ml.*
[b] *$C^* = i_{app}/(2FD/\delta)$.*
[c] *Not available.*

For what concern the experiments performed in system I, is possible to observe that higher values of current density resulted in a marked decrease of the faradic efficiency of the process (Table 5.2 and Figs. 5.4a-5.4c). In particular, in experiments performed with the higher current density, the process is likely to be

under mass transfer control for a large part of the electrolyses, since the oxalic acid concentration $[OA]^b$ is lower than C* (Table 5.2) with the exception of the early stages of the electrolysis. On the other hand, in experiments performed with the lower value of current density, the process is likely to be under charge transfer control for a large part of the electrolysis (e.g [OA] > C*) and to pass under a mass transfer control only in the final part of the electrolysis (e.g [OA] < C*).

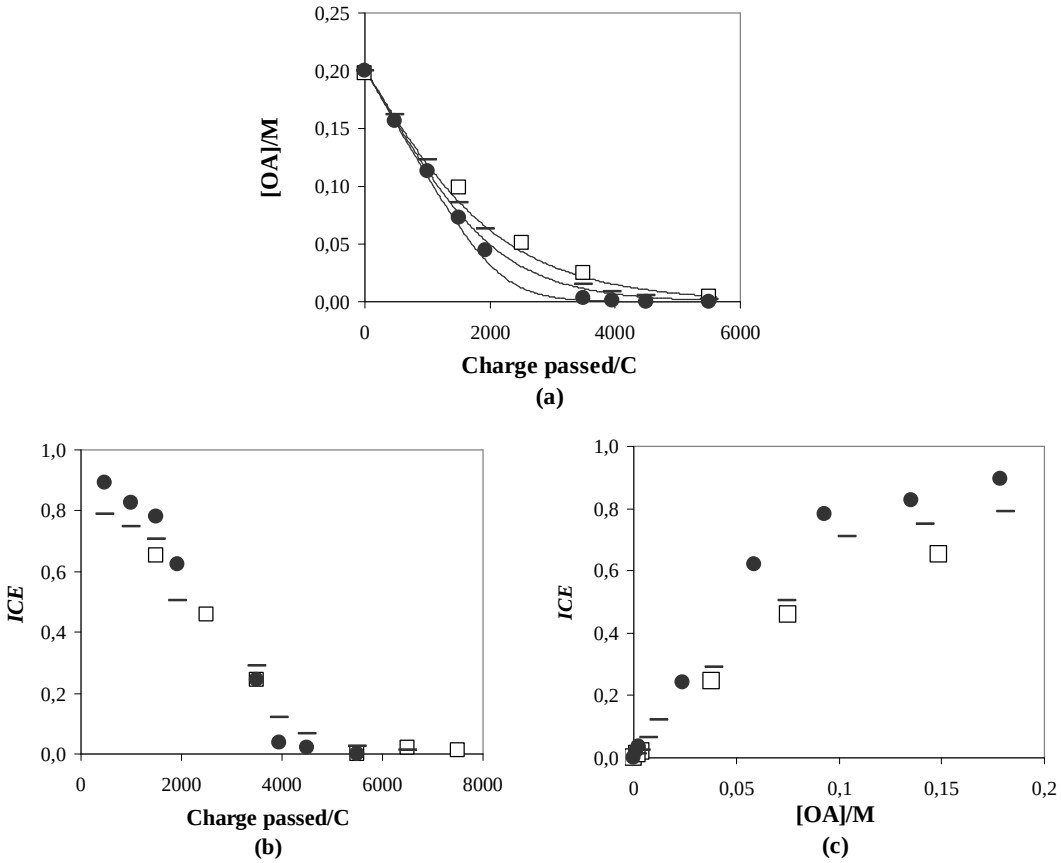

Fig. 5.4 *$[OA]^b$ vs. charge passed (a), ICE vs. charge passed (b) and $[OA]^b$ (c). Current density: 143 (□), 100 (-), 37 mA/cm^2 (•). Amperostatic electrolyses in system I. System solvent supporting electrolyte (SSE): Water, Na_2SO_4,H_2SO_4. Initial oxalic acid concentration: 200 mM. T = 25°C. Theoretical curves (—) obtained by Eq.ns 4.14 with the parameter C* reported in Table 5.2 and with [RH]* = 0.013 M (see Table 4.1).*

Hence, in order to improve the faradic efficiency of the process, on the bases of these preliminary results, it seems important to accelerate the mass transport and to operate with low current density.

It can be observed (Table 5.2) that during amperostatic electrolyses, a gradual increase of the potential with the charge passed was observed, as it is expected if a direct process is involved. As a consequence, amperostatic experiments present lower current efficiency with respect to the potentiostatic ones performed at comparable values of initial current density and initial oxalic acid concentration as a result of the increase of *E* which occurs during the amperostatic electrolyses to compensate the diminution of the acid concentration (see Tables 5.1 and 5.2). In particular (see Figs. 5.4b and 5.4c), a dramatic decrease of the instantaneous current efficiency occurred in the last stages of the experiment as a result of the low residual acid concentration and the working potential increase.

5.2.3.1 INFLUENCE OF CURRENT DENSITY AND FLOW DYNAMIC REGIME ON THE FARADAY EFFICIENCY

As reported on paragraph 2.4.3, very different results were obtained by different groups of researches when the influence of current density and flow rate are investigated separately. Thus, different operative conditions were used in these investigations. In particular, it is possible that the effect of the current density is expected to depend drastically on the hydrodynamics conditions and *viceversa*.

With the aim of evaluating in a systematic way the combined role of current density and flow dynamic regime on the performances of the process, numerous amperostatic experiments were repeated at different flow rates and current densities (Table 5.3).

As shown in Tab 5.3 and in Fig. 5.5, the influence of the flow rate on the process dramatically depends on the adopted *i*: a strong influence was observed for high (Fig. 5.5c) and intermediates values (Fig. 5.5b) while in the case of the electrolyses performed at 17 mA/cm^2 (Fig. 5.5a) a significant influence was observed only in the final part of the experiments.

Indeed, for the electrolyses performed at 17 mA/cm^2, quite low values of C* occur (see Table 5.3). Hence, the process is under charge transfer control for the most part of the electrolysis and as a consequence the flow dynamic regime plays a role only in the last part of the experiments. On the other hand, when the experiments were performed at higher current densities, C* assumes quite high values and, as a consequence, a high influence of flow dynamic regime is expected.

Table 5.3. *Influence of Current Density and of Flow rate on the Incineration of Oxalic Acid*[a]

Entry	I/A (mA/cm^2)	Flow rate (l/min)	Current Efficiency (%)	Conversion (%)	Time Passed (min)	C* (M)[b]
1	17	1.02	67 – 69	98 - 99	778	0.006
2	39	1.02	64 – 66	94 - 96	334	0.015
3	56	1.02	63 – 66	90 – 92	233	0.021
4	17	0.05	65 – 67	95 - 97	778	0.013
5	39	0.05	58 – 60	88 - 90	334	0.042
6	17	0.02	65 – 67	93 - 96	778	0.019
7	39	0.02	56 – 58	82 - 84	334	0.044
8	56	0.02	56 – 58	77 - 79	233	0.063

[a] *amperostatic electrolyses. System solvent supporting electrolyte (SSE): Water, Na_2SO_4, H_2SO_4. Initial oxalic acid concentration: 100 mM. T = 25°C. Charge passed = 7000 C = 1.45 Q^{th}, where Q^{th} = charge necessary for a total conversion of the oxalic acid with a CE = 100%. V = 250 ml.*

[b] $C^* = i_{app}/(2FD/\delta)$.

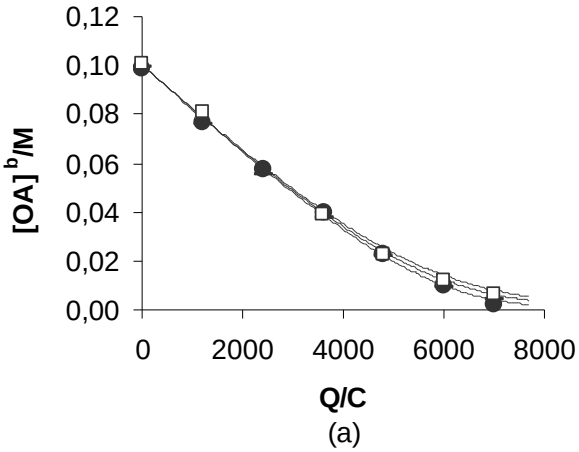

(a)

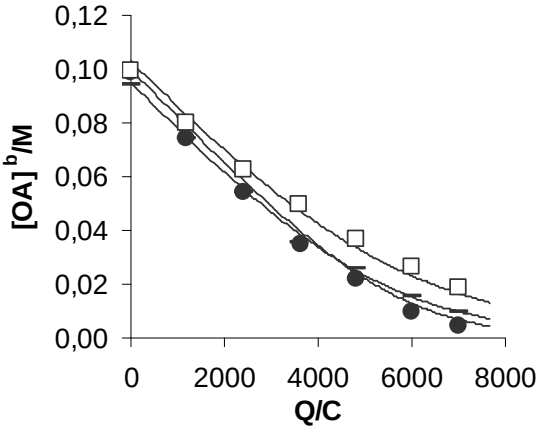

(b)

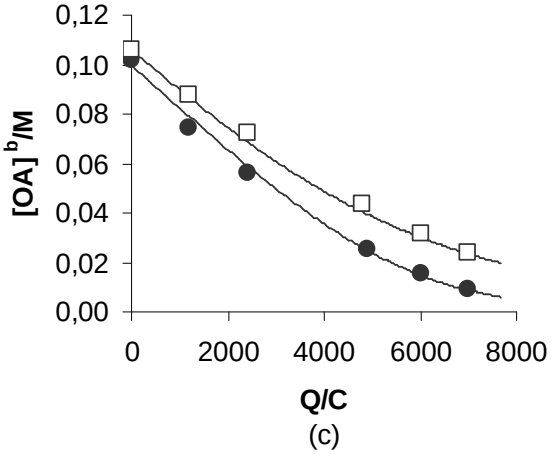

(c)

Fig. 5.5a-5.5c *Profile of oxalic acid concentration vs. charge passed for electrolysis performed with 17 (a), 39 (b), 56 mA/cm^2 (c) at different flow rates. Flow rate: 0.2 (□), 0.5, (-) 1.2 l/min (•). Amperostatic electrolyses in system II. Theoretical curves (—) obtained by Eq.4.14 with the parameter C* reported in Table 5.3 and with [RH]* = 0.013 M (see Table 4.1). System solvent supporting electrolyte (SSE): Water, Na_2SO_4,H_2SO_4. Initial oxalic acid concentration: 100 mM. T = 25°C.*

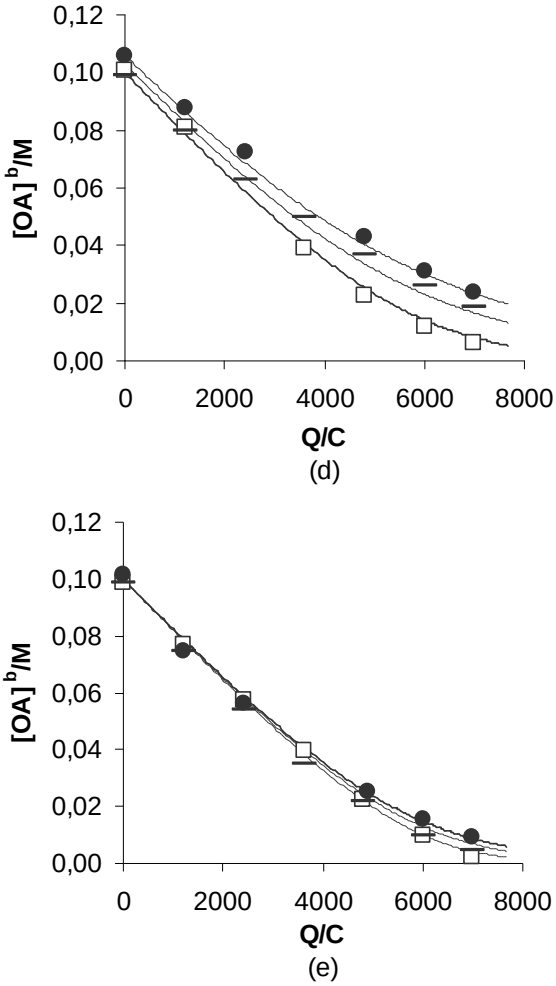

Fig. 5.5d and 5.5e *Data of figures 5.4a-5.4c re-plotted as profile of oxalic acid concentration vs. charge passed for electrolysis performed with 0.2 (d) and 1.2 (e) l/min at different current density. Current density: 17 (□), 39 (-) and 56 (•) mA/cm^2. Theoretical curves (—) obtained by Eq.4.14 with the parameter C* reported in Table 5.3 and with [RH]* = 0.013 M (see Table 4.1).*

When one compares the experiments performed at constant flow rate, the consumption of oxalic acid strongly depends on the current density at the lower value of the flow rate while only a small influence is observed at the higher value of flow rate (Figs. 5.4d and 5.4e).

5.2.3.2 INFLUENCE OF SUBSTRATE CONCENTRATION

To evaluate the role of the acid concentration on the performances of the process, amperostatic experiments were repeated in the best adopted conditions

(flow rate 1.2 l/min, current density: 17 mA/cm^2) at different values of the initial oxalic acid concentration (0.01, 0.05, 0.1 and 0.2 M).

As shown in Fig. 5.6 and according with theoretical previsions, the performances of the process dramatically depend on the OA concentration.

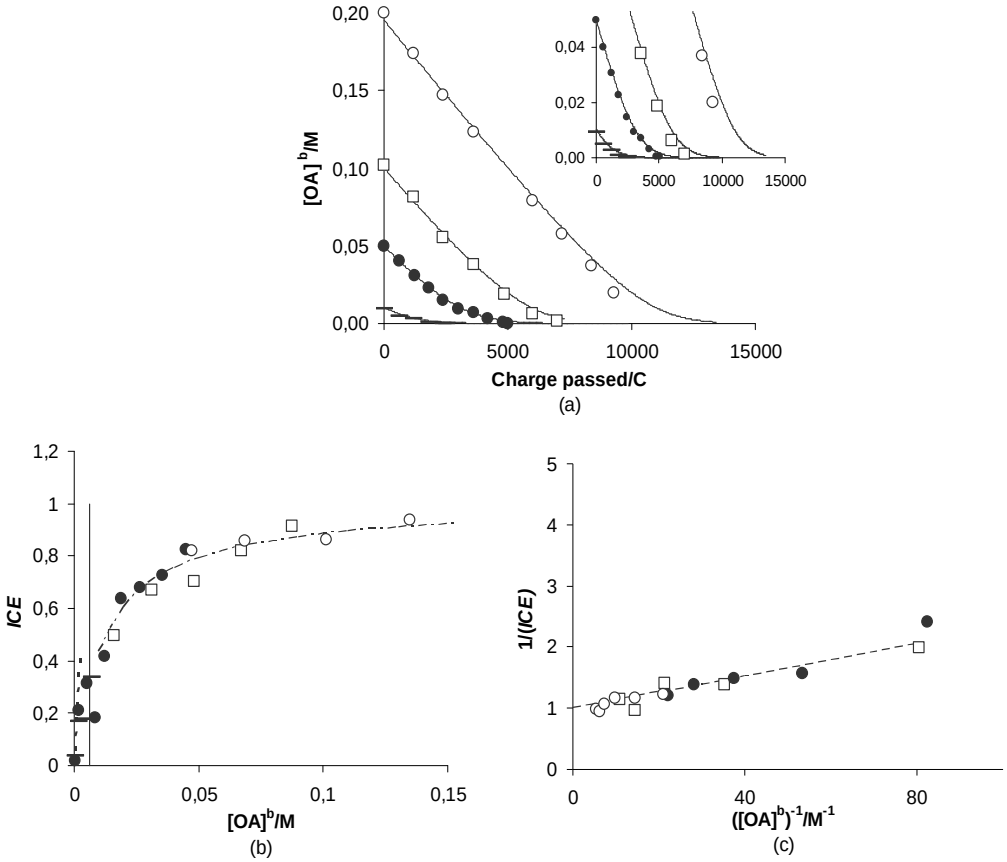

Fig. 5.6 *Oxalic acid concentration vs. charge passed (a), ICE vs. [OA]^b (b) and 1/ICE vs 1/[OA]^b (c). Initial substrate concentration: 0.01 (-), 0.05 (•), 0.1 (□) and 0.2 M (o). Flow rate: 1.2 l/min. Current density: 17 mA /cm^2. Amperostatic electrolyses. System solvent supporting electrolyte (SSE): Water, Na_2SO_4,H_2SO_4. T = 25°C. Theoretical curves (—) in Fig. 5.6a obtained by Eq.ns 4.14 with the parameter C* reported in Table 5.3 and with [RH]* = 0.013 M. Theoretical curves in Figures 5.6b and 5.6c (---) obtained by Eq.ns 4.6 and 4.1 with the parameter C* reported in Table 5.3 and with [RH]* = 0.013 M.*

In particular, the instantaneous current efficiency depends on $[OA]^b$ and not on the charge passed Q, thus confirming that the performances of the electrode are not affected by Q. In particular, the plot of *ICE* vs. $[OA]^b$ (Fig. 5.6b) has a profile consisting in an initial very rapid linear rise followed by a very slow increment towards values higher than 90%. This kind of profile can be associated to the fact that at low substrate concentrations the process is mass transfer controlled ($[OA]^b < C^*$) and as consequence the *ICE* is a linear function of $[OA]^b$ (see Eq. 4.1) while at higher values of concentration ($[OA]^b >> C^*$) the process is under charge transfer control and 1/ICE is expected to be a linear function of $1/[OA]^b$ (see Eq. 4.6).
Indeed, as shown by Figures 5.6b and 5.6c, the experimental data are well fitted by Eq. 4.1 when $[OA]^b < C^*$ and by Eq. 4.6 when $[OA]^b >> C^*$.

5.2.3.3 EFFECT OF THE NATURE OF THE SUPPORTING ELECTROLYTE

In order to study the influence of supporting electrolyte on the performances of the process, we have performed two set of experiments at very different operative conditions:

- set 1 (Fig. 5.7a): initial acid concentration 0.1 M, current density 17 mA/cm^2, flow rate 1.2 l/min, supporting electrolytes: Na_2SO_4-H_2SO_4 and K_3PO_4-H_3PO_4;
- set 2 (Fig. 5.7b): acid concentration 0.01 M, current density 39 mA/cm^2, flow rate 0.2 l/min, supporting electrolyte: Na_2SO_4-H_2SO_4, $HClO_4$ and K_3PO_4-H_3PO_4.

It can be observed (see Fig. 5.7) that in any case, the nature of the supporting medium has a marked influence on the degradation of oxalic acid.

5.3 EFFECT OF pH

To investigate the role of pH, we have performed various experiments, including quasi-steady polarization curves, chronoamperometric measurements and potentiostatic and galvanostatic incineration electrolyses using different concentrations of H_2SO_4 and NaOH. As shown in Fig. 5.1 and 5.8, very different quasi-steady polarization curves were recorded in acid and basic conditions. As

previously mentioned, in acid conditions (pH = 2) the polarization curve shifted to more positive potentials in the presence of OA and the current density increases with a linear dependence on the acid concentration (Fig. 5.1).

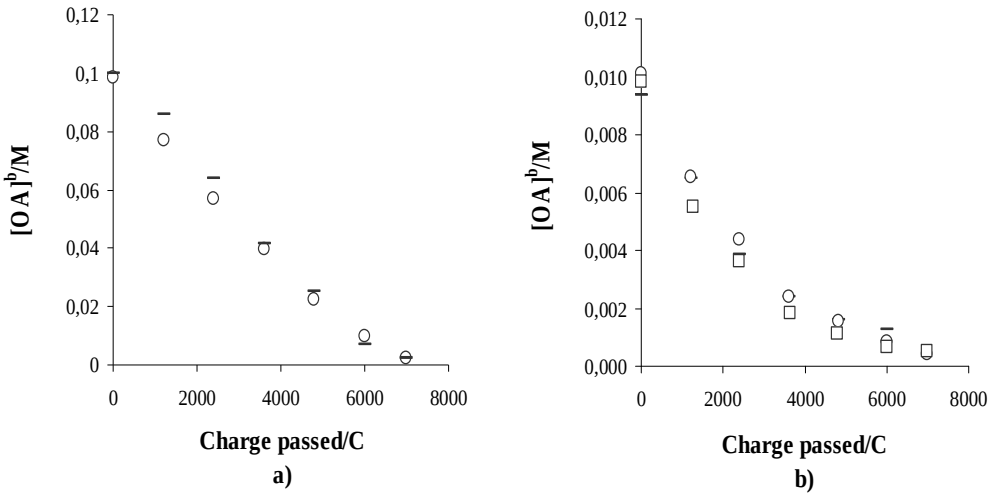

Fig. 5.7 *Oxalic acid concentration vs. charge passed. Fig. 5.7a: initial substrate concentration: 0.1 M, flow rate 1.2 l/min, current density: 17 mA /cm^2. Supporting electrolyte: Na_2SO_4-H_2SO_4 (o) and K_3PO_4-H_3PO_4 (-). Fig. 5.7b: initial substrate concentration: 0.01 M, flow rate 0.2 l/min, current density: 39 mA /cm^2. Supporting electrolyte: Na_2SO_4-H_2SO_4 (o), $HClO_4$ (□) and K_3PO_4-H_3PO_4 (-). Amperostatic electrolyses in system II. T = 25°C. pH = 2*

On the other hand, when OA was added to the solution at pH of about 13, a very low effect on the polarization curve was observed, thus suggesting a lower effective oxidation process.

Chronoamperometric measurements performed in basic conditions are reported in Fig. 5.9. At 2.4 V for the first three additions, the current remained constant or decreased, but gradually increased with further addition of OA, thus showing the possible simultaneous occurrence of different processes such as an hydroxyl radical-mediated reaction, a possible adsorption phenomenon such as that observed by Chang et al. (2006) for the oxidation of formaldehyde at BDD and a direct oxidation at the electrode surface, the last one being detectable at higher OA concentrations.

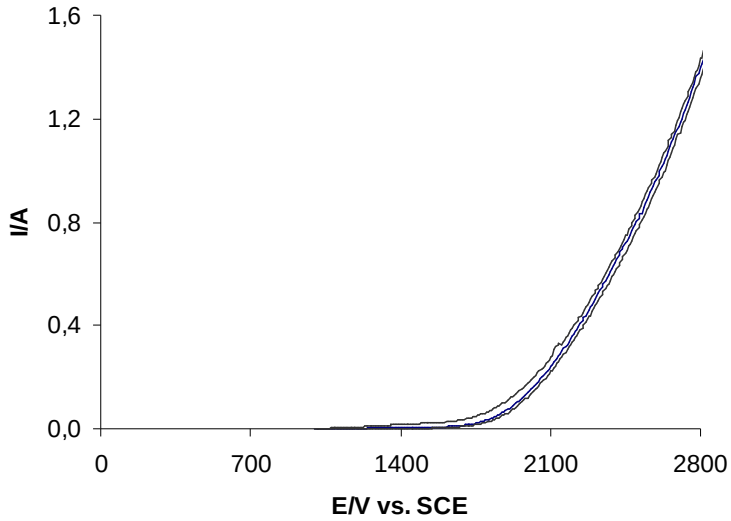

Fig. 5.8 *Current-potential curves in basic conditions for the BDD electrode in the presence of different amounts of oxalic acid: (a) 0; (b) 10 mM; (c) 20 mM. System solvent supporting electrolyte (SSE): Water, NaOH (0.25 M).*

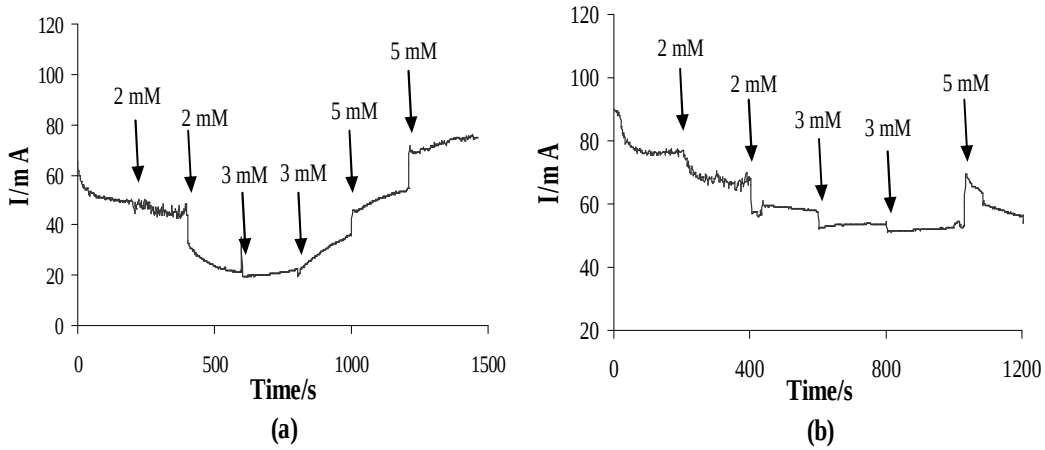

Fig. 5.9 *Chronoamperometric response of BDD anode to step-by-step injection of OA at different potentials: 2.4 V (a) and 2.7 V (b) vs. SCE. System solvent supporting electrolyte (SSE): Water, NaOH (initial pH = 12).*

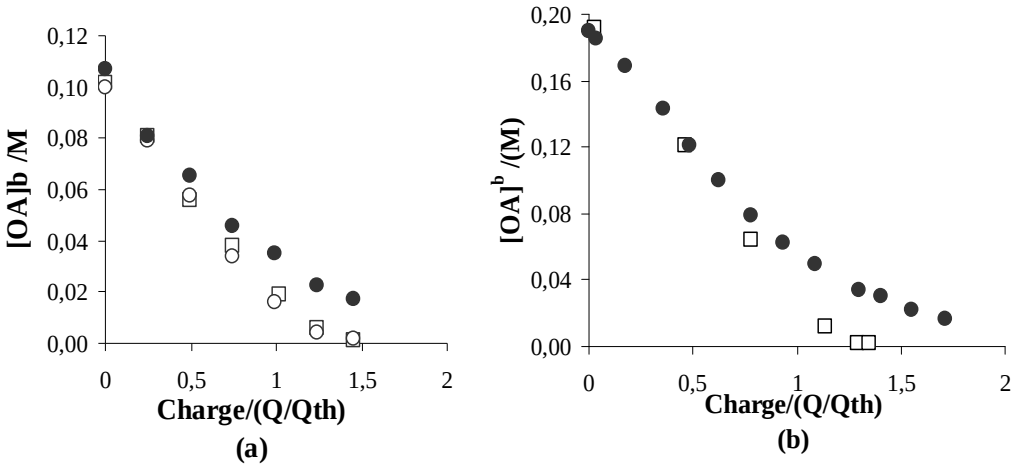

Fig. 5.10 *Oxalic acid concentration vs. charge passed as a function of pH in electrolyses performed under amperostatic (a) and potentiostatic (b) alimentation. Initial pH: 0.3 (o), 2 (□),and 12 (•). Experimental conditions for amperostatic electrolyses: initial substrate concentration: 0.1 M., Flow rate: 1.2 l/min, Current density: 17 mA /cm^2; system II. T = 25°C. Experimental conditions for potentiostatic electrolyses: initial substrate concentration: 0.2 M, E = 2.3 V vs. SCE, system I. T = 25°C.*

When the chronoamperometric measurements were performed at 2.7 V, a higher oxalic acid concentration was necessary to observe a slight increase of the current, according to the fact that at higher potentials hydroxyl radical-mediated reactions are likely to be more favored with respect to direct oxidation.

As shown in Fig. 5.10, when selected experiments were repeated at different values of pH, both with galvanostatic and potentiostatic alimentation, the decrease of the acid content in solution assumes different profiles in acid and alkaline media. In particular, according with literature data, higher faradic efficiencies are obtained in acid media.

5.4 COMPARISON WITH A THEORETICAL MODEL

As previously presented, a good qualitative agreement between theoretical predictions based on the direct anodic oxidation of oxalic acid and experimental

results collected at low pH was observed. In the following we wish to evaluate if also a quantitative agreement can be observed.

Let us focus our attention first, on a process kinetically controlled completely by mass transfer. This was realised by an electrolysis performed in system I with an amperostatic alimentation, a current density of about 15 mA/cm^2 and an initial acid concentration of 7 mM. In these conditions C* can be estimated to be about 14 mM and as a consequence $[OA]^b < C^*$ for the entire electrolysis. Hence, according to Eq. 4.3, in Fig. 5.11 is possible to observe that experimental results are in good agreement with the theoretical predictions.

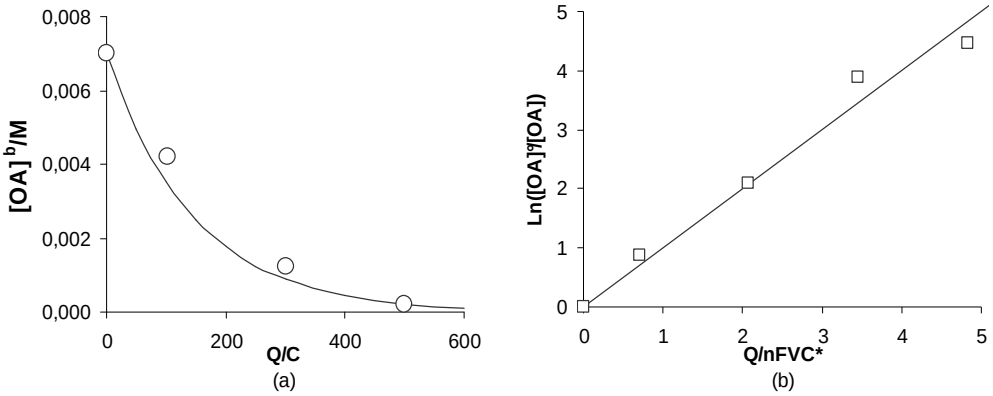

Fig. 5.11 *$[OA]^\upsilon$ vs. charge passed (a) and $ln[OA]^\upsilon/[OA]^\upsilon$ vs. Q/(nFVC*) (b). Amperostatic electrolyses in system **I.** System solvent supporting electrolyte (SSE): Water, Na_2SO_4, H_2SO_4. Initial oxalic acid concentration: 7 mM. T = 25°C. Current density: 15 mA/cm^2. Theoretical curves (—) obtained by Eq. 4.3a with the parameter C* = 0.014 M.*

Let us consider now a process completely controlled by oxidation reaction control regime. This situation arises if one considers, as an example, the electrolyses performed at maximum flow rate with the lower adopted current intensity and the higher initial oxalic acid concentrations. In this case, C* assumes a very low value and as a consequence the process is under charge transfer control for the major part of the electrolysis up to conversion of about 90%.

Hence, experimental data should be in agreement with previsions of Eq. 4.6b. Indeed, when a value of 0.013 M was used for *[RH]**, experimental results are in a

very good agreement with theoretical predictions in the two particular cases of processes purely controlled by charge transfer or mass transfer.

Let now us discuss the general case of a process whose rate determining step during the electrolysis changes from charge transfer control in the first stages to mass transfer control in the last part with a mixed regime between them. In this case a general expression for the instantaneous current efficiency has to be adopted (see Eq. 4.14) and the profiles of the oxalic acid concentration during the electrolysis as a function of charge or time passed can be numerically computed by combining Eq.ns 4.14a and 4.14b, that are functions of the parameters *[RH]** and C*. The last parameter has been estimated for all the experienced electrolyses (Tables 5.2 and 5.3).

Furthermore, by considering again, in a first approximation approach, *[RH]** not to be dependent on the working potential (see paragraph 4.4), this parameter should assume a constant value during all the experiments and as consequence can be computed as a fitting parameter.

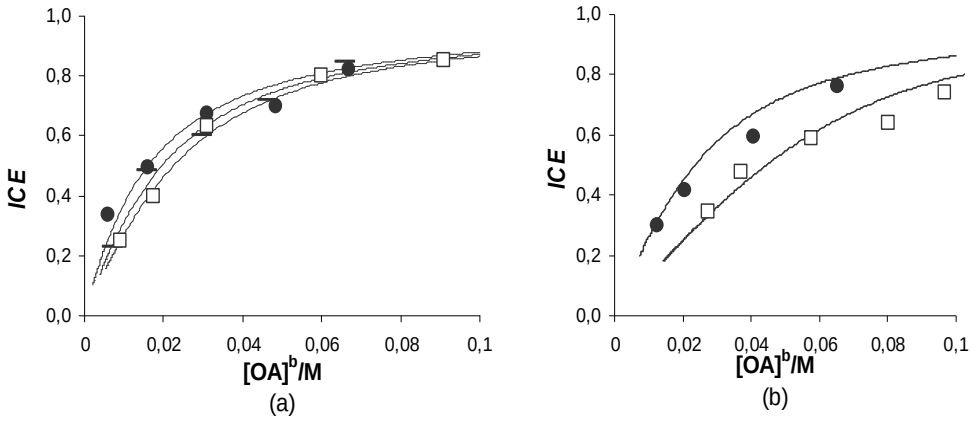

Fig. 5.12 *Data of electrolysis reported in figures 6a and 6c, plotted as ICE vs. $[OA]^b$. Electrolysis performed in system II with 17 (a), 56 mA/cm^2 (b) at different flow rates. Flow rate: 0.2 ( ), 0.5 (-) 1.2 l/min (•).Theoretical curves (—) obtained by Eq.ns 4.14 with the parameter C* reported in Table 5.3 and with [RH]* = 0.013 M.*

Indeed, all the performed experiments gave a profile of *ICE* vs. $[OA]^b$ (see as an example Fig. 5.12a and 5.12b) and of $[OA]^b$ vs. charge passed (see Figures 5.4a, 5.5a-5.5e and 5.6a) in very good agreement with the theoretical predictions when a unique value of 0.013 M was used for *[RH]** (see Table 4.1).

It is interesting to observe that the parameter $x = k'(E)/k(E)$ (see Eq. 4.23) can be computed by the ratio between the intercept (*p*) and the slope (*s*) of regression lines relative to current densities data recorded in the presence of different amounts of OA when the oxidation process is under charge transfer control (e.g. at very low values of *E*). Since the current densities recorded during quasi-steady polarization curves at low pH present for each value of *E* a linear dependence on the acid concentration, it was possible to roughly compute this ratio as a function of *E* and, interestingly, it presents a lower value of about 0.014 M, very close to that derived by the fitting of incineration data with theoretical predictions (see above).

CHAPTER 6

ELECTROCHEMICAL OXIDATION OF OXALIC ACID AT DSA ANODE

6.1 INTRODUCTION

Among the operative parameters that can influence the performances of the electrochemical oxidation process, anodic material is by far the most important.
In order to study the effect of the anodic material, we have performed a set of experiments on the electrochemical oxidation of oxalic acid at IrO_2/Ta_2O_5 anode.
As in the case of electrochemical oxidation at BDD surface, a comparison of theoretical predictions and experimental data was carried out at the end of the chapter.
Furthermore, a comparison between results obtained in the case of the experiments performed at BDD and DSA anodes will be reported.

6.2 QUASI-STEADY POLARIZATION CURVES

Prior to electrochemical incineration experiments, quasi-steady polarization curves and chronoamperometric measurements were recorded in background solutions containing Na_2SO_4, in the absence and in the presence of different concentrations of oxalic acid both in acidic and basic conditions. As shown in Fig. 6.1, the polarization curves at pH of 2 and 12 shifted to less positive potentials in the presence of OA and current density *i* increased with a linear dependence on the OA concentration for a fixed value of the potential *E*.

6.3 CHRONOAMPEROMETRIC MEASUREMENTS

6.3.1 EFFECT OF THE POTENTIAL

To achieve more information on the oxidation mechanism, a series of chronoamperometric measurements of current by the step-by-step injection of oxalic acid into the solution at different fixed potentials (1.5 and 1.8 V vs. SCE) was carried out at pH of 2.

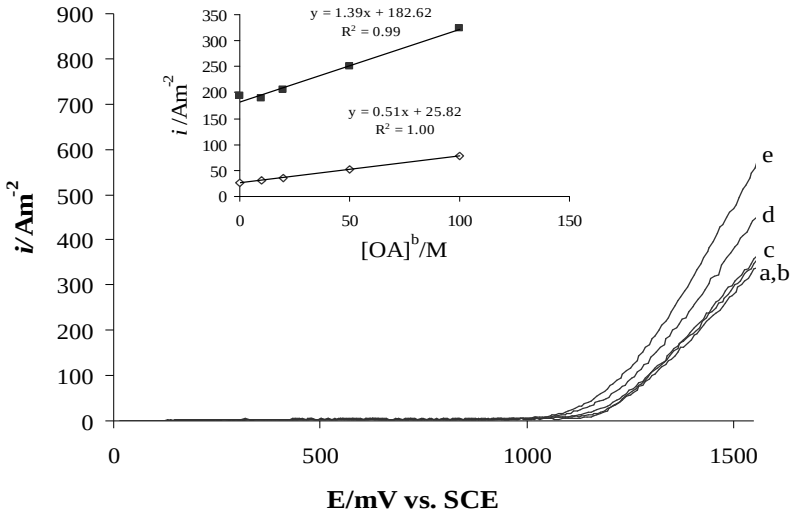

(a)

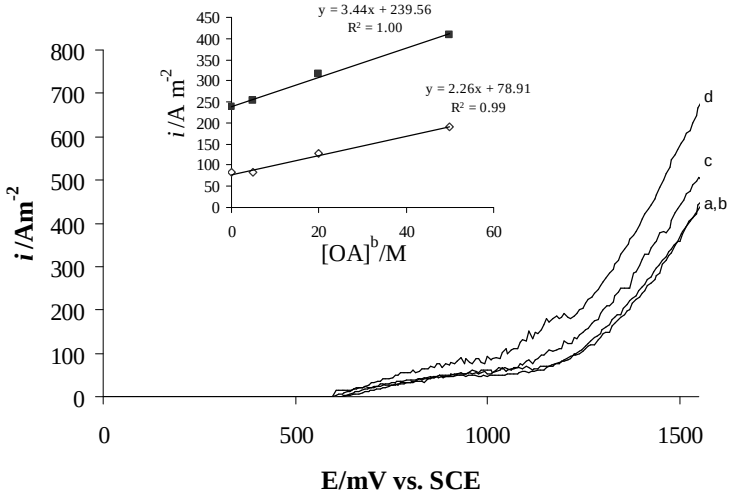

(b)

Fig. 6.1. *Current density - potential curves for the IrO_2-Ta_2O_5 electrode at pH of 2 (Fig. 1a) and 12 (Fig. 1b) in the presence of different amounts of oxalic acid: (a) 0; (b) 10; (c) 20; (d) 50; (e) 100 mM. (Inset) Current vs. $[OA]^b$ at different potentials: 1.2 (◊) and 1.4 (■) V and relative regression lines. Temperature: 25°C. System solvent supporting electrolyte (SSE): Water, Na_2SO_4, H_2SO_4 (pH = 2) or NaOH (pH = 12).*

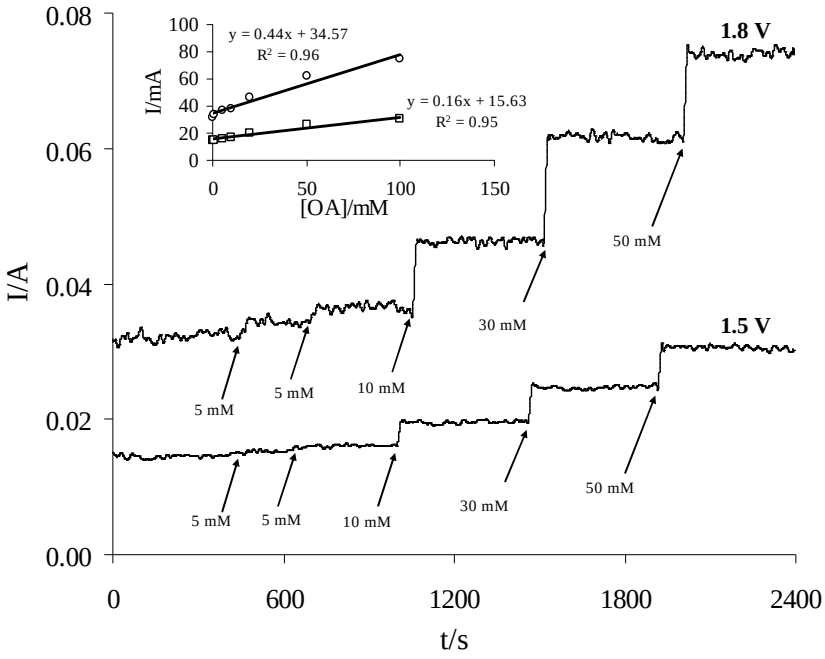

Fig. 6.2 *Chronoamperometric response of IrO_2-Ta_2O_5 anode to step-by-step injection of OA at different potentials: 1.5 V and 1.8 V vs. SCE. Inset shows the correspondent current increase as a function of OA concentration. Temperature: 25°C. System solvent supporting electrolyte (SSE): Water, Na_2SO_4, H_2SO_4 (pH = 2).*

As shown in Fig. 6.2, an increase of the steady-state current was observed, with an increasing concentration of OA, at both polarized potentials examined.

Furthermore, in the adopted range of concentrations, current increased linearly with OA concentration (see inset in Fig. 6.2). Hence, chronoamperometric measurements and quasi-steady polarization may indicate that electrochemical incineration of OA can be at least partially attributed to the direct electrochemical oxidation pathway on the surface of the IrO_2 based anode. Interestingly, also in the case of the anodic oxidation of OA at BDD the occurrence of a direct oxidation process was observed, as discussed in the precedent chapter. This is probably due to the fact that OA is expected to be rather resistant to mediated oxidation processes by means of hydroxyl radicals (Scialdone, 2009) or “adsorbed oxygen” (Comninellis, 1994). For the sake of comparison, let us compare the chronoamperometric measurements of current by the step-by-step injections of OA and of a phenol derivative, the 4-methoxy-phenol.

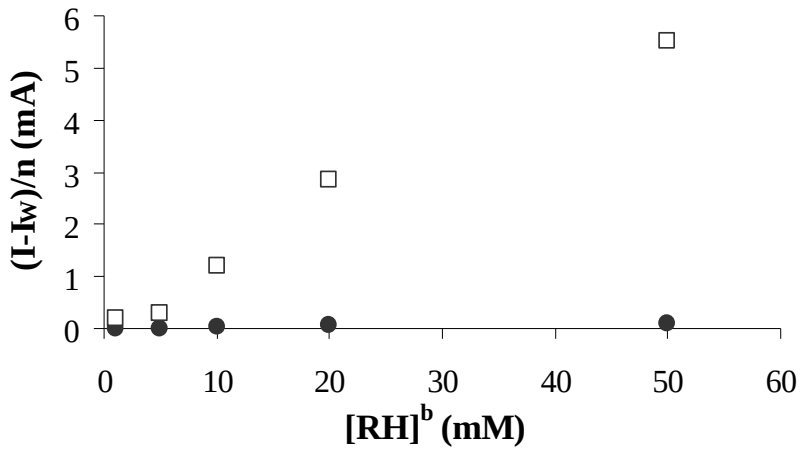

Fig. 6.3 (*I-Iw)/n detected during the chronoamperometric response of IrO_2-Ta_2O_5 anode to step-by-step injection of OA (□) and 4-methoxy-phenol (•) at 25°C at 1.5 V vs. SCE where Iw is the current recorded in the absence of the organic and n is the number of electrons necessary to achieve the total oxidation of the compound. System solvent supporting electrolyte (SSE): Water, Na_2SO_4, H_2SO_4 (pH = 2).*

As shown in Fig. 6.3, the additions of the phenol derivative gives rise to a negligible increase of the current density normalized to the number of electrons necessary for the total oxidation with respect to the case of OA, thus confirming that for the oxalic acid the direct anodic oxidation is of particular relevance with respect to phenolic compounds where, according to literature (Comninellis, 1994), the oxidation is likely to take place by means of adsorbed "oxygen".

6.3.2 EFFECT OF THE TEMPERATURE

A strong effect of temperature towards the electrochemical incineration of oxalic acid was reported by the group of prof. De Battisti (see par. 2.4.5). Thus, polarization curves, performed at DSA anode, were also repeated at a pH of 2 and at a fixed potential of 1.5 V at higher values of the temperature. As shown in Fig. 6.4, higher temperatures resulted in a more marked increase of the current density with the $[OA]^b$, thus probably indicating that at higher values of temperature the OA anodic oxidation process becomes more favorite with respect to water oxidation.

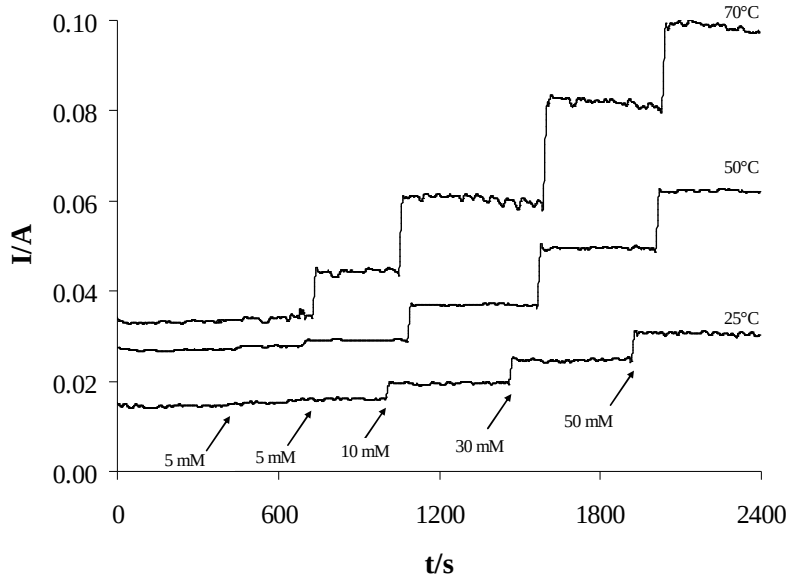

(a)

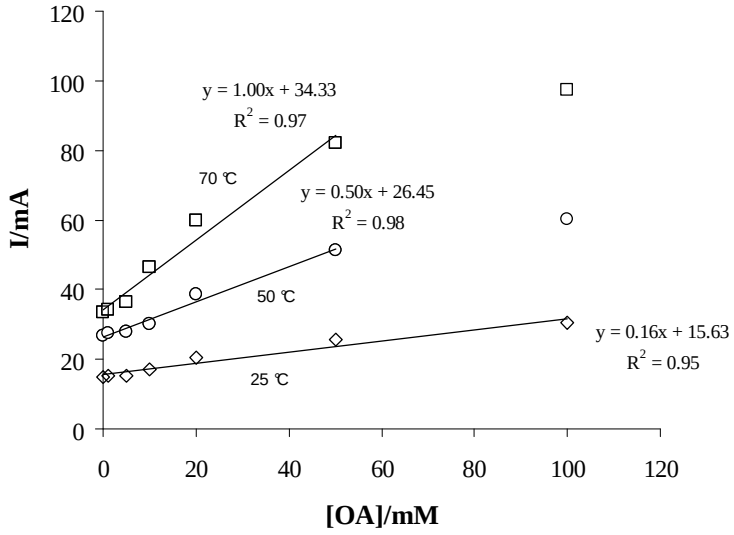

(b)

Fig. 6.4 *Chronoamperometric response of IrO_2-Ta_2O_5 anode to step-by-step injection of OA at 25, 50 and 70 °C at 1.5 V vs. SCE (Fig. 6.4a). Fig. 6.4b shows the correspondent current increases as a function of OA concentration. System solvent supporting electrolyte (SSE): Water, Na_2SO_4, H_2SO_4 (pH = 2).*

It is possible to observe that at temperatures of 50 and 70°C a linear relationship between current density and $[OA]^b$ does not occur for the higher values of $[OA]^b$, thus probably reflecting the fact that at high OA concentrations, quasi-saturation of active sites is likely to be involved.

6.4 ELECTROLYSES

6.4.1 INFLUENCE OF SUBSTRATE CONCENTRATION

A first set of electrolyses was performed with a current density of 39 mA/cm^2, a flow rate of 0.2 l/min, a pH of 2, a T = 25 °C and an initial OA concentration of 0.1 M. The electrolyses were stopped when the charge passed was 7000 C = 1.45 Q^{th}, where Q^{th} = charge necessary for a total conversion of the oxalic acid with a *CE* = 100%. At the end of the experiments a conversion of only about 68% with a current efficiency slightly lower than 50% was achieved (Table 6.1, entry 1).
When the experiment was repeated with a lower initial $[OA]^b$, of 10 mM (Table 6.1, entry 2), a dramatic decrease of the current efficiency arises. Indeed, a conversion of about 60 % was achieved after 3600 C = 7.5 Q^{th} with a final CE of about only 8% caused by the fact that $[OA]^b$ in this case is always significantly lower than $C^* = i_{app}/(2Fk_m)$ so that the ratio $i_{lim}/i_{app} << 1$ and as a consequence most part of the charge passed gives rise to the oxygen evolution reaction (Scialdone, 2009).

6.4.2 INFLUENCE OF pH

To investigate the effect of pH on the incineration of OA at IrO_2 based anodes, we have repeated some galvanostatic incineration experiments at a pH of 12. As shown in Fig. 6.5a and in Table 6.1 (entries 1 and 7), when the experiments are carried with an initial OA concentration of 0.1 M, according with literature data, higher faradic efficiencies are obtained in acid media. Otherwise, when the experiments were carried out with an initial substrate concentration of 10 mM, a less significant effect of pH on the abatement of OA was observed (Fig. 6.5b and Table 6.1, entries 2 and 8). This is probably due to the fact that under these conditions the OA concentration is dramatically lower than C*, the process is prevalently under

mass transfer control and as a consequence the performances of the process are expected to depend mainly on parameters which are not pH dependent such as the flow dynamic regime of the system, the current density and $[OA]^b$ (Scialdone, 2009).

Table 6.1. *Influence of Operative Parameters on the Incineration of Oxalic Acid*[a]

Entry	$[OA]^{b,t=0}$ (M)	pH	I/A (mA/cm^2)	Flow rate (l/min)	Current Efficiency (%)	Conversion (%)	Time Passed (min)	C* (M) [b]
1	0.1[c]	2	39	0.02	45 – 49	66 – 70	334	0.076
2	0.01[d]	2	39	0.02	6 – 10	59 -63	172	0.076
3	0.1[c]	2	17	1.02	62 – 66	91 – 95	778	0.009
4	0.1[c]	2	39	1.02	61 – 65	90 – 94	334	0.020
5	0.1[c]	2	17	0.02	62 – 66	91 - 95	778	0.032
6	0.1[c]	12	17	1.02	20 – 24	29 – 33	778	0.009
7	0.1[c]	12	39	0.02	20 – 24	30 – 34	334	0.076
8	0.01 [d]	12	39	0.02	3 – 8	48 – 54	172	0.076
9	0.35 [e]	12	56	1.02	61 – 65	97 - 99	847	0.028

[a] *amperostatic electrolyses. System solvent supporting electrolyte (SSE): Water, Na_2SO_4, H_2SO_4 or NaOH. T = 25°C. V = 250 ml.*
[b] *$C^* = i_{app}/(2FD/\delta)$.*
[c] *Charge passed = 7000 C = 1.45 Q^{th} where Q^{th} = charge necessary for a total conversion of the oxalic acid with a CE = 100%*
[d] *Charge passed = 3600 C = 7.5 Q^{th}.*
[e] *Charge passed = 25410 C = 1.5 Q^{th}.*

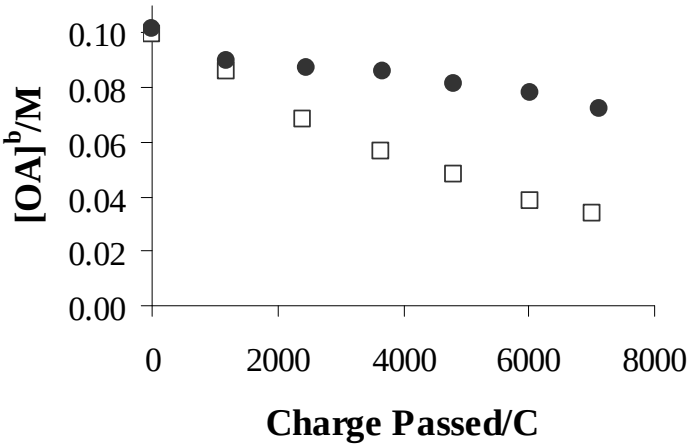

(a)

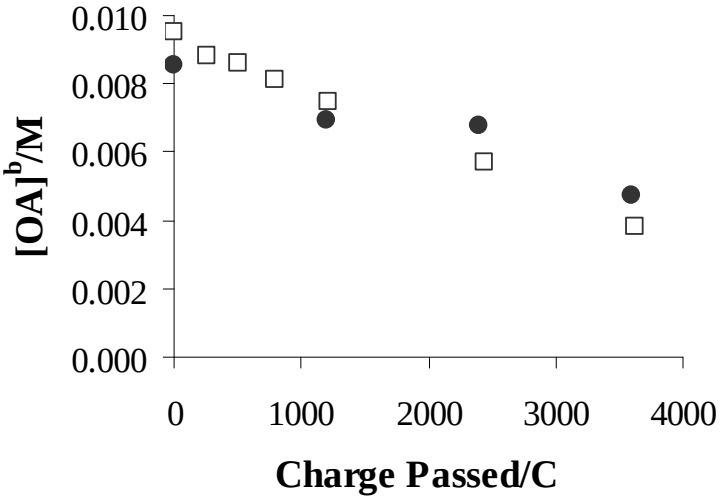

(b)

Fig. 6.5 *Oxalic acid concentration vs. charge passed as a function of pH. Initial pH: 2 (□) and 12 (●). Initial substrate concentration: 0.1 (a) and 0.01 (b) M. Experimental conditions: Amperostatic alimentation, Flow rate: 0.2 l/min, Current density: 39 mA/cm^2, T = 25°C.*

6.4.3 INFLUENCE OF CURRENT DENSITY AND FLOW DYNAMIC REGIME

It has been previously shown that the flow rate and the current density can affect dramatically the performances of the electrochemical incineration. Moreover, we showed in the precedent chapter that the current density and the flow rate effects depend on each other.

Hence, in order to evaluate the effect of both the parameters on the performances of the process, some experiments were carried out at pH of 2 by changing both the flow rate (from 0.2 to 1.2 l/min) and the current density (from 17 to 39 mA/cm^2).

As shown in Table 6.1 and in Fig. 6.6, the influence of the flow rate on the process dramatically depends on the adopted current density: a strong influence was observed for high values (Fig. 6.6a and Table 6.1, entries 1 and 4) while in the case of the electrolyses performed at 17 mA/cm^2 (Fig. 6.6b and Table 6.1, entries 3 and 5) a very small effect was observed. Indeed, for the electrolyses performed at 17 mA/cm^2, quite low values of C* occur (see Table 6.1). Hence, the process is under charge transfer control for the most part of the electrolysis and as a consequence the flow dynamic regime plays a role only in the last part of the experiments.

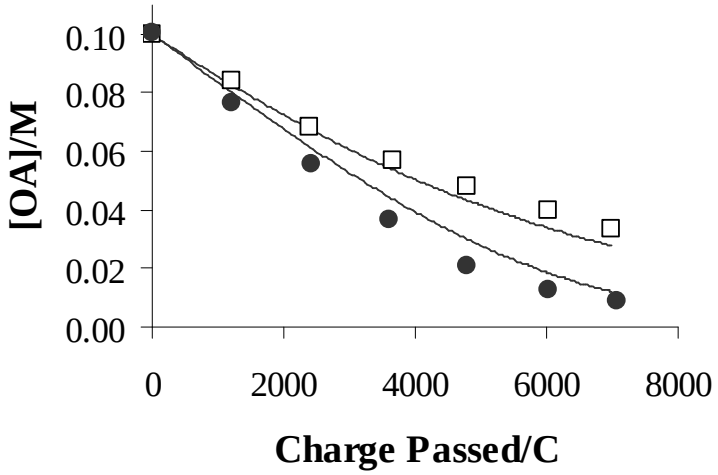

(a)

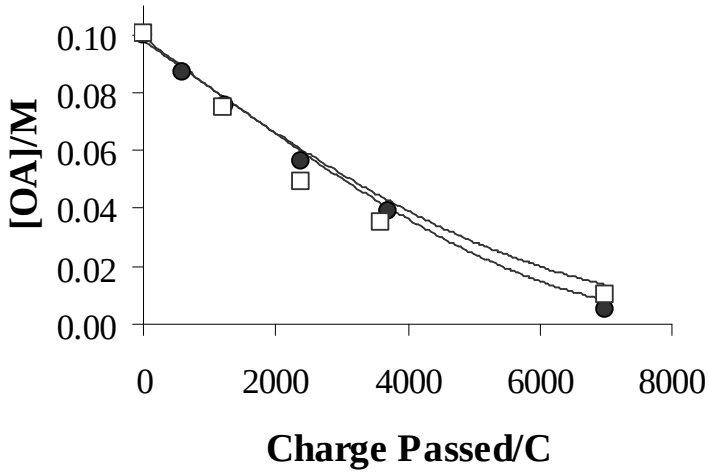

(b)

Fig. 6.6 *Profile of oxalic acid concentration vs. charge passed for electrolysis performed at pH = 2 with 39 (a) and 17 mA/cm^2 (b) at different flow rates. Flow rate: 0.2 (□) and 1.2 l/min (●). Experimental conditions: Amperostatic alimentation, System solvent supporting electrolyte (SSE): Water, Na_2SO_4, H_2SO_4. Initial oxalic acid concentration: 100 mM. T = 25°C. Theoretical curves (—) obtained by Eq.ns 4.14 with the parameter C* reported in Table 6.1 and [RH]* = 0.018 M.*

On the other hand, when the experiments were performed at higher current densities, C* assumes quite high values when the experiments are carried out at low values of the flow rate and, as a consequence, a high influence of flow dynamic regime is expected. When one compares the experiments performed at constant flow rate, the consumption of oxalic acid strongly depends on the current density at the lower value of the flow rate (when mass transfer control arises for a large part of the process) (Table 6.1, entries 1 and 5) while no a significant influence is observed at the higher value of flow rate (Table 6.1, entries 3 and 4).

When some experiments were carried out in basic conditions with an initial $[OA]^b$ of 0.1 M, no effect of a change of the current density and the flow rate was observed (Table 6.1, entries 6 and 7 and Fig. 6.7). This is probably due to the fact that incineration in basic conditions gives rise to very low OA abatement so that in all

the employed experimental conditions the process was always under charge transfer control ($[OA]^b > C^*$).

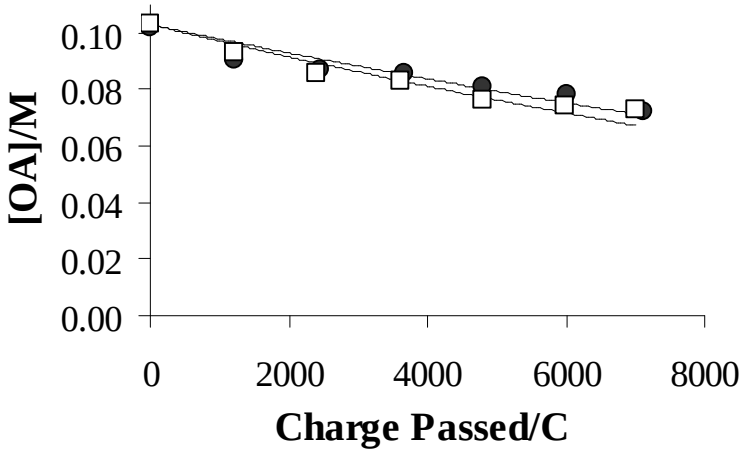

Fig. 6.7 *Profile of oxalic acid concentration vs. charge passed for electrolysis performed at pH = 12 in the following operative conditions: 39 mA/cm^2 and 0.2 l/min (•) and 17 mA/cm^2 and 1.2 l/min (□). Experimental conditions: Amperostatic alimentation, System solvent supporting electrolyte (SSE): Water, Na_2SO_4, NaOH. Initial oxalic acid concentration: 100 mM. T = 25°C. Theoretical curves (—) obtained by Eq.ns 4.14 with the parameter C* reported in Table 6.1 and [RH]* = 0.25 M.*

6.4.4 INFLUENCE OF TEMPERATURE

In order to evaluate the effect of the temperature on the process, we have performed two set of experiments at different temperatures at different operative conditions:

- Current density 39 mA/cm^2 and flow rate 0.2 l/min;
- Current density 17 mA/cm^2 and flow rate about 1.2 l/min

Interestingly, as shown in Table 6.2 and in Fig. 6.8, an increase of the temperature gave rise, in all cases, to a drastic increase of both OA conversion and CE.

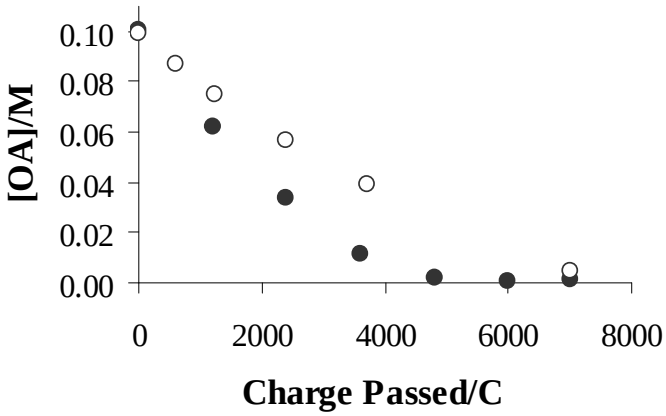

(a)

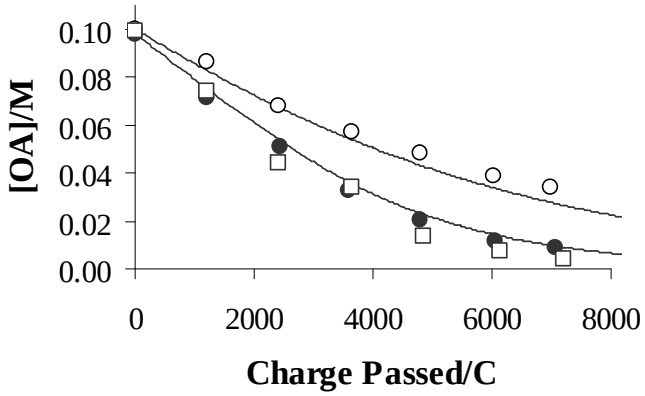

(b)

Fig. 6.8 *Profile of oxalic acid concentration vs. charge passed for electrolysis performed at 17 mA/cm^2 and 1.2 l/min (Fig. 6.8a) and 39 mA/cm^2 and 0.2 l/min (Fig. 6.8b) at different temperatures. T = 25 (o), 50 (•) and 70 °C (□). Experimental conditions: Amperostatic alimentation, System solvent supporting electrolyte (SSE): Water, Na_2SO_4, H_2SO_4. Initial oxalic acid concentration: 100 mM. pH = 2. Theoretical curves (—) obtained by Eq.ns 4.14 with the parameter C* reported in Table 6.2 and [RH]* = 0.018 M and 0.003 M for the experiments performed at 25 and 50°C, respectively.*

In particular, under the best adopted operative conditions (T = 50 °C, high flow rate and low current density) after 6000 C (Q = 1.25 Q^{th}) a conversion of about 99% and a current efficiency close to 80% was obtained which demonstrates that incineration of oxalic acid can be carried out successfully at IrO_2-Ta_2O_5 anodes with very high conversions and CE. In order to explain the positive effect of temperature on the performances of the process, it is useful to remember that higher temperature, according to chronoamperometric measurements (par. 6.3.2), favour the oxidation of OA with respect to that of water.

Table 6.2 *Influence of Temperature on the Incineration of Oxalic Acid*[a]

Entry	T (°C)	I/A (mA/cm^2)	Flow rate (l/min)	Current Efficiency (%)	Conversion (%)	Time Passed (min)	C* (M) [b]
1	25	39	0.02	45 – 49	66 – 70	334	0.076
2	50	39	0.02	59 – 63	90 – 94	334	~ 0.05
3	70	39	0.02	62 - 66	95 - 98	334	n.d.
4	25	17	1.02	62 – 66	91 – 95	778	0.009
5	50	17	1.02	68 - 72	> 99	778	n.d.
6	25	39	0.02	71 - 75	> 98	334	0.076
7	25	39	0.02	71 - 75	> 99	334	0.076

[a] *amperostatic electrolyses. System solvent supporting electrolyte (SSE): Water, Na_2SO_4, H_2SO_4. Initial oxalic acid concentration: 100 mM. pH = 2. Charge passed = 7000 C = 1.45 Q^{th}, where Q^{th} = charge necessary for a total conversion of the oxalic acid with a CE = 100%. V = 250 ml.*

[b] $C^* = i_{app}/(2FD/\delta)$.

6.5 THEORETICAL CONSIDERATION

A general theoretical model for the anodic oxidation of oxalic acid has been presented in the chapter 4, based on the occurrence of both direct and direct processes mediated by adsorbed hydroxyl radicals or adsorbed "oxygen".

In the following we wish to evaluate if a quantitative agreement between the developed theoretical models and the experimental results on the electrochemical incineration of OA at IrO_2 based electrodes above presented can be observed.

Let us focus our attention first, on a process kinetically controlled by oxidation reaction. This situation arises if one performs an electrolysis with a very high initial value of OA concentration so that $[OA]^b$ is drastically higher of C* for the most part of the charge passed. Thus, we have carried out an electrolysis with a flow rate of 1.2 l/min and 56 mA/cm^2 (C* = 0.028 M) and an initial OA concentration of 0.35 M (see Table 6.1, entry 9). Interestingly, as shown in Fig. 6.9, experimental data are in quite good agreement with theoretical predictions if a value of $[RH]^* = 0.018$ M is used, which probably represents $[RH]^* = k'(E)/k(E)$ since a direct anodic oxidation mechanism is likely to be involved according to chronoamperometric and polarization measurements.

Let us focus on a process kinetically controlled completely by mass transfer. This was realised by an electrolysis carried out with an initial OA concentration of 0.01 M, a pH of 2, a low flow rate and an high current density (Table 6.1, entry 2). Indeed, under these conditions $[RH]^b$ is expected to be drastically lower than C* ICE^{OC} during all the experiment, where ICE^{OC} is the instantaneous current efficiency under oxidation reaction control (Scialdone, 2009) and the expression of the current efficiency in this case is reported in Eq. 4.1.

Indeed as shown in Fig. 6.10, experimental results are in very good agreement with the theoretical predictions, in spite of the fact that no adjustable parameters are present.

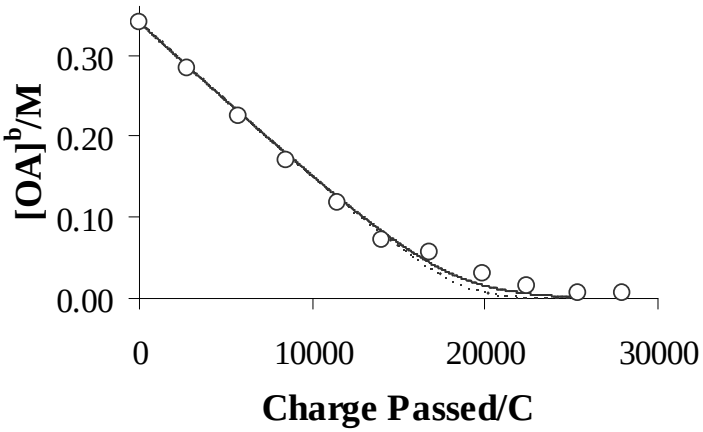

Fig.6.9 *[OA]^b vs. charge passed. Experimental conditions reported in Table 6.1, entry 9. Theoretical curves for a process under oxidation reaction (---) (obtained by combination of Eq.ns 4.6b and 4.14b and for a mixed kinetic regime (—) (obtained by Eq.ns 4.14) with [RH]* = 0.018 M).*

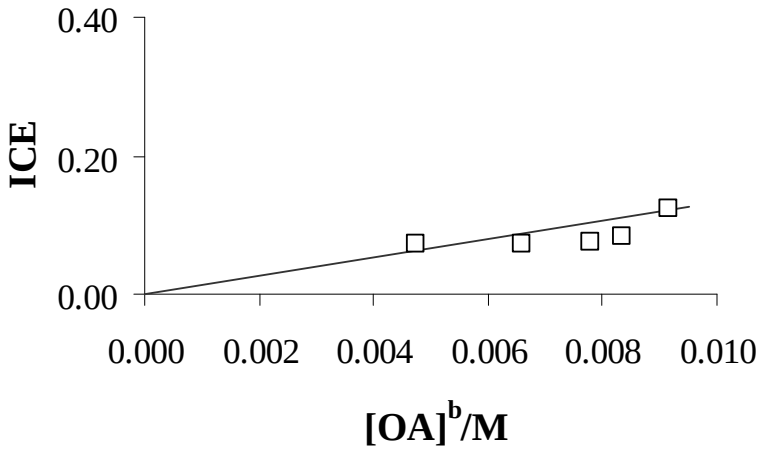

(a)

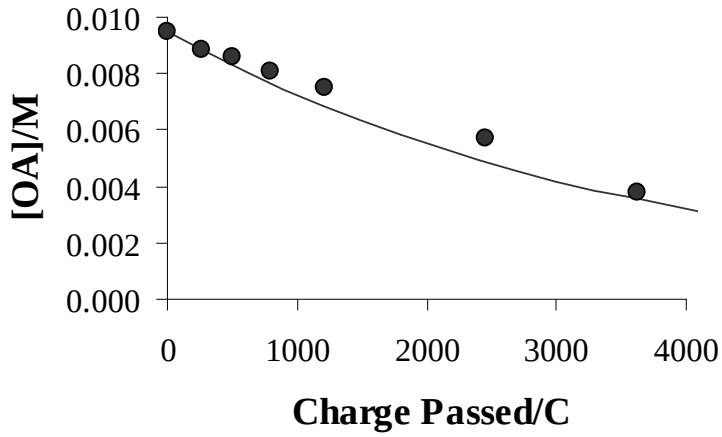

(b)

Fig. 6.10 *ICE vs. $[OA]^b$ (a) and $[OA]^b$ vs. charge passed (b). Experimental conditions reported in Table 6.1, entry 2. Theoretical curves (—) obtained by Eq.ns 4.1 for Fig. 6.9a and 4.3 for Fig. 6.9b with the parameter C* reported in Table 6.1.*

Let now us discuss the general case of a process whose rate determining step during the electrolysis changes from charge transfer control in the first stages to mass transfer control in the last part with a mixed regime between them. In this case, *ICE* is given by the Eq. 4.14a. As shown by Fig. 6.11 and 6.6, experimental results are in quite good agreement with theoretical predictions. In particular, both the effects of the current density and of the flow rate are well predicted by the developed theoretical model.

We have compared also the data obtained during experiments performed in basic conditions with theoretical predictions based on Eq.ns 4.14 and as shown in Fig. 6.7 also in this case a good agreement between experimental data and theoretical predictions is obtained when a value of *[RH]** of about 0.25 M is used as fitting parameter. Finally, let us study the effect of the temperature on the process. Higher temperature should result in higher values of the mass transfer coefficient k_m mainly because the viscosity of a liquid solvent decreases exponentially with T.

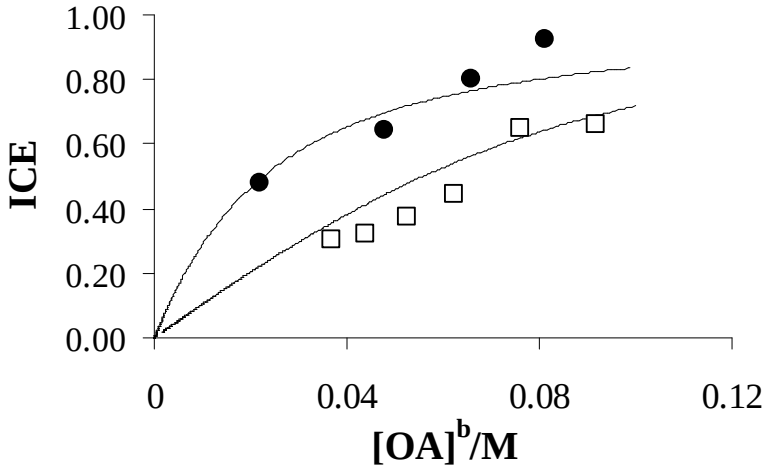

(a)

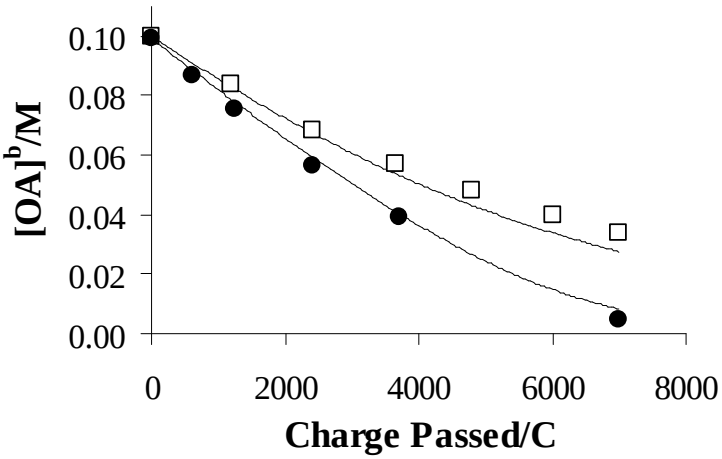

(b)

Fig. 6.11 *ICE vs. $[OA]^b$ (a) and $[OA]^b$ vs. charge passed (b) for electrolysis performed at pH = 2 in the following operative conditions: 39 mA/cm^2 and 0.2 l/min (□) and 17 mA/cm^2 and 1.2 l/min (•). Experimental conditions reported in Table 6.1, entries 1 and 3. Theoretical curves (—) obtained by Eq.ns 4.14 with the parameter C* reported in Table 6.1 and [RH]* = 0.018 M.*

On the other hand, a higher temperature result in a drastic increase of the CE also when the process is likely to be under oxidation reaction control for the most part of the experiment (see Table 6.2, entries 4 and 5). Hence, an increase of the temperature is likely to result also in a significant decrease of the parameter *[RH]** which is likely to coincide with *k'(E)/k(E)*. Comparing theoretical predictions based on Eq.ns 4.14 with experimental data achieved at 50 °C, i = 39 mA/cm^2, flow rate 0.2 l/min (Table 6.2, entry 2), quite interestingly, a good fitting of experimental data and theoretical predictions arise if one use a very low value of *[RH]** of about 0.003 – 0.004 M (see Fig. 6.8b).

6.6 COMPARISION BETWEEN RESULTS OBTAINED AT BDD AND AT DSA ANODES

As mentioned in section 2.3, the role of the anodic material on the electrochemical oxidation processes is determinant. Indeed quite different reaction pathways can take place at BDD and at DSA anodes. With the aim of investigate the influence of the nature of the anodic material on the electrochemical incineration of oxalic acid, let now us observe some results already examined in this and in the precedent chapter.

When electrolyses at the two anodes were performed at a current density of 39 mA/cm^2 and a flow rate of 0.2 l/min, with an initial concentration of oxalic acid 0.1 M, at room temperature and at acid pH, as shown in Fig. 6.12a, after a charge passed of 7000 C = 1.45 Qth, a significantly higher conversion is obtained (higher than 80%) at a boron doped diamond anode (Table 5.3 entry 7), while at iridium based anode the conversion is only of about 68% with a current efficiency slightly lower than 50% (Table 6.2 entry 1). The difference of the performances of the two anodic material decrease when the electrolyses were conducted at lower current density and higher flow rate (see Fig. 6.12b), i.e. when the most part of the process is expected to be under oxidation reaction control. Indeed, at BDD anode a conversion of oxalic acid of about 99% was obtained, while a slight decrease was detected in the case of iridium based anode (conversion of oxalic acid of 93%) (Table 5.3 entry 1 and Table 6.2 entry 4, respectively).

Interestingly, at both BDD and Ti/IrO_2-Ta_2O_5 anodes in acidic conditions the process is expected, according to polarization curves and chronoamperometric measurements reported in section 5.2.1 and 6.2 - 6.3 respectively, to take place at least in part by a direct anodic oxidation process. Otherwise, when chronoamperometric and polarization measurements were carried out at room temperature in the presence of different amounts of OA at BDD and IrO_2-Ta_2O_5, an increase of $[OA]^b$ results in the case of BDD in a higher increase of the current density with respect to that observed at IrO_2-Ta_2O_5. This result, probably, indicates that at room temperature the direct anodic oxidation of OA is more favorite with respect to water oxidation at BDD anodes than at IrO_2-Ta_2O_5.

These data may indicate that different oxidant agents is involved at BDD and DSA anodes. Thus, at active electrodes, such as IrO_2 based anodes, water oxidation involves the formation of chemisorbed oxygen, that, according to literature (Comninellis, 1994; Comninellis and De Battisti, 1996), is consumed in the oxidation of organic compounds with the formation of selective oxidation products and in an easy oxygen evolution. On the contrary, at diamond anodes, free or weakly physical adsorbed hydroxyl radicals are generated which are expected to have a stronger oxidizing power and to cause often a complete combustion of organics.

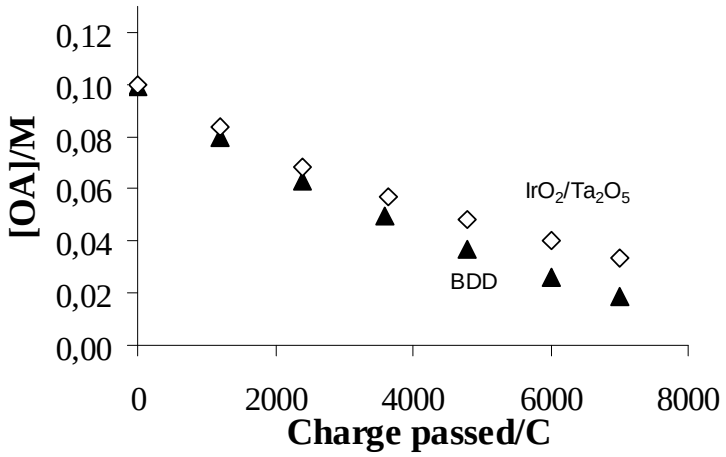

(a)

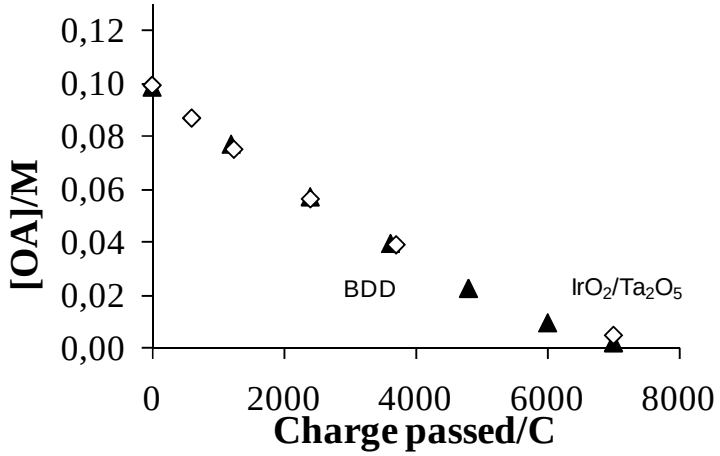

(b)

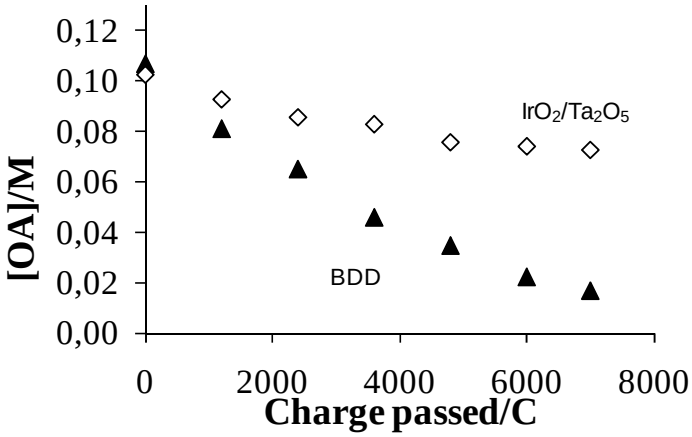

(c)

Fig. 6.12 *Profile of oxalic acid concentration vs. charge passed for electrolyses performed with galvanostatic alimentation: at pH = 2 at 39 mA/cm^2 – 0.2 l/min (a) and at 17 mA/cm^2 – 1.2 l/min (b); at pH = 12 at 17 mA/cm^2 – 1.2 l/min (c). System solvent supporting electrolyte (SSE): Water, Na_2SO_4, H_2SO_4 or NaOH. Initial oxalic acid concentration: 100 mM. T = 25°C.*

Furthermore, in the case of oxalic acid, a direct anodic oxidation process is likely to be involved whose competition with oxygen evolution necessarily depends on the nature of the electrodic material.

A different scenario can be observed at pH 12. Indeed, higher differences between the performances of the two anodes can be noted and quite lower conversion values are observed at DSA anode at both the opposite operative conditions. In particular, conversions of about 32% and current efficiencies of 22% were detected. Thus at basic pH, the influence of the anodic material is strongly enhanced, in particular in the conditions of higher flow rate and lower current density (see Fig. 6.12b and 6.12c).

Furthermore, when the electrochemical incineration of oxalic acid at DSA anode was conducted at acid pH, at a temperature of 50°C, at a flow rate of 1.2 l/min and a current density of 17 mA/cm^2, a conversion of about 99% and a current efficiency close to 80% was obtained (see section 6.4.4), results at least comparable to that obtained at BDD at room temperature (Table 5.3 entry 1). This surprising result seems very interesting if one focus on the fact that a temperature of 50 °C is easily achievable on applicative scale, that DSA anodes are widely industrially used, very stable as confirmed also in our study (comparable performances were achieved after several days of continuous operations), less expensive than Si-BDD and presented lower cell potentials (2.5 – 3.1 V) with respect to BDD (3.2 – 4.7 V).

CHAPTER 7

ELECTROCHEMICAL INCINERATION OF OXALIC ACID IN THE PRESENCE OF SODIUM CHLORIDE

7.1 INTRODUCTION

As previously mentioned, electrochemical oxidation of organic compounds can be performed by means of electrogenerated oxidants such as active chlorine, peroxidisulfuric acid, In particular, we have studied in detail the anodic incineration of oxalic acid in the presence of NaCl with the aim of studying in a systematic way the influence of numerous parameters on the performances of the process and to individuate the optimal operative conditions both in the absence and in the presence of NaCl. A particular aim of this study was to evaluate how the role of operative parameters changes in the presence of chlorides.

Since the effect of NaCl on the process is expected to depend on the nature of the electrodic material, also in this case Ti/IrO_2-Ta_2O_5 and BDD were used.

7.2 PRELIMINARY EXPERIMENTS PERFORMED IN THE ABSENCE OF ORGANICS

7.2.1 POLARIZATION AND CHRONOAMPEROMETRIC MEASUREMENTS IN THE PRESENCE OF NaCl

Quasi-steady polarization and chronoamperometric measurements were recorded at BDD and IrO_2-Ta_2O_5 in background solutions containing Na_2SO_4 and H_2SO_4 or NaOH in the absence and in the presence of different concentrations of NaCl. At pH of 2, according to the literature (Ferro et al., 2000; Trasatti, 1987), a significant increase of the current density is observed upon increasing the halide concentration both at BDD (Fig. 7.1a) and IrO_2-Ta_2O_5 (Fig. 7.2a). Interestingly, according to chronoamperometric measurements, in steady state conditions an higher increase of the current density arises at IrO_2-Ta_2O_5 with respect to BDD.

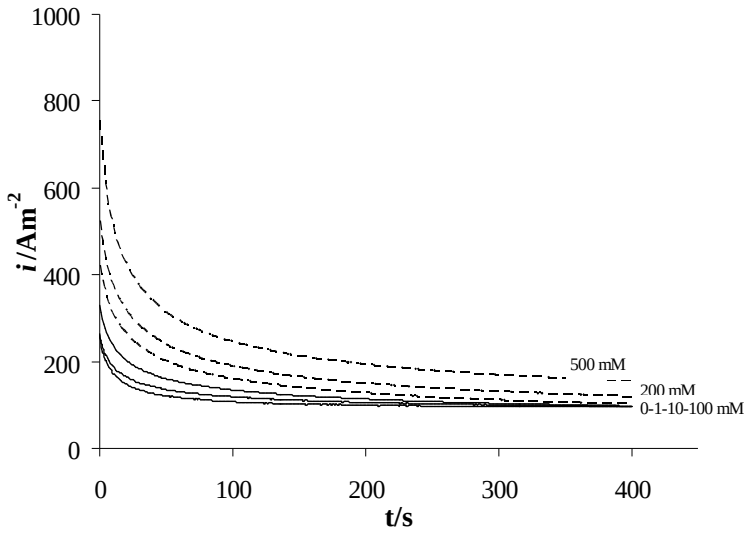

(a)

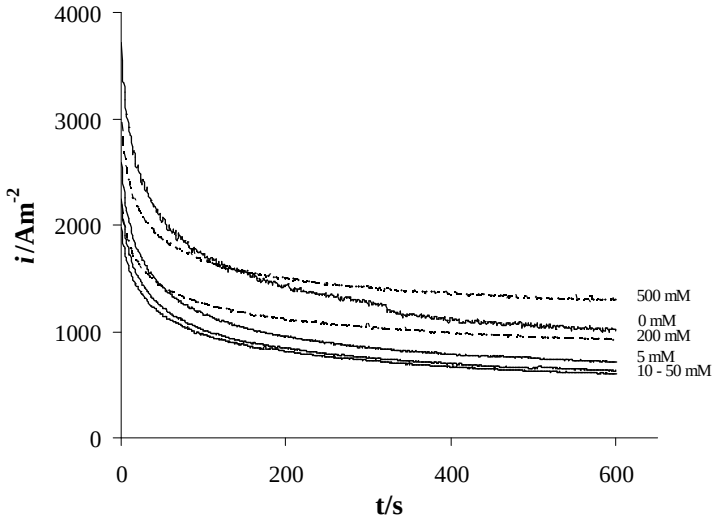

(b)

Fig. 7.1 *Chronoamperometric response of BDD to step-by-step injection of NaCl at 2.44 V vs. SCE at a pH of 2 (a) and 12 (b). System solvent supporting electrolyte (SSE): Water, Na_2SO_4, H_2SO_4 (pH = 2) or NaOH (pH = 12).*

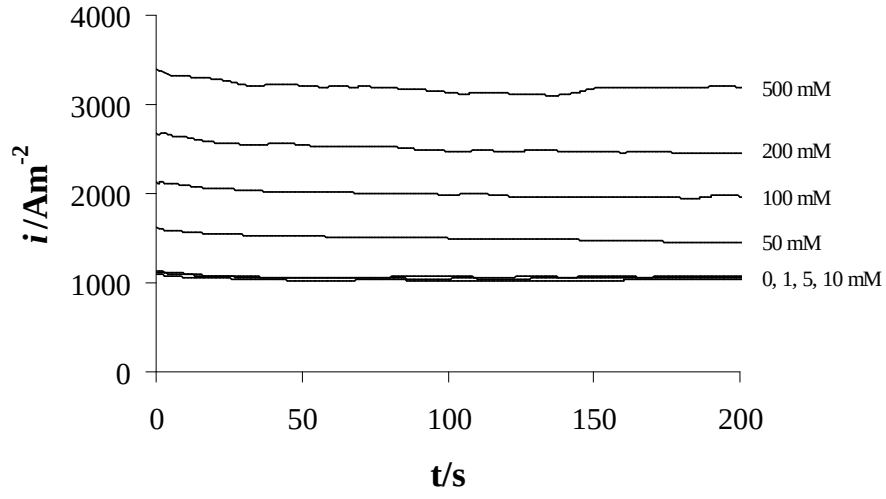

(a)

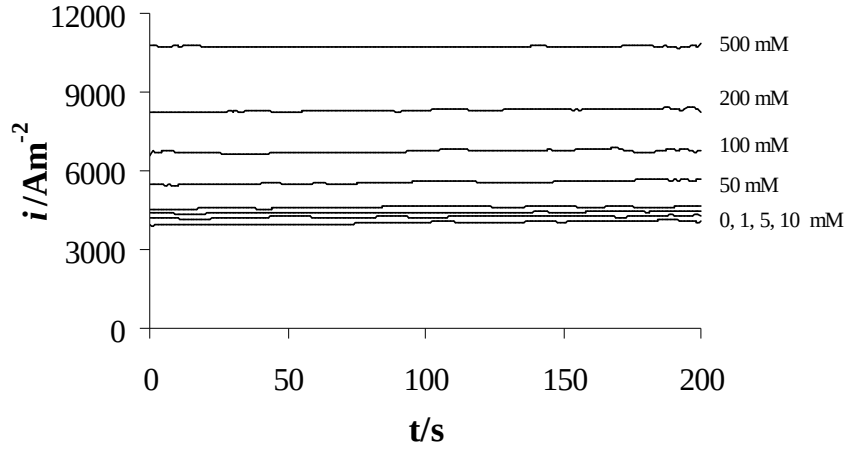

(b)

Fig. 7.2 *Chronoamperometric response of Ti/IrO_2-Ta_2O_5 to step-by-step injection of NaCl at 1.5 V vs. SCE at a pH of 2 (a) and 12 (b). System solvent supporting electrolyte (SSE): Water, Na_2SO_4, H_2SO_4 (pH = 2) or NaOH (pH = 12).*

At the DSA anode, a drastic increase of the current density is observed upon increasing the NaCl concentration also in basic conditions (Fig. 7.2b) in spite of the fact that the competition between chloride and water oxidation is expected to be drastically affect by the pH of the solution, higher pH favoring the water oxidation (Trasatti, 1987).

On the other hand, one can consider that oxygen evolution gives rise to local acidification of the solution. In particular, oxide electrodes prepared by thermal decomposition of suitable precursors, as a rule, consist of porous layers of sintered crystallites and the pH in the pores, as a result of the oxygen evolution reaction, is expected to be very low while mass transfer limitations dampens its sensitivity to the external acidity of the bulk of the solution (Trasatti, 1987), thus favoring the chloride oxidation reaction.

When polarization and chronoamperometric measurements were carried out at BDD at a pH of 12, a decrease of the current densities was observed with respect to the blank in the presence of small concentrations of NaCl. As shown as an example by the chronoamperometric measurements carried out at 2.44 V vs. SCE (Fig. 7.1b), an increase of the NaCl concentration up to 50 mM gave rise to a slight decrease of the current density while above this value a reversal of the trend was observed. A similar behaviour has been observed by Martinez-Huitle et al. (2005b) for the polarization curves of NaCl, NaBr and NaF at Pt in basic solutions. Thus, Authors supposed that the adsorption of Cl^- at the anodic surface can cause the anodic shift of the oxygen evolution.

More in general, our data could be interpreted considering that the adsorption of Cl^- at the anodic surface from one side can hinder the oxygen evolution reaction and from the other side gives rise to the chlorine formation, resulting in a decrease or in an increase, respectively, of the current densities with respect to the blank. Which of the two effects is prevailing should depend on the pH and on the amount of NaCl present in the system. In particular, the different results achieved in the case of BDD and iridium anodes may be tentatively attributed to a lower selectivity of the diamond towards the chlorine evolution in not very acid conditions or to a less porous structure for BDD with respect to the metal oxide electrode, that could result

in a more limited decrease of the pH at active sites when experiments are carried out with high external pH.

7.2.2 ELECTROLYSES CARRIED OUT IN THE PRESENCE OF NaCl

The effect of some operative parameters on the formation of active chlorine during the electrolysis of aqueous solutions of NaCl was investigated by performing a series of electrolyses at both BDD and DSA anodes at different values of pH, flow rate and current density.

Table 7.1. *Effect of operative parameters on the Active Chlorine formation during the electrolyses of a solution of Na_2SO_4 and NaCl* [a]

Entry	Anode	pH	Current density (mA/cm^2)	Flow rate ($l\ min^{-1}$)	Active chlorine concentration (mM)
1	BDD	12	39	0.02	5 – 7
2	IrO_2-Ta_2O_5	12	39	0.02	26 – 28
3	BDD	12	17	1.02	< 1
4	BDD	2	39	0.02	8 – 10
5	IrO_2-Ta_2O_5	2	39	0.02	21 – 23
6	IrO_2-Ta_2O_5	2	39	1.02	17 – 19
7	IrO_2-Ta_2O_5	2	17	1.02	4 – 8

[a] *Amperostatic electrolyses in system II. Initial NaCl concentration = 0.17 M, system solvent supporting electrolyte (SSE): Water, Na_2SO_4, H_2SO_4 (pH = 2) or NaOH (pH = 12). T = 25 °C. V = 250 ml. Active chlorine concentration computed after a charge passed of 2400 C.*

7.2.2.1 EFFECT OF THE ANODIC MATERIAL

As shown in Table 7.1 (Entries 1-2,4-5), a drastic effect of the anodic material on the formation of strongly oxidizing compounds was observed also during our experiments. In particular, dramatically higher concentrations of oxidants, computed as active chlorine, were observed in analogous operative conditions at the iridium based anode with respect to BDD both in acidic and in basic conditions. In order to explain the different behavior of the two electrodes for what concern the formation of oxidants in the solution, different hypotheses can be made. First, it can be supposed that at DSA anodes the formation of chlorine is more favored with respect to the oxygen evolution. Second, some authors have proposed in order to interpret the higher concentration of chlorate detected at BDD with respect to ruthenium oxide anodes, that, at diamond, active chlorine can react with the weakly adsorbed hydroxyl radicals or with the generated peroxides to form Cl^-, chlorite and chlorate (Polcaro et al., 2008). In any cases, from the applicative point of view, one has to observe that BDD, in spite of the reported high selectivity towards chlorine evolution (Ferro et al., 2000), is a not very efficient anode for the formation of active chlorine at least under operative conditions adopted in this study.

7.2.2.2 EFFECT OF pH

As shown in Table 7.1, the pH affected the performances of the process. Indeed, pH is expected to affect both heterogeneous and homogeneous reactions as synthetically reported below:

- for what concern the electrochemical reactions, pH is expected to affect the competition between water and chloride oxidation processes, lower pH favoring the chlorine evolution reaction. Furthermore, very low pH gives rise to a lower concentration of species as hypochlorite and hypochlorous acid that can be further oxidized at the anode to form chlorate (Czarnetzki and Jansenn, 1992);
- the value of the pH affects also the homogeneous decomposition of oxidants through the reaction between hypochlorous acid and hypochlorite (Eq. 2.40)

that is expected to assume the maximum rate at quasi neutral pH and the loss for desorption of chlorine that is maximized for very low values of pH (< 2).

In particular, in the experiments performed at BDD anode, a significant effect of the pH on the performances of the process was observed (Table 7.1, entries 1 and 4). Indeed, in basic conditions lower concentrations of oxidants were computed. This experimental evidence seems in agreement with the fact that, according to polarization curves and chronoamperometric measurements, very high NaCl concentrations are necessary in basic conditions to detect a significant current density increase. A different picture was observed in the case of the iridium oxide based anode. Indeed, at this anode slight higher concentrations of oxidants were observed in basic conditions (Table 7.1, entries 2 and 5).

Hence, one may suppose that in the experiments performed at DSA, the variation of pH affects more drastically homogeneous reactions with respect to electrochemical ones. In particular, in basic conditions, reactions reported in Eq.ns 2.35 and 2.36 are partially shifted towards the presence of chlorite, thus avoiding the loss of chlorine by desorption.

7.2.2.3 EFFECT OF FLOW RATE AND CURRENT DENSITY

As shown in Table 7.1 (entries 1,3 and 5-7), when the electrolyses were performed at higher flow rate and lower current density, the final concentration of active chlorine at fixed amount of circulated charge was dramatically lower. A positive effect of higher current density towards the formation of oxidants was also observed by Bergmann and Koporal (2005) during a study on the electrochemical disinfectant production using anodes of RuO_2 in the absence of added supporting electrolyte. Authors supposed that the positive effect of current density was due to the fact that, in drinking water, ion transfer rate is significantly affected by migration, that at its turn is accelerated by higher current densities. On the other hand, in our experiments a significant concentration of chloride ions and supporting electrolyte was used and so migration should have a minor role in the mass transfer of ions to the anodic surface. Israelides et al. (1997) argued that OCl^- can be involved in mass transport controlled electrochemical reactions (Eq.ns 2.41 and

2.42), that are expected to have a more important effect on the performances of the process in the presence of higher flow rate and lower current density in terms of current efficiencies for the formation of active chlorine.

Hence, in order to explain the effect of flow rate and current density on the performances of the process, one may focus the attention on the anodic processes. In particular, the anodic oxidation of hypochlorus acid and hypochlorite is favorite at higher pH when these specie present higher concentrations. Otherwise, a different local pH is expected at the anodic surface with respect to the bulk of the solution as a consequence of the oxygen evolution reaction that results in the local acidification of the anodic surface. Then, different values of the concentrations of HClO and OCl^- can be expected in the bulk of the solution and at the anodic surface, the last being probably affected by mass transfer kinetics and current density. Hence, on the bases of these consideration one may tentatively speculate that in the presence of low current density and high flow rate, the anodic oxidation of these species can occur with higher current yield.

7.2.2.4 EFFECT OF CATHODIC REDUCTION OF ACTIVE CHLORINE

Additionally, in order to evaluate the possible effect of the cathodic reduction of active chlorine on the performances of the process, we have carried out two electrolyses in another system, constituted of a batch electrochemical cell in undivided and divided cell, respectively. Similar concentrations of active chlorine were detected during all the experiments, thus suggesting that the cathodic reduction of oxidants has not a significant effect on the process, at least under the adopted operative conditions.

7.3 POLARIZATION CURVES AND ELECTROANALYTICAL MEASUREMENTS IN THE PRESENCE OF OXALIC ACID

In order to investigate the performance of electrochemical incineration of oxalic acid in presence of NaCl in solution, chronoamperometric and polarization measurements were, previously, recorded. As shown in the previous chapters, in the

absence of NaCl at fixed potential at both electrodes, the current increased linearly with OA concentration.

Interestingly, when polarization curves and choronoamperomentric measurements were recorded in the presence of NaCl, a change of the polarization curves occurs both in acidic and basic conditions. In particular, both in the cases of IrO_2 and BDD anodes, for a fixed value of the potential, current densities increased with a linear dependence on the acid concentration. Otherwise the increase of the current density was significantly lower if compared with that observed in the absence of NaCl, as shown, as an example, by the comparison between the chronoamperometric measurements carried out in acidic conditions in the absence and in the presence of NaCl (Fig. 7.3).

Hence, it is possible to conclude that the direct oxidation of OA at the anodic surface becomes drastically less relevant (and quasi negligible at Ti/IrO_2-Ta_2O_5) in NaCl solutions, as a result of the chloride ions oxidation.

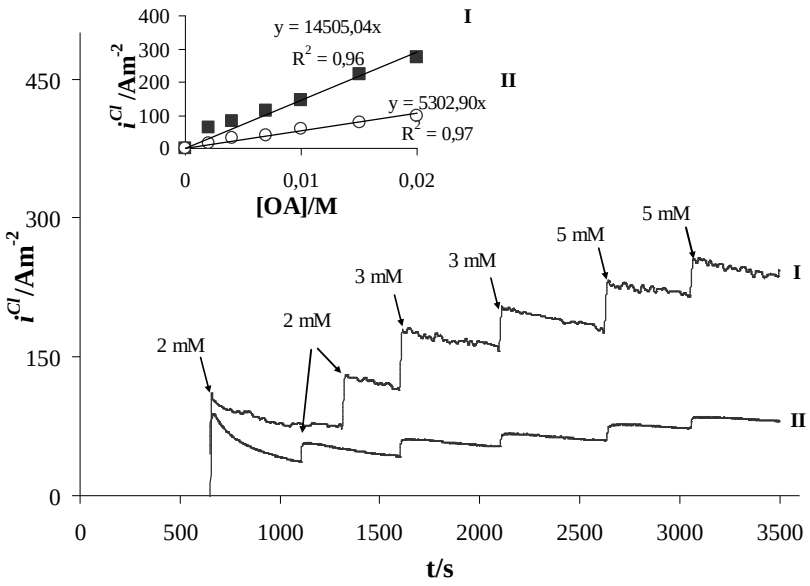

(a)

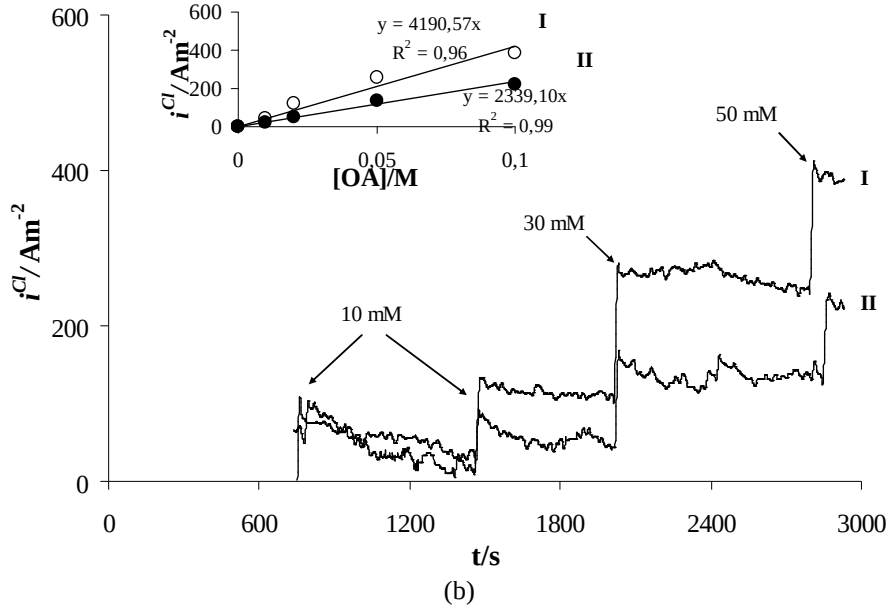

(b)

Fig. 7.3 *Chronoamperometric response of BDD (a) and IrO_2-Ta_2O_5 (b) to step-by-step injection of OA in the absence (I) and in the presence (II) of NaCl 0,17 M at a pH of 2. $i^{Cl} = i - i^w$ (where i and i^w are the current densities observed in the presence and in the absence of chloride, respectively). Inset: i^{Cl} vs. [AO] at the condition (I) and (II) and relative regression lines. System solvent supporting electrolyte (SSE): Water, Na_2SO_4, H_2SO_4. E = 2.44 V and 1.5 V vs. SCE for BDD and IrO_2-Ta_2O_5 anodes, respectively.*

In order to have some preliminary information on the reactivity of active chlorine with oxalic acid, some cyclic voltammograms were recorded without and with addition of NaCl and OA at iridium anode in acidic conditions.

As shown in Fig. 7.4, the addition of NaCl to a water solution gives rise an anodic wave and a small cathodic peak. According to the literature, such behavior can be attributed to oxidation of Cl^- ions to Cl_2 (Szpyrkowicz et al., 2005). The addition of OA to the electrolyte gives rise to a very small change of the voltammograms.

Only a small decrease of both anodic and cathodic currents at potentials close to 1 V was observed, that can be tentatively ascribed to a slight passivation of the electrode due to adsorption of OA as previously observed by Szpyrkowich et al. (2005) in the case of a Red dye. An interesting feature of these cyclic voltammograms is given by

the fact that also at quite low scan rates of 0.1 V/s, the addition of OA has a very small influence on the cathodic wave. Hence, it seems reasonable to assume that a slow homogeneous reaction between active chlorine and OA arises so that this reaction is expected to take place mainly in the bulk of the solution. This result is confirmed by the fact that a significant concentration of active chlorine is detected when electrolyses are carried out in the presence of both NaCl and OA.

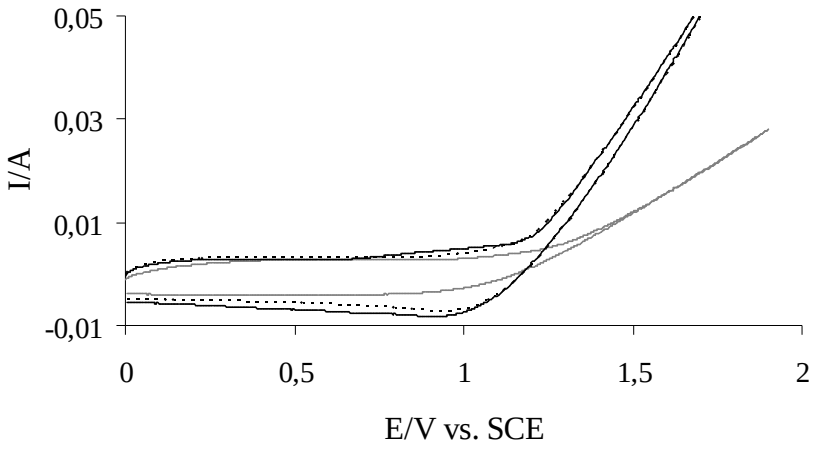

Fig. 7.4 *Cyclic voltammograms performed at IrO_2-Ta_2O_5. (—) System solvent supporting electrolyte (SSE): Water, Na_2SO_4, H_2SO_4 (pH = 2) alone, (---) with addition of oxalic acid 5 mM, (—) with addition of NaCl 0.17 M. Scan rate: 0.1 V/s. T = 25 °C. V = 25 ml.*

7.4 EXPERIMENTAL INVESTIGATION ON THE EFFECT OF OPERATIVE PARAMETERS ON THE ELECTROCHEMICAL INCINERATION OF OA IN THE ABSENCE AND IN THE PRESENCE OF NaCl

7.4.1. COMPARISON OF THE ELECTROCHEMICAL INCINERATION OF OA AT BDD AND IRIDIUM ANODE AT DIFFERENT NaCl CONCENTRATIONS

To study the effect of the anodic material on the process, we performed two series of electrolyses at BDD and IrO_2 anodes in the presence of an initial OA

concentration of 0.1 M, a quite low value of the flow rate (0.2 l/min), a current density of 39 mA/cm^2 at different values of pH (2 and 12) and of NaCl concentrations (0, 5, 10, 40 g/l). Electrolyses were generally stopped when the charge passed was 7000 C = 1.45 Q^{th} where Q^{th} = amount of charge necessary for a total conversion of the oxalic acid with a *CE* = 100%.

As shown in Table 7.2, the addition of NaCl to the solution gives rise to very different effects depending on both the nature of the anodic material and the pH. Let us first examine the experiments carried out at IrO_2 based anodes (Table 7.2, entries 1-7). In this case, the addition of NaCl to the solution gives rise, both in basic and in acidic conditions, to a significant enhancement of the OA abatement which increases upon increasing the NaCl concentration. Quite interestingly in the presence of 5 g/l of sodium chloride, a dramatic improvement of the performances of the process occurred and about 99 % of the initial OA concentration was removed with a CE higher than 70 % (Fig. 7.9) while a further increase of NaCl concentration did not affect significantly the conversion and the CE.

When electrolyses were repeated at BDD anodes, a quite different picture was observed (Table 7.2, entries 8-14). As reported in chapter 4, in the absence of NaCl, a quite good removal of OA was achieved at BDD. The addition of NaCl in acidic conditions gives rise to a very low increase of the OA abatement. Indeed, after 7000 C a conversion of OA of 83 and 90% was achieved when the electrolyses were performed in the absence and in the presence of 5g/l of NaCl, respectively.

Furthermore, when the experiments were performed in basic conditions a significant decrease of OA abatement was observed upon increasing the NaCl concentration.

This is probably due to the fact that in basic conditions NaCl oxidation generates at BDD a very low concentration of oxidants (see section 7.2.2) and that active chlorine is mainly present as hypochlorite that is a less strong oxidant with respect to hypochlorous acid (Deborde and Von Gunten, 2008). Let us focus on the comparison between the electrolyses carried out at BDD and iridium anodes. As shown in Table 7.2 (Entries 1,8 and 4,11), in the absence of NaCl a dramatically higher abatement of oxalic acid takes place at BDD with respect to IrO_2-Ta_2O_5 both in acidic and in basic conditions.

Table 7.2. *Incineration of Oxalic Acid in the presence and in the absence of NaCl*[a]

Entry	Anode	Initial pH	NaCl (g/l)	Charge passed (C)	Conversion (%)	CE (%)
1	IrO_2-Ta_2O_5	2	-	7000	68	47
2	IrO_2-Ta_2O_5	2	5	7000	99	73
3	IrO_2-Ta_2O_5	2	10	7000	> 99	> 70
4	IrO_2-Ta_2O_5	12	-	7000	32	22
5	IrO_2-Ta_2O_5	12	5	7000	39	27
6	IrO_2-Ta_2O_5	12	10	7000	47	32
7	IrO_2-Ta_2O_5	12	40	7000	78	53
8	BDD	2	-	7000	83	57
9	BDD	2	5	7000	90	66
10	BDD	2	10	7000	93	65
11	BDD	12	-	7040	81	56
12	BDD	12	5	7000	73	49
13	BDD	12	10	7000	72	48
14	BDD	12	40	7000	65	45
15	IrO_2-Ta_2O_5	9	10	7000	11	8

[a] *Amperostatic electrolyses in system II. Current density: 39 mA/cm^2. flow rate: 0.2 l/min. System solvent supporting electrolyte (SSE): Water, Na_2SO_4, H_2SO_4 (pH = 2) or NaOH (pH = 12). Initial oxalic acid concentration: 100 mM. T = 25 °C. V = 250 ml. Charge passed was generally 7000 C = 1.45 Q^{th} where Q^{th} = charge necessary for a total conversion of the oxalic acid with a CE = 100%.*

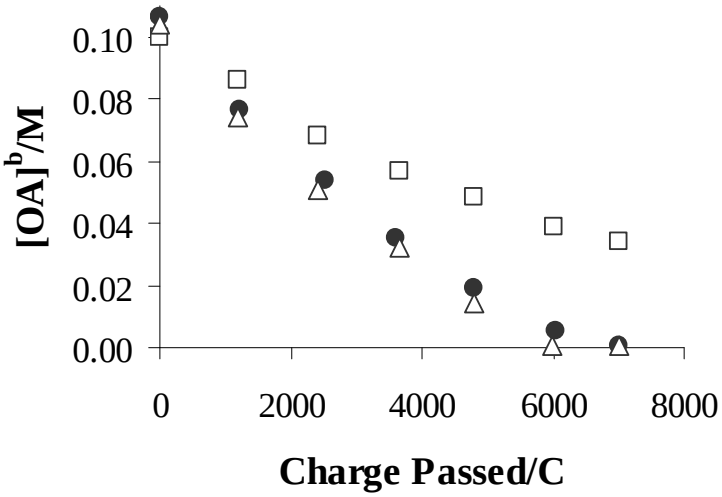

Fig. 7.9 *Oxalic acid concentration vs. charge passed as a function of NaCl concentration. [NaCl]: 0 (□), 5 (•) and 10 (Δ) g/l. Experimental conditions: Amperostatic alimentation, Initial substrate concentration: 0.1 M, Flow rate: 0.2 l/min, Current density: 39 mA /cm^2, T = 25°C. System solvent supporting electrolyte (SSE): Water, Na_2SO_4, H_2SO_4. pH = 2.*

Thus, after 7000 C an abatement of oxalic acid of about 83 and 68% was detected, as an example in acidic conditions, at BDD and IrO_2-Ta_2O_5, respectively.

Otherwise, as a result of the different effects of the NaCl addition on the performances of the process observed at diamond and iridium anodes, when NaCl was added to the system, the picture was readily changed. In particular, in acid conditions, an higher abatement of OA is obtained at IrO_2 anodes with respect to that observed at BDD (see Table 7.2, entries 2,9 and 3,10) for any adopted concentration of NaCl. As an example, when a NaCl concentration of 10g/l was used, after 7000 C abatements of oxalic acid of about 93 and higher than 99% were detected at BDD and IrO_2-Ta_2O_5, respectively. In basic conditions, a more complex scenario was observed: an higher abatement of OA is obtained at BDD with respect to IrO_2-Ta_2O_5 at 5 g/l (Table 7.2, entries 5,12) and 10 g/l (Table 7.2, entries 6,13). Conversely, an higher abatement is observed at iridium anode at 40 g/l (Table 7.2, entries 7,14).

It is important to stress this result, since it demonstrates, according to the theoretical considerations above reported, that, in the presence of significant amounts of NaCl,

the usual picture on the effect of the anodic material on the performances of the process, which indicates BDD as more suitable for electrochemical incineration of organics with respect to DSA characterized by low oxygen overpotential, can be completely inverted.

This complex effect is due to the fact that BDD gives rise with respect to DSA anode, from one side, to an higher current efficiency for organics oxidation at the anodic surface with respect to oxygen evolution but, on the other side, to a lower current efficiency for the formation of oxidants during the electrolysis of NaCl solutions so that one can achieve higher abatement of organics at BDD or DSA anodes depending on the adopted operative conditions and NaCl concentration. According to the literature (Bergmann and Rollin, 2007), the addition of NaCl can give rise to the formation of halogenated byproducts. Hence, the final effluent of two electrolyses carried out at BDD and IrO_2 anodes with an initial concentration of chloride of 170 mM and of OA of 100 mM, were analyzed to determine the presence of halogenated products. Interestingly, the presence of chloroform was observed during the electrolyses with a final concentration lower than 0.1 mM.

In particular, in the case of BDD a very low chromatographic peak was detected that did not present a measurable area.

7.4.2 EFFECT OF pH

As shown in Table 7.2, at the two adopted anodes, higher abatements of OA were achieved in acidic conditions both in the absence and in the presence of chlorides. Indeed, as an example, at iridium anode in the presence of a concentration of NaCl of 5 g/l, an abatement of OA of about 99 and 39% were observed in acidic and in basic conditions, respectively (entries 2 and 5). This result seems quite interestingly if one consider that in most of the studies reported in literature, the electrolyses in the presence of NaCl are carried out in alkaline media in order to minimize the loss of efficiency due to the free chlorine evaporation. On the other hand, our studies show that also low pH can be suitable for the formation of strong oxidants (see Table 7.1). Furthermore, at high pH the active chlorine is present as hypochlorite that is a less strong oxidant towards organic species with respect to

hypochlorous acid which is the main species present at pH close to 2 (Deborde and Von Gunten, 2008). In order to have more information on the effect of pH on the performances of the process, some electrolyses were repeated with an initial pH of 9 (Table 7.2, entry 15). Interestingly, very low abatement of oxalic acid were observed. This is probably due to the fact that at pH close to 7-8 the chemical reaction between hypochlorous acid and hypochlorite (Eq. 2.40) is expected to be maximized since relevant concentrations of both these compounds are present in the solution.

It is important to observe that the pH of the solution changes during the electrolyses. In particular, in the electrolyses performed with an initial pH of 2, an increase of the pH was observed up to values between 4 and 5 while in those performed with an initial pH of 12, the pH decreased to 9-10. A small variation of the pH was also observed for the experiment carried out with an initial pH of 9 that was concluded with a pH of about 8.4. This behavior was similar to that previously observed by Rajkumar et al. (2005) during the electrochemical abatement of phenol in the presence of chlorides. These authors, by changing the initial pH from 3 to 10, found always a final pH of about 8-8.5 that supposed originated by the formation of a bicarbonate buffer during the electrolytic degradation.

7.4.3 EFFECT OF CURRENT DENSITY AND FLOW RATE

According to theoretical considerations reported in section 2.4.3, the performances of the electrochemical incineration of organics can strongly depend on the value of adopted current density and on the flow dynamic regime. In order to elucidate the effect of these operative parameters, we have carried out numerous experiments at both BDD and IrO_2 anodes in the presence of an initial OA concentration of 0.1 M and different amounts of NaCl, under the following operative conditions:

a) Current density 39 mA/cm^2 and flow rate 0.2 l/min
b) Current density 17 mA/cm^2 and flow rate 1.2 l/min

As pointed out in the section 7.2, in the absence of mediators, lower current density and higher flow rates are expected to give rise to higher current efficiency for the

anodic abatement of organics when the process is under mass transfer control or under mixed kinetic regime. Otherwise, when the mass transport of the organics towards the anodic surface is not a rate limiting step, a not significant effect of these two parameters is generally expected. In particular, as shown in Table 7.3 (entries 1 and 2, 11 and 12, 13 and 14), when the electrolyses were carried out in the absence of chlorides, the best performances were obtained, both at BDD and iridium anodes, in the presence of the lower current density and the higher value of the flow rate.

According to theoretical considerations reported above, a different effect of these key parameters is expected in the presence of NaCl. Indeed, as above shown, during the electrolyses of NaCl solutions, an higher concentration of oxidants was generally obtained when lower values of the flow rate and higher values of the current density are adopted.

In particular, as shown in Table 7.3 (entries 5,6 and 17,18) when the experiments were performed in basic conditions in the presence of NaCl in a concentration of 10 g/l, at both adopted anodes, a dramatically higher abatement of OA was achieved in the presence of lower values of the flow rate and higher values of the current density and, as a consequence, in the conditions that not favor the processes under mass transport kinetic control.

Otherwise, no a significant effect of flow rate and current density was observed when the electrolyses were carried out in acidic conditions (entries 3,4 and 15,16).

In order to decouple the effect of the flow rate and of the current density on the performances of the process, some electrolyses were repeated at pH of 12 and with an initial concentration of NaCl of 40 g/l at iridium oxide electrodes by changing separately the flow rate and the current density (Table 7.3).

When an high value of the flow rate was used, an higher current density results in a drastic increase of the OA abatement (Table 7.3, entries 9 – 10), while at low value of the flow rate an insignificant role of the current density was observed (Table 7.3, entries 7 – 8).

Table 7.3. *Effect of flow rate and current density on the electrochemical incineration of OA*[a]

Entry	Anode	pH	NaCl (g/l)	Flow rate (l/min)	Current density (mA/cm^2)	Charge passed (C)	Conversion (%)	CE (%)
1	IrO_2 - Ta_2O_5	2	-	0.02	39	7000	68	47
2	IrO_2 - Ta_2O_5	2	-	1.02	17	7000 (3703)	95	65
							-62	-81
3	IrO_2 - Ta_2O_5	2	10	0.02	39	7000	> 99	> 70
						-3600	70	96
4	IrO_2 - Ta_2O_5	2	10	1.02	17	3632	71	94
5	IrO_2 - Ta_2O_5	12	10	0.02	39	7000	47	32
6	IrO_2 - Ta_2O_5	12	10	1.02	17	7000	12	9
7	IrO_2 - Ta_2O_5	12	40	0.02	39	7000	78	53
8	IrO_2 - Ta_2O_5	12	40	0.02	17	7000	82	55
9	IrO_2 - Ta_2O_5	12	40	1.02	39	7000	60	42
10	IrO_2 - Ta_2O_5	12	40	1.02	17	7000	42	27
11	BDD	2	-	0.02	39	7000	83	57
12	BDD	2	-	1.02	17	7000	99	69
13	BDD	12	-	0.02	39	7000	81	56
14	BDD	12	-	1.02	17	7000	85	62
15	BDD	2	10	0.02	39	7000	93	65

16	BDD	2	10	1.02	17	7000	93	65
17	BDD	12	10	0.02	39	7000	74	50
18	BDD	12	10	1.02	17	7000	67	44

[a] *Amperostatic electrolyses in system II. System solvent supporting electrolyte (SSE): Water, Na_2SO_4, H_2SO_4 (pH = 2) or NaOH (pH = 12). Initial oxalic acid concentration: 100 mM. T = 25 °C. V = 250 ml. Charge passed = 7000 C = 1.45 Q^{th} where Q^{th} = charge necessary for a total conversion of the oxalic acid with a CE = 100%.*

Otherwise, at both 17 and 39 mA/cm^2, a decrease of the current efficiency was observed upon increasing the flow rate (entries 7,9 and 8,10).

Hence, it is possible to conclude that a dramatic change of the effect of the current density and of the flow rate on the performances of the process arises when NaCl is added to the system. As a consequence, and according with the theoretical considerations reported in section 7.2, the comparison between the electrochemical incineration performed in the absence and in the presence of chlorides dramatically depend on the adopted current density and on the flow dynamic regime. As an example, when the anodic oxidation of OA is carried out at an initial pH of 2 at BDD, an higher abatement of OA arises in the absence of NaCl when higher values of flow rate and lower values of the current density are adopted (Table 7.3, entries 12 and 16). Anyway, when the opposite values of flow rate and current density are encountered, an higher abatement is achieved in the presence of chlorides (Table 7.3, entries 14 and 16).

7.4.4 EFFECT OF THE INITIAL CONCENTRATION OF THE OXALIC ACID

In order to evaluate the effect of oxalic acid concentration on the performances of the process, several electrolyses were repeated in basic conditions with an initial OA concentration of 10 mM. This value of concentration was selected to grant the direct process to be under mass transfer control for all the adopted operative conditions. Indeed, [OA][b] in these experiments was always significantly lower than C* = i_{app} /(2Fk_m) (where i_{app} is the applied current density, F is the

Faraday constant and k_m the mass transfer coefficient) so that the ratio $i_{lim}/i_{app} << 1$. As a consequence, in the experiments performed in the absence of chlorides, most part of the charge passed is expected to give rise to the oxygen evolution reaction.

First experiments were carried out in the absence of NaCl and were generally stopped when the charge passed was about 3600 C, corresponding to 7.5 Q^{th} where Q^{th} = amount of charge necessary for a total conversion of the oxalic acid with CE = 100%. As shown in Table 7.4 (entries 1, 4 and 6), current efficiencies from 5 to 12 % were observed as a result of the low oxalic acid concentrations, significantly lower than that observed in the electrolyses performed with an initial OA concentration of 0,1 M (see Table 7.3).

As an example, when experiments were carried out at BDD at pH 12 with a current density of 39 mA/cm^2 and a flow rate of 0.2 l/min, a conversion of 70% was obtained with a current efficiency of about 10 and 64% for an initial oxalic acid concentration of 0.01 and 0.1 M, respectively.

Interestingly, a dramatic effect of the OA concentration towards the performances of the process was observed also when experiments were carried out in the presence of NaCl. Indeed, as an example when similar experiments (under operative conditions reported in Table 7.4, entry 3 and Table 3, entry 7) were carried out at BDD in the presence of 10 g/l a conversion of 65% was obtained with a current efficiency of about 26 and 57% for an initial oxalic acid concentration of 0.01 and 0.1 M, respectively. The effect of OA concentration on the performances of the process is presumably due, according to the considerations reported in section 7.2.2, to the fact that a lower bulk concentration exercises a negative effect both on homogeneous and heterogeneous oxidation reactions. Indeed, a lower concentration of OA in the bulk of the solution results in slower kinetics of homogeneous and heterogeneous oxidation of OA and in a slower mass transfer of OA towards the anodic surface.

Let us focus on the effect of flow rate and current density. As expected for a direct process under mass transfer control, when experiments were carried out at BDD with a low initial value of the OA concentration in the absence of chlorides, a dramatic increase of the current efficiency was observed when higher flow rates and lower current density were adopted (Table 7.4, entries 1 and 4).

Table 7.4. *Effect of operative parameters in the presence of a low initial concentration of OA*[a]

Entry	Anode	NaCl (g/l)	Flow rate (l/min)	Current density (mA/cm^2)	Charge passed (C)	Conversion (%)	CE (%)
1	BDD	-	0.02	39	3600	70	10
2		1	0.02	39	3846	73	9
3		10	0.02	39	3628	99	13
4		-	1.02	17	3600	98	12
5		10	1.02	17	3600	81	11
6	IrO_2–Ta_2O_5	-	0.02	39	3600	45	5
7		1	0.02	39	3600	85	11
8		10	0.02	39	3628	98	13
9		40	0.02	39	3600	90	10
10		10	1.02	17	3600	21	3

[a] *Amperostatic electrolyses in system II. System solvent supporting electrolyte (SSE): Water, Na_2SO_4, NaOH (pH = 12). Initial oxalic acid concentration: 10 mM. T = 25 °C. V = 250 ml. Charge passed = 3600 C = 7.5 Q^{th} where Q^{th} = charge necessary for a total conversion of the oxalic acid with a CE = 100%.*

On the other hand, also in this case, when experiments were repeated in the presence of NaCl, the opposite effect of flow rate and current density was observed (Table 7.4, entries 3 and 5). Similar results were achieved also at iridium anodes (Table 7.4, entries 8 and 10). Hence, it is possible to assume reasonably that in the presence of chlorides, the oxidation of OA takes place mainly by an homogeneous process. To support this hypothesis, one can consider that the abatement of OA, achieved in the operative conditions reported in Table 7.4, entry 8, is higher than the maximum

theoretical abatement for a direct process under mass transfer control computed according to the literature (Panizza et al., 2001) (Fig. 7.5).

As shown in Table 7.4, the effect of NaCl additions on the performances of the process is dramatically dependent on the adopted current densities and flow rates. An increase of the current efficiency was, in fact, observed when higher values of the flow rate and lower values of the current densities were adopted (Table 7.4, entries 1-3) while a decrease was observed in the opposite operative conditions (Table 7.4, entries 4-5). In particular, the highest abatement of OA was obtained at BDD in the presence of 10 g/l (99% conversion with a CE of 13% as reported in Table 7.4 entry 3).

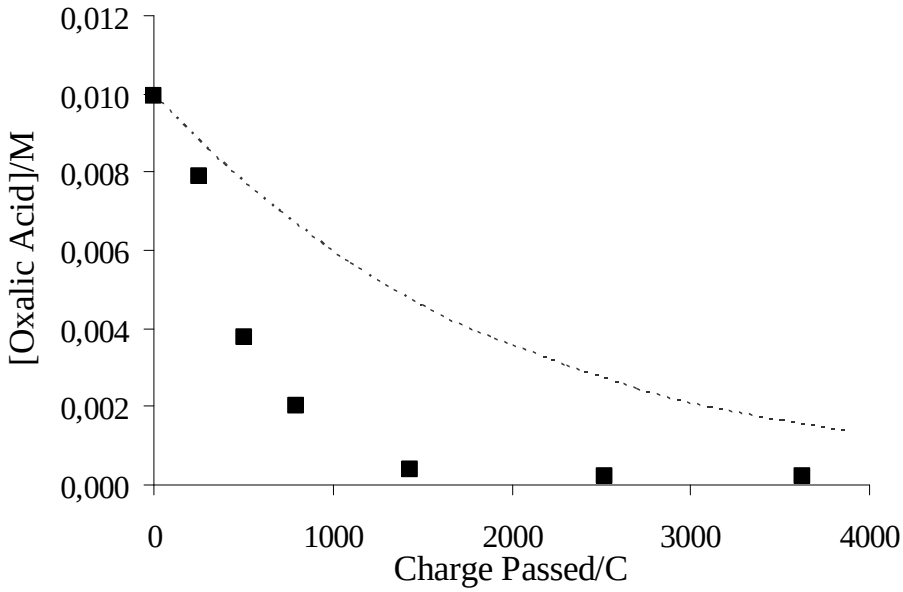

Fig. 7.5 *Oxalic acid concentration vs. charge passed for an amperostatic electrolysis in system II performed at IrO_2-Ta_2O_5. Initial substrate concentration: 10 mM. Flow rate: 0.2 l/min. Current density: 39 mA/cm^2. Amperostatic electrolyse in system II. System solvent supporting electrolyte (SSE): Water, Na_2SO_4, NaOH (pH of 12). T = 25°C. Theoretical curve (---) obtained for a direct process under mass transfer control computed according to chapter 4, with the parameter C* of 0.044.*

Finally let us observe that also in the presence of a low initial OA concentration, higher abatement of OA are obtained at BDD in the absence of chlorides (Table 7.4, entries 1 and 6) and at iridium anodes in the presence of chlorides (Table 7.4, entries 2 and 7). In particular, it was sufficient to operate with a concentration of 1 g/l of NaCl to observe an higher abatement at iridium.

Interestingly, the OA abatement at iridium anodes raises upon increasing the NaCl concentration up to 10 g/l but a further increase of [NaCl] to 40 g/l results in slightly lower current efficiencies (see Table 7.4, entries 6-9), thus showing that in the presence of very high ratio [NaCl]/[OA] between the bulk concentrations of NaCl and OA, a negative effect of an increasing NaCl concentration can be encountered.

CHAPTER 8

INFLUENCE OF THE NATURE OF ORGANIC SUBSTRATE ON THE ELECTROCHEMICAL INCINERATION PROCESS: ANODIC OXIDATION OF FORMIC AND MALEIC ACID

8.1 INTRODUCTION

A study on the influence of some operative parameters on the performances of the electrochemical incineration of two other carboxylic acids, namely formic acid (FA) and maleic acid (MA), was performed in order to compare these results to those referring to oxalic acid (see chapters 5 and 6), with the main aim of study the influence of the nature of the organic substrate on the electrochemical incineration process.

The choice of this kind of compounds was dictated by the fact that carboxylic acids are common intermediates of the oxidative degradation of several compounds. Furthermore, they are rather stable (Gandini et al., 2000; Martinez-Huitle et al., 2004a) and are often mineralized at longer times with respect to the starting substrates (Cañizares et al., 2004a).

In this chapter, electrolyses and chronoamperometries conducted at both Iridium based anode and at BDD, with formic and maleic acids as substrates, are reported.

The first part will be dedicated to the study of the influence of some operative parameters on the electrochemical oxidation of the formic acid, performing a number of experiments under mixed, oxidation reaction control and mass transport control regimes.

The second part of the chapter will be dedicated to the electrochemical oxidation of maleic acid. A series of experiments performed both in divided and undivided electrochemical cells were performed in this case.

Furthermore, we tried to compare the data obtained from the electrochemical oxidation of formic and maleic acids with the theoretical predictions based on the model presented in the chapter 4. For the maleic acid the model was extended in order to consider the formation of intermediate products. In fact, unlike the anodic

oxidation of oxalic and formic acids that lead to the formation of carbon dioxide without the formation of intermediates, maleic acid is a bigger molecule containing four double bonds, that gives rise to the formation of several intermediates during its electrochemical oxidation or reduction. Thus, apart from the electrolyses conducted in undivided cells, in the case of maleic acid a set of experiments was performed in a divided cell, in order to achieve more information about the nature of intermediates. Therefore, a paragraph will be dedicated on the study of the intermediates generated by oxidation and by reduction of the maleic acid, respectively.
Finally, a comparison with the result obtained in the case of oxalic acid will be accomplished, in order to focus on the influence of the nature of the substrate on the electrochemical oxidation process.

8.2 CHRONOAMPEROMETRIC MEASUREMENTS

Prior to electrochemical incineration experiments, chronoamperometric measurements were recorded in background solutions containing Na_2SO_4 and H_2SO_4, in the absence and in the presence of different concentrations of formic and maleic acid at different operative conditions. These experiments were carried out both at BDD and at DSA anodes. To achieve more information on the mechanism of oxidation of these carboxylic acids at the two very different anodic materials, as done in the case of oxalic acid (see par. 5.2.1), chronoamperometric measurements were carried out at different fixed potentials (1.5 and 1.8 V vs. SCE for DSA anode and 2.4 and 2.7 V vs. SCE for BDD) and at different temperatures (25 and 50 °C).
As shown in Fig. 8.1, it is possible to observe that, for low acid concentrations $[OR]^b$, current densities change approximately linearly with the acid concentrations for all the investigated acids, even if the oxalic one gives rise to higher current densities. Conversely, for high acid concentrations, the linear variation is maintained for oxalic and formic acids, while a decrease of the current density occurred upon increasing $[OR]^b$ for the maleic one. Thus this result could suggest the occurrence of the adsorption of maleic acid at anodic surface at high concentration of the substrate, while at lower concentrations, a direct or mediated by hydroxyl radicals oxidation mechanism can be noted.

These trends were explained in literature (Ross and Ross, 1977) assuming that, for low concentrations of the acids, the oxidation of the organic by means of hydroxyl radicals generated by the water oxidation is so fast to be under the kinetic control of the mass transport of the carboxylic acid from the bulk of the solution to the anodic surfaces, while for high acid concentrations, the rate of generation of hydroxyl radicals is not sufficient to oxidize all the molecules that approach the anode, thus allowing the occurrence of lateral reactions, including direct anodic oxidation and adsorption phenomena. Oxalic acid gave rise to higher current densities than other tested acids as a probable consequence of the fact that this acid is involved in a slow reaction with hydroxyl radicals (Ross and Ross, 1977) thus allowing a different oxidation route concerning probably a direct anodic oxidation process also at low concentrations. When experiments were repeated at 50 °C similar trends were observed.

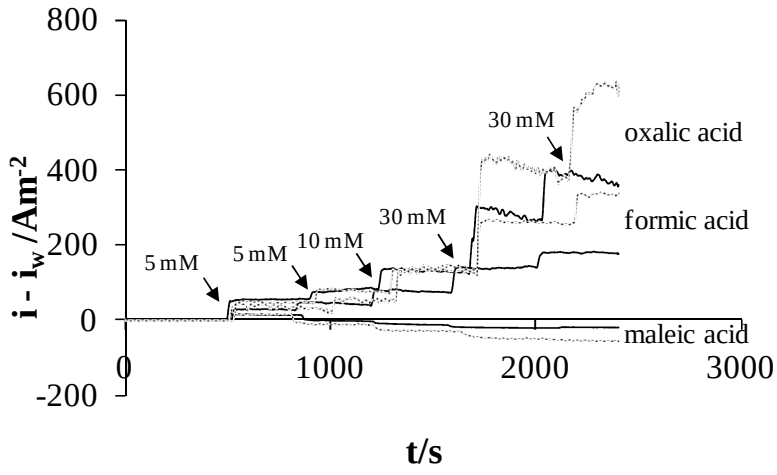

Fig. 8.1 *Comparison of chronoamperometric response of BDD electrode to step-by-step injection of formic, maleic and oxalic acid at 2.7 V vs. SCE at 25 (__) and 50 (__) °C. System solvent supporting electrolyte (SSE): Water, Na_2SO_4, H_2SO_4 (pH = 2). $i - i_w$ (difference between the total current density and the current density recorded in the absence of the acid) vs. acid concentration.*

Interestingly, different results were obtained in the case of chronoamperometric measurements conducted at Iridium oxide based anode both for formic and maleic acid. Indeed, in the first case, the current density seems to be constant or even decreases with an increasing concentration of formic acid, almost for low concentrations. This result was detected at both low and high temperature, and at the two polarized potentials examined. However, at 1.5 V vs. SCE and at 50°C, current density starts to increase when a concentration of 50 mM was reached (see Fig. 8.2).

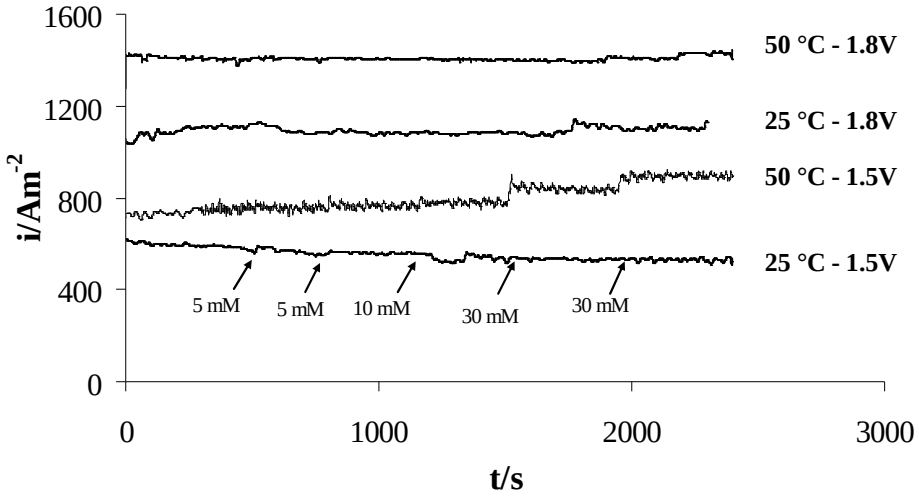

Fig. 8.2 *Chronoamperometric response of DSA anode to step-by-step injection of formic acid at 25 and 50°C, at 1.5 and 1.8 V/SCE. System solvent supporting electrolyte (SSE): Water, Na_2SO_4, H_2SO_4 (pH = 2)*

Nevertheless, in the case of maleic acid, a very different scenario was observed for the chronoamperometry conducted at 1.5 V vs. SCE and 25°C: the current density remains constant for additions of the substrates up to 10 mM and then it increases quite linearly with higher concentrations (see Fig. 8.3 a and b). Analogue results were observed at the temperature value of 50°C and at the higher potential value of 1.8 V vs. SCE, even if higher current densities were detected.

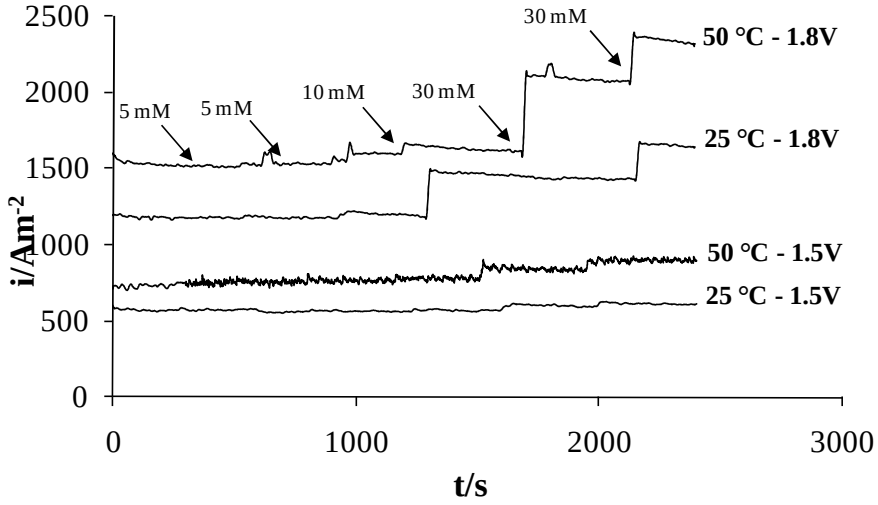

(a)

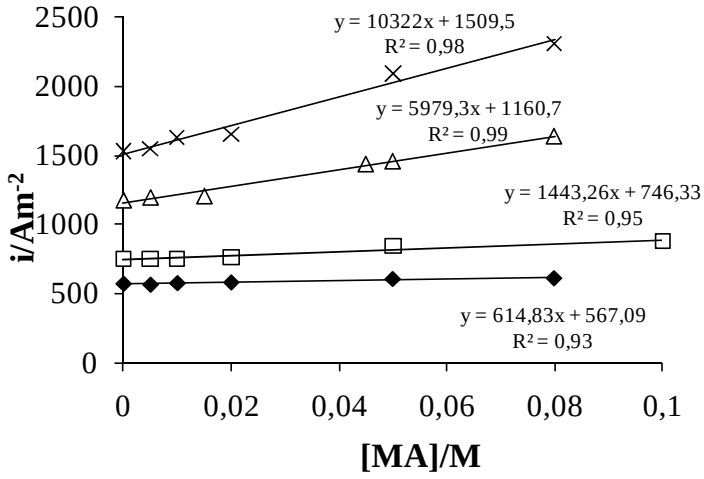

(b)

Fig. 8.3 *(a) Chronoamperometric response of DSA anode to step-by-step injection of maleic acid at 25 and 50°C, at 1.5 and 1.8 V SCE and (b) Correspondent current density as a function of maleic acid concentration. System solvent supporting electrolyte (SSE): Water, Na_2SO_4, H_2SO_4 (pH = 2)*

In order to show the influence of the nature of the substrate on the chronoamperometric measurements, let us plot the difference between the total current density and the current density recorded in absence of the acids versus time, at iridium based anodes (Fig. 8.4). Then, a very different response was observed for the investigated acids.As previously reported in paragraph 6.3 in the case of oxalic acid, an increase of the steady-state current was observed upon enhancing the concentration of the acid, at both polarized potentials examined, thus showing that the oxalic acid is significantly oxidized at iridium anodes in the range of potential of oxygen evolution; while a quite different picture was observed for formic and maleic acids. A current decrease was observed in the presence of formic acid as a probable consequence of adsorption phenomena which hinder the water discharge, while an increase of $[MA]^b$ does not occur upon enhancing *i* unless higher values of $[MA]^b$ are achieved (higher than 20 mM), thus probably reflecting the fact that, at this anode, the oxidation of MA is very limited.

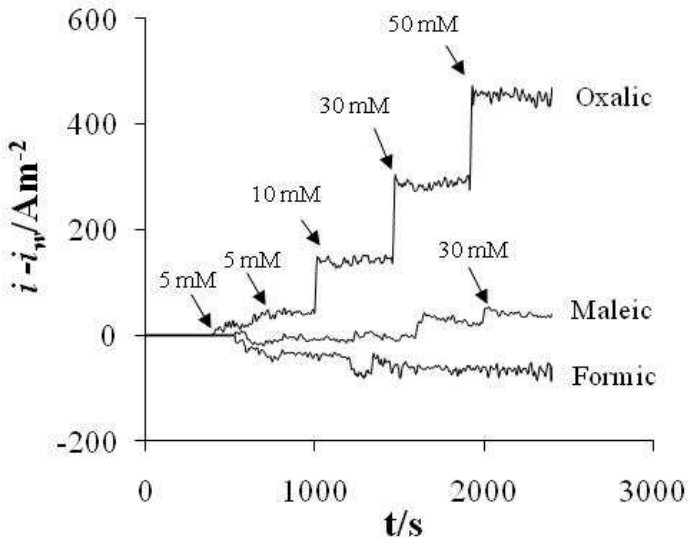

(a)

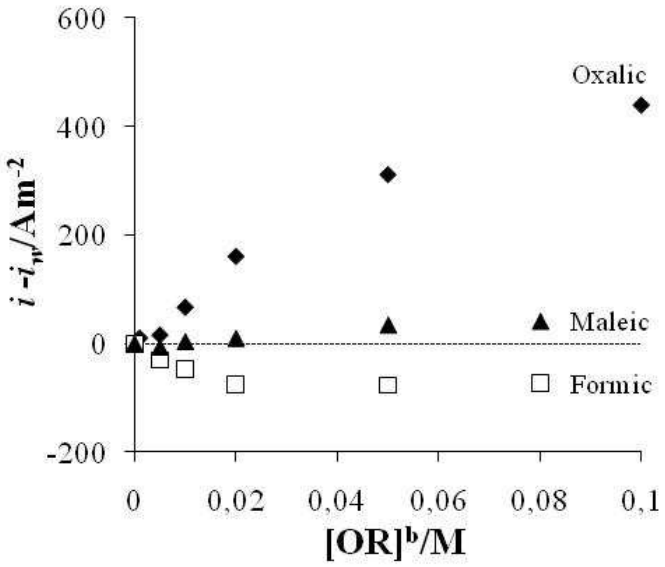

(b)

Fig. 8.4 *Comparison of chronoamperometric response of IrO_2-Ta_2O_5 electrode to step-by-step injection of formic, maleic and oxalic acid at 1.5 V vs. SCE. System solvent supporting electrolyte (SSE): Water, Na_2SO_4, H_2SO_4 (pH = 2). $i - i_w$ (difference between the total current density and the current density recorded in the absence of the acid) vs. time (Fig.8.4a) or acid concentration (Fig. 8.4b)*

8.3 INFLUENCE OF OPERATIVE PARAMETERS ON THE ELECTROCHEMICAL OXIDATION OF FORMIC ACID

To study the effect of some operative parameters on the electrochemical oxidation of formic acid, three different sets of experiments were carried out, under different operative conditions, in order to achieve the kinetic regimes of mass transport control, oxidation reaction control and mixed regime.

8.3.1 MIXED REGIME CONDITIONS

Let us now take in account the general case of a process whose rate determining step changes during the electrolysis from an oxidation reaction control in the first stages to mass transfer control in the last part with a mixed regime between them.

A set of experiments was conducted with galvanostatic alimentation in the recirculation flow cell (see system II in par. 3.2.2) in order to study the influence of some operative parameters, such as the anodic material, the temperature and current density and flow rate.

The electrolytic solution was constituted of sodium sulfate 35 mM as supporting electrolyte and of sulfuric acid in order to achieve a pH of 2. Initial concentration of formic acid was in all the electrolyses of 100 mM and they were stopped when the charge passed was 7000 C = 1.45 Q^{th}, where Q^{th} = charge necessary for a total conversion of the formic acid with a *CE* = 100%.

When the electrolyses was performed at iridium based anodes, with a current density of 39 mA/cm^2, a flow rate of 0.2 l/min and a temperature of 25 °C, a conversion of only about 60% with a current efficiency slightly lower than 50% was achieved at the end of the experiment (Table 8.1, entry 1).

For the sake of comparison, an experiment was performed at similar operative conditions at a boron doped diamond anode (Table 8.1, entry 5), thus obtaining higher conversions an higher faradic efficiency, 88% and 57%, respectively. Interestingly, this result is coherent with chronoamperometric measurements previously reported. Indeed, in acidic conditions, at BDD anode the process is expect to take place at least in part by a direct anodic oxidation process, giving rise to higher conversion during the electrolysis, while at Ti/IrO_2-Ta_2O_5 an evident increase of the current with the concentration of the substrate did not be achieved, thus giving rise to low conversion in the electrolytic experiment. When the experiment was repeated at different operative conditions, in particular with a current density of 17 mA/cm^2, a flow rate of 1.2 l/min (Table 8.1, entry 2 and 7, respectively), very higher conversions were obtained, both for the DSA and for the BDD, even if the best results were observed using BDD as anode(Fig. 8.5): a conversion of about 100% was detected and a faradic efficiency of 66%. These results can be ascribed to the different kinetic regimes involved for the most part of the electrolysis, at the different operative conditions: a prevalent mass transport control at higher current density and minor flow rate, and a charge transfer control at the opposite conditions.

Table 8.1 *Influence of some Operative Parameters on the Incineration of FA*[a]

Entry	Temperature (°C)	Anode	Flow rate (l/min)	Current density (mA/cm^2)	Conversion (%)	CE (%)
1	25	DSA	0.02	39	59 - 61	46 - 48
2	25	DSA	1.02	17	77 - 79	55 - 57
3	25	DSA	1.02	39	84 - 86	54 - 56
4	50	DSA	1.02	17	96 - 98	67 -69
5	25	BDD	0.02	39	87 - 89	56 - 58
6	50	BDD	1.02	17	99 - 100	65 - 67
7	25	BDD	1.02	17	99 - 100	65 - 67

[a] *amperostatic electrolyses. System solvent supporting electrolyte (SSE): Water, Na_2SO_4, H_2SO_4 (pH = 2). T = 25°C. V = 250 ml.*

In order to study the effect of the current density independently from the flow rate at DSA anode, an experiment was conducted at 39 mA/cm^2 and a flow rate of 1.2 l/min. Then, a slight higher conversion of the formic acid with the increasing of the current density was detected (Table 8.1, entries 2 and 3).

To investigate the effect of the temperature, the electrolyses conducted at 17 mA/cm^2 and 1.2 l/min, when the best results were achieved, were repeated at 50°C, at both the used anodes. In the case of the DSA, a dramatic increase of the conversion percentage was observed, from 78 to 97%, while in the case of BDD, no influence of the temperature was detected (Table 8.1, entry 4 and 6, respectively and Fig. 8.6). In particular, the first result is quite similar to that obtained for the oxalic acid when, at the equal operative conditions, higher conversions were obtained at higher temperature at the DSA anode (see paragraph 6.4.4).

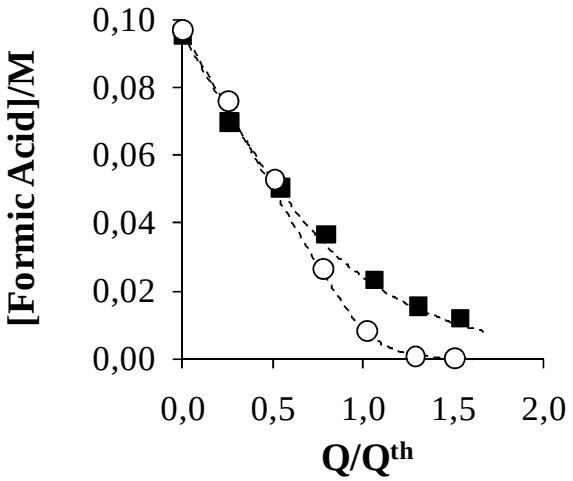

Fig. 8.5 *Effect of flow rate and current density on the anodic oxidation of formic acid at BDD. Electrolyses performed in system II at 1.2 l/min and 17 mA/cm^2 (○), 0.2 l/min and and 39 mA/cm^2 (■). T = 25 °C. System solvent supporting electrolyte (SSE): Water, Na_2SO_4, H_2SO_4 (pH 2). Theoretical curves (---) obtained by Eq. 4.14 with [RH]* = 0.002 M (see Table 4.1).*

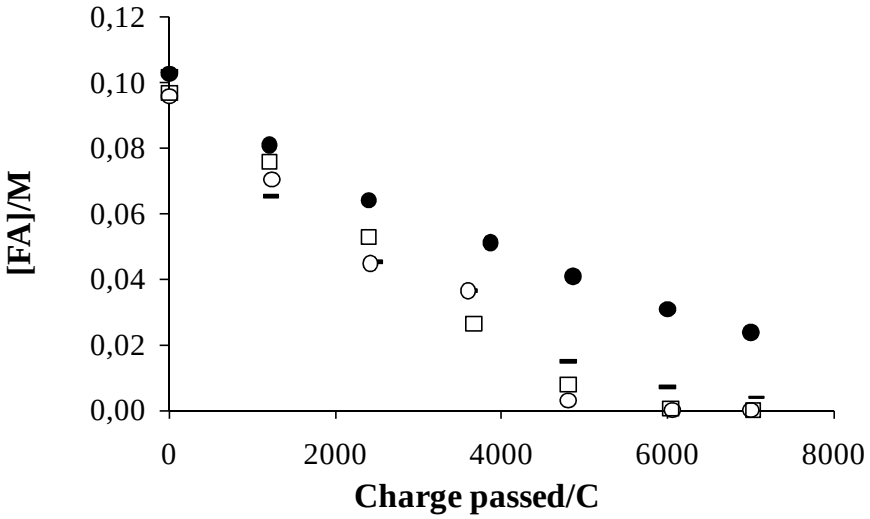

Fig. 8.6 *Formic acid concentration vs. charge passed. BDD anode: T = 25 (o) and 50 (□) °C; IrO_2/Ta_2O_5 anode: T = 25 (•) and 50 (-) °C. Flow rate: 1,2 l/min. Current density: 17 mA /cm^2. System solvent supporting electrolyte (SSE): Water, Na_2SO_4,H_2SO_4 (pH =2). Initial substrate concentration:0,1 M.*

These data indicate, according to the prof. De Battisti (Martinez-Huitle, 2004a), that the rate determining steps for oxalic and formic acids oxidation and for oxygen evolution reaction at iridium oxide anodes, characterized by different activation energy, are different.This result seemed very interesting, focusing on the fact that working at a temperature of 50 °C, easily achievable on applicative scale, could dramatically improve the performances of the DSA anodes in the organic pollutants abatement process via electrochemical oxidation.

Interestingly, as previously discussed in paragraph 4.3.3, the value of *ICE* is readily predictable from Eq. 4.14 for different operative conditions if one estimates k_m and [*RH*]* as above mentioned and consequently the trend of the formic acid concentration vs. charge passed could be easily modelled. Indeed, a good agreement between the mathematical model and the experimental data was observed, as shown in Fig. 8.5, where C* was calculated using the values of k_m estimated according to par. 3.2.1.

8.3.2 OXIDATION REACTION CONTROL REGIME

In order to achieve a process under the kinetic control of the oxidation reaction, lower operative current density were settled, satisfying the condition of C > C*. In particular, an initial concentration of formic acid of 10 mM was used in all the electrolyses, to avoid very long duration of the electrolyses.

Even this set of experiments was conducted with galvanostatic alimentation and in the recirculation flow cell (see system II in par. 3.2.2). The electrolytic solution was constituted of sodium sulfate 35 mM as supporting electrolyte and of sulfuric acid in order to achieve a pH of 2. Electrolyses were stopped when the charge passed was 500 C, close to the value of the theoretical charge, i.e. the charge necessary for a total conversion of the formic acid with a *CE* = 100%.

In particular, the influence of the current density and flow rate, of the initial concentration of formic acid and of the electrodic material was investigated under the adopted operative conditions.

As it is possible to observe in Fig. 8.7 and from Table 8.2 (entries 1-3), a first set of electrolyses at different current density and flow rate values was accomplished and,

whereas the operative kinetic regime was under charge transfer control, no effect of this two parameters was detected.

Table 8.2 *Influence of Formic Acid Initial concentration, Current Density and Flow rate under charge transfer control kinetic regime*[a]

[FA] (mM)[d]	Electrode	i (mA/cm^2)	Flow rate (l/min)	Conversion (%)	Charge Passed (Q/Qth)	Time Passed (min)	C* (M)[b]	i_{lim} for the residual concentration[c] (mA/ cm^2)
10	BDD	1	1.02	80 – 82	1.01	814	0.07	2.09
10	BDD	1	0.02	79 – 81	1.01	832	1.06	1.04
10	BDD	2	1.02	81 - 83	1.01	415	1.04	2.09
10	DSA	1	1.02	54 – 56	1.01	833	0.07	7.04
100	DSA	17	1.02	85- 87	1.00	540	10.09	61.05.00
100	BDD	17	1.02	92 – 94	1.00	533	10.09	12
50	BDD	5.05	1.02	87 – 91	1.00	870	3.06	8.08

[a] *amperostatic electrolyses in system II. System solvent supporting electrolyte (SSE): Water, Na_2SO_4, H_2SO_4. T = 25°C. Q^{th} = charge necessary for a total conversion of the Formic acid with a CE = 100%. V = 250 ml.*
[b] *$C^* = i_{app}/(2FD/\delta)$.*
[c] *$i_{lim} = nFk_m[RH]^b$ computed for the residual concentration of Formic Acid for $Q \sim Q^{th}$*
[d] *Initial concentration of Formic Acid*

Let now us consider the influence of the current density at the constant flow rate of 1.2 l/min. As shown in the Fig. 8.8, an increase of the current density does not affect the conversion of the substrate but results in a faster abatement (e.g., in higher productivity of the electrochemical cell).

Please, observe as the mathematical model elaborated when the process is under the kinetic control of the oxidation reaction (see par. 4.2.2) can satisfactory predict the variation of the applied current density. Indeed, a good agreement between the experimental data and the mathematical model above discussed was detected. When the electrolysis conducted at a current density of 1 mA/cm^2 and a flow rate of 1.2 l/min, at 25°C and with an initial formic acid concentration of 10 mM was repeated at iridium based anode, lower conversion values was obtained. In particular, as shown in Fig. 8.9 and Table 8.2 (Entries 1 and 4), a conversion of about 55% at a charge passed correspondent to the theoretical charge was achieved used DSA anode, while at BDD anode this value was of about 81%. This result, obtained in particular under the oxidation reaction control, can be ascribed to the theoretical consideration of the involvement of an oxidation mechanism mediated by hydroxyl radicals.

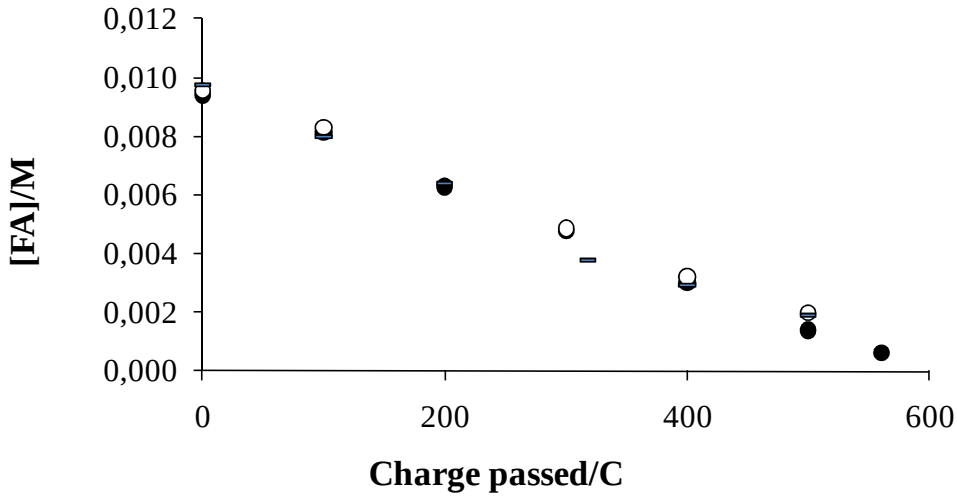

Fig. 8.7 *Formic acid concentration vs. charge passed at BDD anode. Flow rate 1.2 l/min: current density 1 (•) and 2 (-) mA /cm^2. Current density 1 mA /cm^2: 1.2 (•) and 0.2 (o) l/min. System solvent supporting electrolyte (SSE): Water, Na_2SO_4,H_2SO_4 (pH =2). Initial substrate concentration:0.01 M. T = 25 °C.*

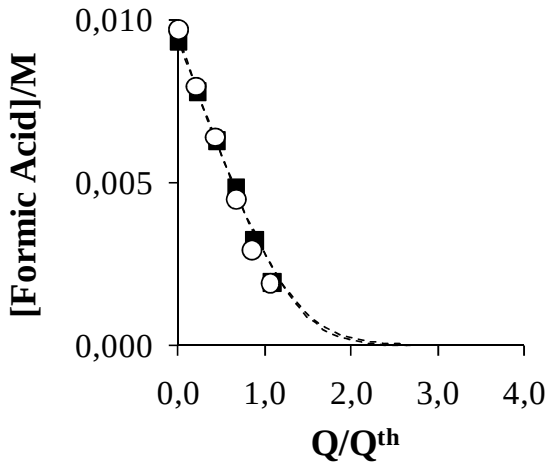

(a)

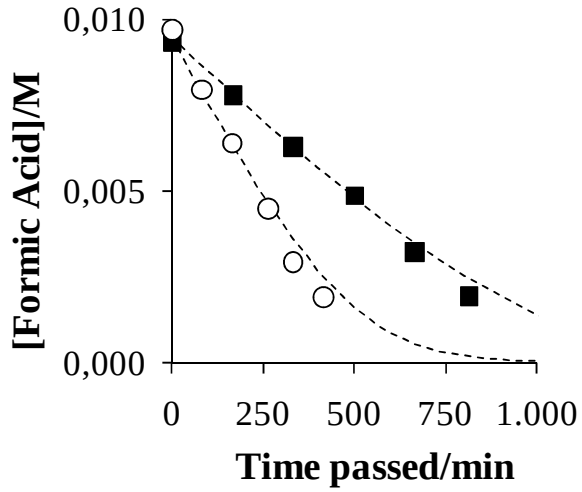

(b)

Fig. 8.8 *Trend of formic acid concentration vs. dimensionless passed charge (a) and vs time (b) for amperostatic electrolyses performed at BDD in system II at 1.2 l/min and 1 (■), 2 (○) and 5 (Δ) mA/cm^2. Initial concentration 10 mM. T = 25 °C. System solvent supporting electrolyte (SSE): Water, Na_2SO_4, H_2SO_4 (pH 2). Theoretical curves (---) obtained by Eq.ns 4.2 and 4.6 with [RH]* = 0.002 M. Q^{th} = charge necessary for a total conversion of FA with a CE = 100%.*

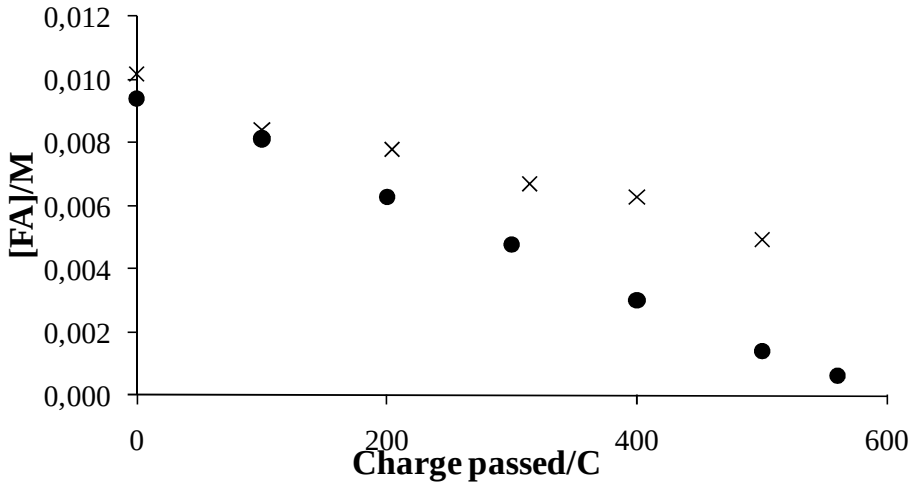

Fig. 8.9 *Formic acid concentration vs. charge passed at (•) BDD and at (x) DSA anodes. Flow rate 1.2 l/min and current density 1 mA /cm^2. System solvent supporting electrolyte (SSE): Water, Na_2SO_4,H_2SO_4 (pH =2). Initial substrate concentration:0.01 M. T = 25 °C.*

Indeed, the kinetic constant of the reaction between the organic pollutant and hydroxyl radical is generally very high for diamond anodes, thus the utilization of this anode is expected to affect positively the abatement of organic pollutants in water if the process is under oxidation reaction control but not if a mass transfer control arises.

Interestingly, an other important parameter investigated, under the oxidation reaction control regime, was the effect of the initial formic acid concentration, since it was difficult to found in literature data on the effect of the organic concentration on the performances of the process when a fast mass transfer kinetic is involved (see par. 2.3.4). In particular, as shown in Table 8.2 (Entries 4 and 5) and in Fig. 8.10a, in the case of the oxidation of formic acid at iridium anodes, for both the experiments performed with C° of 100 and 10 mM, the current efficiency of the process was lower than 100 % and increased significantly upon enhancing the concentration of the organic. For BDD anodes, a different picture was observed.

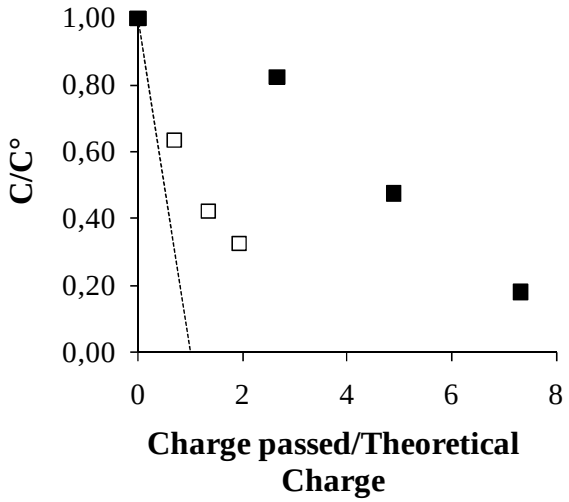

(a)

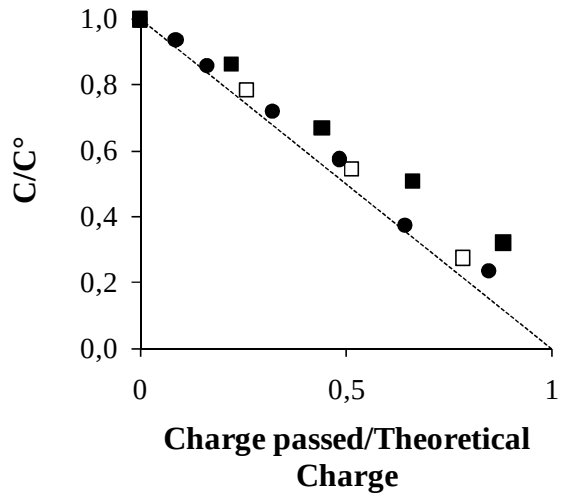

(b)

Fig. 8.10 *C/C° vs. Charge passed/Theoretical Charge for amperostatic electrolyses of formic acid at IrO_2-Ta_2O_5 (8.10a) and at BDD (8.10b). For fig. 8.10a, C° = 10 (■) and 100 mM (□) (Experimental conditions reported in Table 7.2, entries 4 and 5, respectively). For fig. 8.10b, C° = 10 (■), 50 (●) and 100 mM (□) (Experimental conditions reported in Table 7.2, entries 1, 6 and 7, respectively). Electrolyses performed in system II. System solvent supporting electrolyte (SSE): Water, Na_2SO_4, H_2SO_4 (pH about 2). T = 25°C.*

Thus, for an initial concentration of the formic acid of 0.1 M and 0.05 M, current efficiencies were very close to 100 % for a large part of the experiment so that the effect of the organic concentration could not be clearly appreciated (Fig. 8.10b and Table 8.2, entries 6 and 7). On the other hand, when the experiment was performed with an initial concentration of formic acid of 10 mM, conversions decreased appreciably, thus allowing to appreciate the effect of the organic concentration (Fig. 8.10b and Table 8.2, entry 1).

8.3.3 MASS TRANSPORT CONTROL REGIME

When the rate of the mass transfer of the pollutant is dramatically lower than that of its oxidation, the concentration of the pollutant at the anodic surface/reaction layer $[RH]^0$ is close to zero and the oxidation process is under mass transfer control. This case arises, for an oxidation process that proceeds up to the total oxidation of the organic pollutant, when the limiting current density $i_{lim} << i_{app}$ e.g. when $[RH]^b << C^*$ (where $C^* = i_{app}/(nFk_m)$).

In order to better understand the mechanism of oxidation of the formic acid under the mass transport control regime, a set of experiments was performed under potentiostatic alimentation, at BDD anode. All these electrolyses were performed in acid media and in the batch bench-scale cell (system I, par 3.2.2). In particular, potential values were chosen in order to obtain an applied initial current value from three to six times the limiting current one.

Under mass transfer control, the current efficiency *ICE* should depend on the flow dynamic of the system (trough its effect on k_m), on the applied current density and on $[RH]^b$ (with a linear dependence on this parameter) (see par. 4.3.1).

Most of experiments were performed under nitrogen atmosphere and mixing the electrolytic solution by a magnetic stir bar. In order to evaluate the influence of the flow dynamic of the system, a set of experiments was performed stopping the mixing and the introduction of nitrogen into the cell, alternatively. As shown in Fig.8.11, higher conversion were be obtained in the presence of mixing and nitrogen. Indeed, the same bubbles could let to enhance the mixing of the solution near the anode, influencing the flow dynamic of the system. As a general rule, an

increase of the mixing rate, or of the flow rate in the case of a ricirculation cell, lead to a smaller diffusion layer δ, thus a bigger mass transport coefficient, since k_m = D/δ, and consequently to higher i_{lim} and lower C*, favouring the oxidation of organics.

Since this set of experiments was performed with a potentiostatic alimentation, the applied potential was varied with the aim of vary the initial current values and thus investigating the influence of this parameter. As shown in the Fig. 8.12a, an increase of potential leads to lower current efficiencies, according with the theoretical model (see Eq. 4.1). In particular, increasing *E*, the same values of conversion were obtained at shorter times and higher amounts of charge (see Fig 8.12b and 8.12c).

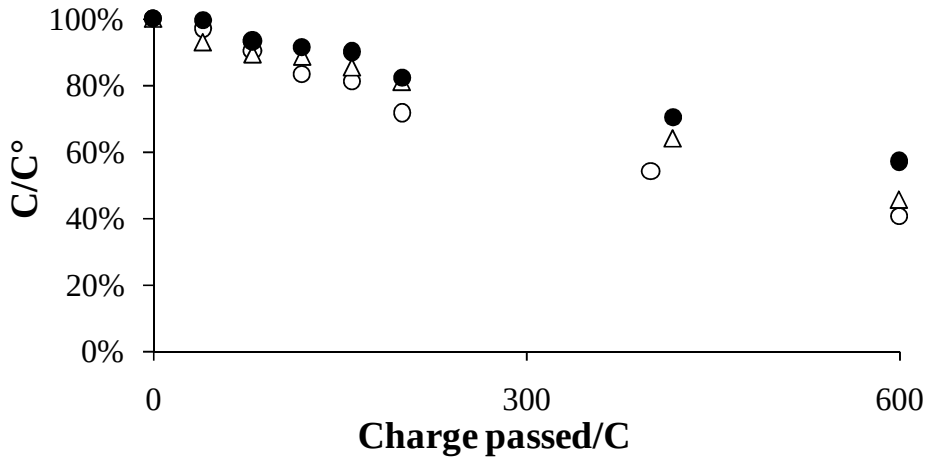

Figure 8.11 *C/C° vs. charge passed for electrolyses performed at BDD anode with an initial concentration of formic acid of 10 mM and with a potential applied of 3.3V/SCE in a mixed and with nitrogen (o), in a not mixed and with nitrogen (Δ) and in a not mixed and without nitrogen (•) system. System solvent supporting electrolyte (SSE): Water, Na_2SO_4,H_2SO_4 (pH =2) T = 25 °C.*

Please, note that in this case conversion values lower than those obtained in the case of oxidation reaction control regime was observed (see par. 8.3.2), since higher

residual formic acid concentrations were detected at the end of the experiments (see Fig. 8.12b).

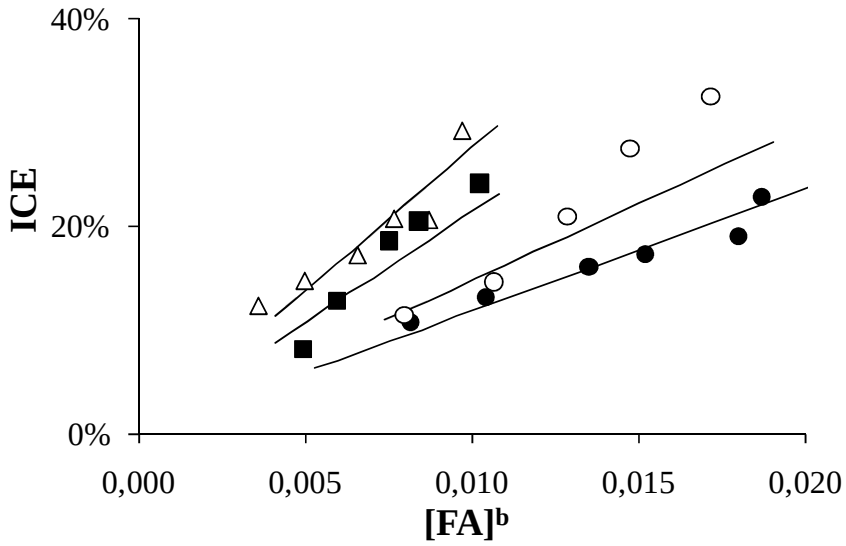

(a)

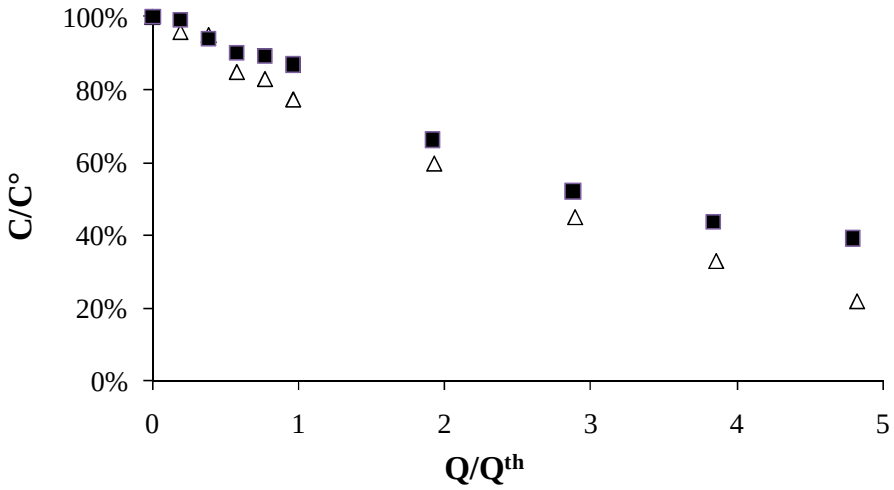

(b)

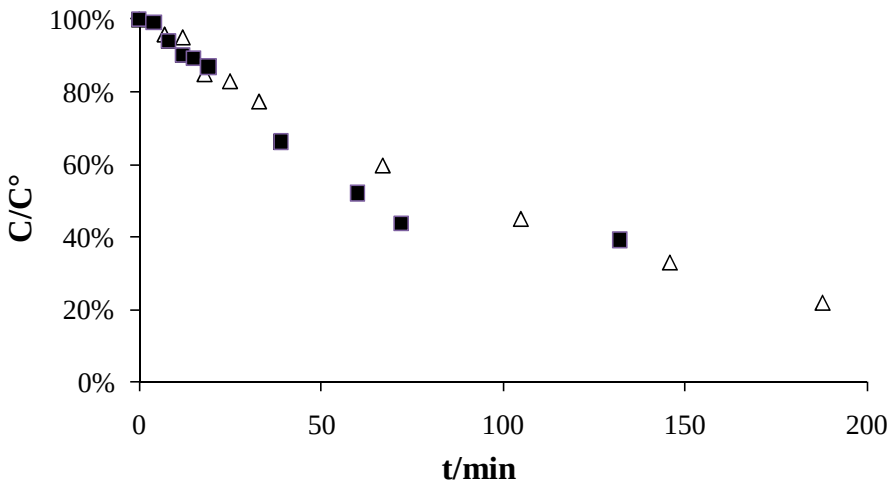

(c)

Fig. 8.12 *Instantaneous Current Efficiency vs. formic acid concentration (a) and trend of dimensionless concentration C/C° vs. dimensionless passed charge (b) and vs. time (c) for potentiostatic electrolyses performed at BDD anode with a C° of 10 mM and a potential applied of 2.6 (Δ) and 2.75 (■) V/SCE and with a C° of 20 mM and a potential applied of 3.3 (o) and 3.75 (●) V/SCE in a mixed and with nitrogen system. System solvent supporting electrolyte (SSE): Water, Na_2SO_4,H_2SO_4 (pH =2) T = 25 °C. Theoretical curves (---) obtained by Eq. 4.1.*

Indeed, conversion values of 81 and 65% were observed when the electrolyses were conducted at BDD anode at 2.6 and at 2.75 V/SCE, respectively. As mentioned in par. 4.4, for a direct process under potentiostatic alimentation (Eq. 4.23), 1/*ICE* should present a linear trend with $1/[FA]^b$ for any value of *E*. Indeed, as shown in the Fig. 8.13, when 1/*ICE* was plotted as a function of $1/[FA]^b$, the experimental points were well fitted by regression lines with an intercept close to 1. Furthermore, for a direct process mediated by hydroxyl radicals under mass transfer control (e.g. for very positive values of the applied potential), the *ICE* should present a linear variation with the formic acid concentration as shown by Eq. 4.28, that was not observed in any electrolysis (see Fig. 8.12a).

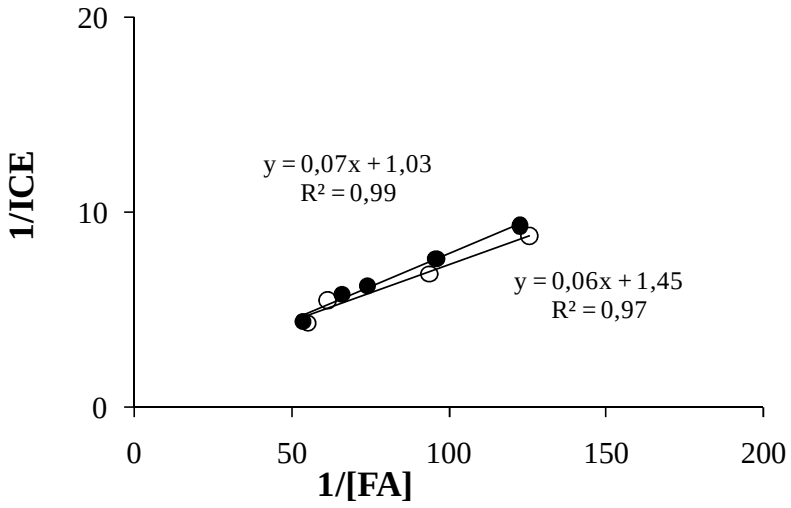

Fig. 8.13 *1/ICE vs. 1/formic acid concentration for potentiostatic electrolyses performed at BDD anode with a C° of 20 mM and a potential applied of 3.3 (o) and 3.75 (•) V/SCE in a mixed and with nitrogen system. System solvent supporting electrolyte (SSE): Water, Na_2SO_4,H_2SO_4 (pH =2) T = 25 °C.*

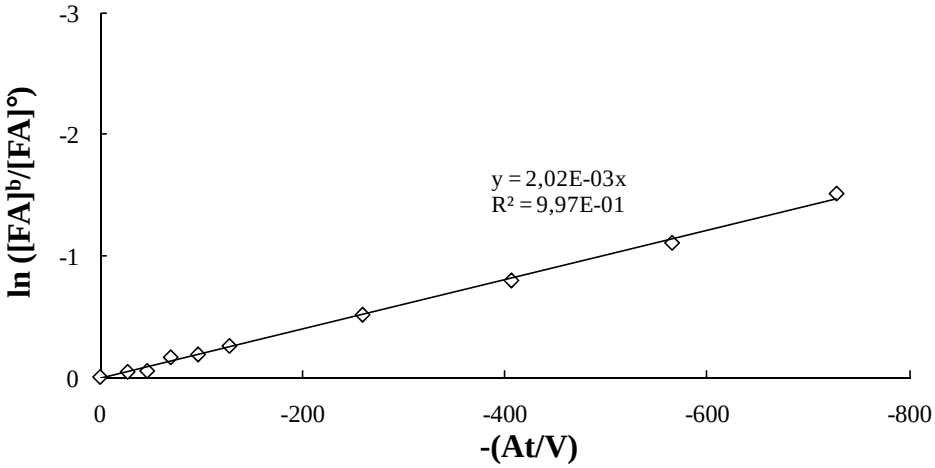

Fig. 8.14 $\ln[FA]^{b,t}/[FA]^{b,t=0}$ *vs. -(A/V)t for potentiostatic electrolysis performed at BDD anode with a C° of 10 mM of formic acid and a potential applied of 2.6 V/SCE in a mixed and with nitrogen system. System solvent supporting electrolyte (SSE): Water, Na_2SO_4,H_2SO_4 (pH =2) T = 25 °C.*

Let now us consider the aspects of the mathematical model discussed in chapter 4, when the experiments were carried out under mass transport control regime, relatively to the dependence of the concentration of formic acid on the charge and on the time passed during electrolyses (see Eq.ns 4.3 and 4.4). Hence, plotting $\ln[RH]^{b,t}/[RH]^{b,t=0}$ versus $-(A/V)t$ is possible to obtain a line with a slope correspondent to the k_m evaluated as described in paragraph 3.2.1 (k_m = 0.0025 cm/s for the system I). As an example, this result is showed in the Fig. 8.14 for the electrolysis performed at 2.6 V/SCE.

8.4 INFLUENCE OF OPERATIVE PARAMETERS ON THE ELECTROCHEMICAL OXIDATION OF MALEIC ACID

A quite different scenario was observed investigating the electrochemical oxidation of maleic acid, since several intermediated products are generated during the electrochemical degradation of this compound, both at the anode and at the cathode. In particular, the compounds detected during these electrolyses were oxalic and formic acids, in higher concentrations and malonic, and acetic acids in lower quantities. These carboxylic acids, produced by oxidation of maleic one, also detected by other authors (Dukkanci and Gunduz, 2009; Feng and Lee, 2003; Flox et al., 2007; Johnson and Gilmartin, 1967; Johnson et al., 1999; Lee and Kim, 2000; Weiss et al., 2007), give rise at their turns to a following oxidation to CO_2.

Succinic acid was also detected, obviously as reduction product, according the following reaction:

$$C_4H_4O_4 + 2\ e^- + 2\ H^+ \rightarrow C_4H_6O_4 \qquad (8.1)$$

Even fumaric acid, the isomer of the maleic acid, was detected in all the experiments. It is a chemically stable molecule at room temperature. Its presence in the electrochemical cell is believed to be formed through the cis-trans isomerization of maleic acid (Lee and Kim, 2000).

8.4.1 EXPERIMENTS PERFORMED IN AN UNDIVIDED CELL

A first set of experiment was performed in the undivided recirculation cell of the system II, in order to study the influence of some operative parameters on the process of electrochemical abatement of the maleic acid as starting compound.

Electrolyses at a current density of 39 mA/cm^2 and a flow rate of 0.2 l/min at room temperature, with an initial concentration of maleic acid of 0.1 M, were performed at both BDD and DSA anodes. As shown in the Fig. 8.15a, higher abatements of maleic acid were obtained at BDD anode.

When the experiment performed at iridium based anode was repeated at a temperature of 50°C (see Fig 8.15b), no influence of this parameter can be detected, according to the chronoamperometric measurements (see par. 8.2).

Moreover, a set of experiments were conducted in order to investigate the influence of current density and flow rate at DSA anodes. Best results were obtained at the higher flow rate of 1.2 l/min and at the lower current density of 17 mA/cm^2 (see Fig 8.15c). The formation of fumaric and succinic acid was observed at both anodes while the presence of oxalic and formic acid was detected only at BDD..

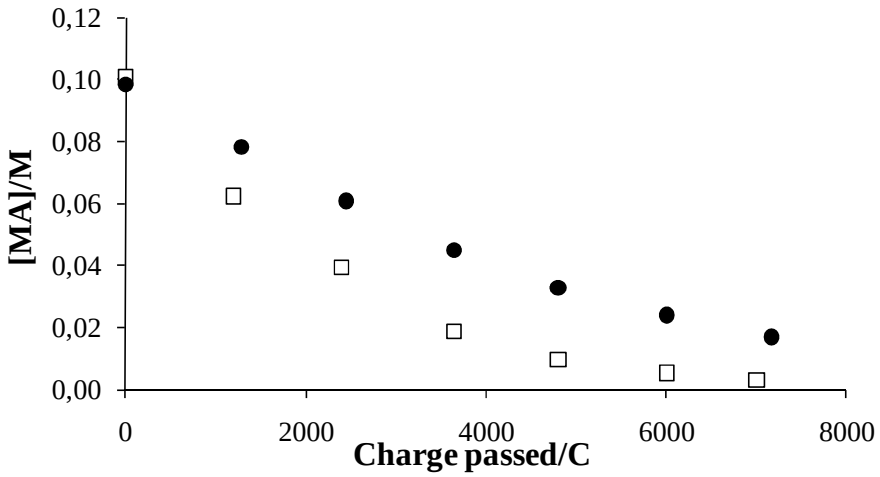

(a)

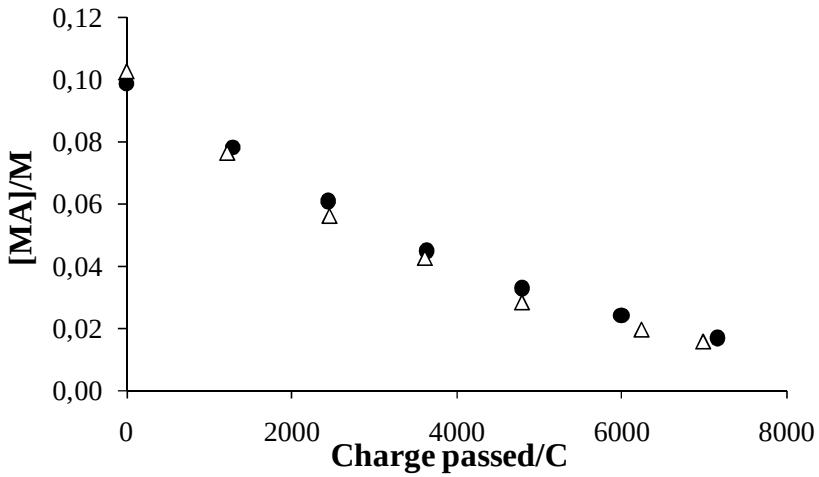

(b)

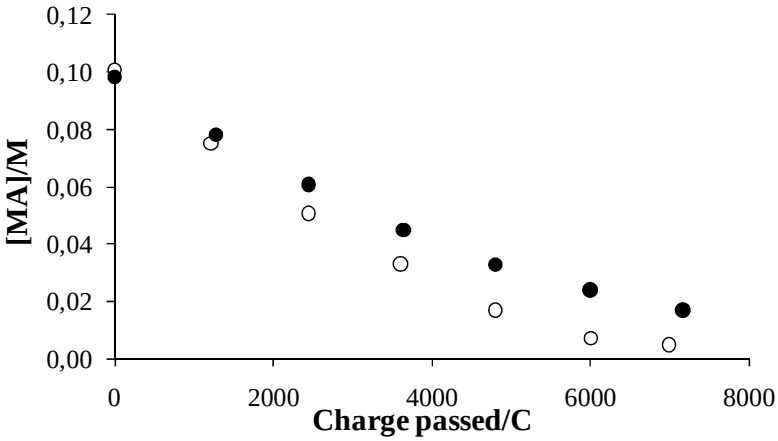

(c)

Fig. 8.15 *Maleic acid concentration vs. charge passed. Fig. 8.15a: electrolyses performed at a flow rate of 0.2 l/min and a current density of 39 mA /cm^2 at BDD (□) and at IrO_2/Ta_2O_5 (•) anodes at 25 °C; Fig. 815b: electrolyses performed at a flow rate of 0.2 l/min and a current density of 39 mA /cm^2 at IrO_2/Ta_2O_5 anode at T = 25 (•) and 50 (Δ) °C; Fig. 8.15c: electrolyses performed at IrO_2/Ta_2O_5 anode at 25 °C at a flow rate of 0.2 l/min and a current density of 39 mA /cm^2 (•) and at a flow rate of 1.2 l/min and a current density of 17 mA /cm^2(o). System solvent supporting electrolyte (SSE): Water, Na_2SO_4,H_2SO_4 (pH =2). Initial substrate concentration:0.1 M.*

When COD was detected for some electrolyses, a slight change of this value was observed against the very fast decrease of the maleic acid concentration. This result was explained considering that a consistent part of maleic acid is cathodically reduced to succinic acid, so that other electrolyes were accomplished at a divided electrochemical cell.

8.4.2 EXPERIMENTS PERFORMED IN A DIVIDED CELL

To overcome the drawback of the experiments performed at an undivided cell, the electrolyses with maleic acid as substrate were repeated in a divided cell in system I, under similar operative conditions in terms of current density and thickness of the stagnant layer.

8.4.2.1 ANODIC COMPARTMENT

Let now us discuss the results obtained investigating the influence of some operative parameters, as the current density, the initial concentration of the substrate, the temperature and the anodic material, on the electrochemical oxidation of maleic acid, considering only the anodic compartment.

As mentioned in the introduction of paragraph 8.4, some by-products were detected at the anodic compartment, such as fumaric, oxalic, formic, malonic and acetic acids, (see Table 8.3). In Fig. 8.16 and in Table 8.3 (Entry 1) the trends of maleic, oxalic and formic acids concentrations is shown for an electrolysis performed at BDD anode, at a current density of 6.2 mA/cm^2 and a temperature of 25°C. An abatement higher than 99% was obtained after a charged passed of 2500 C = 1.5 Q^{th}, where Q^{th} = charge necessary for a total conversion of the maleic acid with a *CE* = 100%. Please, note that in Fig. 8.16b the formic acid presents a higher and lower concentration of the oxalic acid in the first and last stages of the electrolyses, respectively. This is due to the fact that a larger part of maleic acid is converted to formic acid than to the oxalic one. On the other hand, oxalic acid is less easily oxidized at BDD than the formic acid and, as a consequence, tends to accumulate in the system. Interestingly, a similar result was obtained by Weiss et al. (2007), who

observed that the oxidation of maleic acid proceeds with the formation of formic acid as the main intermediate and of small amounts of oxalic acid, whose concentrations showed an increase in the first part of the electrolysis followed by a marked decrease in the last stages of the experiment.

Table 8.3 *Effect of current density and initial concentration of the organic on the electrochemical oxidation of maleic acid and on by-products detected at the anodic compartment during the elcetrolyses*[a]

Entry	[MA] (mM)[b]	i (mA/cm^2)	Charge passed (Q/Q^{th})	Conversion of maleic acid (%)	Yield in oxalic acid[c] (%)	Yield in formic acid[c] (%)	Yield in other carboxylic acids[c,d] (%)
1	20	6.02	1.05	99.08.00	0.8 – 2.1	13 - 0	0.34 – 0
2	2.05	1	2.00	99.07.00	0 – 10.5 – 5.7	2.7 – 13 - 0	-
3	2.05	2	2.01	99.05.00	0.8 – 8 - 0	0 – 6 – 0	-
4	2.05	12.05	5.07	91	1.3 – 2.5 – 7.8	-	-
5	2.05	25	5.07	81	1.2 – 3.6 - 0	0 – 3.8	-
6	20	12.05	2.03	99.09.00	3.4 – 1.4	5.1 - 0.4	0.33 – 0.09
7	20	25	1.08	96	1.7 – 3.4	2.3 – 1.2	0.024 – 0
8	83.5	25	1.05	99.09.00	0 – 1.2 – 0.5	22.7 - 0	0.08 - 0
9	42	25	2.09	99	1.9 – 1.5	6.8 - 0	0.79 - 0
10	5	25	5.09	98	0 – 0.67	-	-

[a] *Amperostatic electrolyses in system I performed at BDD anode. System solvent supporting electrolyte (SSE): Water, Na_2SO_4, H_2SO_4. T = 25°C. Q^{th} = charge necessary for a total conversion of the maleic acid with a CE = 100%. V = 70 ml.*

[b] *Initial concentration of maleic acid*

[c] *Values of yield detected after a charge passed of 600C and at the end of the experiments. a third value is reported in some case to evidence the trend of the by-products concentrations.*

[d] *Other carboxylic acids detected such as malonic and acetic acids*

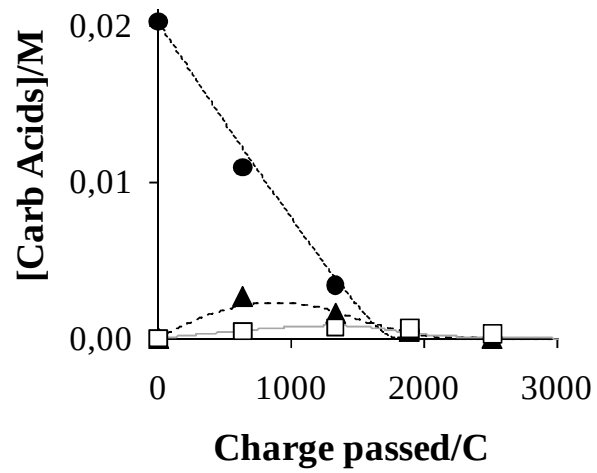

(a)

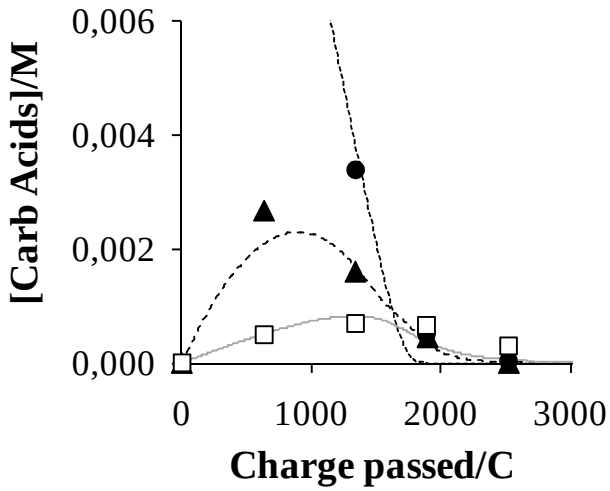

(b)

Fig. 8.16 *Profile of Maleic (●), Formic (▲) and Oxalic (□) acid concentration vs. Charge passed/Theoretical Charge for amperostatic electrolyses performed in system I with* i_{app} *= 6.2 mA/cm*^{2} *at 25 °C. System solvent supporting electrolyte (SSE): Water,* Na_2SO_4*,* H_2SO_4 *(pH 2). Theoretical curves (---) obtained with the values of [RH]*,* p_1 *and* p_2 *listed in Table 1.*

The effect of current density on the abatement of maleic acid and on the formation of formic and oxalic acids as by-products was studied by performing a set of electrolyses at different current densities (from 1 to 25 mA/cm^2), with an initial substrate concentration of 2.5 mM. As shown in Fig. 8.17, at low current densities, thus for a process under oxidation reaction kinetic control (see Table 8.3, entries 2 and 3), no significant effect of current density was observed (see triangle and circles in Fig. 8.17a).

Conversely, for high current densities, when the process takes place under mass transfer control (see Table 8.3, entries 4 and 5), the abatement of maleic acid with the charge passed decreased with current density (see empty and filled squares in Fig. 8.17a).

Furthermore, for what concern by-products, at lower current density it possible to note, as an example, a yield in formic acid of about 2.7% (Table 8.3, entry 2), while at higher current densities no formic acid was detected (Table 8.3, entries 4 and 5), after a charge passed of 100 C, correspondent to a dimensionless charge of 0.4. Hence, higher concentrations of by-products were observed for low current densities, when the process is under oxidation reaction control. Similar results were found by Polcaro et al. (2003) for the degradation of phenol. To understand these data, one can consider that, for a process under mass transfer control, the by-products are formed in an environment rich of hydroxyl radicals that can readily oxidize the organics present in the proximity of the anodic surface. Conversely, for a process under oxidation reaction control the starting pollutant is in excess with respect to the hydroxyl radicals so that direct anodic oxidation processes can take place thus giving rise to less complete oxidation processes. These results could be noted even in Figures 8.18, as shown in Tab 8.3, entries 1-6-7, where the trends of maleic, formic and oxalic acids were plotted in the same figure. Indeed, even at higher initial maleic acid concentration, i.e. 20 mM, higher abatements of the organic substrate were achieved at lower current density. In particular, a decrease of the conversion values, from major than 99% at 6.2 mA/cm^2 to 96% at 25 mA/cm^2 was obtained.

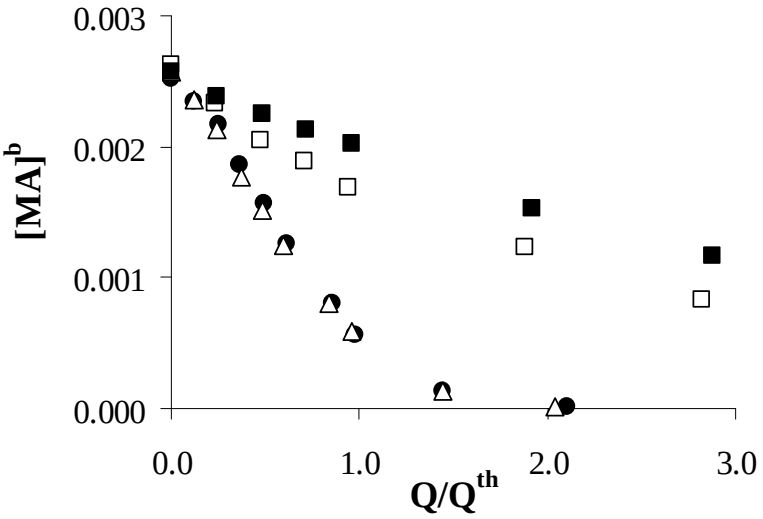
0.003
0.002
0.001
0.000
[MA]b
0.0
1.0
2.0
3.0
Q/Qth

(a)

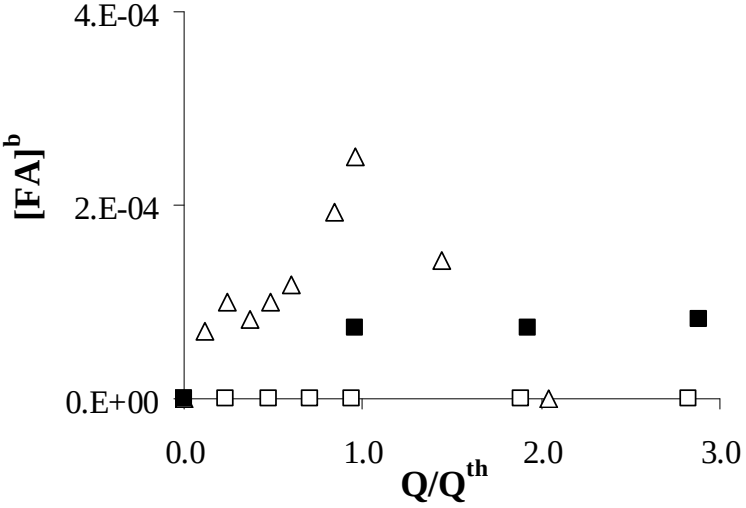
4.E-04
2.E-04
0.E+00
[FA]b
0.0
1.0
2.0
3.0
Q/Qth

(b)

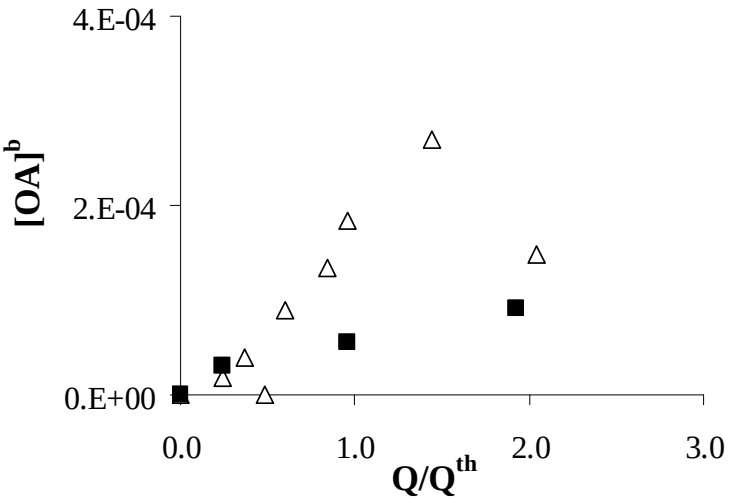

(c)

Fig. 8.17 *Concentration profiles of MA (8.17a), FA (8.17b) and OA (8.17c) vs. dimensionless passed charge obtained in amperostatic electrolyses of a solution of Maleic Acid at BDD with i = 1 (•), 2 (Δ), 12 (□) and 25 (■) mA/cm^2. Initial [MA] = 2.6 mM. Electrolysis performed in system I, divided cell. SSE: Water, Na_2SO_4, H_2SO_4 (pH about 2). T = 25°C. Q^{th} = charge necessary for a total conversion of MA with a CE = 100%.*

Furthermore, for what concern by-products, at lower current density it possible to note, as an example, a yield in formic acid of 13% (Table 8.3, entry 1), while at higher current density this value is of only about 2.3% (Table 8.3, entry 7), after a charge passed of 600 C, correspondent to a dimensionless charge of 0.4.

These experimental data were modelled according the theoretical modelling discussed in chapter 4 relatively to the presence of more organics (see Fig. 8.16 and Fig. 8.18). In particular, Eq.ns 4.11 and 4.12 were used in the case of process under oxidation reaction control, when the lowest current density value was applied (see Fig. 8.18a) and Eq.ns 4.15-4.18 in the case of a mixed kinetic regime (see Fig. 8.18b and 8.18c). Quite interestingly, a good agreement between theoretical model and experimental data was achieved. In particular, also the effect of current density on the concentration profiles of by-products was well captured by the model, thus showing its efficacy also in the presence of more organics in the electrochemical

cell. It is well known that the concentration of the organic affects drastically the performances of the process. In fact, both oxidation reactions and mass transfer rates are expected to decrease linearly with the organic concentration.

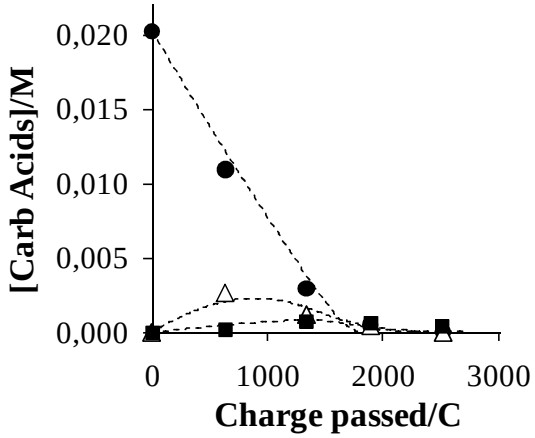

(a)

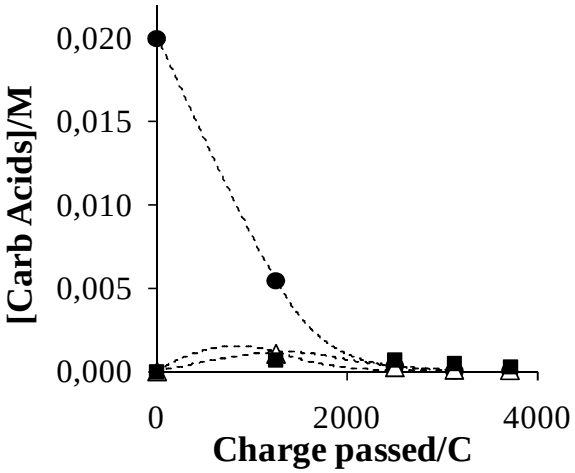

(b)

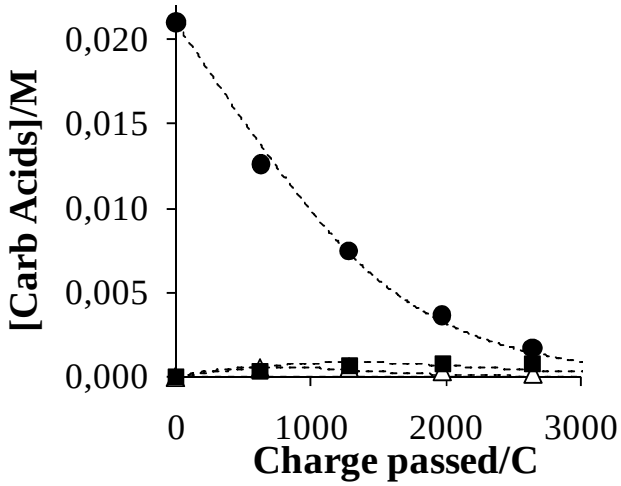

(c)

Fig. 8.18 *Effect of current density on the anodic oxidation of maleic acid at BDD performed in system I at 6.2 (Fig. 8.18a), 12.5 (Fig. 8.18b) and 25 mA/cm^2 (Fig. 8.18c). Profile concentrations of maleic (●), formic (Δ) and oxalic (■) acids were reported. Initial concentration of maleic acid of about 20 mM. T = 25 °C. System solvent supporting electrolyte (SSE): Water, Na_2SO_4, H_2SO_4 (pH 2). Theoretical curves (---) obtained with the values of [RH]* listed in Table 4.1.*

As discussed above, the same effect of the current density was observed both at an initial maleic acid concentration of 20 and 2.5 mM, even if lower abatements were obtained at lower initial organic concentration. Indeed, when the electrolyses, performed at BDD anode, were conducted at a current density of 12.5 mA/cm^2, at 25 °C and at acid pH, a conversion of 91% was detected with an initial maleic concentration of 2.5 mM, while a value higher than 99% was measured at higher concentration (Table 8.3, entries 4 and 6). Thus it appeared of a certain importance to investigate the influence of this parameter, performing some series of electrolyses in the presence of maleic acid with various C°, even in order to observe the effect on the by-products formation. As expected, higher and current efficiency were obtained increasing the initial concentration (Fig. 8.19a). In particular, the reduction of C° resulted in a dramatic decrease of the concentration of the formic acid (Fig. 8.19b) but in a less drastic reduction of the oxalic concentration (Fig. 8.19c).

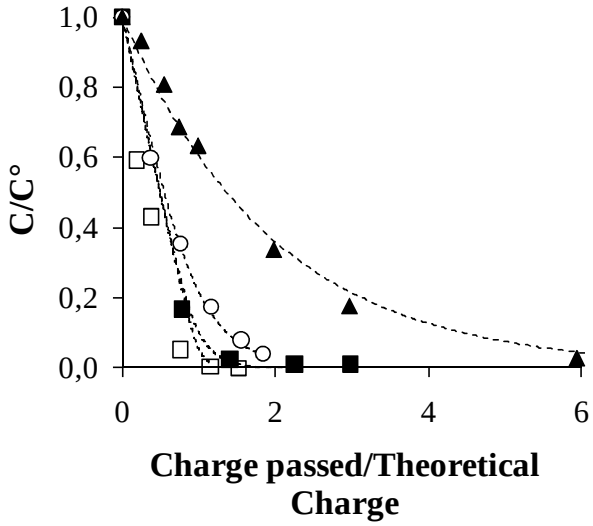
1,0
0,8
0,6
0,4
0,2
0,0
C/C°
0
2
4
6
Charge passed/Theoretical Charge

(a)

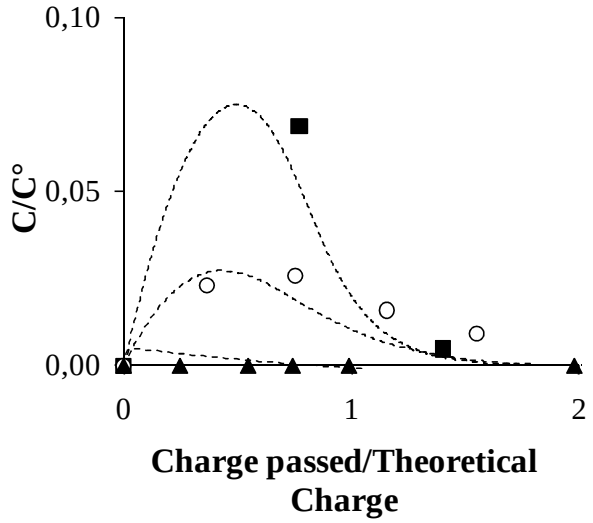
0,10
0,05
0,00
C/C°
0
1
2
Charge passed/Theoretical Charge

(b)

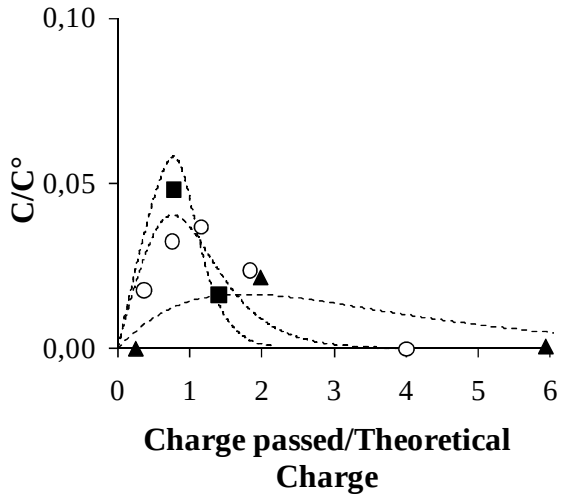

(c)

Fig. 8.19 *Effect of the initial concentration C° on the anodic oxidation of maleic acid at BDD performed with C° = 83.5 (□), 42 (■), 20 (○) and 5 (▲) mM at i = 25 mA/cm^2 (correspondent to Table 8.3, entries 8-9-7-10, respectively) and T = 25°C. Profile concentrations of maleic (Fig. 8.22a), formic (Fig. 8.22b)and oxalic (Fig. 8.22c) acids are reported. Experiments performed in system I. System solvent supporting electrolyte (SSE): Water, Na_2SO_4, H_2SO_4 (pH 2). Theoretical curves (--) obtained with the values of [RH]* listed in Table 4.1.*

This result is effectively predicted by the model and it can be attributed to the lower oxidant ability of BDD for the oxalic acid that, as a consequence, survives in the aqueous medium for longer times also in the presence of an excess of hydroxyl radicals (computed with respect to all the organics present in the system). Thus, as shown in Fig. 8.19, also in this case the model was in good agreement with experimental data.

Finally also the effect of the temperature and of the anodic material were studied. As shown in Fig 8.20a, at room temperature and at a current density of 39 mA/cm^2, very high abatements were obtained at BDD anode with a conversion of about 100%, while at Iridium anodes a conversion of about 10% was achieved. Similar results were previous found by other authors. Quite interestingly, Li et al. (1981) found that the oxidation of phenol at Ru oxide proceeded with the formation of maleic acid which remained in the solution for a very long time.

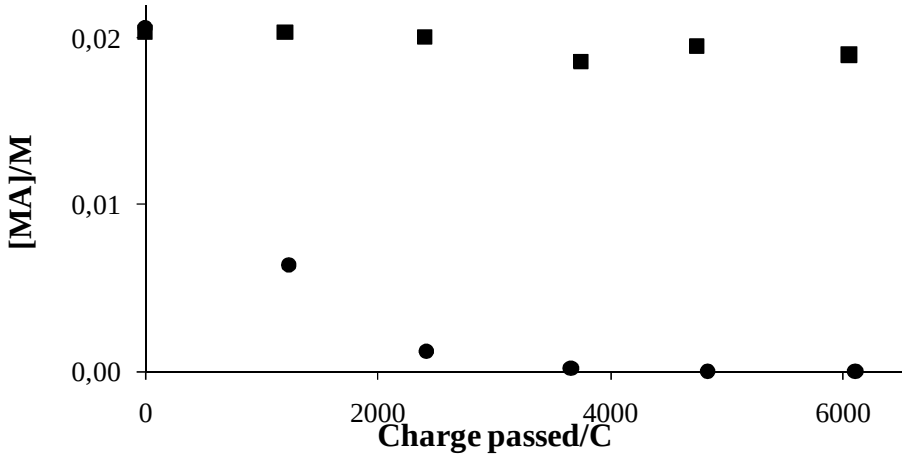

(a)

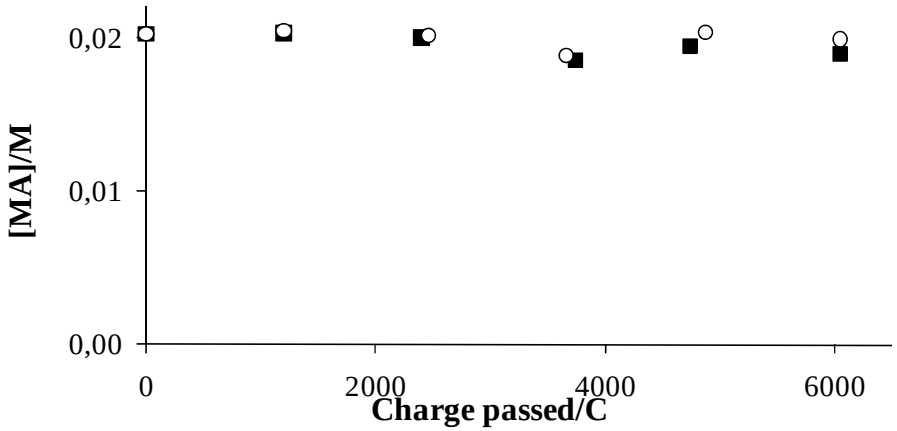

(b)

Fig. 8.20 *Effect of the nature of the anodic material (a) and of the temperature (b) on the anodic oxidation of maleic acid at i = 39 mA/cm^2. Electrolyses performed at BDD (●) and at DSA (■) anode at T = 25 °C and at DSA anode at 50°C (o). Initial maleic acid concentration: 20 mM. System solvent supporting electrolyte (SSE): Water, Na_2SO_4, H_2SO_4 (pH 2).*

Moreover Bock and MacDougall (1999) showed that the performances of iridium anodes in the oxidation of maleic acid decrease with the passed charge probably as a result of irreversible interactions between the anodic surface and maleic acid and/or its oxidation products.When the electrolysis at the iridium based anode was conducted at higher temperature (Fig. 8.20b), no influence of this operative parameter was observed.

This result confirm the high stability of this organic towards anodic oxidation at oxide electrodes, as previously found in chronoamperometric experiments, even at a temperature of 50°C.

8.4.2.2 CATHODIC COMPARTMENT

Let now us make some considerations about the cathodic compartment. In this case, the only reactions of interest that take place are the electro-reduction and the isomerisation of the maleic to succinic and fumaric acids, respectively. Indeed, as shown in the inset of the next figure, the number of moles of maleic acid converted resulted for each sample equal to those of succunic and fumaric acids formed. Moreover, since the number of electrons involved in the reduction of maleic acid are only 2 (see Eq. 8.1), the process results to be under mass transport control kinetic regime for all the electrolyses performed at BDD anode, under the operative conditions adopted. This consideration lead to the conclusion that at the cathodic compartment, the degradation of maleic acid, in particular its conversion to succinic acid, presents lower current efficiencies with respect to its degradation by oxidation at the anode. Conversely, an opposite results was observed for the electrolysis conducted at DSA anode, where very low values of anodic oxidation of the substrate were detected.

Interestingly, the preparation of succinic acid, process of great importance since it finds extensive application in the synthesis of a wide variety of organic compounds, is often accomplished by electrochemical reduction of maleic acid (Arati et al., 2004). In particular, many studies were conducted on the study of the influence of some operative parameters on the electrochemical reduction of maleic acid, in sulphuric media and at different cathodic material (Arati et al., 2004; Kanakam et

al., 1967; Kudryashov and Kochetkov, 1970). Despite the intersting nature of this matter, this kind of studies were outside of the objectives of this work. Thus, no more investigations have been made in this sense.

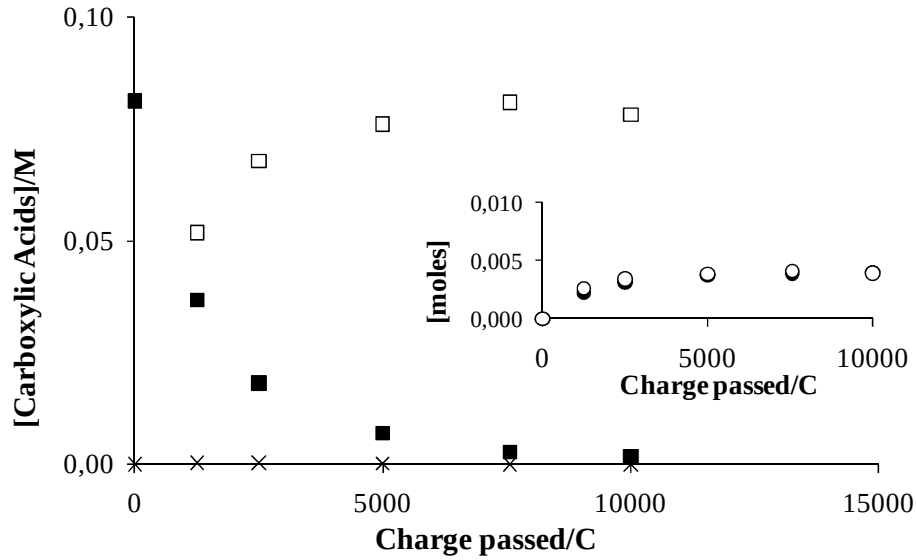

Fig. 8.21 *Profile of maleic (■), fumaric (x) and succinic (□) acids concentrations vs. charge passed for amperostatic electrolyses performed in system II at BDD. The inset reports the moles of maleic reacted (●) and the moles of succinic and fumaric (o) formed during the electrolyses as a function of the charge passed. Experimental conditions: current density = 25 mA/cm^2. Initial maleic acid concentration = 83.5 mM. System solvent supporting electrolyte (SSE): water, Na_2SO_4, H_2SO_4 (pH about 2). T = 25°C.*

8.5 EFFECT OF THE NATURE OF THE SUBSTRATE ON THE AMPEROSTATIC ELECTROLYSES

With the aim of discuss on the influence of the nature of the substrate on the electrochemical oxidation process, let now us observe some results already examined in this and in the precedents chapter, considering in this case COD values in order to compare the obtained results.

As shown in Fig. 8.22, the abatement of the COD obtained by anodic oxidation dramatically depends on the nature of both the anode and the acid. Indeed, at BDD,

high and similar abatements of the COD were obtained for formic and maleic acids (Fig. 8.22a), while solutions of oxalic acid at BDD gave a lower abatement of COD for the same amount of charge passed with respect to the other acids (Fig. 8.22a). Thus, formic and maleic acids are likely to be involved at BDD in a very fast oxidation by means of free or weakly-adsorbed hydroxyl radicals electrogenerated by the oxidation of water, while oxalic acid is considerably less reactive towards hydroxyl radicals (Ross and Ross, 1977), so that it is likely to be involved, at least at low pH, in a direct electrochemical oxidation at the anodic surface (see par chapter 5). At iridium anodes, a very different behavior was observed. A slight higher abatement of COD was observed for oxalic acid with respect to formic one. When maleic acid was used, in agreement with chronoamperometric measurements, very low abatements of both COD (see Fig. 8.22b) and acid concentration were observed. Moreover, as shown in Fig. 8.22, a higher abatement of COD was observed at BDD for all the investigated acids and in particular, the rate of abatement observed was FA ~ MA > OA, while at iridium anodes an opposite trend was observed and the rate of abatement decrease as follows: OA > FA >> MA.

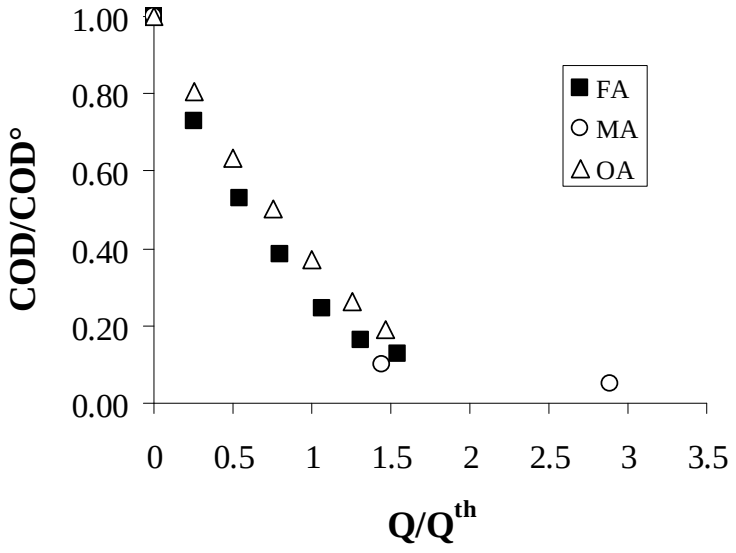

(a)

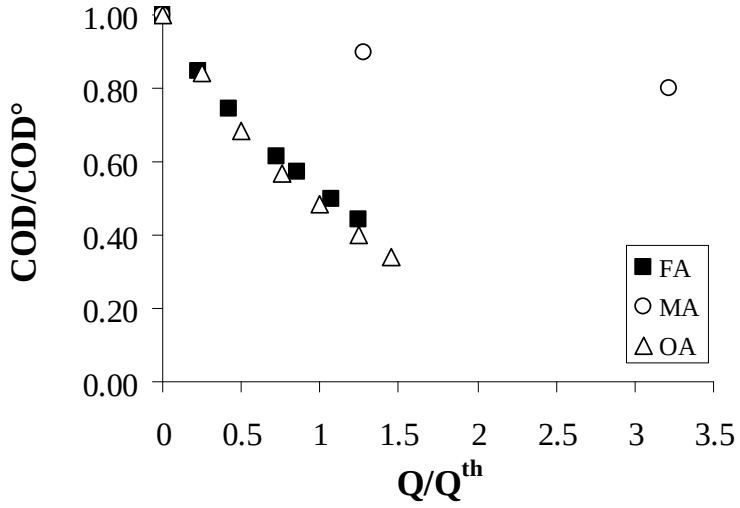

(b)

Fig. 8.22 *Ratio between actual (COD) and initial (COD°) vs. dimensionless passed charge for amperostatic electrolyses of OA (Δ), FA (■) and MA (○) performed at BDD (8.25a) and IrO_2-Ta_2O_5 (8.25b). Initial COD: 0.055-0.066 M. Electrolyses of OA and FA performed in system II in un undivided cell with a flow rate of 0.2 l/min. Electrolysis of MA performed in system I, divided cell. Current density 39 mA/cm^2. System solvent supporting electrolyte (SSE): water, Na_2SO_4, H_2SO_4 (pH about 2). T = 25°C. Q^{th} = charge necessary for a total conversion of organic with a CE = 100%.*

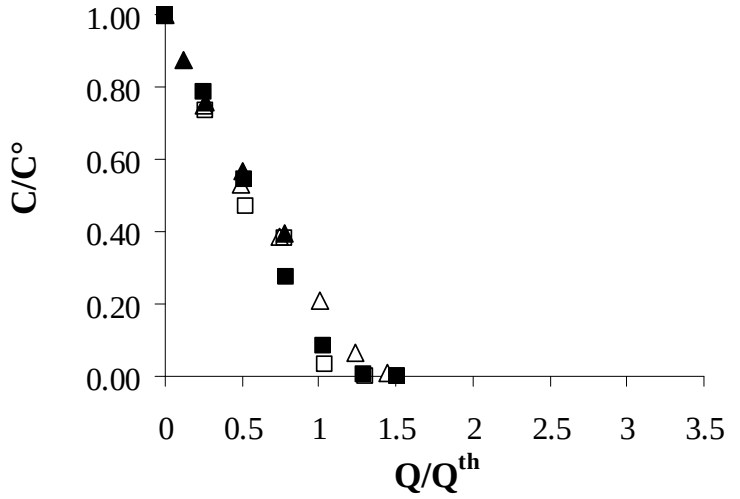

(a)

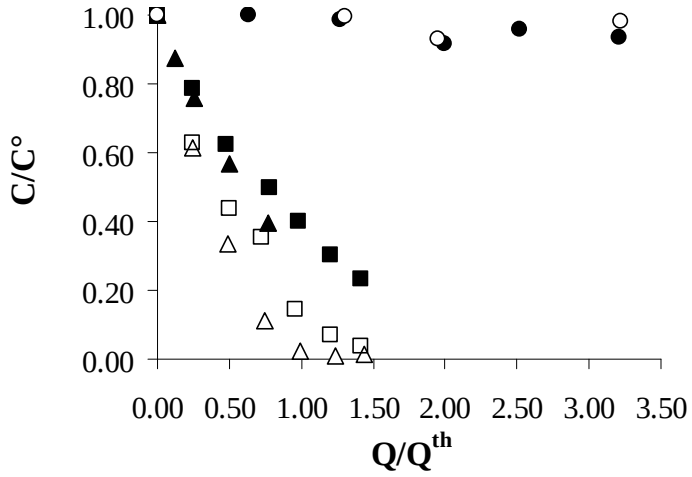

(b)

Fig. 8.23 *Trend of dimensionless concentration C/C° vs. dimensionless passed charge for amperostatic electrolyses at 25 (filled symbols) and 50 °C (open symbols) at BDD (8.26a) and IrO_2-Ta_2O_5 (8.26b) performed in the presence of OA (▲ T = 25°C; Δ T = 50 °C), FA (■ T = 25°C; □ T = 50 °C) and MA (● T = 25°C; ○ T = 50 °C). Initial COD: 0.055-0.066 M. Electrolyses of OA and FA performed in system II with a flow rate of 1.2 l/min and current density of 39 mA/cm^2. Electrolysis of MA performed in system I, divided cell, with current density of 39 mA/cm^2. System solvent supporting electrolyte (SSE): water, Na_2SO_4, H_2SO_4 (pH about 2). T = 25°C. Q^{th} = charge necessary for a total conversion of the organic with a CE = 100%.*

These data indicate that different oxidant agents are involved at BDD and DSA anodes, as reported already in the section 2.5 and 6.6. Finally, for what concern the effect of the temperature, the incineration of formic and oxalic acids was only slightly enhanced by an increase of this operative parameter at BDD anode (see Fig. 8.23a), while at iridium oxide anodes, a strong increase of the abatement was observed by working at 50°C for both the acids (Fig. 8.23b).

These data indicate, according to Martinez-Huitle et al. (2004a), that the rate determining steps for oxalic and formic acids oxidation and for oxygen evolution reaction at iridium oxide anodes are different as indicated by their different temperature sensitivity that is attributed to differences in the activation energies of the rate determining steps. Unfortunately the efficacy of temperature enhancement with DSA electrodes is not general considering that when experiments were

performed in the presence of maleic acid, a very low abatement was obtained also at 50 °C (Fig. 8.23b).

CHAPTER 9

COMPARISON BETWEEN ANODIC OXIDATION AND ELECTRO-FENTON PROCESSES FOR THE TREATMENT OF SOME CHLOROETHANES

9.1 INTRODUCTION

Chlorinated aliphatic hydrocarbons are frequently found in many surface and ground waters, as a result of their widespread use in industry and in various household products and their poor biodegradability (Chemical and Engineering Data, 2007). These substances are often toxic and some of them are present on the US Environmental Protection Agency priority list of pollutants with very low limit values in drinking water. Both destructive and non-destructive methods have been used to remove chlorinated aliphatic hydrocarbons from polluted water.

Recent researches have demonstrated that some AOPs, offer an attractive alternative to traditional routes for treating wastewaters containing toxic or/and refractory organic pollutants.

A study about the application of some AOPs, in particular EAOPs, to the oxidation of two chloroethanes, namely 1,2-dichloroethane (DCA) and 1,1,2,2-tetrachloroethane (TeCA), chosen as model compounds, is reported in this chapter. A comparative study on the degradation of these toxic organics by simple anodic oxidation and electro-Fenton coupled with anodic oxidation process is proposed. For more details about the electro-Fenton (EF) process, see section 1.6.2.

The mineralization of the DCA and TeCA solutions was assessed from the decay of their dissolved organic carbon (DOC), which can be considered as the TOC when treating completely solubilized compounds, as it was in all cases. For both kinds of electrochemical experiments, electrolyses were conducted with a galvanostatic alimentation, at system III (see section 3.2.3), where an BDD/ADE (air diffusion cathode, see experimental section for more details) cell was used, supplying nitrogen instead of compressed air when the pure anodic oxidation process had to be accomplished.

Interestingly, regarding the pure electrochemical route, two different processes can be used in principle for the removal of chlorinated aliphatic hydrocarbons: oxidation to carbon dioxide (often called "electrochemical incineration") (Eq. 9.1), that takes place at the anode, and reduction to de-halogenated aliphatic hydrocarbons (Eq. 9.2) for the conversion of chloroalkanes to corresponding alkanes, that takes place at the cathode.

$$C_mH_nCl_p + 2m\ H_2O \rightarrow m\ CO_2 + (n+4m)\ H^+ + p\ Cl^- + (4m+n-p)\ e^- \quad (9.1)$$

$$C_mH_{2m+2-p}Cl_p + 2p\ e^- + p\ H^+ \rightarrow C_mH_{2m+2} + p\ Cl^- \quad (9.2)$$

In particular, a BDD anode was chosen in this set of experiments, because of its better performance compared with the classical anode materials of industrial electrochemistry, as reported in literature specifically for the oxidation of chlorinated organic compounds (Fiori et al., 2005; Scialdone et al., 2008). In general, very few studies were dedicated up to now to the electrochemical incineration of chlorinated aliphatic hydrocarbons (Chen et al., 1999; Scialdone et al., 2008). Recently, it was studied the effect of the anodic material on the anodic incineration of 1,2-dichlorethane, by using numerous electrodes such as Pt, Au, BDD, Ebonex, stainless steel, Ti/IrO_2-Ta_2O_5 and PbO_2 (Scialdone et al., 2008), and the possibility of an electrochemical route based on the anodic oxidation to carbon dioxide coupled with the cathodic reduction to de-halogenated hydrocarbons, for the first time proposed for the treatment of wastewaters contaminated by chloroethanes (Scialdone et al., 2010).

Furthermore, very few studies were found on the application of Fenton's chemistry, as single or coupled process, for chlorinated compounds. In particular, Vilve and co-authors (2010) have studied the degradation of 1,2-dichloroethane using a simple Fenton's chemical oxidation in order to optimize several operative parameters such as the H_2O_2/Fe^{2+} ratio, temperature, pH and treatment time, while Rodriguez et al. (2005) have focused their study on the photo-Fenton degradation of chlorinated solvents, such as 1,2-dichloroethane, dichloromethane and trichloromethane, with the aim of study the influence of operative conditions also in this coupled process. Nevertheless, no studies upon the application of electro-Fenton process to the oxidation of 1,2-dicholoroethane and 1,1,2,2,-tetrachloroethane have been

accomplished. Thus, the aim of this study was the investigation of the effect of some operating parameters, such as the current, nature and concentration of the initial substrate and anodic material on the electro-Fenton process and the comparison with the anodic oxidation process.

9.2 ACCUMULATION OF ELECTROGENERATED H_2O_2 IN THE ELECTROLYTIC CELL

A fundamental task must be carried out before starting with the study on the degradation and mineralization of the chlorinated hydrocarbons by electrochemical advanced oxidation processes based on the electrogeneration of H_2O_2 using a carbon-PTFE O_2-diffusion cathode (air-diffusion electrode, ADE). In order to assess the ability of the ADE to electrogenerate H_2O_2, several solutions containing 130 ml of 0.035 M Na_2SO_4 at pH 3.0 and at 10 ºC were electrolysed by applying a constant current of 300 mA for 480 min, in the presence and absence of Fe^{2+} catalyst and organic compound. The H_2O_2 concentration accumulated in each solution during the electrolyses was determined by the spectrophotometric measurement of the absorbance of the coloured complex formed between Ti(IV) and H_2O_2 at λ = 408 nm (more detailed in the experimental section). The results in Fig. 9.1 show the trends obtained.

The first electrolysis was performed in the absence of catalyst and organic compound (i.e., anodic oxidation with H_2O_2 electrogeneration). Under these conditions, H_2O_2 can be continuously supplied to the acidic aqueous solution contained in the electrolytic cell from the two-electron reduction of oxygen gas – directly injected as compressed air – by reaction (9.3) with E^o = 0.695 V/SHE, which takes place more easily than its four-electron reduction to water from reaction (9.4) with E^o = 1.23 V/SHE (Brillas et al., 2009):

$$O_{2(g)} + 2\,H^+ + 2\,e^- \rightarrow H_2O_2 \quad (9.3)$$

$$O_{2(g)} + 4\,H^+ + 4\,e^- \rightarrow 2\,H_2O \quad (9.4)$$

There are major parasitic reactions which result in a lower current efficiency. For example, electrochemical reduction at the cathode surface from reaction (9.5) and, to

a much lesser extent, disproportion in the bulk by reaction (9.6) are given regardless the cell configuration (Brillas et al., 2009):

$$H_2O_2 + 2\,H^+ + 2\,e^- \rightarrow 2\,H_2O \quad (9.5)$$

$$2\,H_2O_2 \rightarrow O_{2(g)} + 2\,H_2O \quad (9.6)$$

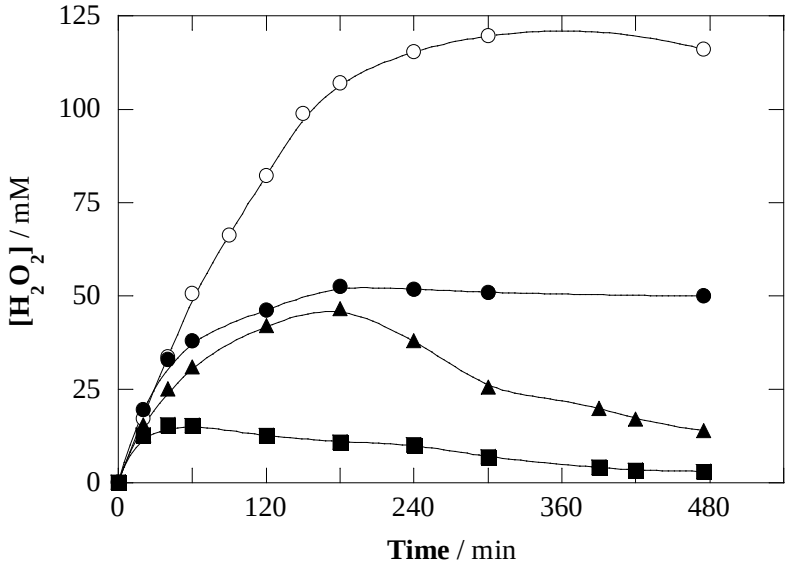

Fig. 9.1 *Time course of the accumulated H_2O_2 during the electrolysis of 130 ml of a 0.035 M Na_2SO_4 solution, at 300 mA, pH 3.0, and at 10 ºC using a BDD/ADE cell. [Fe^{2+}] (mM): (○) 0 and (●,■,▲) 0.5; [DCA] (mM): (○,●) 0, (▲) 2, and (■) 4.*

Since an undivided cell is utilized, H_2O_2 is also oxidized to O_2 at the anode via $HO_2^{\bullet}$ as an intermediate by the following reactions (Brillas et al., 2009):

$$H_2O_2 \rightarrow HO_2^{\bullet} + H^+ + e^- \quad (9.7)$$

$$HO_2^{\bullet} \rightarrow O_{2(g)} + H^+ + e^- \quad (9.8)$$

Consequently, the accumulation of H_2O_2 is lower than its electrogeneration. As observed in Fig. 9.1, the accumulated H_2O_2 concentration increased during the first 240 min, reaching a value of about 120 mM, whereupon a steady state was maintained because the rate of H_2O_2 formation at the cathode became equal to its destruction rate at the cathode, at the anode and in the bulk.

When 0.5 mM Fe^{2+} was used as catalyst (i.e., electro-Fenton process, see section 1.6.2), the steady state H_2O_2 concentration decreased to about 50 mM due to its destruction through the classical Fenton's reaction in acidic medium (9.9) and Fenton-like reaction (9.10), which entail the synchronous formation of $^{\bullet}OH$ and $HO_2^{\bullet}$. Also reaction (9.11) contributes to the destruction of H_2O_2. Such phenomena allow the mineralization of the organic pollutants (RH) once they are present in the solution bulk (apart from their destruction by the $^{\bullet}OH$ adsorbed at the anode).

$$Fe^{2+} + H_2O_2 + H^+ \rightarrow Fe^{3+} + H_2O + {}^{\bullet}OH \quad (9.9)$$

$$Fe^{3+} + H_2O_2 \rightarrow Fe^{2+} + HO_2^{\bullet} + H^+ \quad (9.10)$$

$$H_2O_2 + {}^{\bullet}OH \rightarrow H_2O + HO_2^{\bullet} \quad (9.11)$$

Thus, a similar electrolysis was carried out in the presence of Fe^{2+} and 2 mM DCA. As observed in Fig. 9.1, the maximum H_2O_2 concentration was lower than that obtained in the electro-Fenton process. In addition, the value decreased from 180 min. Such a lower accumulation is accounted for by a higher destruction caused by some particular reaction. Indeed, in the presence of an organic compound, the $^{\bullet}OH$ is continuously consumed by reaction (9.12), thus enhancing the destruction of H_2O_2 by Fenton's reaction.

$$RH + {}^{\bullet}OH \rightarrow R^{\bullet} + H_2O \quad (9.12)$$

Therefore, the destruction of H_2O_2 by reaction (9.9) to yield $^{\bullet}OH$ is directly related to the use of these $^{\bullet}OH$ in the destruction of the organic matter (i.e., DCA and its intermediates). The influence of the DCA on the H_2O_2 accumulation was confirmed by electrolyzing a 4 mM DCA solution. As observed, a much lower concentration was accumulated along the trial due to the greater extent of reaction (9.12), which had an immediate influence on the Fenton's reaction extent.

9.3 COMPARISON BETWEEN THE ADOPTED EAOPs ON THE DEGRADATION RATE OF 1,2-DICHLOROETHANE

The oxidant ability of the EAOPs based on H_2O_2 electrogeneration was firstly studied by treating DCA solutions. Fig. 9.2 shows the decay of DCA vs. the

electrolysis time during the degradation of 130 ml of 4 mM DCA (i.e., 96 mg L^{-1} DOC) in 0.035 M Na_2SO_4 medium, at 300 mA, pH 3.0, and at 10 ºC, by pure anodic oxidation (i.e., 0 mM Fe^{2+} and N_2 supply to the cathode to prevent the H_2O_2 generation) and electro-Fenton (i.e., 0.5 mM Fe^{2+} and air supply to the cathode) using the same BDD/ADE cell. The decay of the DCA concentration was studied by GC/MS. Fig. 9.2 reveals that the trends in both methods were similar, but some differences must be commented. In the absence of metal catalyst, a progressive destruction of DCA could be achieved due to main action of the BDD(•OH) and only 3% remained at 420 min.

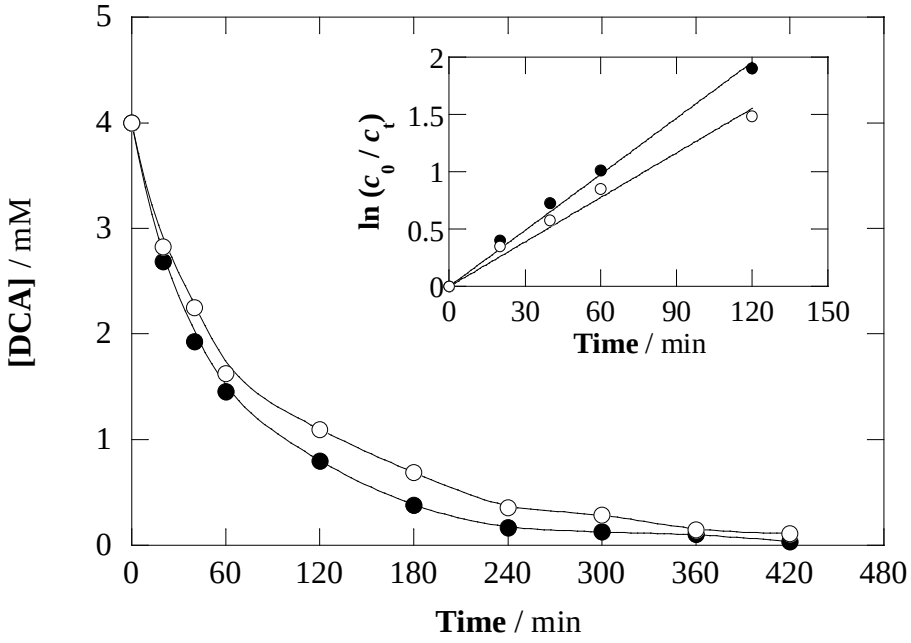

Fig. 9.2 *Decay of the DCA concentration vs electrolysis time during the degradation of 130 ml of 4 mM DCA (i.e., 96 mg L^{-1} DOC) in 0.035 M Na_2SO_4 medium, at 300 mA, pH 3.0, and at 10 ºC, by (○) pure anodic oxidation (i.e., 0 mM Fe^{2+} and N_2 supply to the cathode) and (●) electro-Fenton (i.e., 0.5 mM Fe^{2+} and air supply to the cathode) using a BDD/ADE cell. The inset shows the corresponding kinetic analyses assuming pseudo first-order kinetics for the reaction with •OH.*

A quicker decay was observed in electro-Fenton, with total disappearance in 420 min, which confirms the higher oxidation power of this process. The superior

performance of electro-Fenton can be explained by: (i) the much higher concentration of $^{\bullet}$OH thanks to the simultaneity of two generation ways (i.e., the synergistic action of the large amounts of $^{\bullet}$OH at the anode and in the bulk); and (ii) the minimization of the mass transport limitations inherent to the electrode processes at a given current value. Indeed, since the oxidizing species are not confined to the electrode surface or its vicinity, the interaction between the organic molecules and $^{\bullet}$OH results to be easier within the whole bulk solution (Sirés et al., 2010).

9.4 INFLUENCE OF SOME OPERATIVE PARAMETERS ON THE ELECTROCHEMICAL MINERALIZATION OF 1,2-DICHLOROETHANE AND 1,1,2,2-TETRACHLOROETHANE

Upon the application of the EAOPs, numerous by-products can be formed because the $^{\bullet}$OH radicals do not exhibit high functional group selectivity. It is then necessary to verify that the electrochemical technology is able to mineralize such compounds. Fig. 9.3 shows the effect of several parameters on the mineralization of DCA solutions. In particular, Fig. 9.3a shows the DOC decays vs. electrolysis time for the treatment of 130 ml of 4 mM DCA (i.e., 96 mg L^{-1} DOC) in 0.035 M Na_2SO_4 medium, at pH 3.0 and at 10 ºC using the BDD/ADE cell. The anodic oxidation and electro-Fenton trials were firstly compared in Fig. 9.2 considering the DCA concentration trends. To confirm those previous results, let us now observe that a slower mineralization was achieved by anodic oxidation, with 91% DOC removal at 420 min, while a mineralization higher than 95% was reached by EF. Interestingly, the much higher values of DOC in comparison with those corresponding to the carbon contained as DCA (calculated from the DCA concentration values shown in Fig. 9.2) suggests the presence of other organic compounds dissolved in the electrolytic solution (see par. 9.5).

Moreover, Fig. 9.3a shows the effect of the applied current on the solution DOC removal for the electro-Fenton treatment. The mineralization rate was much lower at 100 mA due to the lower production rate of $^{\bullet}$OH. At 420 min, only 79.5% DOC removal was achieved.

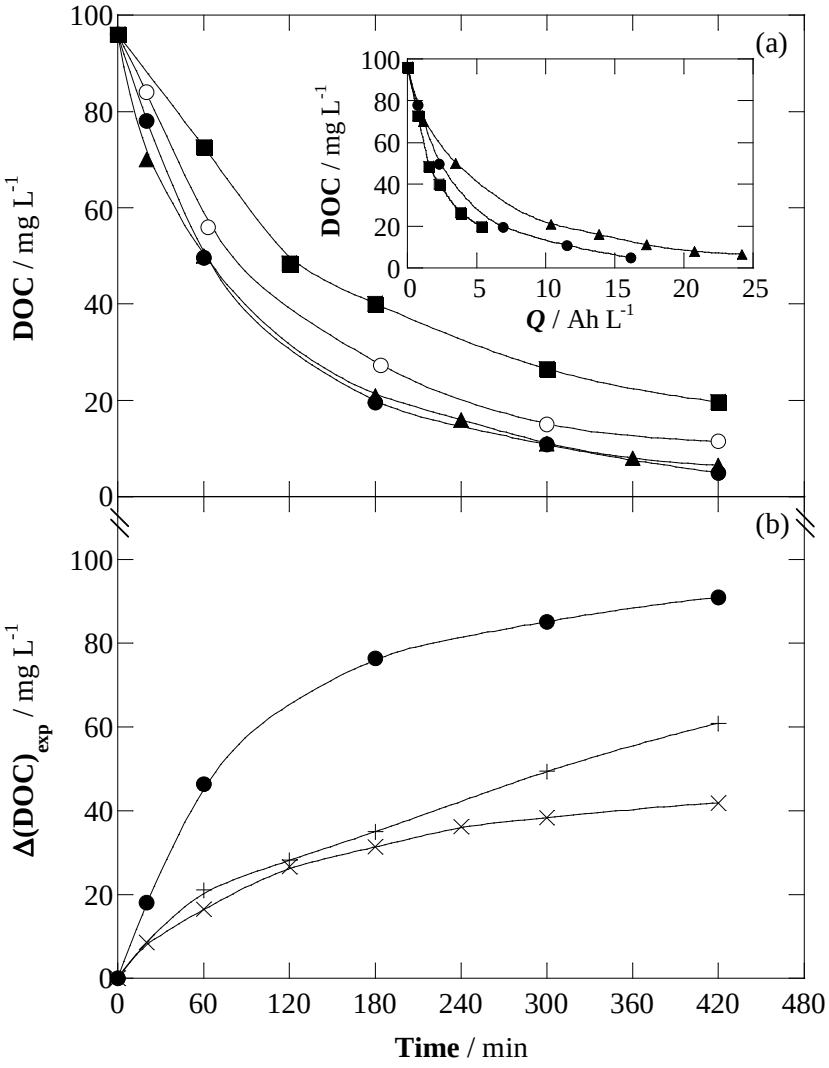

Fig. 9.3 *Effect of several parameters on the mineralization of DCA solutions. (a) DOC decay vs. electrolysis time for the treatment of 130 ml of 4 mM DCA in 0.035 M Na_2SO_4 medium, at pH 3.0 and at 10 ºC using a BDD/ADE cell. [Fe^{2+}] (mM): (○) 0 (with N_2 supply to the cathode) and (●,■,▲) 0.5; Current (mA): (■) 100, (○,●,) 300, and (▲) 450. The inset shows the DOC decay vs. the specific charge for the trials with Fe^{2+}. (b) Evolution of $\Delta(DOC)_{exp}$ vs. electrolysis time for (●), which is shown in plot (a), compared to: (x) a similar experiment, with 2 mM DCA (i.e., 48 mg L^{-1} DOC and (+) a similar experiment, using a Pt anode.*

The faster electrogeneration of H_2O_2 and regeneration of Fe^{2+} at 300 mA largely contributes to the significant acceleration. Interestingly, the enhancement obtained when increasing from 300 to 450 mA is not as remarkable as that produced when increasing from 100 to 300 mA. This result suggests a greater limitation by mass transport under the experimental conditions tested at high applied current (i.e., the oxidation rate becomes mainly determined by the transport of oxygen and iron ions toward the cathode). Therefore, a rise from 300 to 450 mA did not improve the degradation process.

The inset shows the DOC decay vs. the specific charge for the three trials with Fe^{2+}. The increase of the applied current causes a higher consumption of specific charge for attaining a given TOC value. For example, 1.5, 2.3, and up to 3.5 Ah L were required to reach 50% mineralization at 100, 300, and 450 mA, respectively. This result is due to the increasing extent of the parasitic reactions that do not consume hydroxyl radicals to oxidize the organic matter, which leads to the progressive waste of the supplied current.

The effect of the initial pollutant concentration was studied by comparatively treating a 2 mM (i.e., 48 mg L^{-1} DOC) and a 4 mM solution at 300 mA. As shown in Fig. 3b, where $\Delta(DOC)_{exp}$ is plotted against the electrolysis time for these electro-Fenton degradations, a larger amount of DOC was removed when treating 4 mM DCA at any time and, at 420 min, 42 and 91 mg L^{-1} DOC were removed from 2 and 4 mM DCA, respectively. This is an interesting feature because it means that the electro-Fenton process can proceed more successfully when treating a high organic content. Indeed, at a higher pollutant concentration, a smaller fraction of $^{\bullet}OH$ is wasted in parasitic reactions because the oxidizing species interact with a larger number of organic molecules that are available. As a result, a more efficient process was obtained when treating 4 mM DCA.

Finally, the electro-Fenton treatment of 4 mM DCA using the BDD/ADE cell at 300 mA was compared with the same treatment using a Pt/ADE cell. As observed, a much poorer mineralization was achieved, with only 61% DOC removal at 420 min using the cell with a Pt anode. This confirms the important role of the oxidation process at the anode, which supposes a fundamental synergistic contribution to the

oxidation in the bulk. Such enhancement is consistent with other studies reporting the different oxidation power of both anodes (see section 2.3).

The study of the effect of the same operative parameters was also carried out for TeCA solutions (see Fig. 9.4). The conclusions drawn are analogous to those from Figs. 9.3a and 9.3b, although it is important to notice that the mineralization rate was higher than that obtained in the case of DCA solutions. Indeed, the solutions of 4 mM TeCA were completely mineralized at 420 min by electro-Fenton with BDD at 300 and 450 mA. Also in this case, higher abatements were detected using a BDD anode; for example, only a 80% DOC removal was observed with Pt anode at 300 mA. It was worth noting the poorer effectiveness of the anodic oxidation treatment, also using TeCA as organic substrate, that led to a 94% DOC removal at 420 min, instead of the high mineralization achieved by electro-Fenton oxidation.

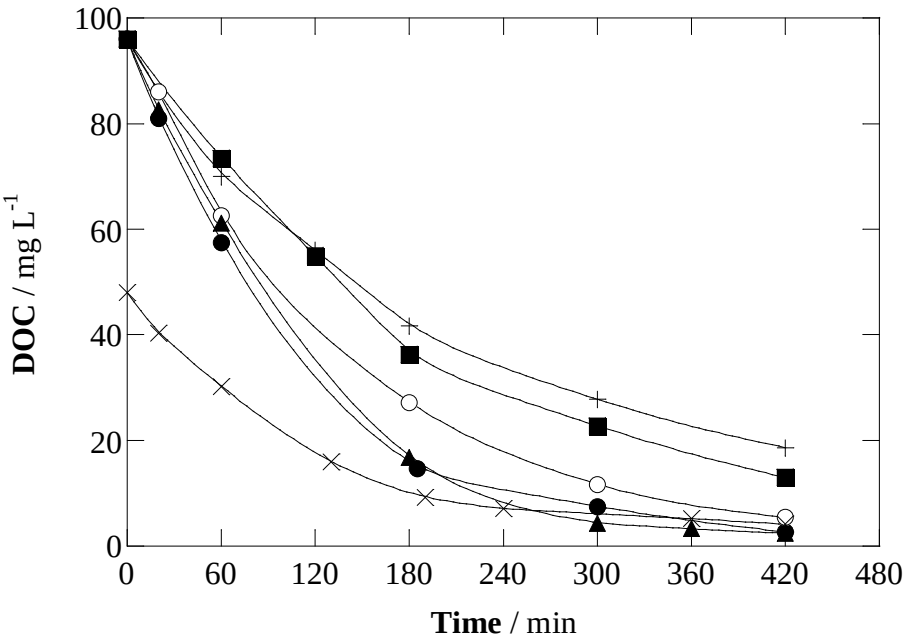

*Fig. **9.4** Effect of several parameters on the mineralization of TeCA solutions given by the DOC decay vs. electrolysis time. Each symbol represents the same experimental conditions described in Figs. 3a and 3b, with TeCA instead of DCA.*

9.5 TIME COURSE OF THE REACTION INTERMEDIATES AND MINERALIZATION PATHWAYS

The previous mineralization and kinetic studies have been accompanied by the identification of intermediates, such as carboxylic acids and inorganic chlorinated ions. Indeed, since $^{\bullet}OH$ is a non-selective oxidizing species, various by-products were formed at relatively low concentration levels. It is always of a great interest to discuss the time course of the intermediates in order to know their nature and concentration, because a progressive transformation of the starting substrates into more biodegradable compounds can be related to the decrease of the toxicity of the solutions (Sirés et al., 2010).

Figs. 9.5-9.7 show the time course of the concentration of the main intermediates accumulated in the electrochemical cell during the anodic oxidation and electro-Fenton treatments of solutions of DCA and TeCA. In particular, short-chain carboxylic acids and chlorinated ions were detected by HPLC and IC, respectively.

It can be seen that the by-products are formed since the very beginning of the electrolyses in concomitance with the disappearance of the primary compound. For the electro-Fenton of DCA, oxalic, formic, chloroacetic and acetic acids were detected (see Fig. 9.5), while for the electro-Fenton of TeCA, dichloroacetic acid was observed besides the others (see Fig. 9.6). Please, note that it was not possible to determine the exact individual concentrations of chloroacetic and acetic acids, since they displayed two overlapped peaks.

Let us now observe the trends of the carboxylic acids detected during the treatments of DCA in Fig. 9.5. Fig.9.5a shows the chlorocetic+acetic acids concentration, present as the main intermediates, under different applied operative conditions. Thus, upon the application of the electro-Fenton to a solution with 4 mM DCA at 300 mA using the ADE/BDD cell, these intermediates reach their complete mineralization at 420 min. A lower current of 100 mA led to a significantly greater accumulation of these intermediates, due to the poorer oxidizing ability of the process at low current (see Fig. 9.3a). Accordingly, a part of the DOC content for this trial at 420 min can be justified by the presence of chloroacetic+acetic. On the other hand, the accumulation-destruction profile yielded at a higher current of 450

mA was similar to that obtained at 300 mA, which agrees with the comments on the DOC removal from Fig. 9.3a. Regarding the effect of the initial concentration of pollutant, it can be observed that a lower concentration of these intermediates is accumulated, finally disappearing at 420 min.

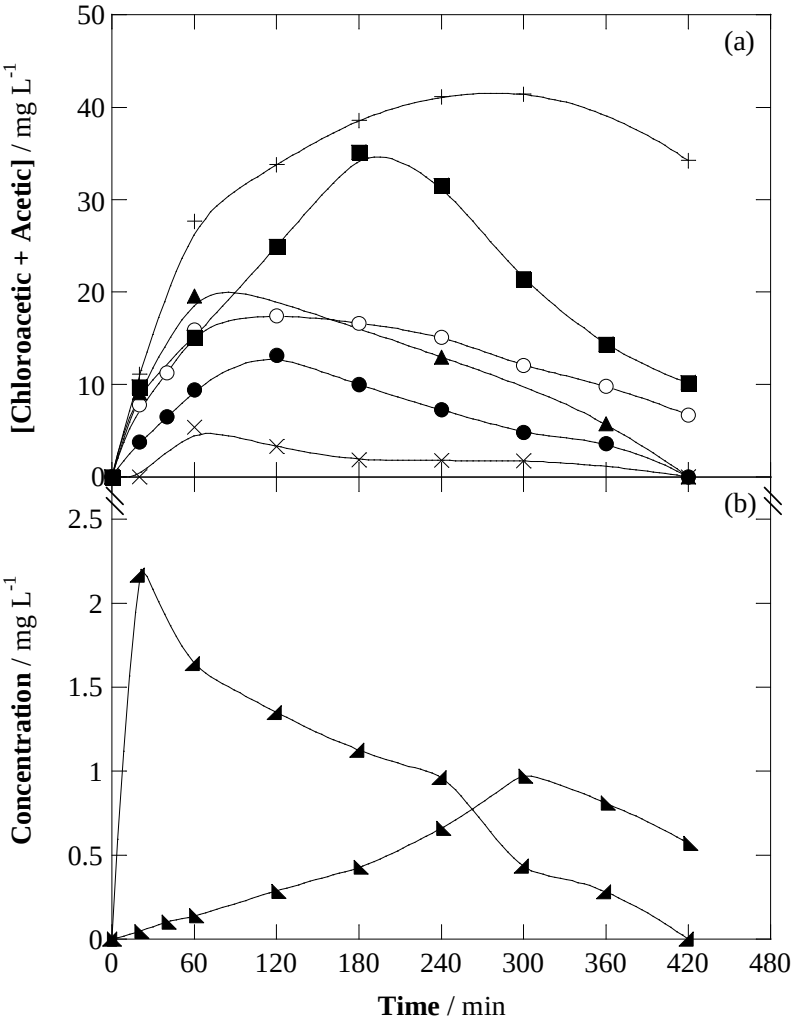

Fig. 9.5 *Time course of the concentration of the short-chain carboxylic acid intermediates accumulated during the treatment of DCA solutions. (a) Total amount of chloroacetic + acetic for different treatments, where each symbol represents the same experimental conditions described in Figs. 9.3a and 9.3b. (b) Trends of (▲) oxalic and (◢) formic for (●) shown in Fig. 9.3a.*

When the treatment of 4 mM DCA was comparatively carried out by EF at 300 mA, with Pt as the anode, much higher values of chlorocetic+acetic acids concentration was observed.Furthermore, these acids were very hardly oxidizable in this system and they remained until the end of the experiment. A concentration of about 35 mg L^{-1} was still present in the solution at 420 min, which reveals their persistence towards oxidation at the Pt surface. It is interesting to observe in Fig. 9.5b that, although the concentration of all the carboxylic acids detected as intermediates in the electro-Fenton experiment performed at 300 mA with BDD anode firstly increases and then decreases with the electrolysis time, that of oxalic acid tends to increase but is finally accumulated in the system. This result, which was also observed in the case of the study of the anodic oxidation of maleic acid, where the oxalic and formic acids were present as the main intermediates (see section 8.4), can be explained considering the higher resistance of oxalic acid to oxidation at the BDD compared to formic acid. Thus, despite formic, chloroacetic and acetic acids disappear after 420 min by electro-Fenton at 300 mA with a BDD anode, a certain concentration of oxalic acid can still be detected. A different scenario can be drawn for the electro-Fenton of TeCA (see Fig. 9.6). As shown in Fig. 9.6a, the main intermediate product in this case is the dichloroacetic acid, because of the higher number of chloride ions present in the TeCA molecule.

Also within this framework, the presence of this by-product was monitored at the different applied operative conditions. In particular, the highest concentration of this intermediate was detected for the electro-Fenton experiment performed at 300 mA with an initial concentration 4 mM TeCA. As in the case of DCA, the profile obtained at 450 mA was very similar. In contrast, a lower concentration was detected at 100 mA, although the persistence of the acid was much higher and thus, about 10 mg L^{-1} were still present in the solution at 420 min. The use of the Pt/ADE cell instead of the BDD/ADE cell, as well as the absence of catalyst led to only a partial destruction of this intermediate at the end of the experiments. Fig. 9.6b shows that the second major components present in solution as intermediates are chloroacetic and acetic acids, while formic is present in minor quantity. For oxalic acid only a small amount was accumulated in comparison to that observed for DCA

and, consequently, all the acids could be finally mineralized at 420 min. Considering the nature of the carboxylic acids detected, the general reaction pathway for the complete mineralization of 1,2-dlchloroethane and 1,1,2,2-tetrachloroethane by the EF process is also proposed.

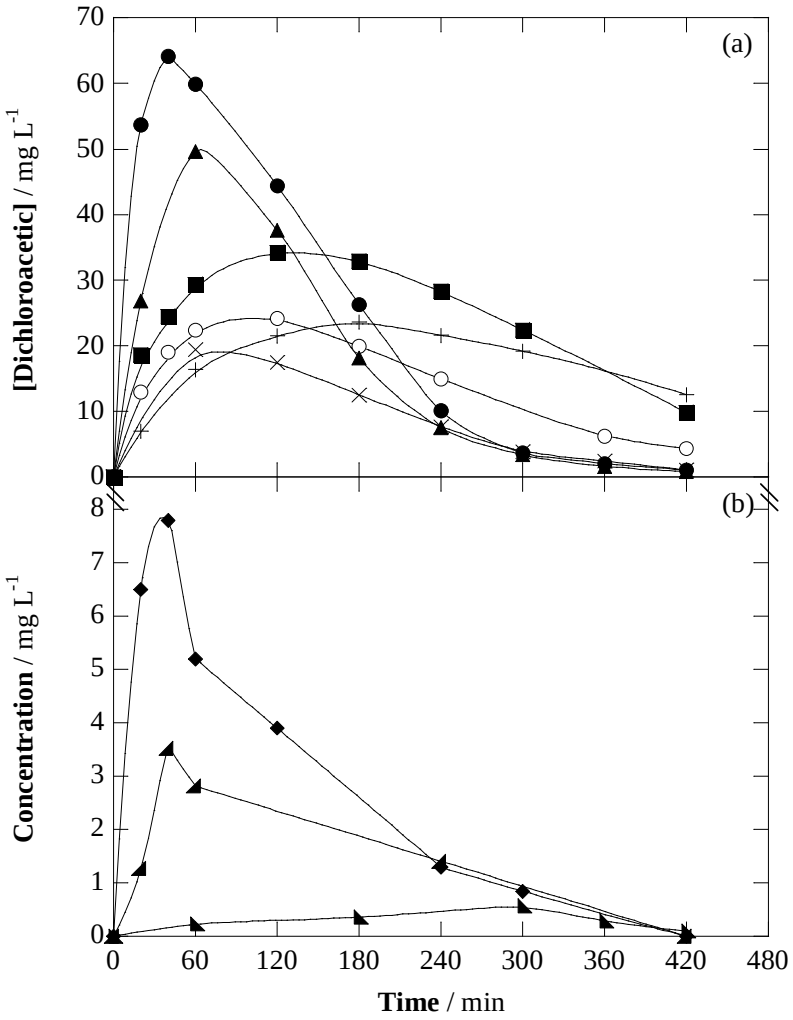

Fig. 9.6 *Time course of the concentration of the short-chain carboxylic acid intermediates accumulated during the treatment of TeCA solutions. (a) Total amount of dichloroacetic for different treatments, where each symbol represents the same experimental conditions described in Fig. 9.4. (b) Trends of (◆) chloroacetic + acetic, (▲) oxalic, and (◢) formic for (●) shown in Fig. 9.4.*

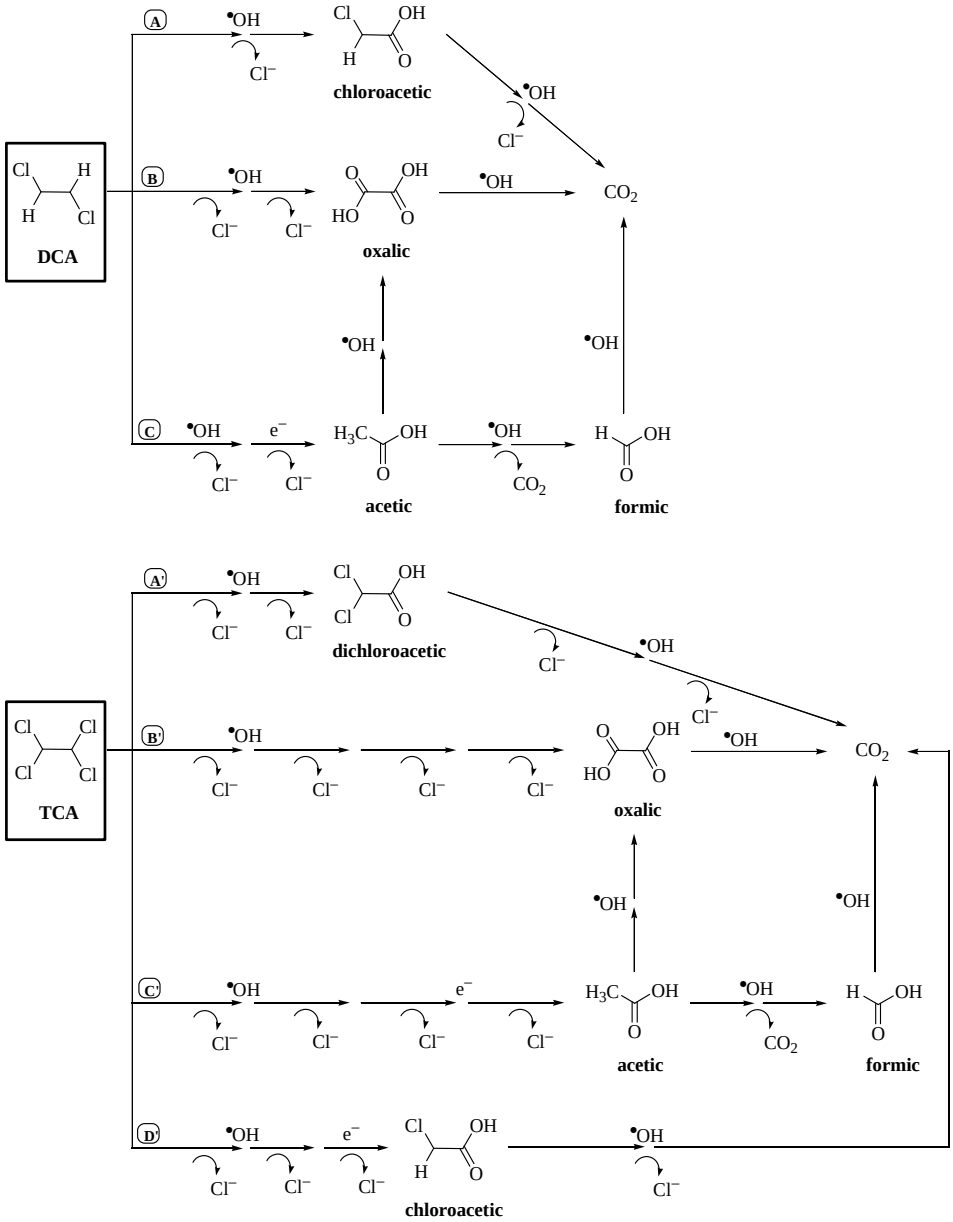

Fig. 9.7 *General reaction schemes proposed for the complete mineralization of acidic aqueous solutions of DCA (upper) and TeCA (lower) by EAOPs using a BDD/ADE cell.* $^{\bullet}OH$ *no drawn in stoichiometric quantities.*

The reaction pathways shown in Fig. 9.7 involve the primary attack of $^{\bullet}OH$ on both chlorinated hydrocarbons as the pre-eminent route. In the case of DCA, chloroacetic is formed as the main by-product, although oxalic acid can also be formed following this kind of process. One or two Cl^- ions are released, respectively (Pathways A and B in Fig. 9.7). Acetic acid is formed by reduction with loss of a chloride ion, which takes place after the attack of $^{\bullet}OH$ on DCA (Pathway C in Fig. 9.7). Acetic acid can then be oxidized to oxalic and formic acids. An analogue reaction scheme was proposed for TeCA. The main difference is the additional formation of dichloroacetic acid from the oxidation of TeCA with loss of two chloride ions. In all cases, further attack by $^{\bullet}OH$ on the reaction intermediates leads to their mineralization to CO_2.

The presence of reductive routes can be ascribed to: (i) the direct reduction at the cathode, and (ii) the presence of Fe^{2+} in solution that can reduce the organic compound in the bulk (Brillas et al., 2009), as shown in the following reaction:

$$R^{\bullet} + Fe^{2+} + H^{+} \rightarrow RH + Fe^{3+} \quad (9.13)$$

For the sake of simplicity, only the first alternative is shown in the schemes, since complexation of the intermediates with the iron species adds more complexity to the reaction pathways.

Also the inorganic products, derived from the presence of chloride ions in solution, were detected as intermediates during the electro-Fenton treatments of DCA and TeCA. In particular, the trends of Cl^-, ClO_3^- and ClO_4^- ions, which were obtained for the electro-Fenton experiment conducted using the BDD anode at 300 mA and with an initial concentration of the chlorinated aliphatic hydrocarbons of 4 mM, are reported in Fig. 9.8. Analogue considerations can be made for the specie observed for DCA (see Fig. 9.8a) and TeCA (see Fig. 9.8b) treatments. Indeed, higher concentrations of chlorides were detected at the beginning of the experiments, as expected from the direct release of the chlorine contained in the pollutants. The maximum concentration of this ion was attained at 60 min. At about 120 min, the concentrations of the three ions were almost equal, because chlorate and perchlorate are increasingly accumulated due to the oxidation of chloride. The maximum

concentration of chlorate was reached at about 180 min. From this time, chloride and chlorate decreased up to very low values at 420 min, whereas perchlorate continuously increased due to the oxidation of chloride and chlorate, reaching a very high value at 420 min.

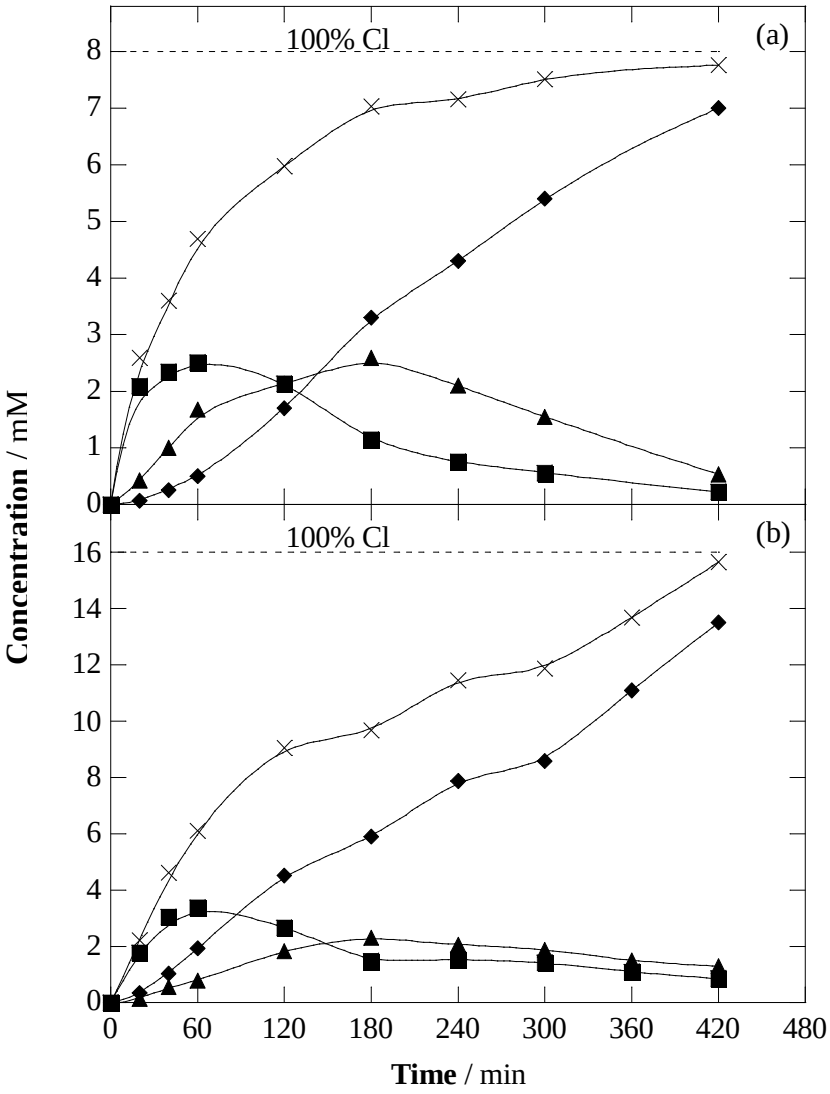

Fig. 9.8 *Time course of the concentration of the chlorinated ions released during the treatment of (a) DCA solutions in the conditions of (●) shown in Fig. 9.3a, and (b) TeCA solutions in the conditions of (●) shown in Fig. 9.4. Ion: (■) Cl^-, (▲) ClO_3^-, (◆) ClO_4^-, and (x) sum of the three ions.*

At this time, 0.2, 0.5 and 7.0 mM of Cl^-, ClO_3^- and ClO_4^- were obtained for DCA, respectively, being 97% the total percentage of chlorine in the form of chlorinated ions (the initial chlorine content in the solution was 8 mM). Similar profiles were yielded upon the treatment of TeCA, and 0.9, 1.3 and 13.5 mM of Cl^-, ClO_3^- and ClO_4^- were obtained at 420 min, respectively, being 98% the total percentage of chlorine in the form of chlorinated ions (the initial chlorine content in the solution was 16 mM).

9.6 STUDY OF THE ELECTRO-FENTON DEGRADATION OF A MULTICOMPONENT SOLUTION

Multicomponent aqueous solutions containing both 1,2-dichloroetane and 1,1,2,2-tetrachloroethane, each one at a concentration of 2 mM, were electrolyzed at 300 mA by the EF process with 0.5 mM of Fe^{2+} at BDD. This is an interesting task because organic pollutants usually occur simultaneously in wastewaters. Fig. 9.9 shows the decay of the normalized DOC of the mixture over the electrolysis time. The solution contained 96 mg L^{-1} DOC (as a result of a DOC of 46 mg L^{-1} for each of the chlorinated aliphatic hydrocarbons). Also in this case, the production of by-products was monitored by HPLC. As shown in the inset of the Fig. 9.9, dichloroacetic, chloroaceti+acetic, oxalic and formicacids are present in quantities comparable to those obtained for the chlorinated compounds alone at an initial concentration of 2 mM. The time required to achieve the almost overall DOC removal was longer than that observed for the two compounds alone at a concentration of 2 mM (see Fig. 9.3, Fig. 9.4 and Fig. 9.9), as expected from the higher content of organic matter. However, the difference was not very large and, in fact, the mineralization rate was higher, since at 300 mA the efficiency of the EF treatment is higher when $^{\bullet}OH$ can encounter a higher number of organic molecules. For example, 34%/30% and 32% DOC removals were achieved after 60 min for single DCA/TeCA and multicomponent solutions, respectively; at 420 min, 87%, 91% and 90% DOC removal was reached for DCA, TeCA and the mixture, respectively. The mineralization degrees where therefore very similar, despite treating twice the initial DOC value in the case of the mixture.

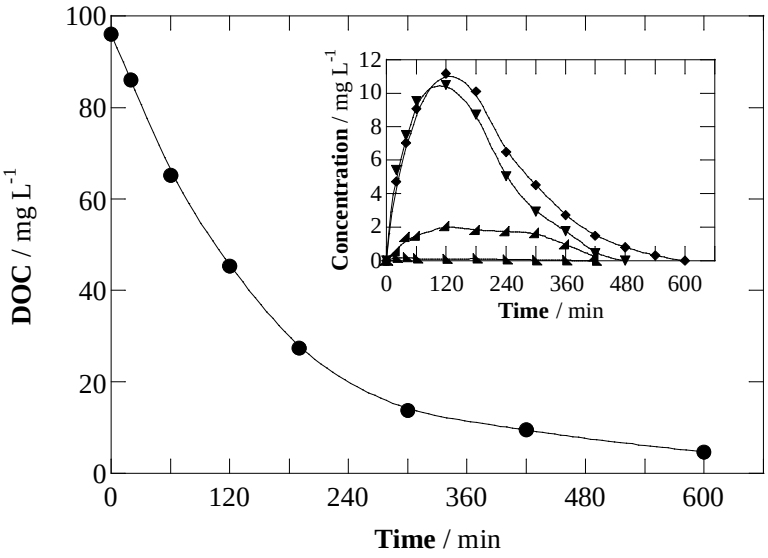

Fig. 9.9 *Study of the mineralization of solutions with DCA + TCA given by the DOC decay vs. electrolysis time. Mixtures of 130 ml containing 2 mM DCA, 2 mM TCA, and 0.5 mM* Fe^{2+} *in 0.035 M* Na_2SO_4 *medium were treated at 300 mA, pH 3.0, and at 10 ºC by electro-Fenton treatment using a BDD/ADE cell. The inset panel shows the time course of the concentration of the short-chain carboxylic acid intermediates accumulated: (◆) chloroacetic + acetic, (▼) dichloroacetic, (▲) oxalic, and (◢) formic.*

CONCLUSIONS

The influence of numerous parameters, such as the nature of the electrodic material and of the organic pollutant, the pH, the flow dynamic regime, the current density, the pollutant concentration and the temperature, on the electrochemical incineration of some carboxylic acids and aliphatic chlorides, chosen as model organic compounds, was studied in detail during the PhD thesis. Moreover, different electrochemical approaches such as direct processes, oxidation by means of electro-generated chlorine and electro-Fenton were investigated to compare their performances.

It was observed that the performances of the direct electrochemical oxidation of carboxylic acids in terms of final conversion and current efficiency depend dramatically on the adopted operative conditions both at iridium based electrodes and BDD. Experiments performed for these purposes have shown that the incineration of carboxylic acids was favored by high flow rate and low current density, i.e. when the most part of the process was under oxidation reaction kinetic control. Moreover, the process resulted to be favored by high initial concentrations of the organic substrate and low pH but did not depend, under the adopted operative conditions, on the nature of the supporting electrolyte. The abatement and the current efficiency of the process was also dependent on the flow dynamic regime and on the current density when the process took place under mass transfer kinetic control or mixed kinetic regime.

When the electrochemical incineration of maleic acid was studied performing electrolyses in an undivided cell, a slight change of COD was observed against the very fast decrease of the maleic acid concentration. Thus, the study of the effect of some operative parameters on the process was carried out in a divided cell, where different by-products were detected, specifically succinic acid in the cathodic compartment, as a reduction product, and mainly formic and oxalic acids in the anodic one. Higher concentrations of by-products were observed for low current densities, when the process is under oxidation reaction control, since starting pollutant is in excess with respect to the hydroxyl radicals formed at the anode.

Finally, at room temperatures a higher abatement of COD was observed at BDD for all the investigated acids and in particular, the rate of abatement observed was FA ~ MA > OA, while at iridium anodes an opposite trend was observed and the rate of abatement decrease as follows: OA > FA >> MA, these data indicating that different oxidant agents are involved at BDD and DSA anodes. While it has been confirmed that electrochemical oxidation using diamond thin film electrodes can be successfully carried out for incinerating oxalic acid wastes, Ti/IrO_2-Ta_2O_5 anodes can be used with good effect for this aim only if suitable operative conditions are used. Indeed, very high oxalic acid and formic acid abatements and current efficiencies were obtained in this case by working in acidic conditions at 50 °C and relatively low current density and high flow rate. Unfortunately, when experiments were performed at iridium based anodes in the presence of maleic acid, a very low abatement was obtained also at 50 °C.

Since in literature some authors had observed that higher abatements of organic pollutants could be obtained in the presence of active chlorine in the electrolytic cell, sodium chloride was added to the electrolytic solution in order to study the effect of the chloride ions on the electrochemical incineration of oxalic acid at BDD and DSA anodes. When experiments were carried out in the presence of only sodium chloride, a strong influence of pH on the active chlorine formation was observed at BDD (higher production at acid pH) but not at IrO_2-Ta_2O_5. Furthermore, active chlorine production was favored for high current density, low flow rate and at IrO_2-Ta_2O_5 anodes. The effect of NaCl on the electrochemical oxidation of oxalic acid was observed to depend on the nature of the anode and on the pH. The best results were achieved at IrO_2-Ta_2O_5 adding sodium chloride at acid pH. Moreover, in the presence of NaCl, a dramatic change of the role of some operative parameters occurred. Indeed, in the presence of high amounts of sodium chloride, a higher abatement of oxalic acid was obtained when high current densities and low flow rates were imposed and at IrO_2-Ta_2O_5.

Comparing the performances of electro-Fenton process coupled with anodic oxidation at BDD anode and simple anodic oxidation, higher abatements of 1,2-

dichloroethane and 1,1,2,2-tetrachloroethane were obtained in the first case thanks to the presence of Fe^{2+} in the solution.

Higher applied currents led to a faster electro-generation of H_2O_2 and regeneration of Fe^{2+}, thus giving rise to a faster degradation of the starting compounds. When the experiments were performed at Pt, much lower DOC removal was detected, thus confirming the important role of the oxidation process at the anode. A time course of the concentration of the main intermediates accumulated in the electrochemical cell during the treatments, in particular, short-chain carboxylic acids and chlorinated ions, was also reported.

REFERENCES

Andreozzi R. et al., *Advanced oxidation processes (AOP) for water purification and recovery*, Catalysis Today, 53 (1999) 51–59.

Arati V.M. et al., *Reduction of maleic acid to succinic acid on titanium cathode*, Organic Process Research & Development, 8 (2004) 685-688.

Bergmann M. and Koparal A., *Studies on electrochemical disinfectant production using anodes containing RuO_2*, Journal of Applied Electrochemistry, 35 (2005) 1321-1329.

Bergmann M. and Rollin J., *Product and by-product formation in laboratory studies on disinfection electrolysis of water using BDD anodes*, Catalysis Today 124, (2007) 198-203.

Bock C. and MacDougall B., *The anodic oxidation of p-Benzoquinone and maleic acid*, Journal of the Electrochemcial Society, 146 (1999) 2925-2932.

Bonfatti F. et al., *Electrochemical Incineration of Glucose as a Model Organic Substrate II. Role of Active Chlorine Mediation*, Journal of the Electrochemical Society, 147 (2000) 592-596.

Brillas E.et al., *Mineralization of paracetamol in aqueous medium by anodic oxidation with a boron-doped diamond electrode*, Chemosphere, 58 (2005) 399–406.

Brillas E. et al., *Electro-Fenton Process and Related Electrochemical Technologies Based on Fenton's Reaction Chemistry*, Chemical Reviews, 109 (2009) 6570-6631.

Busca G.et al., *Technologies for the removal of phenol from fluid streams: A short review of recent developments*, Journal of Hazardous Materials, 160 (2008) 265–288.

Cañizares P. et al., *Electrochemical oxidation of aqueous phenol wastes on synthetic diamond thin-film electrodes*, Industrial and Engineering Chemical Research, 41 (2002) 4187-4194.

Cañizares P. et al., *Electrochemical Oxidation of Aqueous Carboxylic Acid Waste Using Diamond Thin-Film Electrodes*, Industrial and Engineering Chemical Research, 42 (2003) 956-962.

Cañizares P. et al., *Electrochemical oxidation of several chlorophenols on diamond electrodes: Part II. Influence of waste characteristics and operating conditions*, Journal of Applied Electrochemistry, 34 (2004a) 87–94.

Cañizares P. et al., *Electrochemical Oxidation of Polyhydroxybenzenes on Boron-Doped Diamond Anodes*, Industrial and Engineering Chemical Research, 43 (2004b) 6629-6637.

Cañizares P. et al., *Modelling of wastewater electro-oxidation process part I. General description and application to inactive electrodes*, Industrial & Engineering Chemistry Research, 43 (2004c) 1915-1922.

Cañizares P. et al., *Modelling of wastewater electro-oxidation process part II. Application to active electrodes*, Industrial & Engineering Chemistry Research, 43 (2004d) 1923-1931.

Cañizares P. et al., *Costs of the electrochemical oxidation of wastewaters: A comparison with ozonation and Fenton oxidation processes*, Journal of Environmental Management, 90 (2009) 410-420.

Chang C. C. et al., *The electro-oxidation of formaldehyde at a boron-doped diamond electrode*, Analytical Letters, 39 (2006) 2581-2589.

Chatzisymeon E. et al., A*nodic oxidation of phenol on Ti/IrO*$_2$ *electrode: Experimental studies*, Catalysis Today, 151 (2010) 185-189.

Chemical and Engineering Data 87 (2007) 59; *Chlorinated Hydrocarbons*, in Ullmann's Encyclopedia of Industrial Chemistry, Wiley-VCH Verlag GmbH & Co. KGaAed. (2002), electronic edition.

Chen G. et al., *Electrolytic oxidation of trichloroethylene using a ceramic anode*, Journal of the Applied Electrochemistry, 29 (1999) 961-970.

Chen G., *Electrochemical technologies in wastewater treatment*, Separation and Purification Technologies, 38 (2004) 11-41.

Chen W. et al., *Decomposition of dinitrotoluene isomers and 2, 4, 6-trinitrotoluene in spent acid from toluene nitration process by ozonation and photo-ozonation*, Journal of Hazardous Materials, 147 (2007) 97–104.

Chiang L. et al., *Indirect oxidation effect in electrochemical oxidation treatment of landfill leachate*, Water Research, 29 (1995) 671-678.

Choi J.Y. et al., *Anodic oxidation of 1,4-dioxane on boron-doped diamond electrodes for wastewater treatment*, Journal of Hazardous Materials 179 (2010) 762–768.

Comninellis Ch., *Electrocatalysis in the electrochemical conversion/combustion of organic pollutants for waste water treatment*, Electrochimica Acta, 39 (1994) 1857-1862.

Comninellis Ch. and Nerini A., *Anodic oxidation of phenol in the presence of NaCl for wastewater treatment*, Journal of Applied Electrochemistry, 25 (1995) 23-28.

Comninellis Ch. and De Battisti A., *Electrocatalysis in anodic oxidation of organics with simultaneous oxygen evolution*, Journal de Chimie Physique et de Physico-Chimie Biologique, 93 (1996) 673-679.

Comninellis Ch.et al., *Perspective Advanced oxidation processes for water treatment: advances and trends for R&D*, Journal of Chemical Technologies and Biotechnologies, 83 (2008) 769–776.

Czarnetzki L. R. and Jansenn L. J. J., *Formation of hypochlorite, chlorate and oxygen during NaCl electrolysis from alkaline solutions at an RuO_2/TiO_2 anode*, Journal of Applied Electrochemistry, 22 (1992) 315-324.

Deborde M. and Von Gunten U., *Reactions of chlorine with inorganic and organic compounds during water treatment-Kinetics and mechanism: A critical review*, Water Research, 42 (2008) 13-51.

De Laat J.et al., *Etude de l'oxydation de chloroethanes en milieu aqueux dilue par H_2O_2/UV*, Water Research, 28 (1994) 2507-2519.

Dukkanci M. and Gunduz G., *Catalytic wet air oxidation of butyric acid and maleic acid solutions over noble metal catalysts prepared on TiO_2*, Catalysis Communications, 10 (2009) 913-919.

Gimeno O. et al., *Phenol and substituted phenols AOPs remediation*, Journal of Hazardous Materials, B119 (2005) 99–108.

Gulyas H., *Processes for the removal of recalcitrant organics from wastewaters*, Water Science and Technology, 36 (1997) 9-16.

Feng Y.J. and Li X.Y., *Electro-catalytic oxidation of phenol on several metal-oxide electrodes in aqueous solution*, Water Reasearch, 37 (2003) 2399-2407.

Ferro S. et al., *Chlorine evolution at Highly Boron-Doped Diamond Electrodes*, Journal of the Electrochemical Society, 147 (2000) 2614-2619.

Ferro S. et al., *Electroxidation of oxalic acid at different electrode materials*, Journal of Applied Electrochemistry, 40 (2010) 1779-1787.

Fiori G. et al., *Electroreduction of volatile organic halides on activated silver cathodes*, Journal of the Applied Electrochemistry 35 (2005) 363-368.

Flox C.et al., *Degradation of 4,6-dinitro-o-cresol from water by anodic oxidation with a boron-doped diamond electrode*, Electrochimica Acta, 50 (2005) 3685–3692.

Flox C. et al., *Solar photoelectro-Fenton degradation of cresols using a flow reactor with a boron-doped diamond anode*, Applied Catalysis B: Environmental, 75 (2007) 17–28.

Fockedey E. et al., *Coupling of anodic and cathodic reactions for phenol electro-oxidation using three-dimensional electrodes*, Water Research, 36 (2002) 4169–4175.

Gandini D. et al., *Oxidation of carboxylic acids at boron-doped diamond electrodes for wastewater treatment*, Journal of Applied Electrochemistry, 30 (2000) 1345-1350.

Guinea E. et al., *Solar photoassisted anodic oxidation of carboxylic acids in presence of* Fe^{3+} *using a boron-doped diamond electrode*, Applied Catalysis B: Environmental, 89 (2009) 459–468.

Iniesta J. et al., *Electrochemical oxidation of phenol at boron-doped diamond electrode*, Electrochimica Acta 46 (2001) 3573–3578.

Israelides C. et al., *Olive oil wastewater treatment with the use of an electrolysis system*, Bioresource Technology, 61 (1997) 163-170.

Johnson J.W. and Gilmartin L.D., *The anodic oxidation of maleic acid on platinized-platinum, Electroanalytical Chemistry and Interfacial Electrochemistry*, Journal of Electroanalytical Chemistry, 15 (1967) 231-237.

Johnson S.K. et al., *Electrochemical incineration of 4-chloro phenol and the identification of products and intermediates by mass spectrometry*, Enviromental Science and Technology, 33 (1999) 2638-2644.

Jüttner K. et al., *Electrochemical approaches to environmental problems in the process industry*, Electrochimica Acta, 45 (2000) 2575–2594.

Kanakam R. et al., *Electroreduction of maleic and fumaric acids at a rotating cathode*, Electrochimica Acta, 12 (1967) 329-332.

Kapalka A.et al., *Kinetic modelling of the electrochemical mineralization of organic pollutants for wastewater treatment*, Journal of Applied Electrochemistry, 38 (2008) 7–16.

Kapalka A. et al., *The importance of electrode material in environmental electrochemistry. Formation and reactivity of free hydroxyl radicals on boron-doped diamond electrodes*, Electrochimica Acta, 54 (2009) 2018-2023.

Kudryashov I.V. and Kochetkov V.L., *Kinetics of the reduction of maleic acid on nickel catalyst*, D.I. Mendeleev Moscow Institute of Chemical Technology, 11 (1970) 692-695.

Kulas J. et al., *Photocatalytic degradation rate of oxalic acid on the semiconductive layer of n-TiO_2 particles in the batch mode plate reactor Part I: Mass transfer limits*, Journal of Applied Electrochemistry 28 (1998) 843-853.

Lee D.-K. and Kim D-S, *Catalytic wet air oxidation of carboxylic acids at atmospheric pressure*, Catalysis Today, 63 (2000) 249-255.

Li X. et al., *Reaction pathways and mechanisms of the electrochemical degradation of phenol on different electrodes*, Water Research, 39 (2005) 1972-1981.

Mahamuni N.N. and Y.G. Adewuyi, *Advanced oxidation processes (AOPs) involving ultrasound for waste water treatment: A review with emphasis on cost estimation*, Ultrasonics Sonochemistry, 17 (2010) 990–1003.

Martinez-Huitle C.A. et al., *Electrochemical incineration of oxalic acid. Role of electrode material*, Electrochimical Acta, 49 (2004a) 4027-4034.

Martnez-Huitle C.A. et al., *Electrochemical incineration of chloranilic acid using Ti/IrO_2, Pb/PbO_2 and Si/BDD electrodes*, Electrochimica Acta, 50 (2004b) 949–956.

Martinez-Huitle C.A. et al., *Electrochemical incineration of oxalic acid: Reactivity and engineering parameters*, Journal of Applied Electrochemistry, 35 (2005a) 1087–1093.

Martinez-Huitle C. A. et al., *Electrochemical Incineration in the Presence of Halides*, Electrochemical and Solid State Letters, 11 (2005b) D35-D39.

Martinez-Huitle C. A. and S. Ferro, *Electrochemical oxidation of organic pollutants for the wastewater treatment: direct and indirect processes*, Chem. Soc. Rev., 35 (2006) 1324-1340.

Michaud P-A. et al., *Electrochemical oxidation of water on synthetic boron-doped diamond thin film anodes*, Journal of Applied Electrochemistry, 33 (2003) 151-154.

Montanaro D.et al., *anodic, cathodic and combined treatments for the electrochemical oxidation of an effluent from the flame retardant industry*, Journal of Applied Electrochemistry, 38 (2008) 947-954.

Morimtsu M. et al.,Eletrochimica Acta, 46 (2000) 401.

Murugananthan M. et al., *Electrochemical degradation of 17β-estradiol (E2) at boron-doped diamond (Si/BDD) thin film electrode*, Electrochimica Acta, 52 (2007) 3242–3249.

Oturan M.A. et al., *Sonoelectro-Fenton process: A novel hybrid technique for the destruction of organic pollutants in water*, Journal of Electroanalytical Chemistry, 624 (2008) 329-332.

Palma-Goyas R.E. et al., *Electrochemical degradation of crystal violet with BDD electrodes: Effect of electrochemical parameters and identification of organic by-products*, Chemosphere 81 (2010) 26–32.

Panizza M. et al., *Anodic oxidation of 2-naphthol at boron-doped diamond electrodes*, Journal of Electroanalytical Chemistry, 507 (2001) 206-214.

Panizza M. and Cerisola G., *Electrochemical oxidation of 2-naphthol with in situ electrogenerated active chlorine*, Eletrochimica Acta, 48 (2003) 1515-1519.

Panizza M. and Cerisola G., *Application of diamond electrodes to electrochemical processes*, Electrochimica Acta, 51 (2005) 191–199.

Pimblott S. M. et al., *Radiolysis of aqueous solutions of 1,1- and 1-dichloroethane*, Journal of Physical Chemistry A, 109 (2005) 10294-10301.

Pleskov Y. V., *Electrochemistry of Diamond: A Review*, Russian Journal of Electrochemistry, 38 (2002) 1275–1291.

Polcaro A. M. et al., *Kinetic Study on the Removal of Organic Pollutants by an Electrochemical Oxidation Process*, Industrial & Engineering Chemistry Research, 41 (2002) 2874-2881.

Polcaro A. M. et. al., *Electrochemical treatment of wastewater containing phenolic compounds: Oxidation at boron-doped diamond electrodes***,** Journal of Applied Electrochemistry, 33 (2003) 885-893.

Polcaro A.M. et al., *Oxidation at boron doped diamond electrodes: an effective method to mineralize triazines*, Electrochimica Acta, 50 (2005) 1841–1847.

Polcaro, A. M. et al., *Product and by-product formation in electrolysis of dilute chloride solutions*, Journal of Applied Electrochemistry, 38 (2008) 979-984.

Poyatos J. M. et al., *Advanced Oxidation Processes for Wastewater Treatment: State of the Art*, Water Air Soil Polluting, 205 (2010) 187–204.

Rajkumar D. et al., *Indirect electrochemical oxidation of phenol in the presence of chloride for wastewater treatment*, Chemical Engineering and Technology, 28 (2005) 98-105.

Rodrigo M.A. et al., *Oxidation of 4-Chlorophenol at boron-doped diamond electrode for wastewater treatment*, Journal of The Electrochemical Society, 148 (2001) D60-D64.

Rodriguez S.M. et al., *Treatment of chlorinated solvents by TiO_2 photocatalysis and photo-Fenton: influence of operating conditions in a solar pilot plant*, Cremosphere, 58 (2005) 391-398.

Ross F.and Ross A. B., in *Selected specific rates of reactions of transients from water in aqueous solutions*, National bureau of standards Department of commerce, Washington, DC 20234 (1977).

Scialdone O. et al., *Electrochemical incineration of 1,2-dichloroethane: Effect of the electrode material*, Electrochemical Acta, 53 (2008) 7220-7225.

Scialdone O., *Electrochemical oxidation of organic pollutants in water at metal oxide electrodes: A simple theoretical model including direct and indirect oxidation processes at the anodic surface***,** Electrochimica Acta, 26 (2009) 6140-6147.

Scialdone O. et al., *Electrochemical abatement of chloroethanes in water: reduction, oxidation and combined processes*, Electrochimica Acta, 55 (2010) 791-708.

Simond O. et al., *Theoretical model for the anodic oxidation of organics on metal oxide electrodes*, Electrochimica Acta, 42 (1997) 2009-2012.

Sirés I. et al., *Electrochemical degradation of b-blockers. Studies on single and multicomponent synthetic aqueous solutions*, Water Research, 44 (2010) 3109-3120.

Skoumal M. et al., *Mineralization of paracetamol by ozonation catalyzed with* Fe^{2+}, Cu^{2+} *and UVA light*, Applied Catalysis B: Environmental, 66 (2006) 228–240.

Skoumal M.et al., *Electro-Fenton, UVA photoelectro-Fenton and solar photoelectro-Fenton degradation of the drug ibuprofen in acid aqueous medium using platinum and boron-doped diamond anodes*, Electrochimica Acta, 54 (2009) 2077–2085.

Szpyrkowicz L. et al., *Application of electrochemical processes for tannery wastewater treatment*, Toxicology and Environmental Chemistry, 44 (1994) 189-202.

Szpyrkowicz L. et al., *Electrocatalysis of chlorine evolution on different materials and its influence on the performance of an electrochemical reactor for in direct oxidation of pollutants*, Catalysis Today, 100 (2005) 425-429.

Trasatti, S. *Progress in the understanding of the mechanism of chlorine evolution at oxide electrodes*, Electrochimica Acta, 32 (1987) 369-382.

Vilve M. et al., *Degradation of 1,2-dichloroethane from wash water of ion-exchange resin using Fenton's oxidation*, Enviromental Science and Polluting Research, 17 (2010) 875-884.

Wastewater, *ULLMANN'S* encyclopedia of industrial chemistry

Weiss E. et al., *A kinetic study of the electrochemical oxidation of maleic acid on boron doped diamond*, Journal of Applied Electrochemistry, 37 (2007) 41-47.

Wiley, *Synthetic Diamond Films Preparation, Electrochemistry, Characterization and Applications*, Chapter 11, in press.

Zhi J-F et al., *Electrochemical incineration of organic pollutants on boron-doped diamond electrode. Evidence for direct electrochemical oxidation pathway*, Journal of Physical Chemistry B, 107 (2003) 13389-13395.

PUBBLICATIONS

- "Electrochemical incineration of oxalic acid at boron-doped diamond electrodes by potentiostatic and amperostatic electrolyses: role of operative parameters", O. Scialdone, A. Galia, C. Guarisco, Serena Randazzo, G. Filardo, Electrochimica Acta 53 (2008) 2095–2108.
- "Electrochemical oxidation of organics at metal oxide electrodes: The incineration of oxalic acid at IrO2–Ta2O5 (DSA-O2) anode", O. Scialdone, Serena Randazzo, A. Galia, G. Filardo, Electrochimica Acta 54 (2009) 1210–1217.
- "Electrochemical oxidation of organics in water: role of operative parameters in the absence and in the presence of NaCl", O. Scialdone, Serena Randazzo, A. Galia, G. Silvestri, Water Research 43 (2009) 2260-2272.
- "Electrochemical abatement of chloroethanes in water: reduction, oxidation and combined processes", O. Scialdone, A. Galia, Serena Randazzo, L. Gurreri, G. Silvestri, Electrochimica Acta 55 (2010) 701-708.

COMMUNICATIONS

- "Electrochemical oxidation of carboxylic acids at boron doped diamonds", O. Scialdone, Serena Randazzo, A. Galia, C. Guarisco, G. Filardo, comunicazione orale al GEI-ERA, 5 -10 Settembre 2010 Modena, Italy.
- "Electrochemical incineration of organic pollutants: effect of the nature of the pollutants and of the operative conditions", Serena Randazzo, G. Filardo, A. Galia, G. Silvestri, O. Scialdone – VII PhD-Chem Day, CongressoCIRCC, http://www.circc.uniba.it/conferenze/VII_PhD_ChemDay/index.htm, 19 Febbraio 2010, Napoli, Italy.
- " Electrochemical incineration of organic pollutants: effect of the nature of the pollutants and of the temperature",– comunicazione orale al '2nd

European conference on environmental applications of advanced oxidation processes (*EAAOP2)*, 9-11 Settembre 2009, Nicosia, Cyprus.

- "Effect of the temperature on the electrochemical incineration of carboxylic acids", Serena Randazzo, G. Filardo, A. Galia, G. Silvestri, O. Scialdone – poster presentato all'ISE, 16-21 Agosto *2009* Beijing, China.
- "Electrochemical incineration of oxalic acid in the presence of NaCl", Serena Randazzo, G. Filardo, A. Galia, O. Scialdone - comunicazione orale al Convegno GRICU, 14-17 Settembre 2008, Le Castella (KR), Italy.
- "Electrochemical incineration of oxalic acid in presence of NaCl", O. Scaildone, Serena Randazzo, A. Galia, G. Filardo, G. Silvestri - Society of Electrochemistry, 7-12 Settembre 2008**,** Siviglia, Spain.
- "Influence of operative parameters on the electrochemical incineration of oxalic acid", O. Scialdone, Serena Randazzo, A. Galia, C. Guarisco, G. Filardo, G. Silvestri,– ISE, 16-19 Marzo 2008, Foz do Iguaçu, Brazil.
- "Electrochemical incineration of oxalic acid at boron doped diamonds", O. Scialdone, A. Galia, G. Filardo, C. Guarisco, Serena Randazzo, G. Silvestri, poster presentato al GEI-ERA, 15-20 Luglio 2007, Cagliari, Italy.
- "Electrochemical incineration of oxalic acid at boron-doped diamond electrodes: influence of operative parameters", O. Scialdone, G. Filardo, A. Galia, C. Guarisco, Serena Randazzo, G. Silvestri - XXII Congresso Nazionale della *Società Chimica Italiana*, 10-15 Settembre *2006*, Firenze, Italy.

ACKNOWLEDGEMENTS

Dott. Ing Scialdone Onofrio

Dott. Ing. Galia Alessandro

Prof. Filardo, Ing. Guarisco Chiara and the others of our laboratory

Prof. Brillas and his research group

Dr. Nacho Sirés